

MULTI-SCALE MODELING OF
POTATO LATE BLIGHT
EPIDEMICS

Promotor:

Prof. dr. A.A.M. Holtslag
Hoogleraar Meteorologie

Co-promotoren:

Dr. ir. W. van der Werf
Universitair hoofddocent, leerstoelgroep Gewas- en Onkruiddecologie

Dr. ir. G.J.T. Kessel
Onderzoeker, Plant Research International

Dr. ir. W.A.H. Rossing
Universitair hoofddocent, leerstoelgroep Biologische Landbouwsystemen

Promotiecommissie:

Prof. dr. ir. E. Jacobsen, Wageningen Universiteit
Prof. dr. ir. M.C.M. de Jong, Wageningen Universiteit
Dr. A.P. van Ulden, KNMI, De Bilt
Prof. dr. M.R. Finckh, University of Kassel, Germany

Dit onderzoek is uitgevoerd binnen de C.T. de Wit Onderzoekschool: Production Ecology and Resource Conservation.

**MULTI-SCALE MODELING OF
POTATO LATE BLIGHT
EPIDEMICS**

PETE SKELSEY

Proefschrift

ter verkrijging van de graad van doctor

op gezag van de rector magnificus

van Wageningen Universiteit,

Prof. dr. M.J. Kropff,

in het openbaar te verdedigen

op woensdag 3 september 2008

des namiddags te vier uur in de Aula

Pete Skelsey (2008)

Multi-scale modeling of potato late blight epidemics.

PhD thesis Wageningen University. - With ref. -

With summaries in English and Dutch.

ISBN: 978-90-8504-941-8

“Here’s tae us.....”

Dedicated to my parents, David and Mary, my brother Chris,
and the beautiful Jen

Abstract

Skelsey, P. 2008. Multi-scale modeling of potato late blight epidemics. PhD thesis, Wageningen University, the Netherlands. With English and Dutch summaries, 257 pp.

Phytophthora infestans, causal agent of potato late blight, causes multi-billion dollar losses annually in global production of potatoes and other Solanaceous crops. Although the spatial dimension of potato late blight epidemiology is widely acknowledged by researchers who study plant disease, the corresponding theoretical framework is underdeveloped. This is because spatial increase of potato late blight disease is the product of a complex interplay between meteorological driving forces, management practices, and the spatial characteristics of crops and landscapes. The objective of this thesis is to enhance understanding of potato late blight epidemiology at the field- and regional-scale by an integration of epidemiological and aerobiological modeling.

Field-scale disease dynamics were quantified through the development and validation of a spatio-temporal model of the potato late blight pathosystem. The model was used to compare disease dynamics in pragmatic layouts for variety mixtures. A sensitivity analysis of the model resulted in a heuristic for distinguishing epidemics driven by lesion expansion from those driven by lesion propagation. The model was also used to study the vulnerability of potato crops to disease invasion from an initial influx of sporangia, in order to determine the feasibility of spore dispersal modeling as a risk assessment tool. Regional-scale inoculum dynamics were quantified through the development and validation of a numerical and a fully analytical atmospheric spore dispersion and deposition model.

Two modeling tools for management were developed. In the first instance, a full complement of aerobiological models (release of spores from sporangiophores, escape from the canopy, numerical dispersion model and survival during transportation) were combined with an existing decision support system (DSS) to develop a novel concept for inclusion of regional aerobiological modeling in disease risk warning forecasts for an aerially transmitted plant pathogen. A field trial with the new system showed adequate disease control while the number of chemical treatments was reduced in comparison to a non-spatial DSS. In the second instance, the potato late blight model was combined with the full complement of aerobiological models (including the analytical dispersion model) and a landscape generator to create a multi-scale simulator of the late blight pathosystem. The simulator was used to evaluate various landscape designs for the suppression of invasions of resistance breaking pathogen strains. Simulation results showed that the large capacity of *P. infestans* for long-distance transport of viable inoculum nullified the effectiveness of spatial barriers to disease spread at scales up to several kilometers. The most successful landscape designs for suppressing disease spread were those that increased the level of genetic diversity in host populations, and/or the degree of mixing of host genotypes.

Many of the modeling tools and concepts developed in this research are extendable to other pathosystems characterized by airborne inoculum.

Keywords: *Solanum tuberosum*, *Phytophthora infestans*, potato late blight, spatial epidemiology, spore dispersal, decision support system, landscape design, integrated late blight management.

Acknowledgements

The threads of this thesis have woven their way through 4 years of my life, and have encompassed many people. It is therefore with gratitude that I take this opportunity to thank those who made it all possible.

I am sincerely grateful to Dr. Wopke van der Werf; a wise and trusted mentor for whom I have the utmost respect. To merely label you as a supervisor is to do you an injustice. I cannot thank you enough for all your hard work, encouragement, and inspiration; all delivered in fine style with good humor and a revolving office door.

Many thanks also to Dr. Walter Rossing. I will never forget the day I arrived on your doorstep, nervously clutching my "Beginners guide to calculus." Your patience in those early days (and beyond) seemed boundless and is a true credit to your role as a teacher and scientist. There will always be a glass of malt for you in my house.

It is difficult to know where to begin with Dr. Geert Kessel. Thanks for all the advice, support, knowledge, laughs, and of course - parameter values. I had a great time working and traveling with you, and of course with the rest of the PRI tribe.

I am also deeply grateful to my promoter Prof. Bert Holtslag. When I was lost in a maze of meteorology, you had an uncanny knack at making the unfathomable seem transparent. You have succeeded where many textbooks have failed.

A special thanks to Adrie Jacobs and Peter Hofschreuder for introducing me to the wonderful world of dispersal, and Dr. Jordi Vilá-Guerau de Arellano for fruitful discussions on turbulence and football. I must also thank the many learned scientists from around the world with whom I have enjoyed rewarding discussions on my travels. Thanks also to the staff at Agrovision-Opticrop and Dacom PLANT Service for making me welcome on my visits, and for sharing their experiences.

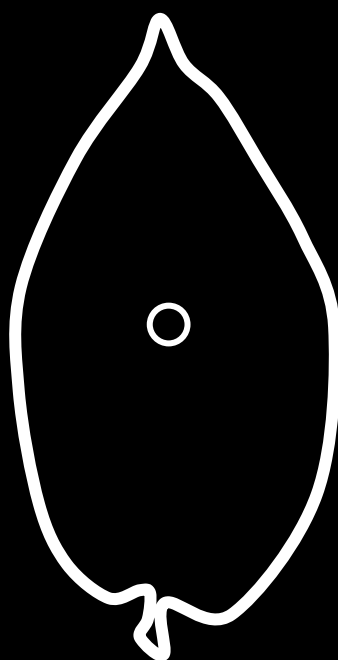
These acknowledgements would not be complete without saying "cheers" to two very special people - Sander and Nuray - who provided me with my second home, and much more besides. Slainte to the rest of the De Zaaier crew, who are far too numerous to mention.

Finally, it is time to thank those closest to my heart. None of this would have been possible without the unwavering support of my mum and dad, whom I love dearly. Thanks to my brother Chris who has always encouraged me - I couldn't let you get one up on me bro! And Jen, you have been an ocean of calm and tranquility amidst the tempest of the last few years; without you, I would be a much poorer man.

Contents

Chapter 1	General introduction	1
Chapter 2	Influence of host diversity on development of epidemics: an evaluation and elaboration of mixture theory	21
Chapter 3	Parameterization and evaluation of a spatio-temporal model of the late blight pathosystem	55
Chapter 4	Scenario approach for assessing the utility of dispersal information in decision support for aerially spread plant pathogens, applied to <i>Phytophthora infestans</i>	87
Chapter 5	Development and validation of a quasi-Gaussian plume model for the transport of botanical spores	111
Chapter 6	Regional spore dispersal as a factor in disease risk warnings for potato late blight: a proof of concept	141
Chapter 7	Invasion of a virulent <i>Phytophthora infestans</i> genotype at the landscape level; does spatial heterogeneity matter?	171
Chapter 8	General discussion	221
	Summary	239
	Samenvatting	245
	List of publications	251
	Curriculum vitae	253
	PE&RC PhD Education Statement Form	255
	Funding	257

CHAPTER 1



Introduction

Potato (*Solanum tuberosum* L.) is the world's number one non-grain food commodity. In the developed world, potato has long been a major part of the staple diet, and up until the 1990s most potatoes were grown and consumed in Europe, North America and countries of the former Soviet Union. Since then, there has been a dramatic increase in potato production and demand in Asia, Africa and Latin America, where output rose from less than 30 million tons in the early 1960s to more than 165 million tons in 2007 (FAO, 2008). Global potato production reached a record 320 million tons in 2007 (FAO, 2008), and is set to rise even further. As concern grows over the risk of food shortages and instability in dozens of low-income countries, global attention is turning to the potato crop to try to ease the strain of food price increase. The United Nations has designated 2008 as the "International Year of the Potato," and potato is now being promoted as an important contributor to the solution to global hunger. Potato is not without its problems, however. *Phytophthora infestans*, causal agent of potato late blight, is a highly aggressive plant pathogen that can destroy a potato crop in a matter of days. The costs of losses to potato late blight, and of controlling it, are enormous; it is estimated that *P. infestans* is responsible for multi-billion dollar losses annually in global tomato and potato production (Duncan 1999; Birch and Whisson, 2001; Haverkort et al., *in press*). Given that potato is now being pushed as a major component of strategies aimed at feeding the poor and hungry, this destroyer of plants could become an important biotic threat to global food security.

This thesis describes experimental and simulation work aimed at improving our understanding of potato late blight epidemiology. Knowledge of plant pathology, epidemiology, meteorology, potato production and spatial modeling is combined and analyses are made to gain insight into the spatial dimension of potato late blight epidemiology. Our aim is to evaluate how knowledge of spatial epidemiology can be used to improve local and regional management of the disease.

Background

P. infestans has shaped nations. Its legacy is one of death, displacement, and economic loss. In Europe in the mid-nineteenth century, potato late blight spread like wildfire. Crop losses were most severe in Ireland, where the notorious "great hunger"

or “Irish potato famine” resulted in the death of 1 million people and the displacement of 1.5 million more (Large, 1940). Undoubtedly, this is still the most striking example of the damage that can be wrought on plants and human society through invasion of a virulent plant pathogen. *P. infestans* has been the subject of intense academic interest ever since. Nonetheless, potato late blight continues to be a problem today. This is despite daily attention from growers, and a concentrated effort from the plant breeding and agrochemical industries.

Part of the potato late blight problem in developed countries is the devotion of most growers to susceptible potato varieties. This is not for reasons of sentiment; varietal choice is dictated by end-users who demand potatoes with certain quality traits for consumption or processing that are difficult to combine with resistance to the disease. Potato production today is therefore heavily reliant on the use of fungicides to keep blight off the landscape. In developing countries growers are often poor at diagnosis and decision making, leading to liberal application of fungicides on a rather ad-hoc basis. This situation is generally perceived as unsustainable. In the Netherlands alone around 1.4 Mkg of chemicals are used in an average growing season to combat potato late blight (Haverkort et al., *in press*). Fungicide costs globally are estimated at around \$1 billion per annum (Forbes and Landeo, 2006). Not surprisingly, there is mounting pressure from governments, retailers and public alike to reduce the intensive use of fungicides in potato cultivation. To further complicate the situation, pathogen populations around the world have changed dramatically during the last two decades of the twentieth century with the replacement of the old “clonal” population by a new, genetically more diverse and more aggressive population that is capable of sexual recombination. This has led to a further intensification in chemical usage. This potent, persistent and pervasive plant pathogen appears to be getting the upper hand.

Pathogen

Taxonomy

Although in everyday parlance *P. infestans* is a “fungus,” it does not actually belong to the Kingdom Fungi. The genus *Phytophthora*, the closely related genus *Pythium*, and the downy mildews (i.e., *Bremia*, *Sclerospora*, *Plasmopara*, *Peronospora*, etc.) are the three major groups that comprise the Oomycetes. Oomycetes are stramenopiles; a group which includes multicellular brown algae, the planktonic diatoms, and most

other algae of similar pigmentation, the fungus-like water molds and other colorless forms. Oomycetes produce asexual spores called zoospores. These are formed inside sporangia. Zoospores are propelled by flagella and capitalize on surface water for movement. Oomycetes also produce sexual spores, called oospores, that develop from the joining of oogonia (female reproductive structure) and antheridia (male reproductive structure). A few, such as *P. infestans*, produce asexual spores (sporangia) that are distributed by wind. Many species of Oomycetes are still described or listed as types of fungi and may sometimes be referred to as pseudofungi, or lower fungi. The reader is referred to Erwin and Ribeiro (1996) for a discussion on changes in the understanding of the taxonomic position of this group of organisms. The following is considered to be the correct taxonomic classification of *P. infestans* by many pathologists:

Phytophthora infestans (Mont.) de Bary - Kingdom Chromista, Phylum Oomycota, Order Peronosporales, Family Peronosporaceae, Genus *Phytophthora*, of which it is the type species (Birch and Whisson 2001).

Origins and distribution

Speculation as to the origins of *P. infestans* began soon after the catastrophic potato famines of the mid-nineteenth century, and the debate still continues today. Some suggest that the center of origin of *P. infestans* is in the central highlands of Mexico because of the high diversity of both potato and pathogen that occurs there (e.g., Niederhauser, 1991; Grünwald and Flier, 2005). Furthermore, major genes for resistance to potato late blight were first discovered in endemic potato species in Mexico, suggesting long-term coevolution between host and pathogen (Grünwald and Flier, 2005). An alternative theory is that *P. infestans* originated in the South American Andes, the center of diversity of Solanaceous plant species (Spooner et al., 2005). As only a few clonal lineages of the pathogen have been described from this area, this hypothesis has not been generally accepted (e.g., Niederhauser, 1991; Grünwald and Flier, 2005).

At least two major migrations of the pathogen from its center of origin (lets say Mexico) to Europe and North America have shaped the historical significance of the pathogen. The first took place in the mid-nineteenth century and led to the “Irish potato famine” already mentioned. Apparently this migration involved a limited number of genotypes, and all were of the A1 mating type (Goodwin et al., 1994). This lack of genetic diversity was not limiting to the pathogen, and it soon spread to almost every area where potatoes were grown. Meanwhile, the occurrence of the A2

mating type was confined to an area of the highlands of central Mexico (Niederhauser, 1956). This situation changed dramatically in 1976. The summer that year was hot and dry and the largely unirrigated potato crop failed in most of Europe. Import restrictions were relaxed and large tonnages of potato were imported from Mexico. Hidden inside these now infamous tubers were many new strains of the pathogen, including the A2 mating type (Duncan, 1999). The pathogen population in Europe is now highly diverse and there is evidence for sexual reproduction in several European countries (Drenth, 1994; Andersson et al., 1998; Flier et al., 2002). This new population has replaced the old clonal population throughout most of Eurasia (Duncan, 1999). Similar introductions occurred in North America around the same time. As a result, both the A1 and A2 mating types now have a global distribution on potato and tomato.

Hosts

P. infestans infects members of the *Solanaceae* family. Erwin and Ribeiro (1996) list 89 host species of *P. infestans*, but *P. infestans* is probably aggressive on all tuber bearing species in the genus *Solanum*. Of the non-tuber bearing *Solanum* hosts, tomato (*Lycopersicon esculentum*) is the most important economically. Other domesticated *Solanum* species are also hosts of *P. infestans*, including pear melon (*S. muricatum*) (Turkensteen 1978), tree tomato (*S. betaceum*) (Oliva et al., 2002), and naranjilla (*S. quitoense*) (Adler et al., 2004). There have also been references to infection in Solanaceous plants outside the genus *Solanum*, e.g., *Nolana* species (Abad et al., 1995).

Symptoms

Initial symptoms on potato appear as water-soaked, irregular, pale lesions on above ground foliage. These grow rapidly into dark, necrotic spots. Lesion appearance then depends very much on lesion age. Young lesions are generally irregular in shape and are often surrounded by a halo of pale, collapsed tissue. Older lesions tend to be more circular, and as they are not limited by leaf veins they will expand right up to the leaf margins. A white fluff can be observed around lesion edges during morning hours. This consists of the sporangiophores (stalks) and sporangia of the pathogen. Lesions on stems can cause girdling and leaf wilt above the point of infection. Stem lesions are generally light to dark brown and brittle, leading to frequent stem breakage. Late blight can attack tubers when spores are washed down into the soil. Infected tubers show irregular reddish/purplish depressions that can extend deep

into the tissue. Although infected tubers are generally hard and firm, secondary bacterial infections can take hold leading to soft rot. Badly infected fields generally give off a distinctive smell of rotting tissue.

Epidemiology

“Damp is conducive to the progress of the disease.....dryness retards it.”

[David Moore, 1845]

The epidemiology of potato late blight has been investigated for over 150 years, therefore we know much about the factors that influence epidemic dynamics. It could in fact be argued that the terrors of the “Irish potato famine” in the mid-nineteenth century led to a new understanding of plant disease and the birth of plant pathology. Within months of the arrival of potato late blight in Ireland, David Moore, curator of the Royal Dublin Society’s Botanic Gardens, provided the first insight into what makes this disease tick, and he is quoted above (cited in Nelson, 1995). Since those initial observations, plant disease epidemiologists have worked tirelessly to discover and quantify the effects of weather on epidemic development, as well as other factors that may be of importance.

In cold, temperate zones, *P. infestans* must survive freezing winter conditions in order that the epidemic phase can begin anew each growing season. Increase of disease in time and space then requires a repeated cycle of infection, multiplication of inoculum, and dispersal of inoculum to new sites. A potato late blight epidemic therefore has three basic components: survival of the pathogen between cropping seasons; increase of disease through growth of the pathogen in living host tissue (*in planta*); and increase of disease through new infections, which follows directly from pathogen dispersal and host encounter (Aylor, 1990). There is a vast corpus of information on *P. infestans* epidemiology, therefore only a short summary is possible here.

Between-season survival

There are a number of ways that survival between cropping seasons is achieved in the potato agro-ecosystem. In the cold temperate zones, *P. infestans* may overwinter as mycelium in tubers. Tuber infection can occur before harvest due to rain-splash of inoculum from infected foliage into the soil. It can also occur during harvest

if tubers are lifted through soil that contains viable sporangia, or come into contact with infected foliage or sporangia from other sources of inoculum. If the infected tubers are protected from freezing, either in storage or in soil, then they can act as localized sources of inoculum in the following cropping season. Stored tubers may be used as seed potatoes for next years crop, or discarded in refuse piles. Infected tubers that are not harvested produce “volunteer” potato plants in the following season. In all three cases mycelium can spread up through the new shoots and produce sporangiophores in the foliage. This then is the *primary* inoculum that initiates the epidemic phase anew each growing season. Another source of primary inoculum is provided by the sexual cycle of the disease. Oospores resulting from mating between A1 and A2 strains are hardy, thick-walled structures that can survive in soil over winter. In fact, oospores are able to survive for several years in the soil before germinating and infecting a new crop (Drenth et al., 1995).

Disease cycle

Part of the reason why *P. infestans* is so successful as a pathogen comes from the fact that the disease cycle is actually two cycles: a very efficient and effective asexual cycle, and a sexual cycle (Fig. 1). As a hemibiotroph, *P. infestans* requires living host tissue for part of its infection cycle and it can infect most parts of the potato plant. Infection usually starts with deposition of an asexual reproductive structure, called a sporangium, on a host leaf or stem. *P. infestans* sporangia are lemon-shaped with a length ranging between 29 and 36 μm and width between 19 and 22 μm . In warmer conditions, the sporangium germinates directly through production of a germ tube that penetrates the host tissue. In cooler conditions, the sporangium will produce and release around 6 to 12 motile zoospores. These have two flagella, one tinsel type that is directed forward and a second whiplash type that is directed backward. This allows the zoospore to swim in free moisture. When zoospores lose their flagellae they become cystospores, which also germinate and infect through a germ tube. After penetration, threadlike filaments called hyphae begin intracellular colonization of host tissue (vegetative growth). Together these form the mycelium of the pathogen. Haustoria develop that extract nutrients from within the cells of the host and thus destroy the plant tissue, giving rise to a necrotic lesion. After a latency period of a couple of days, spore-bearing sporangiophores emerge around the edge of the lesion. The sporangia may be dispersed by the wind to cause new foliar infections in the same crop or in neighboring fields. Alternatively, they may be splashed onto other leaves or down into the soil by rain or irrigation water. Once in the soil, tuber

infections can occur via eyes, lenticels or wounds in the tuber tissue. Given favorable environmental conditions, regeneration time is rapid and the whole asexual cycle can be repeated every 5 to 7 days. Thus, the asexual cycle is the driving force behind rapid polycyclic epidemics that can be observed in potato crops during the growing season. The net result is significant loss of photosynthetic capacity in the potato crop, and direct losses of harvestable product due to tuber infections.

P. infestans is heterothallic, meaning that two mating types are required for sexual reproduction. These are named A1 and A2. Sexual reproduction involves the production of a male sex organ (antheridium) and a female sex organ (oogonium) that may contain one or several eggs. Oogonial hyphae grow through the antheridium and then swell to form the oogonium. Meiosis occurs within these sex organs and fertilization is achieved by the transfer of a single haploid nucleus through a fertilization tube to each haploid egg. Fertilization leads to the development of one or more round, thick-walled zygotes called oospores. These can survive adverse

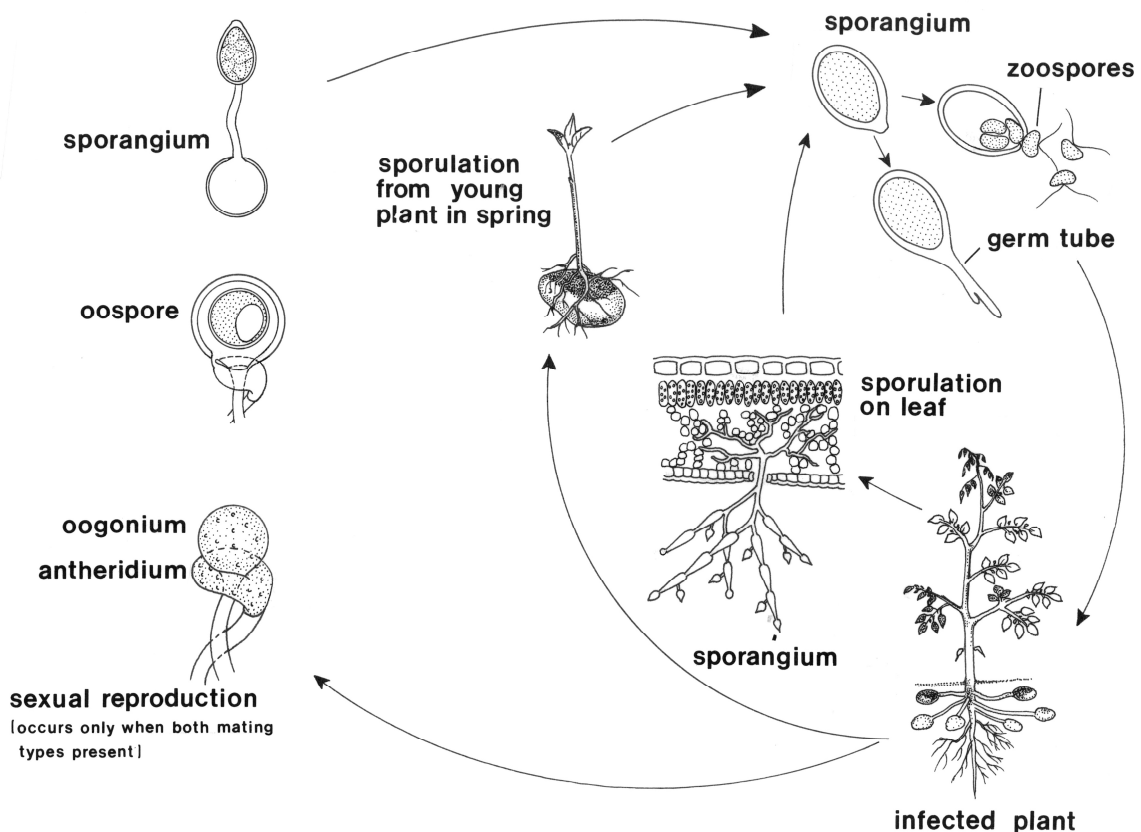


Fig. 1. Disease cycle of potato late blight, caused by *Phytophthora infestans* (Reprinted with permission from Schumann, 1991).

conditions better than other forms of the pathogen.

Disease development *in planta*

Temperature and moisture play major roles in the development of disease *in planta*. These environmental factors determine the mode of sporangial germination, how successful the pathogen will be at establishing a parasitic interaction with the host, and the rate at which the pathogen can grow through the host tissue (Beckett et al., 2005). Environmental conditions influence infection, the incubation period (time period from inoculation to appearance of lesions), and the production of sporangia. In other words, the weather determines if pathogen establishment will occur at all. Although not extensive, the following list captures some of the most important weather dependent relations for development of disease (Beckett et al., 2005): infection requires a minimum of 2 to 3 hours of leaf wetness at the optimum temperature of 20°C (Crosier, 1934); the transition between direct and indirect germination of sporangia occurs at approximately 15°C, (Harrison, 1992; Judelson and Blanco, 2005) with indirect infection via zoospores being most common below this temperature and direct infection dominating above 15°C; incubation period is shortest between 20 and 28°C (Crosier, 1934; Mizubuti et al., 1998; Andrade-Piedra et al., 2005); the most rapid sporangium production occurs at around 21°C (Crosier, 1934); and the optimum temperature range for maximum spore production is 15 to 21°C (Crosier, 1934; Mizubuti et al., 1998; Andrade-Piedra et al., 2005).

Spatial spread of disease

Once epidemics are underway, wind or splash-borne sporangia are the primary means for spatial increase in disease. Splash dispersal involves the removal of spores from their sporangiophores by rain or irrigation water. Splash-borne sporangia are generally deposited very close to the inoculum source, and have a good chance of survival given the moisture requirements of the germination process. Most airborne sporangia are deposited within several meters of the inoculum source (Fry and Mizubuti, 1998), but dispersal over larger distances can take place. Wind, atmospheric turbulence, temperature, humidity and solar radiation all play major roles in the aerial transport of spores, which can be divided into a number of weather dependent stages (Fig. 2):

- i) Spore release from sporangiophores. As humidity drops, hygroscopic twisting of the sporangiophore releases the sporangia into the air (Pinckard, 1942).

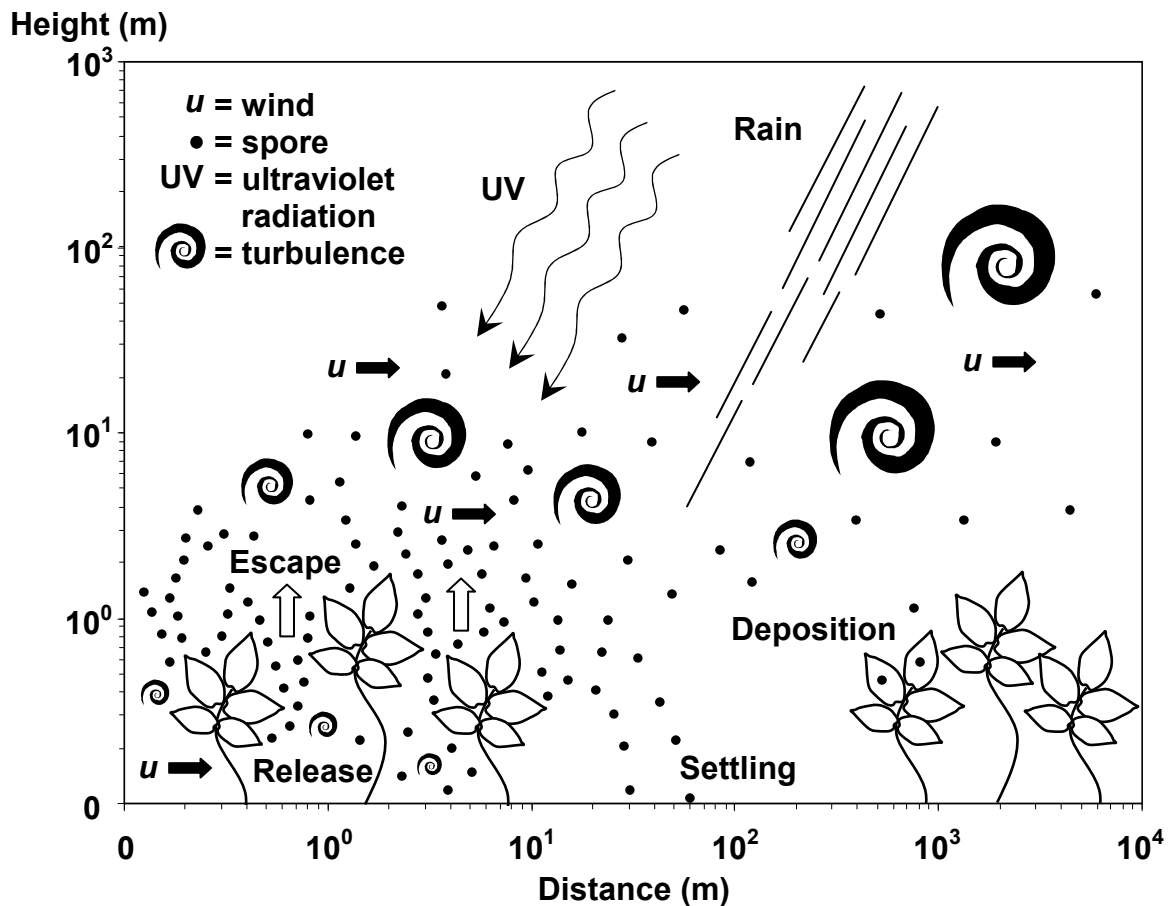


Fig. 2. Aerial component of the disease cycle of potato late blight, caused by *Phytophthora infestans*.

- ii) Spore escape from the potato canopy. Wind and atmospheric turbulence lift spores up through the canopy making them available for long-distance transport. Time of day of spore release, height of spore release, and canopy structure all affect wind and turbulence statistics and the probability of spore escape (Aylor, 1990).
- iii) Transport to distant potato crops. This requires a favorable wind direction. During transportation, atmospheric turbulence spreads and dilutes the spore cloud, and spores are lost through gravitational settling and wash-out by rain.
- iv) Survival during transportation. Detached sporangia are sensitive to drying out (temperature and humidity), but mainly to DNA damage caused by ultraviolet radiation (Mizubuti et al., 2000).
- v) Deposition on susceptible host tissue. Deposition can be broadly classified as one of two types: wet deposition (wash-out by rain), or dry deposition (gravitational settling and inertial impaction). Wet deposition, or deposition

onto a wet surface, greatly increases the chances that the spore will stick (and germinate), whereas dry deposition can lead to rebound and re-entrainment of spores into the atmosphere.

Unfortunately, we can only speculate about the full range of dispersal distances of *P. infestans* sporangia that occur in nature. Quantitative data on dispersal distances that could account for between-field dispersal are practically non-existent in the literature. This is due to the difficulties associated with collection of experimental dispersal data over large spatial scales, and the difficulties of locating and verifying donor fields in the real world. Empirical data on the survival of detached sporangia reveal that most spores are killed within 1 hour on sunny days, but many survive for very long periods on cloudy days (Mizubuti et al., 2000; Sunseri et al., 2002). Such information suggests a wide range of possible dispersal distances. The only study in the literature that provides hard evidence of long-distance dispersal is by Zwankhuizen et al. (1998), who used DNA fingerprinting to establish that infested organic crops led to the dispersal of at least two *P. infestans* genotypes over an area of 25 km² in a period of 2 weeks. In one instance, sporangia of *P. infestans* from a refuse pile were found/inferred to infect potato fields up to 900 m away.

Other means of dispersal include transport of sporangia from one location to another on farm equipment and by wild/farm animals. Many anecdotal stories exist of such occurrences, but these are hard to verify and not thought to be of great importance to potato late blight epidemiology. Of far more importance is the transport of infected seed tubers to other growing areas. As described above, this mode of dispersal has resulted in spatial spread of the pathogen at intercontinental scales.

Management

Cultural

The first step in integrated control is reducing the primary sources of inoculum. This can be achieved by use of healthy, certified seed potatoes. Elimination of potato refuse piles, volunteer potatoes and prevention of formation of oospores are also major components of most late blight management strategies. In organic production systems, field selection and preparation, seed sprouting and selection, plant nutrition and weed control are additional important agronomic practices that contribute to

reduced disease severity. Various crop diversification strategies such as multiline cultivars and cultivar mixtures, and mixing potato varieties with other crop species in row-cropping systems can also significantly reduce disease pressure (Garrett and Mundt, 2000; Mundt, 2002; Andrivon et al., 2003; Pilet et al., 2006).

Host resistance

Plant breeders have been searching for a long time for sources of genetic resistance to *P. infestans* among wild species of potato. In the early 20th century, resistance was found in the Mexican species *S. demissum* and was introduced into potato breeding programs. *S. demissum* was the source of (at least) 11 race-specific resistance (*R*) genes (Turkensteen, 1989). Race-specific (or vertical) resistance is usually highly effective, but often not durable due to selection and build-up of virulent populations of the pathogen. Current potato varieties carry subsets of the 11 *R*-genes (Turkensteen, 1989). The resistance this affords depends on the genotypic composition of *P. infestans* populations in the area of cultivation.

Race-non-specific resistance (partial, horizontal, or field-resistance) against *P. infestans* is believed to be more durable as it “covers all races” of the pathogen. It consists of multiple resistance genes that affect various stages of the disease cycle. This slows down development of disease in the crop, but does not offer complete protection.

Genetic engineering of host resistance is currently a hot topic in plant breeding. There has been much political and public opposition to genetically modified crops, and many genetic engineers have long resented the regulatory procedures imposed on transgenic crop plants. Transgenic plants contain genes from noncrossable organisms (e.g., a selection marker gene originating from a microorganism), synthetic genes or artificial combinations of a coding gene with regulatory sequences, such as a promoter, from another gene (Schouten et al., 2006). In contrast, in the “cisgenic” approach crop plants are modified with one or more genes (containing introns and flanking regions such as native promoter and terminator regions in a sense orientation) isolated from a crossable donor plant. This is the approach adopted by projects such as DuRPH (Sustainable resistance against *Phytophthora* through cisgenic marker-free modification) in the Netherlands (Haverkort et al., *in press*). It is hoped that the DuRPh project and the cisgenic approach will not only contribute to prevention of crop loss and reductions in chemical usage, but also to public acceptance of genetic modification as an acceptable method for plant improvement.

Chemical

Chemical control is still the most important measure used, and many growers anticipate that disease control requires regular applications of fungicides at high rates and short intervals throughout the growing season. Protectant fungicides coat the surface of the plant and are used to prevent infection. Curative and eradicator fungicides penetrate and enter plant tissues and are used to eliminate infection. Desiccants are used to destroy “hot-spots” of infected foliage during the cropping season, and to destroy all above ground foliage prior to harvest. In the Netherlands, anywhere from 7 to 20 applications of protectant fungicides are used in a growing season (Schepers and Spits, 2005). This intensive use of fungicides that now characterizes potato production is not only damaging to the environment, it is often ineffective as *P. infestans* evolves rapidly and often emerges resistant to commercially available pesticides (e.g., Fry and Goodwin, 1997).

Forecasting

The heavy weather dependence of potato late blight has long been used to guide decisions concerning fungicide applications. Several models, or “decision support systems” (DSS) for forecasting potato late blight are available today and are being used in different zones of potato production throughout the world (e.g., Smith, 1956; Ullrich and Schrödter, 1966; Krause et al., 1975; Hansen et al., 1995; Hansen et al., 1996; Hadders, 1998; Nugteren, 2004). DSSs integrate and organize information on the life cycle of *P. infestans*, the weather (historical and forecast), plant growth, fungicides, cultivar resistance, and disease pressure in order to make decisions regarding the need for plant protection products. In The Netherlands, the DSSs ProPhy (Agrovision - Opticrop) and PLANT-Plus (Dacom PLANT Service B.V) are used commercially. In total, about 4,500 Dutch potato growers (36%) use the recommendations of these DSSs; given via PC, internet, e-mail or fax. Moreover, recommendations based on PLANT-Plus reach all Dutch potato growers through an automated telephone service.

Problem statement and research objective

The aerial spread of pathogen inoculum to uninfected hosts is crucial to the epidemic phase of potato late blight. Epidemic development is therefore a spatial process, or more specifically, a combination of spatial processes with length scales ranging from

a few millimeters to several kilometers, or more. Host encounter by dispersing spores is highly dependent on meteorological conditions and the spatial characteristics of crops and landscapes. Variation in meteorological driving forces and heterogeneity in the structure of host populations are therefore of fundamental importance to the epidemic process. The paucity of quantitative data concerning spatial aspects of the disease cycle is testament to the difficulty of conducting experiments at relevant spatial scales, and to the difficulty of unraveling the complex interplay between meteorological and spatial variables. As a result, the spatial dimension of potato late blight epidemiology has been scarcely incorporated into integrated crop protection strategies. It is possible that knowledge of the spatial epidemiology of the pathogen could be used to improve local and regional management of the disease, and reduce the need for fungicide applications.

DSSs play an important role in integrated crop protection, as they serve to rationalize the use of fungicides in potato cultivation. Despite the success and widespread use of these systems, it is important to realize that day-to-day spray advice is formed at the individual plant/field-scale. Little or no consideration is given to the wider spatial environment. Spatial aspects of the disease cycle, such as inoculum dispersal and survival during transportation, are not considered as risk influencing factors and such information has been scarcely used in DSS development. There may be potential to improve operational decision support through the development and inclusion of spatial risk factors for disease. Simulation models are ideally suited to generate information on the spatial epidemiology of late blight. A special challenge is to determine the utility of such an approach. Further challenges exist in the development of this concept as models for atmospheric dispersion processes must be utilized in such a way that a lack of knowledge on the whereabouts of inoculum sources can be overcome.

P. infestans has a high evolutionary potential, by virtue of its effective mixed reproductive system; once a mutation to virulence occurs, it can be “tested” in different environments and recombined into many different genetic backgrounds (McDonald and Linde, 2002). It would therefore be profitable to ascertain how the rate of invasion of resistance breaking genotypes could be minimized, in order to avert crop loss and win time to mount appropriate control action. For instance, landscape design and placement of crops with different resistance genes may be used to such effect. Such spatially informed strategies could serve to minimize the consequences of a breakthrough of resistance, improve the durability of resistance resources, and further reduce the need for chemical applications. With the

anticipated advent of genetically engineered *Phytophthora*-resistant potato varieties, new options for the regional spatial deployment of engineered host resistance emerge. A special challenge here is to combine field-scale epidemiological models with a regional model for the transport of viable inoculum between fields.

The overall aim of this research is to improve insight into the spatial dynamics of *P. infestans* epidemics at the field- and regional-scale, by developing and integrating epidemiological and aerobiological models, and to conduct scenario studies with those models towards the elucidation of options for disease control that make use of spatial “weaknesses” of the pathogen, would these exist.

Outline of the thesis

Chapter 2 describes the development of a spatio-temporal field-scale model of the potato late blight pathosystem. The effects of different scales and patterns of host genotypes on the development of focal and general epidemics are investigated, and three different analytical dispersal functions are compared.

In Chapter 3, extensions to the potato late blight model and laboratory experiments used to determine parameter values are described. Both the spatial and temporal components of the model are evaluated through comparison to real measured epidemics in experimental field plots.

Chapter 4 presents a scenario based simulation approach for evaluating the utility of dispersal information in decision making. Further extensions to the potato late blight model are described, and the yield response of potatoes to incoming inoculum is calculated under a range of disease management scenarios. Model results are used to indicate where use of spatial information in decision support is appropriate, and where it carries greatest risk of economic loss to the farmer.

In Chapter 5 the development and validation of a numerical atmospheric dispersion model is described. A Gaussian plume model is combined with a Lagrangian similarity diffusion model and a source depletion method for spore deposition. The potential of the integrated model for predicting and describing spore transport between fields is investigated through validation against spore dispersal data.

Chapter 6 details the integration of the numerical transport model with a suite of additional aerobiological models, and the MM5 weather forecast model, to create a supplementary spatial component for DSSs. The new system works by modifying the

predictions of existing (non-spatial) DSSs according to the degree of risk of long distance transport of viable inoculum. Field trials are conducted to test the ability of the system to reduce fungicide inputs and maintain control of potato late blight, and results are presented.

In Chapter 7 a fully analytical, partial reflection Gaussian plume model is developed and validated against spore dispersal data. This model is integrated with a suite of additional aerobiological models, a landscape generator, and the field-scale potato late blight model to produce a multi-scale, spatio-temporal epidemic simulator. This modeling framework is then used to investigate various spatial strategies for the deployment of host resistance in agricultural landscapes.

Chapter 8 is a synthesis and discussion of the findings and implications of this study.

References

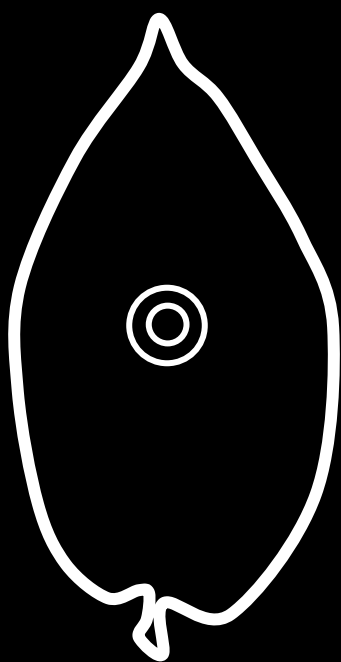
- Abad, Z.G., Abad, J.A., Fernandez-Northcote, E.N., and Ochoa, C. 1995. Host range of *Phytophthora infestans* in central Peru and list in the world since 1840's. Resistance on wild tomatoes. (Abstr). *Phytopathology* 85:1173.
- Adler, N.E., Erselius, L.J., Chacón, M.G., Flier, W.G., Ordoñez, M.E., Kroon, L.P.N.M., and Forbes, G.A. 2004. Genetic diversity of *Phytophthora infestans sensu lato* in Ecuador provides new insight into the origin of this important plant pathogen. *Phytopathology* 94:154-162.
- Andersson, B., Sandstrom, M., and Strömberg, A. 1998. Indications of soil borne inoculum of *Phytophthora infestans*. *Pot. Res.* 4:305-310.
- Andrade-Piedra, J.L., Hijmans, R.J., Forbes, G.A., Fry, W.E., and Nelson, R.J. 2005. Simulation of Potato Late Blight in the Andes. I: Modification and Parameterization of the LATEBLIGHT Model. *Phytopathology* 95:1191-1199.
- Andrивon, D., Lucas, J.M., and Ellisseche, D. 2003. Development of natural late blight epidemics in pure and mixed plots of potato cultivars with different levels of partial resistance. *Plant Pathol.* 52:586-594.
- Aylor, D.E. 1990. The role of intermittent wind in the dispersal of fungal pathogens. *Annu. Rev. Phytopathol.* 28:73-92.
- Beckett, M.C., Daughtrey, M.L., and Fry, W.E. 2005. Temperature and leaf wetness requirements for pathogen establishment, incubation period, and sporulation of *Phytophthora infestans* on *Petunia × hybrida*. *Plant Dis.* 89:975-979.

- Birch, P.R.J., and Whisson, S.C. 2001. *Phytophthora infestans* enters the genomics era. *Mol. Plant Pathol.* 2:257-263.
- Crosier, W.F. 1934. *Studies in the Biology of Phytophthora infestans* (Mont.) de Bary. Cornell University, Ithaca, NY.
- Drenth, A. 1994. Molecular genetic evidence for a new sexually reproducing population of *Phytophthora infestans* in Europe. PhD thesis, Wageningen University, Wageningen, the Netherlands, pp. 150.
- Drenth, A., Janssen, E.M., and Govers, F. 1995. Formation and survival of oospores of *Phytophthora infestans*. *Plant Pathol.* 44:86-94.
- Duncan, J.M. 1999. *Phytophthora* - an abiding threat to our crops. *Microbiol. Today* 26:114-116.
- Erwin, D.C., and O.K. Ribeiro. 1996. *Phytophthora* Diseases Worldwide. St. Paul, Minnesota, APS Press.
- FAO, 2008: <http://faostat.fao.org/default.aspx>
- Flier, W.G., Kessel, G.J.T., Schepers, H.T.A.M., and Turkensteen, L.J. 2002. The impact of oospores of *Phytophthora infestans* on late blight epidemics. In: Lizarraga, C. (Ed.), *Late Blight: Managing the Global Threat*. European Association for Potato Research, pp. 18-22.
- Forbes, G.A., and Landeo, J.A. 2006. Late Blight. In: Gopal, J., and Khurana, S.M.P. (Ed.), *The Handbook of Potato Production, Improvement, and Postharvest Management*. Haworth Press Inc., Binghampton, New York, USA, pp. 279-320.
- Fry, W.E., and Mizubuti, E.S. 1998. Potato late blight. In: Jones, D.G. (Ed.), *The Epidemiology of Plant Diseases*. Luwer Publishers, Dordrecht, Netherlands, pp. 371-388.
- Fry, W.E., and Goodwin, S.B. 1997. Resurgence of the Irish potato famine fungus. *Bioscience* 47:363-370.
- Garrett, K.A., and Mundt, C.C. 2000. Host diversity can reduce potato late blight severity for focal and general patterns of primary inoculum. *Phytopathology* 90:1307-1312.
- Goodwin, S.B., Cohen, B.A., and Fry, W.E. 1994. Panglobal distribution of a single clonal lineage of the Irish potato famine fungus. *Proc. Nat. Acad. Sci., U.S.A.* 91:11591-11595.
- Grünwald, N.J., and Flier, W.G. 2005. The biology of *Phytophthora infestans* at its center of origin. *Annu. Rev. Phytopathol.* 43:171-190.
- Hadders, J. 1998. Experiences with Plant-Plus in 1998. In: Schepers, H.T.A.M., and Bouma, E. (Ed.), *Proceedings of the Workshop on the European network for development of an integrated control strategy of potato late blight*, Uppsala Sweden. PAV Special Report no. 5:194-200.
- Hansen, J.G., Andersson, B., and Hermansen, A. 1995. NEGFY - A system for scheduling chemical control of late blight in potatoes. In: Dowley, L.J., Bannon, E., Cooke, L.R., Keane, T., and O'Sullivan, E. (Ed.), *Phytophthora infestans*. Boole Press Ltd., Dublin, Ireland, pp. 201-208.

- Hansen, J.G., and Andersson, B. 1996. Development and practical implementation of a system for potato late blight forecasting in potatoes. In: Dalezios, N.R. (Ed.), International Symposium on Applied Agrometeorology and Agroclimatology. European Commission, Cost 77, 79, 711, pp. 251-258.
- Harrison, J.G. 1992. Effects of the aerial environment on late blight of potato - a review. *Plant Pathol.* 41:384-416.
- Haverkort, A.J., Boonekamp, P.M., Hutten, R., Jacobsen, E., Lotz, L.A.P., Kessel, G.J.T., Visser, R.G.F., and van der Vossen, E.A.G. 2008. Societal costs of late blight in potato and prospects of durable resistance through cisgenic modification. *Pot. Res.*, *in press*.
- Judelson, H.S., and Blanco, A.B. 2005. The spores of *Phytophthora*: Weapons of the plant destroyer. *Nat. Microbiol. Rev.* 3:47-58.
- Krause, R.A., Massie, L.B., and Hyre, R.A. 1975. BLITECAST: a computerized forecast of potato late blight. *Plant Dis. Rep.* 59:95-98.
- Large, E.C. 1940. The advance of the fungi. Jonathan Cape, London, pp. 488.
- McDonald, B.A., and Linde, C. 2002. Pathogen population genetics, evolutionary potential, and durable resistance. *Annu. Rev. Phytopathol.* 40:349-379.
- Mizubuti, E.S.G., and Fry, W.E. 1998. Temperature effects on developmental stages of isolates from three clonal lineages of *Phytophthora infestans*. *Phytopathology* 88:837-843.
- Mizubuti, E.S.G., Aylor, D.E., and Fry, W.E. 2000. Survival of *Phytophthora infestans* sporangia exposed to solar radiation. *Phytopathology* 90:78-84.
- Mundt, C.C. 2002. Use of multiline cultivars and cultivar mixtures for disease management. *Annu. Rev. Phytopathol.* 40:381-410.
- Nelson, E.C. 1995. The cause of the calamity: the discovery of the potato blight in Ireland, 1845-1847, and the role of the National Botanic Gardens, Glasnevin, Dublin. In: Dowley, L.J., Bannon, E., Cooke, L.R., Keane, T., and O'Sullivan, E. (Ed.), *Phytophthora infestans*. Boole Press Ltd., Dublin, Ireland, pp. 1-11.
- Niederhauser, J.S. 1956. The blight, the blighter, and the blighted. *New York Acad. of Sci.* 19:55-63.
- Niederhauser, J.S. 1991. *Phytophthora infestans* - the Mexican connection. In: Lucas, J.A., Shattock, R.C., Shaw, D.S., and Cooke, L.R. (Ed.), *Phytophthora*. Cambridge University Press, pp. 272-294.
- Nugteren, W. 2004. ProPhy advice in the Netherlands: what's new? In: Westerdijk, C.E., and Schepers, H.T.A.M. (Ed.), Proceedings of the eighth workshop of an European network for development of an integrated control strategy of potato late blight, Jersey, England/France. PAV Special Report no. 10:27-34.
- Oliva, R.F., Erselius, L.J., Adler, N.E., and Forbes, G.A. 2002. Potential of sexual reproduction among host-adapted populations of *Phytophthora infestans sensu lato* in Ecuador. *Plant Pathol.* 51:710-719.

- Pilet, F., Chacón, G., Forbes, G.A., and Andrivon, D. 2006. Protection of Susceptible Potato Cultivars Against Late Blight in Mixtures Increases with Decreasing Disease Pressure. *Phytopathology* 96:777-783.
- Pinckard, J.A. 1942. The mechanism of spore dispersal in *Peronospora tabacina* and certain other downy mildew fungi. *Phytopathology* 32:505-511.
- Schepers, H.T.A.M., and Spits, H.G. 2005. The development and control of *Phytophthora infestans* in Europe in 2004-2005. In: Westerdijk, C.E., and Schepers, H.T.A.M. (Ed.), Proceedings of the Ninth Workshop of an European network for development of an integrated control strategy of potato late blight, Tallinn, Estonia. PAV Special Report no. 11:11-22.
- Schouten, H.J., Krens, F.A., and Jacobsen, E. 2006. Do cisgenic plants warrant less stringent oversight? *Nat. Biotechnol.* 24:753.
- Schumann, G. 1991. Plant diseases: their biology and social impact. The American Phytopathological Society, St. Paul, MN.
- Smith, L.P. 1956. Potato late blight forecasting by 90 % humidity criteria. *Plant Pathol.* 5:83-87.
- Spooner, D.M., McLean, K., Ramsay, G., Waugh, R., and Bryan, G.J. 2005. A single domestication for potato based on multilocus AFLP genotyping. *Proc. Nat. Acad. Sci.* 120:14694-14699.
- Sunseri, M.A., Johnson, D.A., and Dasgupta, N. 2002. Survival of detached sporangia of *Phytophthora infestans* exposed to ambient, relatively dry atmospheric conditions. *Am. J. Potato. Res.* 79:443-450.
- Turkensteen, L.J. 1978. *Phytophthora infestans*: three new hosts and a specialized form causing a foliar blight of *Solanum muricatum* in Peru. *Plant Dis. Rep.* 62:829.
- Turkensteen, L.J. 1989. Interaction of *R*-genes in breeding for resistance of potatoes against *Phytophthora infestans*. In: Fungal diseases of the potato. International Potato Center, Lima, pp. 85-96.
- Ullrich, J., and Schrödter, H. 1966. Das Problem der Vorhersage des Auftretens der Kartoffelkrautfäule (*Phytophthora infestans*) und die Möglichkeit seiner Lösung durch eine "Negativprognose". *Nachrichtenblatt Deutsch. Pflanzenschutzdienst (Braunschweig)* 18:33-40.
- Zwankhuizen, M.J. 1998. Development of potato late blight epidemics: disease foci, disease gradients, and infection sources. *Phytopathology* 88:754-763.

CHAPTER 2



Influence of Host Diversity on Development of Epidemics: An Evaluation and Elaboration of Mixture Theory

P. Skelsey¹, W.A.H. Rossing², G.J.T. Kessel³, J. Powell⁴, and W. van der Werf¹

¹ Wageningen University, Department of Plant Sciences, Crop and Weed Ecology Group, P.O. Box 430, 6709 RZ Wageningen, The Netherlands.

² Wageningen University, Department of Plant Sciences, Biological Farming Systems Group, P.O. Box 9101, 6709 PG Wageningen, The Netherlands.

³ Plant Research International, P.O. Box 16, 6700 AA Wageningen, The Netherlands.

⁴ Department of Mathematics and Statistics, Utah State University, Logan, Utah 84322-3900, USA.

Phytopathology 95:328-338

Abstract

A spatio-temporal/integrodifference equation model was developed and utilized to study the progress of epidemics in spatially heterogeneous mixtures of susceptible and resistant host plants. The effects of different scales and patterns of host genotypes on the development of focal and general epidemics were investigated, using potato late blight as a case study. Two different radial Laplace kernels and a two-dimensional Gaussian kernel were used for modeling the dispersal of spores. An analytical expression for the apparent infection rate, r , in general epidemics was tested by comparison with dynamic simulations. A genotype connectivity parameter, q , was introduced into the formula for r . This parameter quantifies the probability of pathogen inoculum produced on a certain host genotype unit reaching the same, or another unit of the same genotype. The analytical expression for the apparent infection rate provided accurate predictions of realized r in the simulations of general epidemics. The relationship between r and the radial velocity of focus expansion, c , in focal epidemics, was linear in accordance with theory for homogeneous genotype mixtures. The findings suggest that genotype mixtures that are effective in reducing general epidemics of *Phytophthora infestans* will likewise curtail focal epidemics, and *vice versa*.

Additional keywords: crop arrangement, dispersal kernels, genotype mixtures, *Solanum tuberosum*.

Introduction

Modern agricultural practices have resulted in a decline in crop diversity and an increase in genetically and spatially uniform plant populations. This lack of host diversity can lead to an escalation in the frequency and severity of epidemics. Conversely, many natural ecosystems are less prone to severe epidemics, due to the diversity of host genotypes and their patchy distribution (Andrивon et al., 2003). Spatial diversification of host resistance therefore appears as an important approach in the effort to achieve successful and sustainable management of crop pathogens. Applications of this approach have included inter- and intra-specific diversity (Jensen, 1952; Borlaug, 1958; Zadoks, 1958; Zadoks, 1959; Groenewegen and Zadoks, 1979; Wolfe, 1985) both within fields, e.g., alternate strips or rows, and between fields, e.g., cultivar rotation and mosaic cropping.

The potential of genotype mixtures to slow down or prevent epidemic development has been established through the use of computer simulation (Kampmeijer and Zadoks, 1977; Mundt and Leonard, 1986a,b; Mundt et al., 1986; Mundt and Brophy, 1988) and by experimentation (Robinson, 1976; Jeger et al., 1983; Mundt and Browning, 1985; Mundt and Leonard, 1985; Wolfe, 1985; Panse et al., 1989; Mundt et al., 1996; Garrett and Mundt 2000; Zhu et al., 2000; Garrett et al., 2001; Andrивon et al., 2003). Three factors account for disease reduction in genotype mixtures: (i) the dilution of inoculum due to the presence of resistant plants (lack or reduction of inoculum production on resistant plants, and loss of inoculum infectious to susceptible hosts as a result of spore deposition on resistant plants); (ii) the physical barrier to successful deposition created by the resistant plants; and (iii) the potential for induced host resistance when propagules are deposited on a neighboring plant for which they are avirulent (Garrett and Mundt, 1999). With regard to the spatial arrangement of genotypes within a mixture, the ground-area of individual genotype units (genotype unit area) is an important configuration variable influencing epidemic development (Barrett and Wolfe, 1980; Mundt and Browning, 1985; Mundt and Leonard, 1985; Mundt and Leonard, 1986b, Mundt et al., 1986). A genotype unit is defined as a spatially delineated unit of space planted with a single host genotype. A genotype unit can therefore refer to a single plant, a row or patch of plants of the same genotype, or an entire field as in a monoculture.

The rate of progress of epidemics that develop from initial blanket infections originating from large external sources of inoculum (general epidemics) can be characterized by the apparent infection rate, r (day^{-1}) (e.g., Powell et al., 2005). The

apparent infection rate is therefore a good candidate parameter for describing the impact of spatial configuration in a genotype mixture upon the development of the disease in the field. The parameter r can be approximated by utilizing the theory of age-structured populations (e.g., Keyfitz, 1985), whereby the apparent infection rate is related to the net lifetime reproduction (average number of daughter lesions produced per mother lesion) and the generation time (average time between birth of an individual and birth of its offspring); see also Segarra et al. (2001).

For epidemics that develop from an initial point of infection (focal epidemics), the radial velocity of focus expansion, c (m day^{-1}), can be used to describe the impact of spatial variation upon disease progress. According to theory (Van den Bosch et al., 1988a-c; 1990), focal expansion reaches a constant velocity after an initial phase of focus build-up. This rate has been shown (in theory) to increase linearly with the logarithm of the fraction of susceptible plants in ideal mixtures of susceptible and resistant cultivars. This relationship has been confirmed experimentally in the field for stripe rust (*Puccinia striiformis*) on wheat (*Triticum aestivum*) (Van den Bosch, 1988a) and for bean rust (*Uromyces appendiculatus*) on bean (*Phaseolus vulgaris*) (Assefa et al., 1995). An ideal mixture is infinitesimally fine-grained. In practice, ideal mixing is approximated when the spore cloud around a lesion on a plant encompasses a large number of other susceptible plants. An ideal mixture can therefore often be approximated in the field through random seed mixing prior to planting, provided that the pathogen spreads its propagules over distances well exceeding the plant and row distances of the crop.

For the potato late blight pathosystem (*Phytophthora infestans* - *Solanum tuberosum*), the relatively large size of potato plants, as the smallest genotype unit possible, can result in high levels of autoinfection (Scherin, 1996), defined as infection caused by a propagule from within the same genotype unit. The radial expansion of lesions further increases the extent of autoinfection, suggesting a somewhat negative outlook on the potential of genotype mixtures to control *P. infestans*. However, recent experimental studies (Garrett and Mundt, 2000; Garrett et al., 2001; Andrivon et al., 2003) indicate that increased host-diversity can contribute to a reduction of disease progress. There is evidence for a potentially beneficial effect of host diversity in reducing potato late blight in temperate regions such as France (Andrivon et al., 2003) and the United States (Garrett and Mundt, 2000), where late blight epidemics tend to develop from obvious foci. Recent experiments conducted by Andrivon et al. (2003) suggest that part of the mixture effect might be due to differences in the spatio-temporal pattern of disease spread,

with disease progressing mainly along the rows in mixed-cultivar plots (lines of least resistance) as opposed to spatial spread in direct correspondence with the mean wind direction. This new evidence indicates the need for further research into the effects of patch size, shape, and distribution (crop arrangement) on the development of epidemics in genotype mixtures of potato. However, recent field studies by Garrett et al. (2001) suggest that the results of studies into host-diversity effects on potato late blight from temperate regions cannot be extrapolated to humid, tropical regions where general epidemics are commonly observed and success in the use of genotype mixtures has been variable. A hypothesis has been proposed that the level of outside inoculum is an important factor driving the magnitude of host-diversity effects, and that lower amounts of outside inoculum generally improve the efficacy of mixtures against potato late blight (Garrett et al., 2001).

The primary objective of this paper is to determine whether predictions on the effect of genotype mixing in homogeneous mixtures hold also in non-ideal mixtures. A non-ideal mixture is defined here as having a coarser grain than an ideal mixture, i.e., there is a level of aggregation of matching genotypes, e.g., into rows or blocks. A spatio-temporal modeling framework is developed to run disease scenarios for general and focal epidemics in non-ideal genotype mixtures at different scales and patterns and deduct from these simulations predictive relationships regarding the use of genotype mixtures in non-ideal configurations. The model is parameterized for potato late blight. As disease epidemics occur in both large and small-scale production systems around the world, we develop a theoretical framework for evaluating effects of host-diversity that encompasses both general and focal epidemics. This will provide theoretical support for future experimental research efforts aimed at developing globally applicable management strategies based on diversified landscapes/mosaics. The secondary objectives of this paper are as follows: (i) investigate theories relating to the importance of crop arrangement in the use of genotype mixtures for disease suppression; (ii) assess the effects of crop arrangement and different descriptions of dispersal on the growth rate parameters, r and c ; (iii) develop a method for predicting trends in r and c in non-ideal mixtures; (iv) investigate the potential use of r as a predictor of c ; and (v) develop an approximation formula for r .

Theory and approaches

Theoretical framework

Epidemics may be classified on a scale ranging from focal to general, depending on the extent of primary infections. Following the groundbreaking work on ideal genotype mixtures by Van den Bosch et al. (1988a-c; 1990), temporal progress in focal epidemics may be characterized by the radial velocity of focus expansion, c . According to the theory, c approaches a constant value after an initial phase of focus build-up. Van den Bosch et al. (1990) showed that the rate c in monocultures can be approximated as:

$$c = a \ln(R_0) + b \quad (1a)$$

where R_0 (-) is the net lifetime reproduction, defined as the average number of offspring per mother, and a and b are parameters. Table 1 provides a summary of symbol definitions and dimensions.

For ideal cultivar mixtures, equation 1a is changed to include f (-), the fraction of susceptible host plants in the mixture (Asefa et al., 1995):

$$c = a \ln(f R_0) + b \quad (1b)$$

As the mixing of susceptible and resistant plants is assumed to occur at a very fine grain ("ideal mixture"), net lifetime reproduction within a mixture can be equated to the product of the net lifetime reproduction of a population of only susceptible individuals and the fraction of susceptible plants.

The apparent infection rate, r , is a frequently used measure of temporal progress of general epidemics. This apparent infection rate is a parameter in the logistic growth equation (e.g., Zadoks and Schien, 1979), and may be estimated from a time series of disease progress after logit transformation of severity (Berkson, 1944):

$$\text{logit}(X) = rt + C \quad (2)$$

where X (-) is disease severity on a scale from 0 to 1, t (days) is time and C is $\text{logit}(X_0)$, with $\text{logit}(X) = \ln(X/(1-X))$. Another way of conceptualizing r is offered by life history theory, whereby r is related to R_0 and to generation time T (days), the average age of the mother at birth (Keyfitz, 1985; Gotelli, 1998):

$$r \approx \frac{\ln(R_0)}{T} \quad (3)$$

Table 1. Symbols used in this study

Symbol	Units	Description
A	m^2	Total area of the landscape
A_L	m^2	Area of a lesion
A_p	m^2	Area of a plant
c	$m \text{ day}^{-1}$	Radial velocity of focus expansion
f	$-^a$	Fraction of susceptible host plants in the mixture
H	-	Heaviside function
K	m^{-2}	Dispersal kernel: probability distribution of dispersal distances
LAI	-	Leaf area index
N_t	#	Number of infected plants
q	-	Genotype connectivity
Q_t	m^2	Area of infected plant material
r	day^{-1}	Apparent infection rate
r_1	day^{-1}	Approximation formula for the apparent infection rate
r_2	day^{-1}	Approximation formula for the apparent infection rate
R	m	Radius of a leaflet
R_f	m	Focal radius
R_L	m	Radius of a lesion
R_0	-	Net lifetime reproduction
s	$\# m^{-2}$	Density of spores
S	#	Total spore production on a leaflet
t	days	Time
T	days	Mean generation time: average time between birth of an individual and birth of its offspring
x	m	Coordinate
X	-	Disease severity: overall proportion of diseased tissue on the susceptible genotype
y	m	Coordinate
α	m^{-1}	Steepness of disease gradient
δ	-	Deposition efficiency
ϑ	m	Standard deviation in the two-dimensional Gaussian kernel
ι	-	Infection efficiency
I	days	Infectious period
κ	-	Disease severity threshold
λ	days	Latent period
μ	days	Mean of the entire sporulation curve
μ_d	m	Mean dispersal distance
π	-	Mathematical constant
ρ	$m \text{ day}^{-1}$	Radial growth rate of lesions
ρ_m	$m \text{ day}^{-1}$	Cultivar specific potential radial lesion growth rate
σ	$\# m^{-2}$	Sporulation intensity (per unit of infectious leaf area)
σ_c	days	Standard deviation of the entire sporulation curve

^a - signifies that the defined quantity is dimensionless.

For ideal mixtures, R_0 is replaced by fR_0 , similar to equation 1b. It follows from equation 1a and equation 3 that there must be a linear relationship between c and r .

In this paper, we move from ideal mixtures of susceptible and resistant plants to mixtures in arbitrary spatial configurations. The primary mechanism driving epidemic dynamics in time and space is successful propagation, which in turn depends on the spatial arrangement of the host population. We hypothesize that for such cases net lifetime reproduction within the mixture depends on both the fraction of susceptibles and on their spatial configuration and we summarize these two effects in a new parameter q (-), the genotype connectivity. In landscape ecology, connectivity generally refers to the spatial connectedness of like habitat units in a landscape, as it affects the influence of landscape structure on the ability of an organism to move through the landscape (Merriam, 1984). An increasing interest in connectivity research has led to a proliferation of connectivity measures; see Tischendorf and Fahrig (2000). However, what constitutes a spatial connection between genotype units clearly depends on the application or process of interest; genotype units that are connected for insect dispersal are not necessarily connected for pathogen dispersal. It is therefore apparent that spatial connectivity must be assessed with consideration for the nature and scale of the interaction between the organism of interest and the landscape. The parameter q expresses the overall probability that a propagule produced in a susceptible genotype unit in the field (or landscape), when dispersed according to the dispersal kernel, will be deposited within (upon) a susceptible genotype unit (whether the same unit or another unit). In an ideal mixture, $q = f$. For any spatially heterogeneous mixture, q can be calculated by taking into account the dispersal kernel of propagules and the spatial pattern and scale of genotype units. Let $s(x,y)$ express the density of spores at location (x,y) ; $s(x,y)$ is 1 m^{-2} if the genotype is susceptible and 0 m^{-2} otherwise. Inoculum dispersal from a source at location $(0,0)$ is described by a kernel (normalized to a volume or probability mass under the kernel of 1), denoted by $K(x,y)$. Let (x',y') denote source locations, and (x,y) target locations. Then we can write:

$$q = \frac{\int \int_{x,y} H(s(x,y)) \int \int_{x',y'} s(x',y') K(x-x',y-y') dy' dx' dy dx}{\int \int_{x',y'} s(x',y') dy' dx'} \quad (4)$$

where H is the Heaviside function, which is 1 when its argument is greater than 0, and 0 otherwise. The interpretation is that the top integral measures the total number of

spores produced by susceptibles, which when dispersed fall on a susceptible plant, and the bottom integral measures the total number of spores produced by susceptibles. Parameter q is therefore the probability that the spores produced will land on a susceptible genotype; q expresses connectivity between genotypes. In ideal mixtures, q equals f , but in non-ideal mixtures with large genotype units and a high degree of autoinfection within genotype units, q will tend to unity. In general: $f \leq q \leq 1$. As the area of all the susceptible genotype units in the landscape is fA , where A (m^2) is the total area of the landscape, the above equation can be simplified to:

$$q = \frac{1}{fA} \int \int_{x,y} H(s(x,y)) \int \int_{x',y'} s(x',y') K(x-x',y-y') dy' dx' dy dx \quad (5)$$

To investigate these hypothesized relations a spatio-temporal model of the potato late blight pathosystem was constructed.

Development of a spatio-temporal potato late blight model

A spatially explicit age-structured integrodifference equation (IDE) model was developed to simulate general and focal epidemics of *P. infestans*, and to explore the effect of heterogeneous genotype mixtures on the two parameters characterizing the rate of spread in both situations: r and c . IDEs are the spatially explicit equivalent of difference equation models. They are discrete-time, continuous-space models for the growth and spread of biological populations. As noted by Neubert et al. (1995): "IDEs contain two components: (i) difference equations, which model growth and interactions during a sedentary stage and, (ii) redistribution kernels, which characterize movement during a dispersal stage." Often, IDEs are used to describe populations with discrete, non-overlapping generations, but in this model the IDE approach is applied at a daily time step to an age-structured population of expanding lesions. This facilitates the simulation of overlapping lesion generations.

Space is described as a two-dimensional grid, in which each cell represents a potato plant that is either susceptible or resistant to *P. infestans*. In addition to its coordinates, each cell is characterized by state variables describing the number of lesions and their associated radius in age classes of 1 day. All other variables are derived from these basic state variables. The equations describing the number and area dynamics of lesions for each plant are based on the following principles. Every day there is a new generation of lesions and these belong to the same age class. Lesions are latent during the first λ days of their existence, the latency period, which was set at 5 days based on the popular Dutch variety "Bintje" (Flier and Turkensteen,

1999). Concomitant to development, the lesion grows radially. It is assumed that the center part of a lesion becomes infectious at lesion age $(\lambda + 1)$ day. Infectiousness of a segment of leaf area is taken to last 1 day. During each successive day, as another annulus of daily radial growth reaches age $(\lambda + 1)$ day, this annulus will sporulate. Spore production per unit of infectious leaf area is accounted for by the parameter σ (set at 10^8 m^{-2}). A recent paper by Berger et al. (1997) indicates the importance of lesion expansion as an epidemic component in polycyclic epidemics. In this model, the lesion growth rate on a particular plant, ρ (m day^{-1}), is area-limited, i.e., there is a limit to lesion expansion due to competition:

$$\rho = \rho_m(1 - X) \quad (6)$$

where ρ_m (m day^{-1}) is a cultivar specific potential lesion growth rate and X is disease severity, the fraction of the host plant that is either latently infected, infectious or removed. Thus, lesion size is restricted by the leaf area per plant as opposed to the leaf area per leaflet. A limit to lesion expansion due to the size of an “average” leaflet was removed from the model as model outputs were found to be insensitive to this parameter. This is in agreement with analysis of a Leslie matrix model by Powell et al. (2005), which shows that a leaflet restriction is not important in the calculation of the apparent infection rate.

For each individual potato plant, the model thus keeps track of the number and radius of lesions of all age classes and calculates the number of new lesions per plant at each time step. The areas of latent, infectious and dead lesion area on each host plant are calculated by multiplying the annuli of lesions in the appropriate age category with their respective areas, and summing over all lesions. The age-structured population model for lesions on each plant is updated daily, by “aging” the existing lesions by 1 day, and starting new lesions at a rate calculated as the product of: (i) the number of landed spores per m^2 leaf area in a day; (ii) the infection efficiency, ι (-), and (iii) fraction of area not yet occupied by *P. infestans*, $(1-X)$. No calculations are made involving individual lesions.

Dispersal

Host plants are linked through dispersal of spores. Ecological data on short-range dispersal of *P. infestans* are available (Paysour and Fry, 1983). We described where spores land with dispersal kernels, which describe the probability distribution of landing locations of spores in the two-dimensional plane. Spores were dispersed according to a radial Laplace kernel:

$$K(x,y) = \frac{\alpha^2}{2\pi} \exp\left(-\alpha\sqrt{x^2 + y^2}\right) \quad (7)$$

or a radial Gaussian kernel:

$$K(x,y) = \frac{1}{2\pi\vartheta^2} \exp\left[-\left(\frac{x^2 + y^2}{2\vartheta^2}\right)\right] \quad (8)$$

In the Laplace kernel, α (m^{-1}) is a factor describing disease gradient steepness, while ϑ (m) represents the standard deviation in the two-dimensional Gaussian kernel. The positions x and y are distances from the source plant, and $K(x,y)$ is the probability density at location (x,y) . Both dispersal kernels describe the net results of aerial dispersal of spores in time coupled with precipitation to the ground.

The radial Laplace and the radial Gaussian kernels can be compared in terms of the mean dispersal distance, μ_d (m), in the plane, i.e., the mean distance traveled by spores. For a radial Laplace kernel $\mu_d = 2/\alpha$, whereas for a radial Gaussian kernel $\mu_d = \vartheta\sqrt{\pi/2}$. We used three dispersal kernels in simulation experiments (Fig. 1). Two of these are radial Laplace kernels, parameterized with data from Paysour and Fry (1983) for dispersal of spores of *P. infestans*, yielding $\alpha = 0.82 \text{ m}^{-1}$ in non-irrigated potatoes and $\alpha = 2.1 \text{ m}^{-1}$ in irrigated potatoes. The associated mean dispersal distances are $\mu_d = 2.44 \text{ m}$ in non-irrigated potatoes and $\mu_d = 0.95 \text{ m}$ in irrigated potatoes, providing a “wide Laplace kernel” and a “narrow Laplace kernel” respectively. A radial Gaussian kernel was included in order to investigate the sensitivity of model outcomes to a differently shaped kernel (thinner tails) for the same μ_d . The value of ϑ for the Gaussian kernel was 1.95 m, yielding the same value for μ_d as the radial Laplace kernel for non-irrigated potatoes, i.e., 2.44 m.

Solution and Implementation

The integrodifference equation (IDE) model was implemented in MATLAB Version 5.3.0.10183. Spatial phenomena in the model are solved by performing convolutions between spatial distributions of spores and dispersal kernels. Convolutions are implemented in the model via fast Fourier transforms; a technique that greatly enhances the speed and accuracy of the numerical solution of the model. Spatial distributions (i.e., a kernel and a distribution of spores) are transformed into the Fourier domain, multiplied, and the result is back-transformed into the spatial domain, giving the spatial distribution of dispersed spores. This solution method

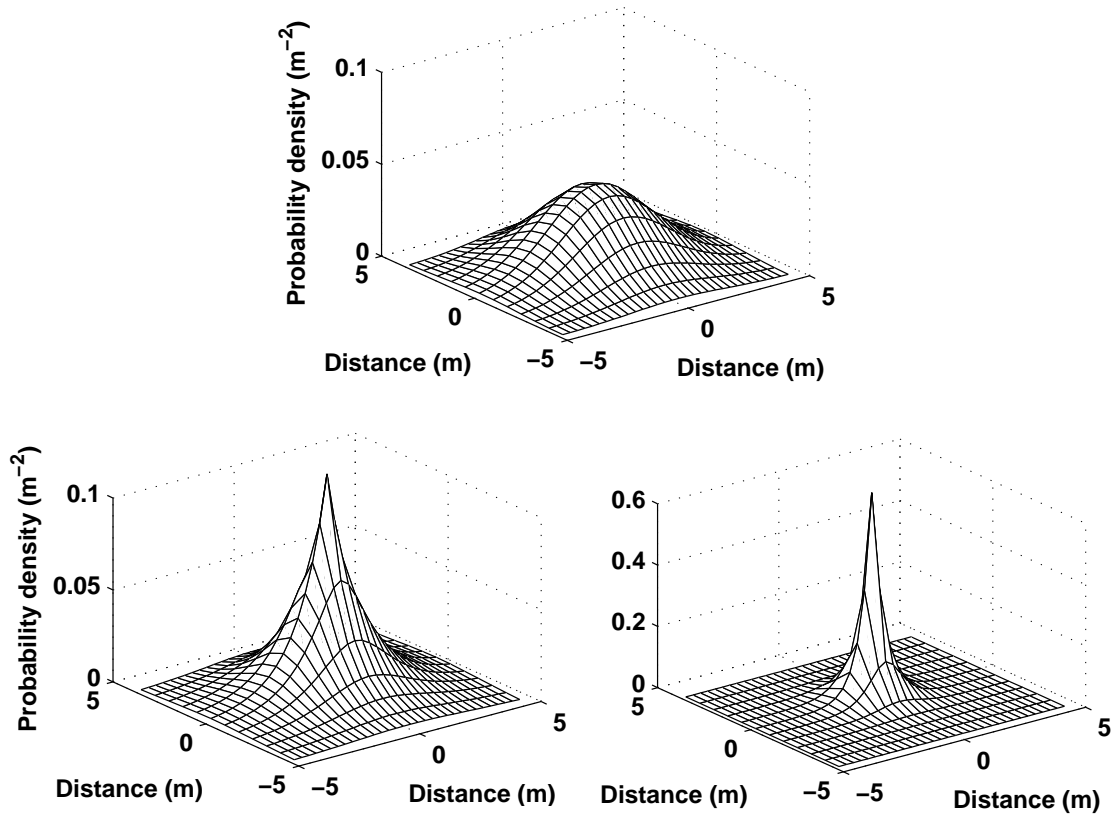


Fig. 1. Dispersal kernels describing the probability distributions of landing locations of spores around the source in the two-dimensional plane, as used in model simulations of potato late blight. Top = Gaussian; bottom left = wide Laplace; and bottom right = narrow Laplace, with mean dispersal distances of 2.44, 2.44 and 0.95 m respectively.

requires periodic boundary conditions, therefore Fourier domain arrays are duplicated an infinite number of times to the left, right, top and bottom. This means that each edge of the array is connected to the opposite edge of an identical array. This leads to “wrap-around” effects, or toroidal symmetry, whereby any spore dispersing outside of the field’s borders will “reappear” on the opposite edge of the field when spatial distributions are back-transformed into the spatial domain. Thus, the simulated domain should be interpreted as a “window” on an infinite repetition of identical windows contiguously over space.

Simulation

As a result of the solution methodology, each field we define in our simulation experiments is not an isolated “island,” but is part of, and is influenced by, a larger virtual environment. Furthermore, any spore that leaves the edge of the field and then reappears on the opposite edge is assumed to be from a distant source of

inoculum, i.e., a neighboring or distant potato field. This provides a representation of general epidemics of potato late blight in dense potato growing regions, where background inoculum levels can be high. For the simulation of general epidemics in isolated fields, spatial distributions are “zero-padded” with a large border of “non-host” space prior to convolution. Spores that are redistributed by the kernel into the non-host space are lost from the system and do not contribute to epidemic development. This prevents wrap-around effects and facilitates spore loss from the simulated domain. In this case the simulated domain can be thought of as a window onto an infinite repetition of identical, isolated genotype mixtures (padded mixtures). For the simulation of focal epidemics, we assume that the initial inoculum is from a smaller, local source, e.g., a volunteer plant, and that the influence of the larger virtual environment can be ignored. As an alternative to zero-padding, all focal simulation experiments are simply stopped long before the focus, or any spores, can reach the field edges, therefore wrap-around effects do not interfere with focal expansion.

In the simulation of general epidemics, a simulation time of 15 days was sufficient to reach a disease severity level of approximately 40 % and make robust estimates of r using equation 2. The length of each simulation for the focal simulation experiments was determined by a need for sufficient focus build-up with which to gain a reliable calculation of c , but also prevention of significant travel of spores over the field boundaries (and wrap-around effects). Simulation times were chosen appropriate for the dispersal kernel used and were derived by measuring the time taken to reach a final disease severity of 20 % in a pure-line susceptible population, under each dispersal kernel. This ensured that focus expansion was stopped sufficiently early in each field. The resultant simulation times were 34 days for the wide Laplace kernel, 54 days for the narrow Laplace kernel and 37 days for the Gaussian kernel.

Based upon planting patterns in the Netherlands, the length of the side of a compartment cell was set at 0.75 m (distance between rows) and the width of each compartment cell at 0.3 m (distance between plants). The growth of the host plant was not considered in this model therefore leaf area index (LAI , -) was held constant at a value of 5. This is approximately the maximum LAI that a potato crop can reach and was used to represent a well-developed potato crop in prime condition. We assume perfect weather conditions for late blight development therefore other variables held constant include: $\lambda = 5$ days, $l = 1$ day, $\rho = 0.004 \text{ m day}^{-1}$, $\iota = 0.01$ and $\sigma = 10^8 \text{ m}^{-2}$. These are estimates (averages) as found in the Netherlands (Flier and

Turkensteen, 1999). In the absence of any information in the literature, an estimate of 0.1 was used for the deposition efficiency, δ (-); defined as the proportion of redistributed spores “captured” by encountered foliage.

Data analysis

Disease severity, X , was derived by calculating the overall proportion of diseased tissue on the susceptible genotype. In all simulation experiments for general epidemics, progress of disease was expressed as r , the potential apparent infection rate that was estimated by linear regression of logit (X) versus time (equation 2) as simulated with the IDE model.

The radial velocity of focus expansion, c , was calculated as the slope of the linear regression of the calculated focus radius on time. Focal radius, R_f (m), was derived by first calculating the crop area infected. This was determined by counting the number of plants with a disease severity greater than a threshold of 1 % (κ), multiplying this number by the area of a plant, and dividing the result by the fraction of susceptible host plants in the mixture:

$$Q_t = \frac{N_t A_p}{f} = \text{area covered by focus} = \pi R_f^2 \quad (9)$$

where Q_t (m^2) is the area infected at time t , N_t is the number of infected plants above the severity threshold κ , A_p (m^2) is the ground area of a plant, and f is the fraction of susceptibles in the mixture. Rewriting equation 9 to make R_f the subject gives:

$$R_f = \sqrt{Q_t / \pi} \quad (10)$$

Radius calculations prior to day 25 were not used in order to avoid distortion of the final statistic created by the initial phase of focus build-up.

For focal epidemics in a non-ideal mixture, the spread of the focus can be restricted by the spatial configuration of the host plants, and thus non-circular foci can occur, e.g., spread of disease along the length of an isolated row. In such cases there would be benefit to measuring spread velocity in several different compass directions; however, the area metric described above is sufficient to describe the impact of crop arrangement on the expansion of disease foci as it represents an average radial expansion over time.

There is evidence for an increasing frontal velocity when larger spatial scales are considered; the theory of turbulent diffusion suggests that spread could become more efficient as the focus expands (Ferrandino, 1993, Scherm, 1996; Mundt, 2002).

However, a constant c is an emergent property of this model and as this model operates at the field-scale, it gives a realistic description of the life cycle of the pathogen and a realistic description of short-scale dispersal.

Importance of scale in the use of genotype mixtures for disease suppression

Pioneering simulation and experimental work (Barrett and Wolfe, 1980; Mundt and Browning, 1985; Mundt and Leonard, 1985; Mundt and Leonard, 1986a,b; Mundt et al., 1986) revealed the importance of crop arrangement, in particular the genotype unit area, in the effectiveness of genotype mixtures for disease control. However, the results of further simulation studies by Mundt and Brophy (1988) suggested that the number of host genotype units in a population is a more important determinant of the effectiveness of mixtures for disease control than is the genotype unit area. In order to investigate this conjecture, we tested the following null hypothesis: the size of the field (window) will not affect model results. The null hypothesis was tested by exploring the effects of increasing the number of genotype units in a field, whilst maintaining the proportion of susceptible crop and its spatial configuration. Mundt and Brophy (1988) simulated potato late blight epidemics in mixtures that were surrounded by non-host space and isolated from external sources of inoculum but in this study we will test this null hypothesis by simulating epidemics in mixtures that are isolated from outside inoculum (padded mixtures), and in mixtures that are part of an inter-connected network of like fields (unpadded mixtures). Individual host plants of a genotype unit area of 0.225 m^2 ($0.3 \times 0.75 \text{ m}$) were first arranged in a 1:4 mixture (25 % susceptible) with an area of 3.6 m^2 ($1.5 \times 2.4 \text{ m}$) (Fig. 2A). This area was successively quadrupled to give identical mixtures in terms of the configuration and proportion of susceptible host plants, but with areas of 14.4 m^2 ($3 \times 4.8 \text{ m}$), 57.6 m^2 ($6 \times 9.6 \text{ m}$), 230.4 m^2 ($12 \times 19.2 \text{ m}$), 921.6 m^2 ($24 \times 38.4 \text{ m}$), and 3686.4 m^2 ($48 \times 76.8 \text{ m}$) respectively (Fig. 2B-F). In order to simulate epidemic development in fields that are isolated, each of the defined mixtures was zero-padded with a large border of non-host plants. In order to simulate the influence of a larger network of host fields on epidemic development, two further simulation experiments were devised, whereby the border of non-host space around the two largest padded mixtures previously defined was removed to give an infinite repetition of identical genotype mixtures contiguously over space (Fig. 2G-H). Only the two largest mixtures were used, as smaller landscapes result in a small number of coefficients in the Fourier transform, which may not be enough to represent the functions adequately.

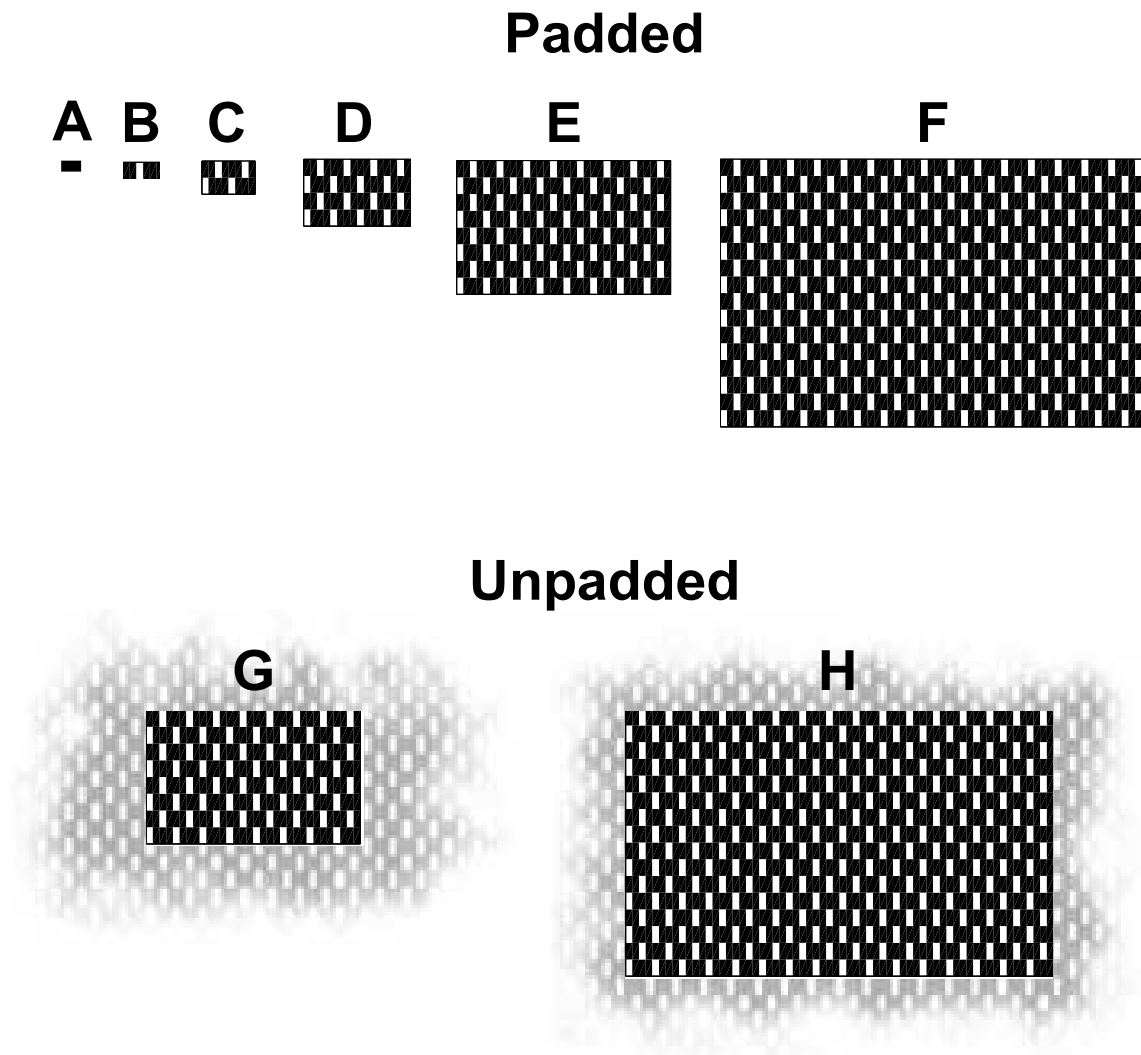


Fig. 2. Genotype mixtures used to study the effect of number of genotype units on the behavior of simulated potato late blight epidemics. White blocks represent plants susceptible to *Phytophthora infestans* and black areas represent resistant plants. Field dimensions are: 1.5 x 2.4 m (A), 3 x 4.8 m (B), 6 x 9.6 m (C), 12 x 19.2 m (D), 24 x 38.4 m (E), 48 x 76.8 m (F), 24 x 38.4 m (G), and 48 x 76.8 m (H) – providing areas of 3.6 m² (A), 14.4 m² (B), 57.6 m² (C), 230.4 m² (D), 921.6 m² (E), 3686.4 m² (F), 921.6 m² (G), and 3686.4 m² (H) respectively. Patterns A-F are “zero-padded” with a large border of non-host plants, isolating them from the influence of a larger virtual environment. Fields G-H have no border of non-host space and are influenced by a larger virtual environment. Genotype unit area is held constant at 0.3 x 0.75 m, providing (A-H), 4, 16, 64, 256, 1024, 4096, 1024, and 4096 susceptible genotype units respectively. The fraction, f (-), of susceptible host plants in the population is held constant at 0.25. Genotype units for patterns A-H are rectangular as the distance between rows is 0.75 m whilst the distance between plants is 0.3 m. The number of genotype units shown in each pattern has been decreased to enhance clarity.

General inoculation in each experiment proceeds with the allocation of 1 cm² of infectious tissue to each host plant. This gives an initial disease severity of approximately 0.01 %. Spore dispersal was provided by the wide Laplace kernel. The disease severities reached in each genotype mixture were then compared with those of pure-line susceptible populations of the same size to provide relative disease severity ratings.

Effect of crop arrangement and dispersal kernel on r and c

In order to investigate the effects of altering the configuration and density of susceptible genotype units on r and c in non-ideal mixtures, two further sets of simulation experiments were devised. General epidemics were simulated in the first set of experiments and focal epidemics were simulated in the second set. In both sets of simulation experiments, we assume that the genotype mixtures are part of a larger inter-connected network of like fields, therefore unpadded mixtures are defined. In each set, block and row patterns with genotype unit areas of 0.3 x 0.75 m and 76.8 x 0.75 m respectively were generated for four different fractions, f , of susceptibles in the genotype mixtures: 0.125, 0.25, 0.5 and 1 (Fig. 3). Thus, identical mixture compositions were used in each set of simulation experiments. The different f values were created by doubling the number of susceptible units in a mixture with each successive f category and locating the new susceptible units equidistantly between the old units. The genotype unit areas were held constant throughout at the aforementioned values. The size of the field remained fixed throughout at 76.8 x 48 m. General inoculation proceeded as above with the allocation of 1 cm² of infectious tissue to each host plant, whilst focal inoculation proceeded with the allocation of 1 cm² of infectious tissue to each of the central nine host plants. In order to gain insight into the effects of different dispersal kernels on our results, each individual simulation experiment outlined in this section was repeated for each of the three dispersal kernels described in the dispersal section.

Parameter q as a predictor of r and c

For the set of general simulation experiments outlined in the previous section, r was plotted against $\ln(q)$ to investigate if q could provide reliable predictions of crop arrangement on the progress of disease, in a similar manner as the rate of focus expansion, c , is linearly related to $\ln(f)$ (Van den Bosch et al., 1990). The same procedure was then repeated for the set of focal simulation experiments; c was

plotted against $\ln(q)$ to investigate if q could predict or characterize the impact of crop arrangement on the progress of disease in focal epidemics.

Parameter r as a predictor of c

In order to develop a theoretical framework for host-diversity that incorporates both general and focal epidemics, it is necessary to determine whether the results of studies into host-diversity effects on potato late blight from temperate regions can

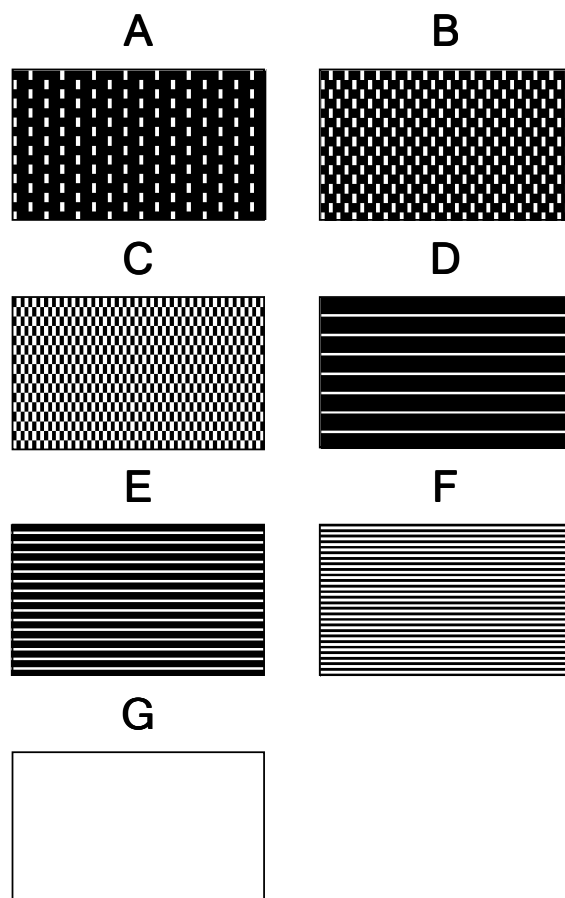


Fig. 3. Genotype mixtures used to study the effect of spatial configuration and fraction, f (-), of susceptible host plants on the behavior of simulated potato late blight epidemics. White blocks represent plants susceptible to *Phytophthora infestans* and black areas represent resistant plants. f values are: 0.125 (A&D), 0.25 (B&E), 0.5 (C&F), 1 (G). The size of the field is held constant at 76.8 x 48 m. Genotype unit areas are: 0.3 x 0.75 m (A-C), 76.8 x 0.75 m (D-F), and 76.8 x 48 m (G) - providing 2048, 4096, 8192, 8, 16, 32, and 1 susceptible genotype units respectively. Genotype units for patterns A-C are rectangular as the distance between rows is 0.75 m whilst the distance between plants is 0.3 m.

be extrapolated to humid, tropical regions. The hypothesized relationship between the two emergent measures of epidemic development, r and c , was investigated by regressing radial velocity calculations against the apparent infection rates in corresponding genotype mixtures.

Approximation formulae for r

In addition to calculation of r based on simulation results, life table analysis for lesions was used to predict the value of r . This analysis is based on an original idea of Spijkerboer (2004). A predictive estimate of r has been derived from q and equation 3, based on the following components: the genotype connectivity, q , the sporulation intensity, σ , the deposition efficiency, δ , the infection efficiency, ι , the radius of a leaflet, R , the latency period, λ , the potential radial growth rate of a lesion, ρ_m , and time, t . The radius of a lesion, R_L (m), is calculated as follows:

$$R_L = \rho_m t \tag{11}$$

in which it is assumed that $R_L = 0$ at $t = 0$ and only one infection occurs on the leaflet at $t = 0$. So, restriction of lesion expansion due to competition for space (equation 6) does not need to be taken into account. It therefore follows that the area of a lesion, A_L (m²), is given by the equation:

$$A_L = \pi R_L^2 = \pi(\rho_m t)^2 = \pi \rho_m^2 t^2 \tag{12}$$

The rate of change of lesion area over time is therefore given by the equation:

$$\frac{dA_L}{dt} = 2\pi \rho_m^2 t \tag{13}$$

Total spore production on a leaflet, S (#), is now written as:

$$S = \int_{\lambda}^{\lambda + \frac{R}{\rho_m}} 2\pi \sigma \rho_m^2 (t - \lambda) dt = \sigma \pi R^2 \tag{14}$$

where R was derived from an average leaflet area of 11 cm², approximating the size of small leaflets. The generation time T (days) can now be written as:

$$T = \frac{1}{S} \int_{\lambda}^{\lambda + \frac{R}{\rho_m}} t 2\pi \sigma \rho_m^2 (t - \lambda) dt = \lambda + \frac{2}{3} \frac{R}{\rho_m} \tag{15}$$

Multiplication of equation 14 by the deposition efficiency, δ , and the infection efficiency, ι , gives the final equation for the calculation of R_0 :

$$R_0 = \sigma \delta \iota \pi R^2 \quad (16)$$

where R_0 represents the net lifetime replacement of infected leaflets, assuming only one infection per leaflet. Substitution of equation 15 and 16 into equation 3 gives an approximation of r in homogenous space:

$$r_1 \approx \frac{\ln(\sigma \delta \iota \pi R^2)}{\lambda + \frac{2 R}{3 \rho_m}} \quad (17)$$

Incorporation of q into the numerator of equation 17 gives a predictive measure for r in heterogeneous space:

$$r_1 \approx \frac{\ln(q \sigma \delta \iota \pi R^2)}{\lambda + \frac{2 R}{3 \rho_m}} \quad (18)$$

Recent theory provides a second approximation formula for r (Segarra et al., 2001):

$$r_2 \approx \frac{\ln R_0}{\mu} \left[1 + \frac{1}{2} \left(\frac{\sigma_c}{\mu} \right) \ln R_0 \right] \quad (19)$$

where μ and σ_c values can be calculated from measurements of the sporulation curve, and R_0 from equation 16 multiplied by q . In order to investigate the accuracy of these approximation formulae, r_1 and r_2 will be used to predict emergent r in the set of simulation experiments for general epidemics.

Results

Importance of scale in the use of genotype mixtures for disease suppression

For simulation experiments A-F (Fig. 2), an increase in the number of genotype units via an increase in the size of the field always resulted in an increase in q and in the final disease severity (Table 2). Relative disease severities decreased from patterns A-C (Fig. 2) and stabilized thereafter. For simulation experiments G and H (Fig. 2), an

increase in the number of genotype units via an increase in the size of the field had no effect on q , or the final or relative severity values (Table 2)

Effect of crop arrangement and dispersal kernel on r and c

In all simulation experiments, q was found to increase with increasing f values, with consistently higher values for the row patterns and the narrow Laplace dispersal kernel, followed by the wide Laplace and Gaussian kernels (Table 3). In the simulated general epidemics, r increased with increasing f values in an analogous fashion to q , and also demonstrated consistently higher values for the row patterns and the narrow Laplace dispersal kernel, followed by the wide Laplace and Gaussian kernels (Table 3). In the simulated focal epidemics, c reached a constant value and increased linearly with the logarithm of the fraction, f , of susceptible plants (Table 3; Fig. 4). Unlike the results for q and r , higher velocities were reached with the wide Laplace kernel, followed by the Gaussian and narrow Laplace kernels (Table 3; Fig. 4).

Table 2: Modeled effect of the number of susceptible host genotype units on disease severity.

Pattern ^a	Overall area (m ²)	Number of units (#)	q^b (-)	Disease severity ^c (%)		
				Pure-line ^d	Mixture ^e	Relative ^f
A	3.6	4	0.05	5.41	3.01	0.56
B	14.4	16	0.10	15.23	6.73	0.44
C	57.6	64	0.16	29.43	12.02	0.41
D	230.4	256	0.20	40.04	16.27	0.41
E	921.6	1024	0.23	45.89	18.74	0.41
F	3686.4	4096	0.24	48.94	20.04	0.41
G	921.6	1024	0.25	52.08	21.40	0.41
H	3686.4	4096	0.25	52.08	21.40	0.41

^a Spatial configuration of host plants as given in Fig. 2.

^b Genotype connectivity calculated according to equation 5. Spore dispersal was provided by a wide radial Laplace kernel in order to simulate dispersal in non-irrigated potato plots.

^c Disease severity calculated as the percentage of diseased foliar surface on the susceptible genotype.

^d Final disease severity for pure-line susceptible population.

^e Final disease severity for mixtures consisting of 25 % susceptible and 75 % immune plants.

^f Relative disease severity, i.e. disease severity for the mixture divided by disease severity of the pure-line susceptible population of the same size.

Parameter q as a predictor of r and c

Plotting r as a function of $\ln(q)$ gave an effective indication of trends in r for all three dispersal kernels for the block patterns ($R^2 > 0.99$, $p \leq 0.005$) (Fig. 5). For the row patterns, plotting r as a function of $\ln(q)$ gave an effective indication of trends in r for the wide Laplace and Gaussian kernels ($R^2 > 0.99$, $p \leq 0.005$); however, this relationship was weaker for the narrow Laplace kernel ($R^2 = 0.90$, $p = 0.05$) (Fig. 5).

Table 3. Modeled effect of dispersal kernel and configuration, density, and aggregation of susceptible genotype units on development of general and focal potato late blight epidemics.

Dispersal kernel	Pattern ^a	f^b (-)	Genotype unit area (m ²)	Number of units (-)	q^c (-)	r^d (day ⁻¹)	r_1^e (day ⁻¹)	r_2^f (day ⁻¹)	sev ^g (%)	c^h (md ⁻¹)
Wide Laplace	A	0.125	0.23	2048	0.13	0.40	0.33	0.34	14.85	0.68
	B	0.250	0.23	4096	0.25	0.47	0.41	0.42	21.40	0.78
	C	0.500	0.23	8192	0.50	0.54	0.49	0.51	33.22	0.89
	D	0.125	57.60	8	0.21	0.42	0.38	0.40	18.89	0.68
	E	0.250	57.60	16	0.28	0.47	0.42	0.44	22.77	0.79
	F	0.500	57.60	32	0.51	0.54	0.50	0.51	33.50	0.90
	G	1.000	3686.40	1	1.00	0.63	0.58	0.60	52.08	1.03
Narrow Laplace	A	0.125	0.23	2048	0.20	0.42	0.38	0.39	18.72	0.28
	B	0.250	0.23	4096	0.30	0.48	0.43	0.45	23.80	0.31
	C	0.500	0.23	8192	0.52	0.54	0.50	0.52	34.15	0.35
	D	0.125	57.60	8	0.49	0.46	0.49	0.51	32.87	0.29
	E	0.250	57.60	16	0.50	0.50	0.49	0.51	33.10	0.32
	F	0.500	57.60	32	0.60	0.55	0.52	0.54	37.41	0.35
	G	1.000	3686.40	1	1.00	0.63	0.58	0.60	52.08	0.40
Gaussian	A	0.125	0.23	2048	0.13	0.40	0.32	0.33	14.55	0.52
	B	0.250	0.23	4096	0.25	0.47	0.41	0.42	21.22	0.58
	C	0.500	0.23	8192	0.50	0.54	0.49	0.51	33.15	0.63
	D	0.125	57.60	8	0.16	0.41	0.35	0.36	16.27	0.48
	E	0.250	57.60	16	0.25	0.47	0.41	0.42	21.23	0.58
	F	0.500	57.60	32	0.50	0.54	0.49	0.51	33.15	0.63
	G	1.000	3686.40	1	1.00	0.63	0.58	0.60	52.08	0.69

^a Spatial configuration of host plants as given in Fig. 3.

^b Fraction of susceptible host plants in the mixture.

^c Genotype connectivity calculated according to equation 5 and the wide Laplace kernel.

^d Apparent infection rate (equation 2).

^e Approximation formula for the apparent infection rate (equation 18).

^f Approximation formula for the apparent infection rate (equation 19).

^g Percentage of diseased foliar surface on the susceptible genotype.

^h Radial velocity of focus expansion.

Plotting c as a function of $\ln(q)$ also gave an effective indication of trends in c for all three dispersal kernels for the block patterns ($R^2 > 0.99$, $p \leq 0.005$), and for row patterns for the wide Laplace and Gaussian kernels ($R^2 > 0.95$, $p \leq 0.05$), whereas this relationship was again weaker for the row patterns under the narrow Laplace kernel ($R^2 = 0.88$, $p = 0.05$) (Fig. 6). This slight disparity resulted from similarly high values of q for f values of 0.125 and 0.25. In these simulation experiments, the combination of a steep dispersal gradient, with $\mu_d = 0.95$ m, and relatively large gaps between susceptible genotype units resulted in spore deposition only within rows. As a result, similar q values were observed in these two cases.

Parameter r as a predictor of c

Fig. 7 shows that in all simulation experiments, r and c were highly correlated ($R^2 > 0.95$), with little difference in the strength of the relationship for the three dispersal kernels. For the block patterns, these relationships were highly significant ($p \leq 0.001$),

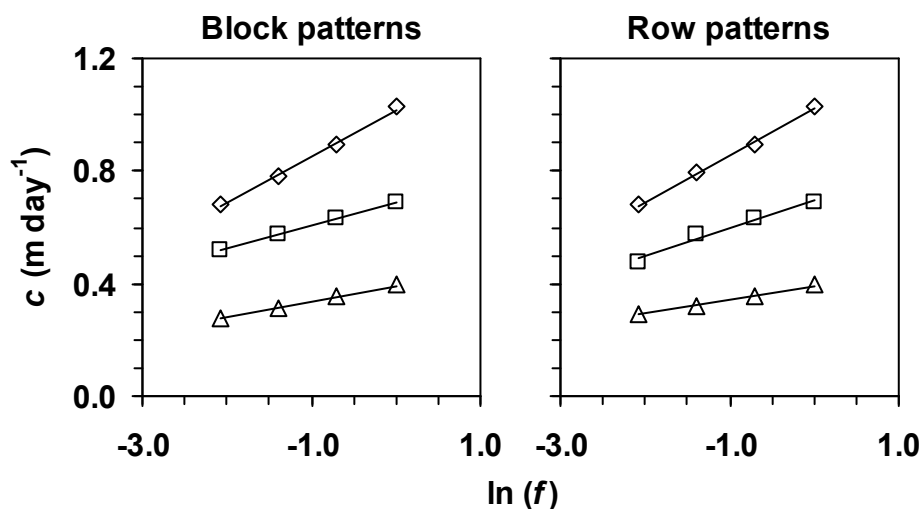


Fig. 4. Relationship between the radial velocity of focus expansion, c , and the logarithm of the fraction of susceptible host plants, f (-), in simulated potato late blight epidemics in genotype mixtures of susceptible and fully resistant potato cultivars. Spores were disseminated using three dispersal functions: ◇ = wide Laplace kernel, △ = narrow Laplace kernel, □ = Gaussian kernel, with mean dispersal distances of 2.44, 0.95, and 2.44 m respectively. The four points in each data set relate to calculations of c at four fractions, f (-), of susceptible plants in the host population: 0.125, 0.25, 0.5, and 1. Genotype unit area was held constant at 0.3 x 0.75 m for block patterns, 76.8 x 0.75 m for row patterns, and 76.8 x 48 m for pure-line susceptible host populations. Block and row patterns are given in Figure 3.

and also for the row patterns ($p \leq 0.05$). The spatial configuration of genotype units had little effect on these relationships.

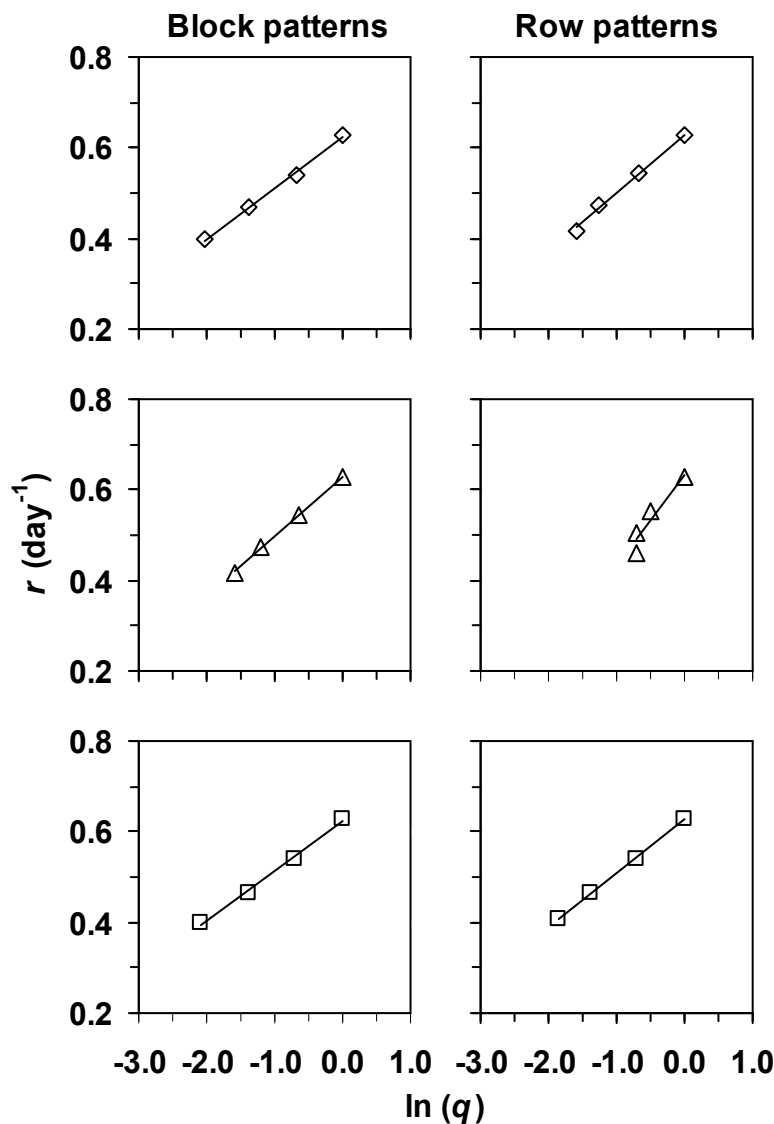


Fig. 5. Relationship between the apparent infection rate, r , and the logarithm of the genotype connectivity parameter, q (-), in simulated potato late blight epidemics in genotype mixtures of susceptible and fully resistant potato cultivars. Spores were disseminated using three dispersal functions: ◇ = wide Laplace kernel, △ = narrow Laplace kernel, □ = Gaussian kernel, with mean dispersal distances of 2.44, 0.95 and 2.44 m respectively. The four points in each data set relate to calculations of r and q at four fractions, f (-), of susceptible plants in the host population: 0.125, 0.25, 0.5, and 1. Genotype unit area was held constant at 0.3 x 0.75 m for block patterns, 76.8 x 0.75 m for row patterns, and 76.8 x 48 m for pure-line susceptible host populations. Block and row patterns are given in Figure 3.

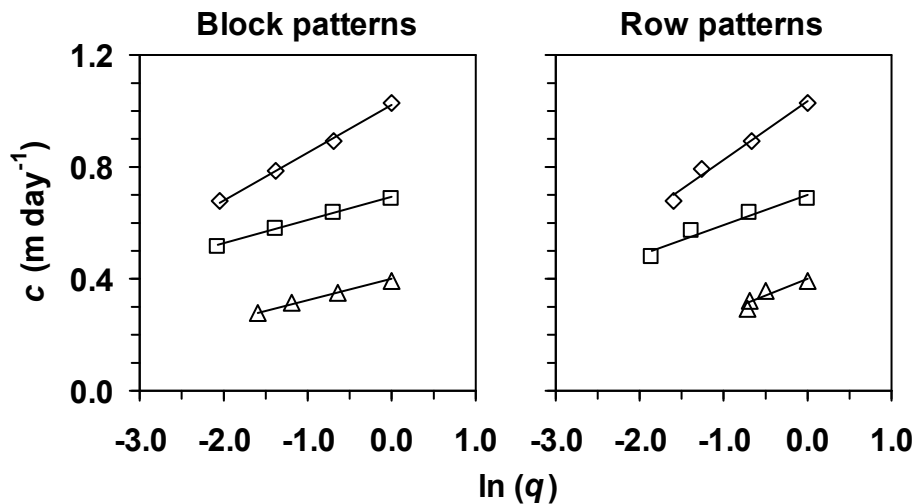


Fig. 6. Relationship between the radial velocity of focus expansion, c , and the logarithm of the genotype connectivity parameter, q (-), in simulated potato late blight epidemics in genotype mixtures of susceptible and fully resistant potato cultivars. Spores were disseminated using three dispersal functions: \diamond = wide Laplace kernel, \triangle = narrow Laplace kernel, \square = Gaussian kernel, with mean dispersal distances of 2.44, 0.95 and 2.44 m respectively. The four points in each data set relate to calculations of velocity at 4 fractions, f (-), of susceptible plants in the host population: 0.125, 0.25, 0.5, and 1. Genotype unit area was held constant at 0.3 x 0.75 m for block patterns, 76.8 x 0.75 m for row patterns, and 76.8 x 48 m for pure-line susceptible host populations. Block and row patterns are given in Figure 3.

Approximation formulae for r

Values of r_1 closely resembled those of r (Table 3) with the bias $((r - r_1 / r) * 100)$ ranging between 1.97 and 19.05 %. The mean bias for the entire set of simulation experiments was 9.79%. A slightly better approximation to r was achieved with r_2 (Table 3), with the bias ranging between 1.65 and 17.10 % and a mean bias of 7.22 %.

Discussion

The results from the first set of simulation experiments lead to the rejection of the null hypothesis; an increase in the number of genotype units via an increase in the size of the field did have an effect on the results, but only in the simulations of isolated fields, where padded mixtures were used (Table 2, A-F). For simulation experiments G and H, an increase in the size of the field clearly had no effect on model results. These differences in model results were due to differences in assumptions regarding dispersal; in patterns A-F the genotype mixtures are

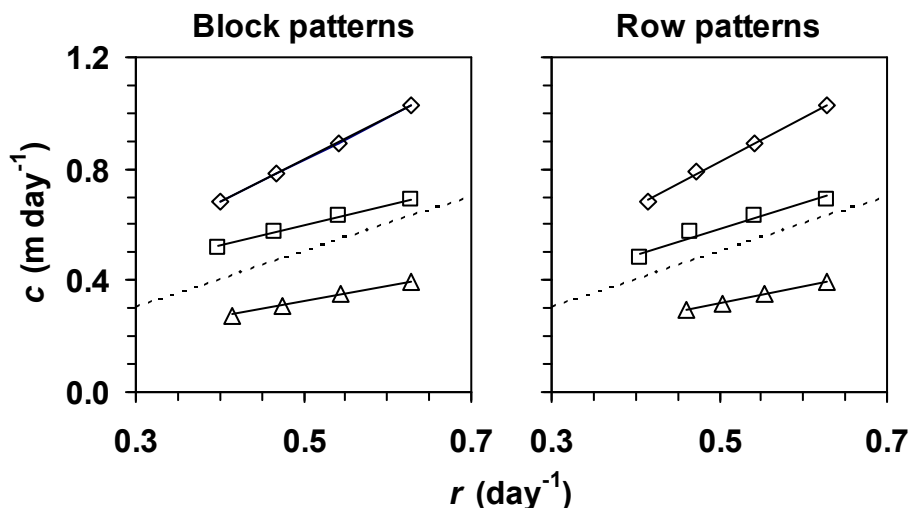


Fig. 7. Relationship between apparent infection rate, r , and radial velocity of focus expansion, c , in simulated potato late blight epidemics in genotype mixtures of susceptible and fully resistant potato cultivars. Spores were disseminated using three dispersal functions: \diamond = wide Laplace kernel, \triangle = narrow Laplace kernel, \square = Gaussian kernel, with mean dispersal distances of 2.44, 0.95 and 2.44m respectively. The four points in each data set relate to calculations of c and r at four fractions, f (-), of susceptible plants in the host population: 0.125, 0.25, 0.5, and 1. Genotype unit area was held constant at 0.3 x 0.75 m for block patterns, 76.8 x 0.75 m for row patterns, and 76.8 x 48 m for pure-line susceptible host populations. The dashed line represents a 1:1 line. Block and row patterns are given in Figure 3.

surrounded by non-host space that facilitates spore loss from outside the mixture boundaries, whereas in patterns G and H, we assume that inoculum from the surrounding (alike) environment compensates this loss. It is clear from Table 2 that the final disease severities for both the pure-line populations and the mixtures increase from patterns A-F. This is an expected result and can be interpreted with the use of q . As we increase the size of the field, a smaller proportion of inoculum is lost outwith the field edges and by corollary, the connectivity between the host plants increases; thus, q increases until its value approaches that of f . When we examine the relative severity values we see that the effectiveness of a mixture, in terms of disease control, increases with an increase in the number of genotype units within a field, then finally stabilizes. Thus, if a genotype mixture is surrounded by non-host space and isolated from external sources of inoculum, then the number of genotype units will exert an influence on model results and the null hypothesis is rejected. These results are in agreement with those of an earlier simulation study by Mundt and Brophy (1988) where potato late blight epidemics were also simulated in isolated

mixtures. As a result, they conclude that the epidemiological impact of the number of genotype units is of more importance than the genotype unit area. However, in simulation experiments G and H, we make a different assumption regarding spore dispersal; the simulated domain is a window onto an infinite lattice of identical, contiguous windows, i.e., there is no non-host space between the mixtures in the lattice. As a result, increasing the size of the field but holding all other aspects of crop arrangement constant has no effect on q (or other model results) as spore loss does not occur in these two simulation experiments. This clearly demonstrates that spore loss from outwith the field boundaries is the mechanism responsible for the difference in model results in patterns A-F. As spore loss from any field is the net result of the influx of external inoculum and the dispersal of inoculum outwith the field boundaries, it is clear that the number of genotype units within a field should not be considered independently from the space that surrounds the field. As *P. infestans* sporangia have been found/inferred to disperse and infect potato fields at up to 900 m distance from the source (Zwankhuizen et al., 1998), it may be of more relevance, particularly in potato growing regions, to assume that individual potato fields are part of an inter-connected network of fields, rather than isolated patches of host plants. This is particularly true in highland, tropical regions, where year round potato production and the continuous presence of late blight has been described by researchers (Oyarzun et al., 1998; Hijmans et al., 2000). Our results suggest that in such regions, where there may be a continual inflow of outside inoculum, the pattern and scale of the genotype units could be of more importance to the individual farmer than the size of his field.

In any spatial model of an aerially disseminated pathogen, the function used to disperse the propagules is of prime importance. The radial Laplace and Gaussian dispersal kernels represent two such commonly used functions and in this study, the mean dispersal distances for these kernels were taken from the results of experiments on potato late blight contained in a seminal paper on interplot interference by Paysour and Fry (1983). In the simulations of general epidemics, q and r values were slightly higher under the narrow Laplace kernel, followed by the wide Laplace and Gaussian kernels. This is an expected result as steeper pathogen dispersal gradients often result in smaller host-diversity effects on disease due to a reduction in mixing effect (Garrett and Mundt, 1999). For focal epidemics, the simulation experiments showed that c can be calculated in non-ideal mixtures; constant velocities were reached in all simulation experiments and c was found to increase linearly with the logarithm of f in all cases. Despite the occurrence of non-

circular foci, the simulation results show that c can still be used as a measure of spatial spread over time. This is by virtue of the area method adopted to derive c , whereby the final velocity obtained represents an average radial expansion over time, in m day^{-1} . For the focal simulation experiments, c values were highest under the wide Laplace kernel, followed by the Gaussian and the narrow Laplace kernels. Here, there was a marked difference between the three sets of results. Unlike general epidemics, where each plant is a source, in non-ideal mixtures focus expansion is governed by the spatial arrangement of susceptible genotypes in the host population. Table 3 shows that q values are higher for both block and row patterns under the narrow Laplace kernel; here, dampening of the spore cloud results in an increase in the number of autoinfections as a larger proportion of spores land back on the source plant. However, despite a loss in mixing effect, c values are considerably lower under this dispersal kernel. It is therefore apparent that simulated c values are greater under dispersal functions that afford the opportunity to breach areas of host resistance. These results reinforce the need to study dispersal when epidemics have a focal aspect and illustrate the importance of future experimental research aimed at gathering ecological data on the short-range dispersal of *P. infestans*.

Our results show that q can be used to predict the impact of crop arrangement on the development of both general and focal epidemics. The linear relationships between $\ln(q)$ and r , and $\ln(q)$ and c , were highly significant, indicating that q can be used effectively to predict changes in both r and c across heterogeneous host populations. However, simulation results for dispersal according to the narrow Laplace kernel in row patterns at f values of 0.125 and 0.25 did not reveal a linear relationship between $\ln(q)$ and r or $\ln(q)$ and c . Here, the combination of a steep dispersal gradient, with $\mu_d = 0.95$ m, and multiple resistant rows of 0.75 m width each, result in the pathogen being unable to breach the gap between neighboring susceptible rows. As a consequence, spores are deposited only within rows, leading to similarity in q values and in disease for these two cases (Table 3). In all other cases, the linear relationships between $\ln(q)$ and r , and $\ln(q)$ and c approached direct proportionality. It is therefore apparent that parameter q is a sound measure for predicting the disease suppressiveness of landscapes. However, caution must be used in interpreting these results. In general epidemics, variation in the landscape is being "averaged out" because each plant is a source. This may be inferred from Fig. 5 where the lines (excluding the anomaly caused by very wide inter-rows) for the various kernels and landscapes seem to almost coincide when superimposed. For focal epidemics, however, variation in the landscape at the scale of the dispersal

kernel has a strong effect on the development rate of the epidemic. This can be inferred from Fig. 6, where the lines, if combined in one graph, do not overlap. This demonstrates clearly that for focal epidemics, information on q proves information on c only if information on the dispersal function is also available.

The results of this modeling study indicate that the spatial arrangement of the host population impacts the development of general epidemics and the spread of focal epidemics by a common mechanism. This explains the high degree of correlation between r and c across different spatial configurations of host plants and for different dispersal kernels. These findings act as evidence against the conjecture that results from studies of host-diversity effects on potato late blight in temperate regions cannot be extrapolated to more tropical regions (Garrett et al., 2001). Variation in empirical results cannot be attributed to fundamentally different responses to changes in spatial configuration of host plants between focal and general epidemics.

The predictive measures of apparent infection rate, r_1 and r_2 , showed that information relating to emergent growth in time and space can be inferred from life table characteristics. The theory of age-structured populations, (e.g., Keyfitz, 1985), has been used to approximate temporal growth without any explicit reference to spatial constraints (equation 3). The inclusion of q in equation 16 provides a link between the space-less world of temporal growth and the spatial variation that shapes the growth of the pathogen population in its habitat. The proposed approximation r_1 was therefore able to produce accurate predictions of r ; on average within 9.79 % of r . The high degree of correlation between r and c suggests that r_1 would also be capable of predicting epidemic spread in focal epidemics.

The measures of epidemic progress developed in this study could be of benefit in the design of new experiments. Using the genotype connectivity parameter, q , it is possible to quickly gauge the efficacy of landscape designs for disease control, without the need for any dynamic epidemic simulation. In addition, q could be used to predict trends in r and c for new pathogens or pathogen races where little is known of epidemic development in the field. If sufficient ecological information regarding life table processes is available, then q can be used as a spatial component as part of other indices, such as r_1 , to produce direct predictions of the effects of host diversity on epidemic development. Similarly, such predictive measures could be used to predict epidemic development in new cultivars via incorporation of the infection efficiency of the pathogen, for that cultivar, into the calculations of q . In this way, intermediate levels of host resistance could be incorporated into q values.

Acknowledgements

This research was funded by a Marie Curie Fellowship from the EU. We thank Hans Heesterbeek and Maria Tsesmeli for their contributions to the model.

References

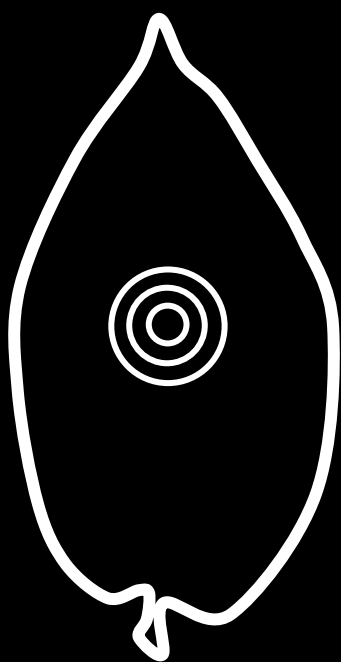
- Andrison, D., Lucas, J.M., and Ellisseche, D. 2003. Development of natural late blight epidemics in pure and mixed plots of potato cultivars with different levels of partial resistance. *Plant Pathol.* 52:586-594.
- Assefa, H., Van den Bosch, F., and Zadoks, J.C. 1995. Focus expansion of bean rust in cultivar mixtures. *Plant Pathol.* 44:503-509.
- Barrett, J.A., and Wolfe, M.S. 1980. Pathogen response to host resistance and its implications in breeding programmes. *EPP0 Bulletin* 10:341-347.
- Berger, R.D., Bergannin-Filho, A., and Amorim, L. 1997. Lesion expansion as an epidemic component. *Phytopathology* 87:1005-1013.
- Berkson, J. 1944. Application of the logistic function to bio-assay. *J. Am. Statist. Assoc.* 48:565-599.
- Borlaug, N.D. 1958. The use of multiline and composite varieties to control air-borne epidemic diseases of self-pollinated crop plants. In: *First International Wheat Genetics Symposium Proceedings*. University of Manitoba, Winnipeg, pp. 12-29.
- Ferrandino, F.J. 1993. Dispersive epidemic waves: I. Focus expansion within a linear planting. *Phytopathology* 83:795-802
- Flier, W.G., and Turkensteen, L.J. 1999. Foliar aggressiveness of *Phytophthora infestans* in three potato growing regions in the Netherlands. *Eur. J. Plant Pathol.* 105:381-388.
- Garrett, K.A., and Mundt, C.C. 1999. Epidemiology in mixed host populations. *Phytopathology* 89:984-990.
- Garrett, K.A., and Mundt, C.C. 2000. Host diversity can reduce potato late blight severity for focal and general patterns of primary inoculum. *Phytopathology* 90:1307-1312.
- Garrett, K.A., Nelson, R.J., Mundt, C.C., Chacon, G., Jaramillo, R.E., and Forbes, G.A. 2001. The effects of host diversity and other management components on epidemics of potato late blight in the humid highland tropics. *Phytopathology* 91:993-1000.
- Gotelli, N.J. 1998. *A Primer of Ecology*. Sinauer Associates, Sunderland, MA, 236 pp.
- Groenewegen, L.J.M., and Zadoks, J.C. 1979. Exploiting within-field diversity as a defence against cereal diseases: a plea for 'poly-genotype' varieties. *Indian J. Genet. Plant Breed.* 39:81-94.

- Hijmans, R.J., Forbes, G.A., and Walker, T.S. 2000. Estimating the global severity of potato late blight with a GIS-linked disease forecaster. *Plant Pathol.* 49:697-705.
- Jeger, M.J., Jones, D.G., and Griffiths, E. 1983. Disease spread of non-specialized fungal pathogens from inoculated point sources in intraspecific mixed stands of cereal cultivars. *Ann. App. Biol.* 102:237-44.
- Jensen, N.F. 1952. Intra-varietal diversification in oat breeding. *Agron. J.* 44:30-4.
- Kampmeijer, P., and Zadoks, J.C. 1977. EPIMUL, a simulator of foci and epidemics in mixtures, multilines, and mosaics of resistant and susceptible plants. *Simulation Monograph*, Pudoc, Wageningen.
- Keyfitz, N. 1985. *Applied Mathematical Demography*, 2nd Edition. Springer Verlag, New York, 441 pp.
- Merriam, G. 1984. Connectivity: a fundamental ecological characteristic of landscape pattern. *Proc. Int. Assoc. Landscape Ecol.* 1:5-15.
- Mundt, C.C. 2002. Microbial dispersal and epidemic velocity: Does scale matter? *Phytopathology* 92 (Suppl.): S96-S97.
- Mundt, C.C., and Brophy, L.S. 1988. Influence of number of host genotype units on the effectiveness of host mixtures for disease control: a modeling approach. *Phytopathology* 78:1087-1094
- Mundt, C.C., Brophy, L.S., and Kolar, S.C. 1996. Effect of genotype unit number and spatial arrangement on severity of yellow rust in wheat cultivar mixtures. *Plant Pathol.* 45:215-222.
- Mundt, C.C., and Browning, J.A. 1985. Development of crown rust epidemics in genetically diverse oat populations: effect of genotype unit area. *Phytopathology* 75:607-610.
- Mundt, C.C., and Leonard, K.J. 1985. Effect of host genotype unit area on epidemic development of crown rust following focal and general inoculations of mixtures of resistant and susceptible oat plants. *Phytopathology* 75:1141-1145.
- Mundt, C.C., and Leonard, K.J. 1986a. Analysis of factors affecting disease increase and spread in mixtures of resistant and susceptible plants in computer-simulated epidemics. *Phytopathology* 76:832-840
- Mundt, C.C., and Leonard, K.J. 1986b. Effect of host genotype unit area on development of focal epidemics of bean rust and common maize rust in mixtures of resistant and susceptible plants. *Phytopathology* 76:895-900.
- Mundt, C.C., Leonard, K.J., Thal, W.M., and Fulton, J.H. 1986. Computerized simulation of crown rust epidemics in mixtures of resistant and susceptible oat plants with different genotype unit areas and spatial distributions of initial disease. *Phytopathology* 76:590-598.
- Neubert, M.G., Kot, M., and Lewis, M.A. 1995. Dispersal and pattern formation in a discrete-time predator-prey model. *Theor. Popul. Biol.* 48:7-43.

- Oyarzun, P.J., Pozo, A., Ordonez, M.E., Doucett, K., and Forbes, G.A. 1998. Host specificity of *Phytophthora infestans* on tomato and potato in simple communities of wheat and wild oats. *Phytopathology* 88:708-714.
- Pansee, A., Davis, J.H.C., and Fischbeck, G. 1989. Compensation-induced yield gains in mixtures of common bean (*Phaseolus vulgaris* L.). *J. Agron. Crop Sci.* 162:347-53.
- Paysour, R.E., and Fry, W.E. 1983. Interplot interference: A model for planning field experiments with aerially disseminated pathogens. *Phytopathology* 73:1014-1020.
- Powell, J.A., Slapničar, I., and van der Werf, W. 2005. Epidemic spread of a lesion-forming plant pathogen - analysis of a mechanistic model with infinite age structure. *Linear Algebra Appl.* 398:117-140.
- Robinson, R.A. 1976. *Plant Pathosystems*. Springer-Verlag, New York.
- Scherm, H. 1996. On the velocity of epidemic waves in model plant disease epidemics. *Ecol. Model.* 87:217-222.
- Segarra, J., Jeger, M.J., and van den Bosch, F. 2001. Epidemic dynamics and patterns of plant diseases. *Phytopathology* 91:1001-1010.
- Spijkerboer, H.P. 2004. From lesion to region: epidemiology and management of potato late blight. PhD thesis, Wageningen University, The Netherlands, 113 pp.
- Tischendorf, L., and Fahrig, L. 2000. On the usage and measurement of landscape connectivity. *Oikos* 90:7-19.
- Van den Bosch, F., Frinking, H.D., Metz, J.A.J., and Zadoks, J.C. 1988a. Focus expansion in plant disease. III. Two experimental examples. *Phytopathology* 78:919-25.
- Van den Bosch, F., Verhaar, M.A., Buiel, A.A.M., Hoogkamer, W., and Zadoks, J.C. 1990. Focus expansion in plant disease. IV. Expansion rates in mixtures of resistant and susceptible hosts. *Phytopathology* 80:598-602.
- Van den Bosch, F., Zadoks, J.C., and Metz, J.A.J. 1988b. Focus expansion in plant disease. I. The constant rate of focus expansion. *Phytopathology* 78:54-8.
- Van den Bosch, F., Zadoks, J.C., and Metz, J.A.J. 1988c. Focus expansion in plant disease. II. Realistic parameter sparse models. *Phytopathology* 78:59-64.
- Wolfe, M.S. 1985. The current status and prospects of multiline cultivars and variety mixtures for disease resistance. *Annu. Rev. Phytopathol.* 23:251-73.
- Zadoks, J.C. 1958. Het gele-roest onderzoek. Tienjarenplan Voor Graanonderzoek (Wageningen) 5:109-19.
- Zadoks, J.C. 1959. Het gele-roest onderzoek. Tienjarenplan Voor Graanonderzoek (Wageningen) 6:139-50.
- Zadoks, J.C., and Schein, R.D. 1979. *Epidemiology and Plant Disease Management*. Oxford University Press, New York, 427 pp.
- Zhu, Y., Chen, H., Fan, J., Wang, Y., Li, Y., Chen, J., Fan, J., Yang, S., Hus, L., Leung, H., Mew, T.W., Teng, P.S., Wang, Z., and Mundt, C.C. 2000. Genetic diversity and disease control in rice. *Nature* 406:718-722.

Zwankhuizen, M.J., Govers, F., and Zadoks, J.C. 1998. Development of potato late blight epidemics: Disease foci, disease gradients, and infection sources. *Phytopathology* 88:754-763.

CHAPTER 3



Parameterization and Evaluation of a Spatio-Temporal Model of the Potato Late Blight Pathosystem

P. Skelsey¹, G.J.T. Kessel², W.A.H. Rossing³, and W. van der Werf¹

¹ Wageningen University, Department of Plant Sciences, Crop and Weed Ecology Group, P.O. Box 430, 6709 RZ Wageningen, The Netherlands.

² Plant Research International, P.O. Box 16, 6700 AA Wageningen, The Netherlands.

³ Wageningen University, Department of Plant Sciences, Biological Farming Systems Group, P.O. Box 9101, 6709 PG Wageningen, The Netherlands.

Phytopathology (*in press*)

Abstract

A spatio-temporal, integrodifference equation model of the potato late blight pathosystem is described. Formerly, the model was used in a theoretical context to analyze and predict epidemic dynamics in spatially heterogeneous mixtures of host genotypes. The model has now been modified to reflect a research interest in interactions between genotype, environment, landscape and management. New parameter values describing host-pathogen interactions were determined and new environment-pathogen relationships included. A new analytical equation describing lesion expansion and associated necrosis has also been developed. These changes prompted a need to assess the quality of model predictions.

Cultivar-isolate specific interactions were characterized in the model using three quantitative components of resistance: infection efficiency, lesion growth rate, and sporulation intensity. These were measured on detached potato leaflets in the laboratory. Results of a sensitivity analysis illuminated the effect of different quantitative components of resistance and initial conditions on the shape of disease progress curves. Using the resistance components, the epidemic process of lesion expansion was separated from the epidemic process of lesion propagation, providing two reference curves for diagnosing observed epidemics.

The spatial component of the model was evaluated graphically in order to determine if realistic rates of focal expansion for potato late blight are produced. In accordance with theory, the radius of a predicted focus increased linearly with time and a constant focal velocity was reached that compared well with published experimental data.

Validation data for the temporal model came from 20 late blight epidemics observed in field trials conducted in the Netherlands in 2002 and 2004. The field data and model were compared visually using disease progress curves, and numerically through a comparison of predicted and observed t_5 and t_{50} points (time in days until 5 and 50 % disease severity was reached, respectively)

and relative areas under the disease progress curve values. Temporal model predictions were in close agreement with observational data and the ability of the model to translate measured resistance components, weather data and initial conditions into realistic disease progress curves without the need for calibration confirms its utility as a tool in the analysis and diagnosis of epidemics.

Additional keywords: dispersal, kernels, convolution, Fourier transforms.

Introduction

It is well documented that aerial dispersal of sporangia is a crucial process in the development of potato late blight epidemics (e.g., Hyre, 1950; Hirst, 1953; van der Zaag, 1956); however, knowledge of the spatial aspects of spore dispersal is still limited. Management of potato late blight could benefit from prediction of the risk posed to potato fields from external inoculum sources of *Phytophthora infestans*, but as spore influx depends on a complex interplay of population biological, atmospheric and spore survival processes, it is difficult to predict. Further questions remain regarding how the composition, configuration and connectivity of landscapes influence pathogen population dynamics. Optimizing the spatial deployment of host resistance could lead to improvements in disease control, an increase in the durability of resistance gene resources, and a reduction in the chemical requirements of potato cultivation in large growing areas. An enhanced understanding of the spatial aspects of epidemic development at the field- and landscape-scale could therefore lead to the identification of new operational and strategic management practices for potato late blight. Spatio-temporal simulation models will be particularly useful in this endeavor as they facilitate a rapid evaluation of disease management practices at scales where experimentation is not always possible.

The model described in this study is a spatio-temporal/integrodifference equation model of the potato late blight pathosystem (*Phytophthora infestans* - *Solanum tuberosum*). Previously, the model was used to study the influence of different scales and patterns of host genotypes on development of focal and general epidemics (Skelsey et al., 2005). In this theoretical context it was not of prime importance to use parameter values relating to real potato cultivars. As it is the long term aim of our research to further develop and utilize this model to investigate new strategies for the regional management of potato late blight, some modifications were required. With these objectives in mind, the model was recently updated to

include a simple set of climatic relations based on the experimental results of Zwankhuizen and Zadoks (2002) and Rotem et al. (1970). Parameter values describing cultivar-isolate interactions have also been modified. Three quantitative components of resistance were measured in the laboratory using a sample of potato cultivars and isolates from the Netherlands: the infection efficiency, ι (-), the radial lesion growth rate, ρ (m day⁻¹), and the sporulation intensity, σ (# m⁻²). A new analytical equation for describing lesion expansion has also been incorporated. In light of these recent changes, it is now useful to assess the quality of model predictions in comparison with observed epidemics in the field.

The primary value of the model is heuristic; i.e., targeted towards increasing our understanding of epidemic dynamics. The model must therefore remain logically tractable and transparent, yet it must produce realistic results that are sufficiently close to real world observations to be considered “useful.” Thus, our goal in model evaluation is neither to achieve nor force a high level of predictive accuracy *per se*; evaluation in this context refers to the ability of the model to translate measured resistance components, weather data and initial conditions into realistic disease progress curves, using as simple and transparent a model as possible, based on the principle of parsimony, also referred to as Ockham’s razor (e.g., Forster and Sober, 1994; Turchin, 2003).

Extensions to the model and laboratory experiments used to derive quantitative components of resistance for a number of potato cultivar-isolate combinations are described. A sensitivity analysis is conducted in order to improve understanding about the effect of new model parameter values and initial conditions on the shape of disease progress curves. The spatial component of the model is evaluated by comparing emergent focal expansion velocities with a rate previously determined by Minogue and Fry (1983). The quality of temporal model predictions is then tested through comparison with measured epidemics in experimental field plots in the Netherlands. The degree of confirmation of temporal model predictions by observational data is assessed using graphical and numerical methods.

Theory and approaches

A spatio-temporal potato late blight model

Integrodifference equations (IDEs) are the spatially explicit equivalent of difference equation models. They are discrete-time, continuous-space models for the growth

and spread of biological populations. As noted by Neubert et al. (1995): “IDEs contain two components: (i) difference equations, which model growth and interactions during a sedentary stage and, (ii) redistribution kernels, which characterize movement during a dispersal stage.”

In the model, space is described as a two-dimensional grid, in which each cell represents a potato plant. The *Phytophthora* population in the model is age- and spatially-structured and internal model accounting keeps track (for every plant in the field) of the number of lesions according to the day of establishment; thus, after t days of simulation there will be t age classes of lesions. Thus, the time step is taken to be one day, and not a generation, as is done in some difference equation models. Lesions in the model are circular and grow radially, producing a new ring of growth (annulus) each day, the area of which is calculated as:

$$dA_t = 2\pi\rho^2 t \left(1 - \frac{A}{K}\right) dt \quad (1)$$

where A_t = the area (m^2) of a single lesion of age class t (days), ρ = the radial lesion growth rate (m day^{-1}), A = the total diseased area per plant (m^2), and K = leaf area of a plant (m^2). Table 1 provides a summary of symbol definitions and dimensions (all parameters are given in standard SI units). New lesion annuli are latent for a period of time, λ (days), set at 5 days for all cultivar-isolate interactions. At age $\lambda + 1$ day, latent areas become infectious and produce spores. The infectious period is set to 1 day for all cultivar-isolate interactions. During each successive day, as another annulus of daily radial growth reaches age $\lambda + 1$ day, this annulus will sporulate. The areas of latent, infectious and dead lesion area on each host plant are calculated by summing over age classes the number of lesions in each age class, multiplied by the age-specific area of latent, infectious and necrotic area per lesion. Lesions are aged at a daily time step. Spore production intensity per unit of infectious leaf area is accounted for by the parameter σ ($\# \text{m}^{-2}$). All spores that are produced are assumed to be released. Spores are redistributed according to a radial Laplace kernel (Skelsey et al., 2005). After sporulation, infectious areas are classed as necrotic. Necrosis of host tissue is also caused by the “girdling” of leaves and stems by lesions. Following van Oijen (1992a), girdling proceeds at a rate equal to the increase in severity, i.e., for every increase in latent area calculated by equation 1, an equal amount of healthy tissue is classed as necrotic. Leaf lesion coverage and areas of necrotic leaf tissue caused by *P. infestans* are assumed to be distributed homogeneously throughout the canopy.

Table 1. Symbols used in this study

Symbol	Units	Description
a	%	y-intercept of an ordinary least squares regression of predicted on observed RAUDPC
A	m^2	Total diseased area per plant
A_{dis}	m^2	Observed area of damage on each plant
A_g	m^2	Ground area of the plant
A_t	m^2	Area of a single lesion of age class t
b	- ^a	Slope of an ordinary least squares regression of predicted on observed RAUDPC
C_p	-	Coefficient of prediction
f_e	-	Escape fraction
K	m^2	Leaf area of plant
LAI	-	Leaf area index
MAE	%	Mean absolute error for RAUDPC
MD	days	Mean absolute deviation between observed and predicted t_5 and t_{50} points
n	#	Number of observations
O	-	Observed output variable
\bar{O}	%	Mean observed RAUDPC
P	-	Predicted output variable
\bar{P}	%	Mean predicted RAUDPC
RAUDPC	%	Relative area under the disease progress curve
RMSE	%	Root mean square error for RAUDPC
RMSE _s	%	Systematic root mean square error for RAUDPC
RMSE _u	%	Unsystematic root mean square error for RAUDPC
s_o	%	Standard deviation of observed RAUDPC
s_p	%	Standard deviation of predicted RAUDPC
S	%	Disease severity
t	days	Time
t_i	days	Time of initiation of the simulated epidemic
t_0	days	Time of the last evaluation when no disease was observable
t_1	days	Time of the first severity observation
t_5	days	Time until 5 % disease severity is reached
t_{50}	days	Time until 50 % disease severity is reached
T_{inf}	°C	Average temperature during consecutive infection-hours
u	$m s^{-1}$	Wind speed
v_d	$m s^{-1}$	Deposition velocity
v_s	$m s^{-1}$	Settling velocity
α	-	Factor of collateral damage due to “girdling” of leaves and stems by lesions
γ	#	Initial number of lesions per plant
δ	-	Deposition efficiency
l	-	Infection efficiency
κ	-	Von Kármán constant (0.35)
λ	days	Latent period

Table 1 continued

Symbol	Units	Description
π	-	Mathematical constant
ρ	m day ⁻¹	Radial growth rate of lesions
σ	# m ⁻²	Sporulation intensity

^a - signifies that the defined quantity is dimensionless.

The age-structured population model for lesions on each plant is updated daily, by “aging” the existing lesions by 1 day, and starting new lesions at a rate calculated as the product of the number of landed spores per m² leaf area in a day, the infection efficiency, ι (-), and the fraction of area not yet occupied by colonies of *P. infestans*, (including latent, infectious, and necrotic tissue). This fraction is also used to limit areal expansion of lesions (due to competition for space at the plant level).

Solution of spatial phenomena

As described in Skelsey et al. (2005), spatial phenomena in the model are solved by performing convolutions between spatial distributions of spores and dispersal kernels. Convolutions are implemented in the model via fast Fourier transforms; a technique that greatly enhances the speed and accuracy of the numerical solution of the model. Spatial distributions (i.e., the kernel and a distribution of spores) are transformed into the Fourier domain, multiplied, and the result is back-transformed into the spatial domain. This solution method requires periodic boundary conditions, therefore Fourier domain arrays are duplicated an infinite number of times to the left, right, top and bottom. This means that each edge of the array is connected to the opposite edge of an identical array, leading to “wrap-around” effects, whereby any spore dispersing outside of the field’s borders “reappears” on the opposite edge of the field when spatial distributions are back-transformed into the spatial domain. This artifact of the solution methodology can be used to provide a representation of interplot interference (spore exchange between neighboring plots), which is based on the spatial characteristics of the experimental site. Prior to convolution, spatial distributions are “padded” with a border of “non-crop” area (“zero-padding”) that matches the spacing between experimental plots. Spores that are redistributed by the kernel into the non-crop area are lost from the system and do not contribute to epidemic development. Spores that are redistributed beyond the border of non-crop area (i.e., further than the spacing between plots) reappear on the opposite edge of

the source plot and are assumed to come from a neighboring donor plot. The extent of zero-padding can also be increased to completely mitigate wrap-around effects. This is useful in the simulation of completely isolated plots or fields.

Environment-pathogen interactions

The model has a daily time step, which is suitable for a study of epidemic dynamics over the length of an entire growing season, but inappropriate for the incorporation of environment-pathogen interactions. Some meteorological variables that have profound effects on the pathogen, such as relative humidity, can show a marked variation over a 24 hour period and therefore it is not possible to average these variables over a day and use them in any meaningful analysis of epidemic dynamics. In the model a simplifying assumption is made that colony growth continues within the leaf tissue and sporangia are produced, dispersed and deposited irrespective of the weather; however, successful germination of dispersed sporangia is weather dependent. Two simple rules are used to analyze hourly weather data and determine if the conditions during a 24 hour period (16:00-16:00 hours; one time step in the model) are suitable for sporangia to cause infection. The first rule determines if the conditions each hour are suitable for the germination process to take place. Following Zwankhuizen and Zadoks (2002), an “infection-hour” is defined as any hour where the temperature is between 10 and 27°C and the relative humidity is greater than 90 %. The second rule determines the number of consecutive infection hours required to allow germination to reach completion in a 24 hour period. This rule is based on the average temperature during consecutive infection-hours, T_{inf} (°C), and the experimental results of Rotem et al. (1970): for $10^{\circ} \leq T_{inf} \leq 15^{\circ}$, 12 consecutive infection-hours are required; for $15^{\circ} < T_{inf} \leq 20^{\circ}$, 18 consecutive infection-hours are required; for $20^{\circ} < T_{inf} \leq 27^{\circ}$, 24 consecutive infection-hours are required; and for $T_{inf} < 10^{\circ}$ and $T_{inf} > 27^{\circ}$, penetration does not occur. If the conditions of these rules are not met, then infection does not take place and the parameter ι is set to 0 for that 24 hour period. These rules therefore act as a simple “switch”; the polycyclic component of the epidemic is allowed to proceed under suitable conditions and it is “switched off” under adverse conditions.

Model parameterization - pathogenicity experiments

Unsprayed, fully grown new leaves from the Wageningen field experiments (described below) were sampled in 2002, 2003 and 2004 and taken to the laboratory to determine ι , ρ , and σ . Five different potato cultivars with different levels of

resistance against *P. infestans* were used: Agria (5.5), Aziza (7.5), Bintje (3), Remarka (6.5) and Sante (4.5). Foliar resistance ratings to potato late blight according to the Dutch National variety list are given in brackets (on a scale of 1 = very susceptible to 9 = very resistant). Two different *P. infestans* isolates (IPO82001 and IPO428-2) were used as inoculants in both the pathogenicity studies and the field experiments. Isolates and their key characteristics, as determined by Flier and Turkensteen (1999), are listed in Table 2.

Culturing and preparation of inoculum

P. infestans isolates IPO82001 and IPO428-2 were stored in liquid nitrogen as sporangial suspensions in a 15 % dimethylsulphoxide solution. Isolates taken from long-term storage were first cultured on tuber slices of the general susceptible potato cultivar Bintje by incubation in the dark at 15°C for 5-7 days. When sporulating mycelium was present, small pieces of mycelium were placed on the abaxial (lower) epidermis of leaflets of cultivar Bintje, which were placed with the abaxial side up in 9 cm petri-dishes containing 10 ml 2 % water agar. Inoculated leaflets were kept in a climate chamber at 15°C with a 16 hour light period. Leaflets densely covered with sporulating mycelium were obtained after seven days of incubation. Sporangial inoculum was prepared by washing these leaves in 20 ml of tap water. The concentration was adjusted to 1×10^4 or 1×10^5 sporangia ml⁻¹ using a Coulter Counter Z1 (Coulter Electronics Inc.) and kept at 18°C. The suspensions were used as inoculum within 30 min after preparation.

Plant material

Potato cultivars Agria, Aziza, Bintje, Remarka and Sante were grown in 3.75 x 3.75 m

Table 2. Isolates of *Phytophthora infestans* used to determine cultivar specific resistance components and to inoculate the field experiments used for model validation

Isolate	Year of collection	Location	Race ^a	Mating type	mtDNA Haplotype
IPO82001	1982	Gembloux ^b	1.2.3.4.5.6.7.10.11	A2	1a
IPO428-2	1992	Ede ^c	1.2.3.4.5.6.7.8.9.10.11	A2	1a

^a Determined by Flier and Turkensteen (1999) using the R-gene differential set of potato clones for race identification: r0 (Bintje), R1, R2, R3, R4, R5, R6, R7, R8, R9, R10 and R11 (Black et al., 1953; Malcolmson and Black, 1966).

^b Belgium.

^c Netherlands.

plots under field conditions during the spring of 2002, 2003 and 2004 in Wageningen, the Netherlands. Leaf material not protected with fungicides was sampled from the fourth and fifth leaf layer from the top when the plants were 7 - 9 weeks old.

Quantification of resistance components

Resistance components ι , ρ , and σ were quantified in a series of bioassays. Lateral leaflets were placed in 9 cm petri dishes containing 10 ml 2 % water agar, one leaflet per petri-dish, lower (abaxial) side up. To determine ι , ten 10- μ l droplets of a sporangial suspension containing 1×10^4 sporangia ml^{-1} were placed on the abaxial side of each leaflet. Petri-plates with the inoculated leaf discs were placed in plastic trays, which were then enclosed in a transparent polythene bag to avoid desiccation. The trays were placed in the dark in a climate chamber at 15°C. After 24 hours, incubation was continued at 15°C and 16 hour photo period. The number of successful inoculations (spreading lesions) per leaflet was determined after seven days incubation and ι was calculated according to Swallow (1987). To determine ρ and σ , one 10- μ l droplet of a sporangial suspension containing 5×10^4 sporangia ml^{-1} was placed on the abaxial side of each leaflet. Petri-plates containing inoculated leaf discs were placed in plastic trays, which were then enclosed in a transparent polythene bag to avoid desiccation. The lesion diameter was measured along two perpendicular axes at least twice before the lesion reached the edge of the leaflet, and ρ was calculated from these measurements. Following the last measurement, the sporangia were released from the lesions by shaking the leaflet in 10 ml of Isoton II electrolytic buffer (Coulter Electronics Inc.) using a vortex mixer. After dilution, the sporangial concentration was measured in three 0.5 ml sub-samples using a Coulter counter and σ was calculated from the lesion surface area and the number of sporangia produced on the lesion.

Statistical analysis

Data came from seven laboratory experiments (described above): two experiments in 2002, three experiments in 2003 and two experiments in 2004. Within the separate experiments, each petri-dish containing one potato leaflet was considered a replicate. Four replicate leaflets per experiment were used to determine ι and ρ in 2002 and 2004. Five replicate leaflets per experiment were used to determine ι and ρ in 2003. Two replicate leaflets were used to determine σ in all five experiments. Linear Mixed Modeling was used to test for possible interactions between year and experiment, year and cultivar, cultivar and inoculum, and between year and

inoculum, using the statistical package Genstat for Windows 9th edition (VSN International Ltd, Hemel Hempstead, 2007), extended with the Biometris procedure library (Goedhart and Thissen, 2006).

No significant interactions were present between year and cultivar, and between year and inoculum, therefore the Linear Mixed Model (LMM) was fitted with fixed factor cultivar*inoculum and random factor year*experiment (treating the experiments of 3 years as 7 independent experiments). The dataset was unbalanced and therefore the LMM was estimated using REML (REsidual Maximum Likelihood). A normal distribution was assumed for ι and ρ and analysis of residuals supported this assumption. Some residual plots showed a small number of values reaching a lower limit (0) or an upper limit. Residuals showed a significant departure from a normal distribution for σ , therefore a Poisson distribution was assumed and σ was analyzed using a GLMM (Generalized Linear Mixed Model).

Sensitivity analysis

In order to gain insight into possible causal effects for any differences between observed and predicted epidemics, the influence of individual resistance components, the parameter deposition efficiency, and initial inoculum level on the shape of disease progress curves were studied. Environment-pathogen interactions were not simulated so that the influence of the parameters of interest on model results was separated from the influence of the weather. In order that this assumption did not result in rapid epidemic development, which could obscure subtle changes in disease progress curves arising from model manipulations, parameters defining a resistant host-pathogen interaction were selected for analysis. Measured parameter values for cultivar Aziza and isolate IPO428-2 (results section; Table 4), together with assumed standard values of $\lambda = 5$ days (latent period) and $\delta = 1$ (deposition efficiency, -), and an initial severity level, γ , of 10 lesions per plant provided the values for the “standard” epidemic. Additional necrosis caused by girdling of leaves and stems by lesions was not simulated. Plot size was fixed at 3.75 x 3.75 m in accordance with the field data used to validate temporal model predictions (see field experiments section below). The simulated plot was padded with a large border of non-crop area (isolated plot) in order to facilitate net loss of spores from the spatial domain (see solution of spatial phenomena section). Parameters δ , γ , ι , ρ , and σ were varied in turn over a range of -/+ one order of magnitude, whereas λ ranged between 2 and 7 days.

In some plant pathosystems, e.g., *Puccinia* spp. on many hosts, the pathogen causes discrete lesions that remain constricted in size over the lifespan of the host. In contrast, in potato late blight, lesions continue to expand after their initial appearance; thus, potato late blight epidemics can be abstracted to a combination of two processes: lesion expansion and the polycyclic process of lesion propagation. A further set of analyses was conducted whereby the relative importance of these two epidemic processes was demonstrated through adjustment of the value of resistance components. Parameters defining the less resistant host-pathogen interaction of cultivar Remarka and isolate IPO82001 (results section; Table 4) were selected for analysis, with assumed standard values of $\lambda = 5$ days and $\delta = 1$. Epidemics were initiated with an initial severity level, γ , of 10 lesions per plant. Additional necrosis caused by girdling of leaves and stems by lesions was not simulated. Complete dominance of the lesion expansion process was obtained by setting δ , ι , or σ to zero. Dominance of the polycyclic process was obtained by reducing ρ and increasing σ by three orders of magnitude respectively. Plot size was again fixed at 3.75 x 3.75 m and padded with a large border of non-crop area (isolated plot).

Evaluation of the spatial component of the model

The two-dimensional radial Laplace kernel used in the model is parameterized for the dispersal of *P. infestans* spores under non-irrigated conditions (Paysour and Fry, 1983). It is of interest to confirm if the kernel and the model can produce realistic rates of focal expansion for potato late blight. Such data were not collected as part of this study but a spread velocity of 3.0 m day⁻¹ was determined experimentally by Minogue and Fry (1983) for potato late blight for a susceptible cultivar not protected with fungicide. In order to replicate these field experiments exactly, the model requires cultivar-isolate specific parameters and site-specific weather data, and these are unknown. However, as the intention of this comparison is simply to evaluate if predicted focal expansion rates lie within the realm of biological plausibility, we proceeded using parameter values for cultivar Bintje and isolate IPO82001 (results section; Table 4).

An epidemic was simulated in a 1 ha field via inoculation of the center plant with 1 lesion. The field was padded with a large border of non-crop area (isolated field) in order to facilitate net loss of spores from the spatial domain (see solution of spatial phenomena section). No weather data were available so perfect weather conditions for disease were assumed. Focal radius was derived at each time step by first calculating the crop area infected. The area of the focus was determined by counting

the number of plants with a disease severity greater than 1 %, and multiplying this number by the ground area occupied by a plant. Focal radius was calculated through manipulation of the formula for the area of a circle, and the focal expansion rate determined through linear regression of focal radius on time. Radius calculations prior to day 15 were ignored in order to avoid distortion of the result created by the initial phase of focus build up.

Evaluation of temporal model predictions - field experiments

Observational data used to validate temporal model predictions came from field trials conducted in the Dutch location of Wageningen in 2002 and 2004 (Table 3). The two different inocula used in the pathogenicity studies described above (Table 2) were each assigned to a separate area of the experimental site. The two areas were separated by 5 m of bare soil, 5 m of maize and another 5 m of bare soil. Each area contained a randomized block experiment with the appropriate cultivars in three replications. Individual plots within the randomized block experiments measured 3.75 x 3.75 m and were separated by 3 m of bare soil. Plots were spray inoculated (on a wet crop) with 300 ml of *P. infestans* sporangial suspension (1.0×10^4 sporangia ml⁻¹) just before dark on 24/6/2002 and 8/7/2004. Disease severity was assessed twice per week using a percentage scale adapted from James (1971). Experimental plots were desiccated after 35 days in 2002, and 29 days in 2004. Temperature and relative humidity measurements for the 2002 field trials came from the nearby (< 1 km) Wageningen University weather station (Haarweg). During the 2004 field trials, relative humidity and temperature were monitored using an electronic sensor (Pow 8-35VDG, Rotronic AG, Bassersdorf, Switzerland) positioned within the canopy at 0.35 m above ground level. Data were recorded every 15 minutes by a data logger (Delta-T

Table 3. Experiments used to validate the potato late blight model.

Year	n ^a	Cultivar ^b	Isolate ^c
2002	3	Agria (1), Aziza (2), Bintje (3), Remarka (4), Sante (5)	IPO428-2
	3	Agria (6), Aziza (7), Bintje (8), Remarka (9), Sante (10)	IPO82001
2004	3	Agria (11), Aziza (12), Bintje (13), Remarka (14), Sante (15)	IPO428-2
	3	Agria (16), Aziza (17), Bintje (18), Remarka (19), Sante (20)	IPO82001

^a Number of replicates.

^b The number in parenthesis identifies the epidemic. The same code is used in Fig. 4. Foliar resistance ratings according to the Dutch National variety list (scale of 1 = very susceptible to 9 = very resistant): Agria (5.5), Aziza (7.5), Bintje (3), Remarka (6.5) and Sante (4.5).

^c Table 2 gives a description of the isolates.

Devices LTD., Cambridge, UK).

Estimation of initial inoculum

Lesion count data were absent from the field data, therefore it was necessary to develop a scheme with which to estimate the initial number of lesions for the simulations, based upon severity observations. It was assumed that late blight first became observable between the last field evaluation on which no lesions were observed and the first observed severity measurement. The method of Andrade-Piedra et al. (2005) was followed to estimate the time of initiation, t_i (days), of the simulated epidemic:

$$t_i = [(t_0 + t_1) / 2] - \lambda \tag{2}$$

where t_0 = the day of the last evaluation when no disease was observable, and t_1 = the day of the first severity observation. The observed area of damage on each plant, A_{dis} (m²) at t_1 was given by:

$$A_{dis} = LAI_{t_1} A_g S_{t_1} / 100 \tag{3}$$

where LAI = leaf area index (-), A_g = the ground area of the plant (m²), calculated on the basis of planting patterns in the Netherlands as the product of the distance between plants and the distance between rows (0.3 x 0.75 m), and S = severity (%). In order to calculate the area of damage caused by a single lesion that had been growing since t_i , equation 1 was rewritten to include the additional necrotic area caused by girdling of leaves and stems by a lesion:

$$\frac{dA_t}{dt} = \alpha 2\pi\rho^2 t \left(1 - \frac{A}{K} \right) \tag{4}$$

where t = the growing time of the lesion ($t_1 - t_i$, days), and α = a constant (-) used to describe the factor of additional necrotic area (set to 2 as described previously). Integrating with respect to time provided an analytical equation describing lesion expansion and associated necrosis caused by girdling of stems and leaves:

$$A_t = K [1 - \exp(-\alpha \pi \rho^2 t^2 / K)] \tag{5}$$

The initial number of lesions, γ (-), applied to each plant in the simulated epidemics was then calculated as the quotient between the diseased area of a plant and the damage caused by a single lesion:

$$\gamma = A_{\text{dis}} / A_t \quad (6)$$

It is of fundamental importance to obtain an accurate measurement of initial disease severity when observational data are to be used for model validation. Initial severity measurements were low ($\ll 1\%$) in all the observed epidemics, and at such low levels the possibility for human error in the visual assessment of disease cannot be ignored. The model was sensitive to initial conditions, and in approximately half of the simulated epidemics, model predictions were improved by using a (larger) severity observation at a later date than t_1 to calculate γ . This meant that in certain cases, very small, initial severity estimates were assumed to be subject to human error and were set to zero: in epidemics 3, 7, 8, and 12 (Table 3), severity was assumed to be 0% for all observed values where $S \leq 0.001\%$; in epidemics 4 to 6, 14, and 15, severity was assumed to be 0% for all observed values where $S \leq 0.01\%$; in epidemic 2, severity was assumed to be 0% for all observed values where $S \leq 1\%$; and in epidemics 1 and 16, severity was assumed to be 0% for all observed values where $S \leq 2\%$.

Statistical analysis

The quality of temporal model predictions is first assessed through a graphical comparison of disease progress curves and a numerical comparison of t_5 and t_{50} points (time at which 5 and 50% severity was reached, respectively). Linear interpolation is used to determine observed and predicted t_5 and t_{50} points for each epidemic, then the mean absolute deviation, MD (days), between predicted and observed values is calculated. The performance criterion to consider the model valid for correctly predicting the shape of observed disease progress curves is that the mean t_5 and t_{50} deviations (MD) should not exceed 3 days (approximately 10% of the duration of observed epidemics).

Observed and predicted relative area under the disease progress curve (RAUDPC, %) values are also calculated (e.g. Campbell and Madden, 1990) for each epidemic and according to the criteria of Willmott (1981) a complement of summary and difference statistics are used to evaluate model performance: the mean absolute error, MAE (%); the root mean square error, RMSE (%); the systematic root mean square error, $RMSE_s$ (%); the unsystematic root mean square error, $RMSE_u$ (%); and Turchin's coefficient of prediction, C_p (-), which is a relative and bounded measure (Turchin, 2003). Turchin considers an ecological model to be "successful" if a value

between 0.4 and 0.9 is attained for the coefficient of prediction and this is used as a second performance criterion. All statistical formulae are described in the appendix.

Simulation

Observational plots were separated by 3 m of bare soil on all sides therefore simulated plots used to assess the quality of temporal model predictions are padded on all sides with a 3 m border of non-crop area. Length and width of each compartment cell in the model is set at 0.75 m (distance between rows) and 0.3 m (distance between plants) in accordance with these data. The foliage in all experimental plots was fully developed and epidemics progressed rapidly, therefore host growth is not modeled and leaf area index, LAI , is fixed at 5 in all simulations. Further simplifying assumptions are made with regard to the disease cycle. Under field conditions, with a sparse, open canopy and vigorous ventilation, a fraction of spores may escape the canopy and contribute to long distance dispersal. At the spatial scale of a micro-plot, these spores would be considered as “lost” from the system. Escape fractions are ignored in this study for two reasons. In the first instance the foliage in all observational plots was fully developed, which would reduce escape considerably. Secondly, vigorous ventilation of potato canopies was unlikely as the experimental site was surrounded on all sides by a tall, thick border of maize, and by a row of mature trees on two sides. In order to verify if this assumption was justified, an escape fraction, f_e (-), was calculated using the mechanistic model for spore escape developed by de Jong et al. (2002):

$$f_e = \exp \left[-LAI \sqrt{v_d / (\kappa u)} \right] \quad (7)$$

where v_d = deposition velocity (m s^{-1}), κ = the von Kármán constant (-), and u = wind speed (m s^{-1}). Deposition velocity is calculated as (Ferrandino and Aylor, 1985; Aylor, 1999):

$$v_d = (1 + LAI) v_s \quad (8)$$

where v_s = settling velocity (m s^{-1}), given by Gregory (1973) as 0.0085 m s^{-1} for *P. infestans* sporangia. Wind speeds were not measured within the experimental site but data from the nearby Wageningen University weather station were available (Haarweg, <http://www.met.wau.nl>). Over the course of the 2004 field experiments, wind speeds averaged 2 m s^{-1} at 2 m height. Assuming a wind speed of 1 m s^{-1} within the sheltered experimental site, and a conservative estimate that wind speeds were

half that again within each canopy at half crop height, equations 7 and 8 give an escape fraction of 2 %. This low value suggests that the assumption of no spore escape from the canopy is a useful simplification for these data. Continuing with the premise that wind speeds within the experimental site were low, and given that canopies were fully developed, a further simplifying assumption is made that all spores that disperse to another plant deposit on host tissue ($\delta = 1$).

Results

Pathogenicity experiments

The interactions between cultivar and isolates were statistically significant for ι ($p < 0.001$), ρ ($p < 0.001$), and σ ($p < 0.05$). Results for mean resistance component values and significance groupings are given in Table 4.

Sensitivity analysis

Of the six parameters investigated (δ , γ , ι , λ , ρ , σ), only four have a fundamentally different effect on the shape of disease progress curves (Fig. 1). The effect of manipulation of δ , ι , or σ on the relative growth rate of epidemics was identical. The same increase in δ , ι , or σ resulted in an identical reduction in the length of the lag period or exponential phase (defined here as the time till 5 % disease severity), and an identical increase in the steepness of the disease progress curve. This was expected as all three parameters exert an influence on the number of new lesions formed in the next generation; σ affects the number of spores that are produced and hence arrive at a new site, δ affects the number that deposit on leaf tissue, and ι affects the fraction of deposited spores that germinate. In terms of their effect on the shape of disease progress curves, these three parameters can thus be grouped together into a single “propagation parameter,” where the aggregate effect depends not so much on the value of each single parameter as on their product.

Manipulation of ρ resulted in the largest deviations from the standard curve (Fig. 1). Changes in the value of this parameter had a major effect on the length of the lag period and the steepness of the disease progress curve. This was also expected since ρ represents the radial growth rate of lesions and therefore affects the areal growth rate quadratically (van Oijen, 1992b). Moreover, the value of ρ also affects the rate of production of new lesions.

Table 4. Mean infection efficiency (ι), radial lesion growth rate (ρ), and sporulation intensity (σ) of five potato cultivars inoculated with two *Phytophthora infestans* isolates from the Plant Research International collection in the Netherlands^a

Fitness component ^b	Cultivar ^c	Isolate IPO428-2 ^d		Cultivar	Isolate IPO82001	
		Mean ^e			Mean	
ι ($\times 10^{-2}$)	Agria	3.29	a	Bintje	3.12	a
	Bintje	2.65	b	Remarka	2.97	b
	Remarka	2.35	b	Sante	2.84	b
	Sante	2.04	b c	Aziza	2.21	b
	Aziza	0.07	c	Agria	1.01	b
ρ ($\times 10^{-3}$)	Agria	5.09	a	Bintje	4.76	a
	Bintje	4.75	b	Remarka	3.92	b
	Sante	3.14	b	Sante	3.39	b
	Remarka	2.71	c	Aziza	3.05	b c
	Aziza	0.30	c	Agria	1.70	c
σ ($\times 10^8$)	Bintje	2.31	a	Bintje	4.55	a
	Sante	1.99	a	Aziza	3.47	a b
	Remarka	1.49	a	Remarka	3.42	b c
	Agria	1.42	a	Sante	2.60	b c
	Aziza	0.57	a	Agria	1.63	c

^a Inoculated leaflets were placed in petri-dishes containing 10 ml 2 % water agar, incubated at 15°C in the dark for 24 hours, followed by a 16 hour photoperiod.

^b ι (-); ρ (m day⁻¹); σ (# m⁻²).

^c Foliar resistance ratings according to the Dutch National variety list (scale of 1 = very susceptible to 9 = very resistant): Agria (5.5), Aziza (7.5), Bintje (3), Remarka (6.5) and Sante (4.5).

^d Isolates are described in Table 2.

^e Data came from seven laboratory experiments: two in 2002, three in 2003 and two in 2004. Within the separate experiments, each petri-dish containing one potato leaflet was considered a replicate. Four replicate leaflets per experiment were used to determine ι and ρ in 2002 and 2004. Five replicate leaflets per experiment were used to determine ι and ρ in 2003. σ was determined using 2 replicate leaflets in all five experiments. Within each resistance component, means followed by the same letter are not significantly different according to a t-test ($\alpha = 0.05$).

The latency period, λ , also plays a role in the polycyclic process but its effect on disease progress curves was minimal in comparison with the other parameters tested (Fig. 1). As λ was increased, the lag period lengthened and the steepness of the curve reduced very slightly. This was expected as when λ is longer, the exponential growth rate of an epidemic decreases (van der Plank, 1963). The reason λ had a seemingly minimal effect in comparison to the propagation parameters δ , ι , and σ , is because it was varied over a narrow, but realistic range; λ would have to be very short for a

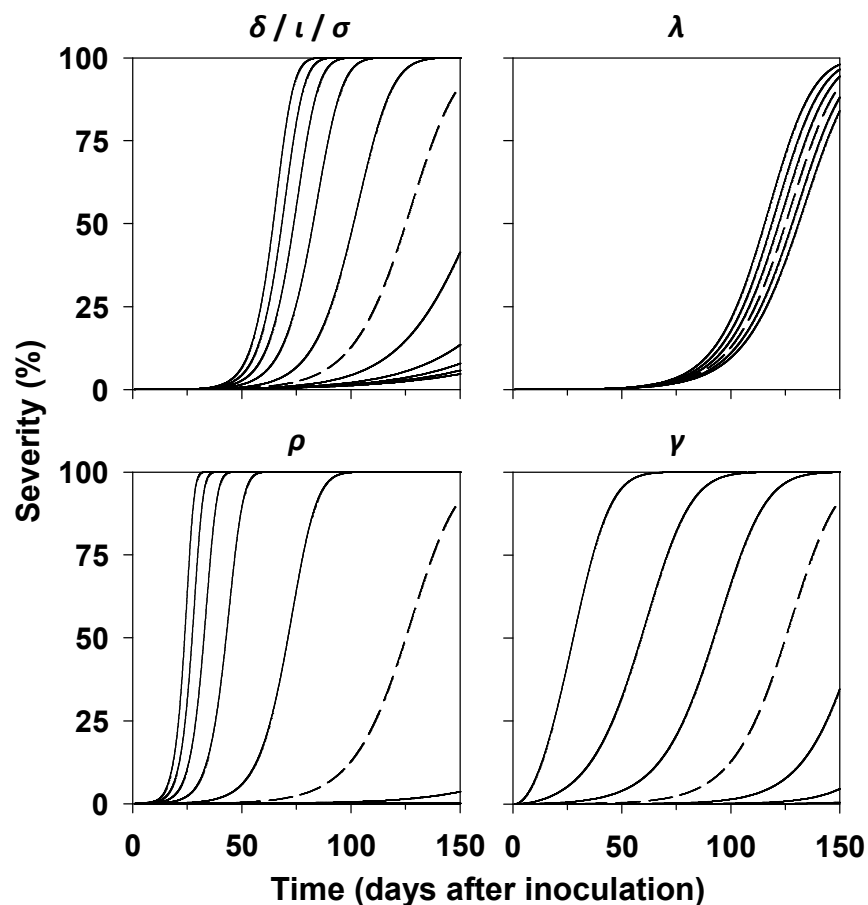


Fig. 1. Sensitivity of predicted disease severity to model parameters and initial conditions: δ = deposition efficiency (-), ι = infection efficiency (-), σ = sporulation intensity ($\# \text{ m}^{-2}$), ρ = lesion growth rate (m day^{-1}), λ = latent period (days), and γ = initial number of lesions per plant (-). Disease progress curves for the “standard” genotype” (dashed lines) produced using parameter values for the interaction between potato cultivar Aziza and isolate IPO428-2 (Table 4) with assumed standard values of $\lambda = 5$ days, $\delta = 1$, and $\gamma = 10$ lesions per plant. Disease progress curves for hypothetical genotypes (solid lines) produced by varying either δ , ι , σ , ρ or γ over a range of $-/+$ one order of magnitude, or λ between 2 and 7 days. Simulated plots were 3.75×3.75 m and isolated from external sources of inoculum with a large border of non-crop area.

change in the order of one or two days to have a significant effect on the rate of epidemic development. Furthermore, lesion expansion (as determined by ρ) gives rise to new inoculum in a shorter time than the cycling through latent periods (Lannou et al., 1994).

The effect of γ on the shape of the disease progress curve was slightly different from the other parameters (Fig. 1). Lesions act independently of one another in the exponential phase of an epidemic; thus an increase in the initial number of lesions did

not alter the relative growth rate of the epidemic. The shape of the disease progress curve was therefore unaltered; the increased lesion input only quickened the onset of the epidemic and shifted the disease progress curve to the left on the time-axis.

Two extreme examples of a disease progress curve are illustrated in Fig. 2. The first curve represents a *Phytophthora* strain with no local spore production. It is assumed that the initial inoculum came from an external source and that the polycyclic process of reproduction and establishment of new lesions is effectively shut off. This was achieved by setting either δ , ι , or σ to zero. Thus, the pure consequences of lesion expansion are realised, resulting in a gentle s-shaped curve with a short lag period, that is very rounded in the terminal phase. Alternatively, for a *Phytophthora* strain that has very little lesion expansion, the polycyclic process - involving reproduction and establishment of new lesions - dominates the epidemic progress curve, as for a rust disease. To produce the second curve, the contribution of lesion expansion was attenuated by reducing ρ to a minimal amount, and dominance of the polycyclic process increased by boosting sporulation via the parameter σ . Thus, the epidemic was driven by the formation of new lesions as opposed to the growth of existing lesions. Lesion expansion could not be switched off completely due to the model assumption that lesions have no area immediately after completion of the infection process. This near exponential process, plotted on a linear scale, yields a curve with a long lag period followed by a sudden "explosion" towards 100 % infection. These two curve types can be thought of as the extreme end points of the range of shapes of disease progress curve that can be observed in nature.

Evaluation of the spatial component of the model

Focal radius increased linearly with time and focal velocity reached a constant value of 2.7 m day⁻¹ (Fig. 3). This compares well with the velocity of 3.0 m day⁻¹ determined experimentally by Minogue and Fry (1983), indicating that the spatial component of the model is operating within the bounds of reality.

Evaluation of temporal model predictions

Based on a visual assessment, the disease progress curves generated by the model were a reasonably accurate fit of the observed epidemics in the field (Fig. 4). Observed and predicted t_5 and t_{50} points, and RAUDPC are presented in Table 5. The mean (absolute) difference, MD, between observed and predicted t_5 points was 2.3 days with a slightly higher mean difference of 2.7 days for observed and predicted t_{50}

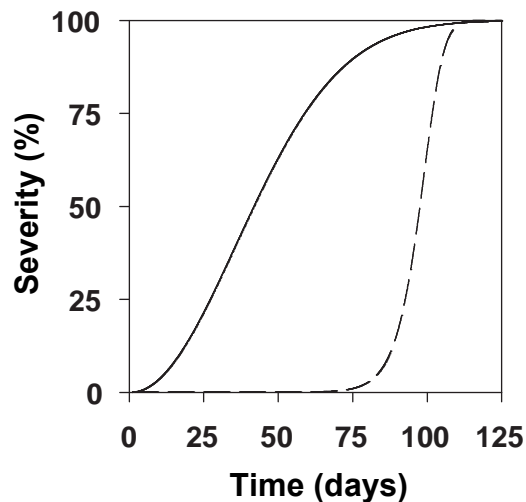


Fig. 2. Division in the effect of resistance components on disease progress curves of potato late blight epidemics. Simulated disease progress curves were obtained by manipulating measured parameter values for the interaction between potato cultivar Remarka and isolate IPO82001 (Table 4). Complete dominance of the lesion expansion process (solid line) is obtained by setting deposition efficiency (δ , -), infection efficiency (ι , -), or sporulation intensity (σ , # m^{-2}) to zero. Dominance of the polycyclic process of lesion propagation (dashed line) is obtained by reducing radial lesion growth rate, ρ (m day^{-1}), and increasing σ by three orders of magnitude respectively. Simulated plots were 3.75×3.75 m and isolated from external sources of inoculum with a large border of non-crop area. Epidemics were initiated with $\gamma = 10$ lesions per plant.

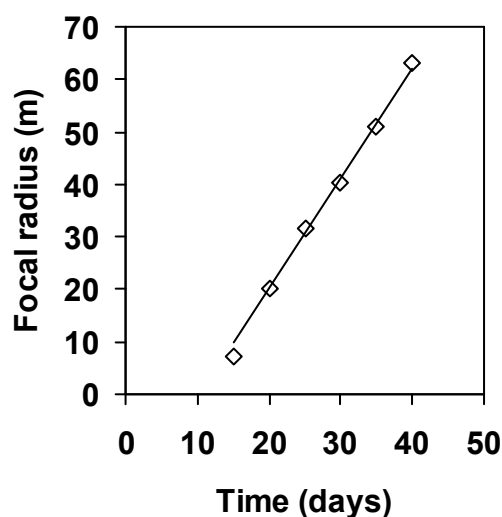


Fig. 3. Radial expansion of a simulated potato late blight focus. Parameter values for the interaction between potato cultivar Bintje and isolate IPO82001 were used (Table 4), with $\lambda = 5$ days, $\delta = 1$, and $\gamma = 1$ lesion on the center plant in the field. Field size was approximately 1 ha. The solid line is a linear regression of calculated focus radius on time (ignoring the initial phase of focus build up): $y = 2.7x - 25.07$, $R^2 = 0.99$.

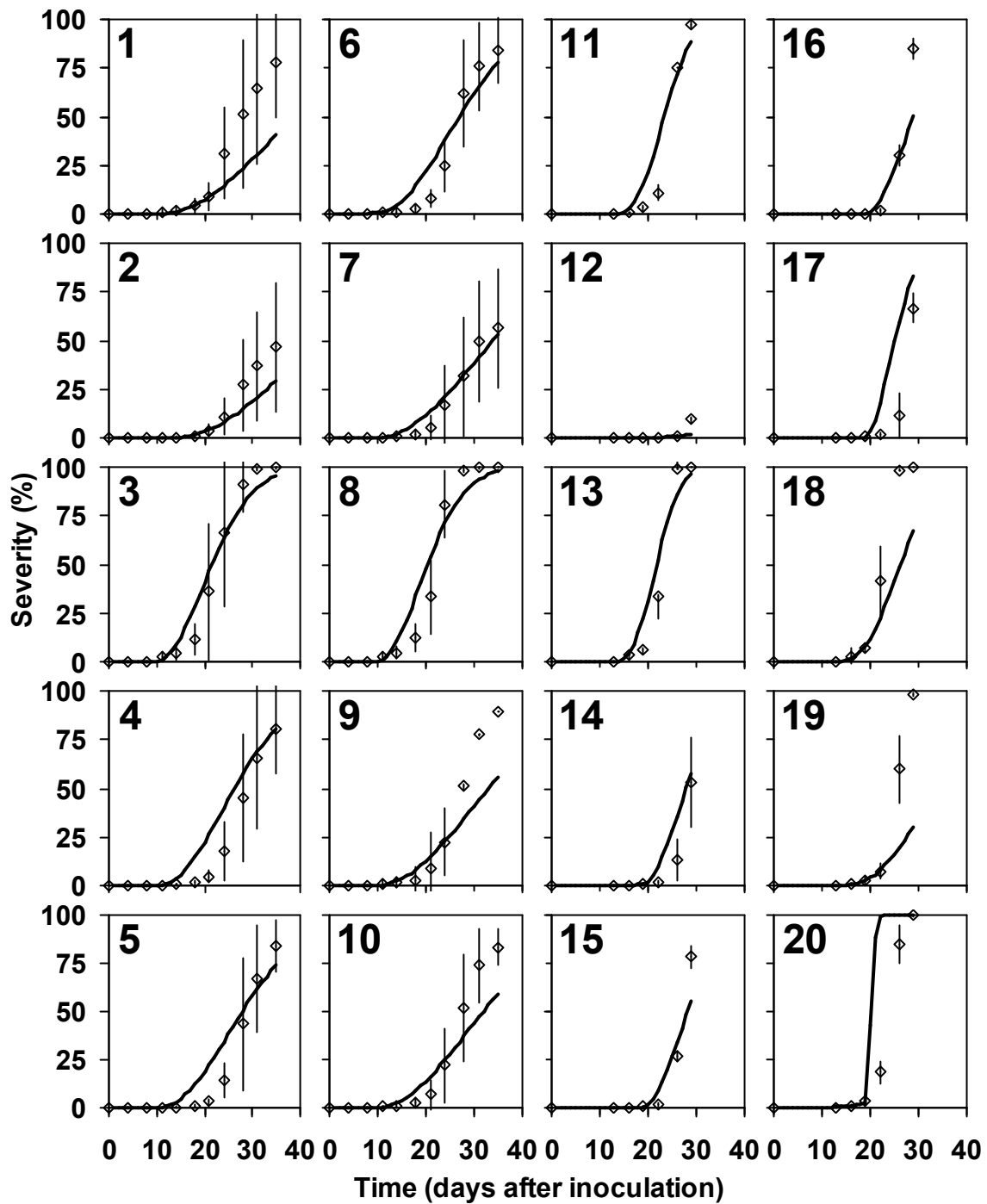


Fig. 4. Observed (\diamond) and predicted (—) disease progress curves of potato late blight epidemics under field conditions in the Netherlands in 2002 and 2004. Vertical lines represent the standard deviation of the observed mean blight severity. Table 3 provides a description of each epidemic as identified by the panel numbers.

Table 5. Observed (O) and predicted (P) t_5 and t_{50} values (time until 5 and 50 % severity, respectively), and relative area under the disease progress curve (RAUDPC, %) values for 20 potato late blight epidemics in the Netherlands.

Code ^a	t_5 (days)		t_{50} (days)		RAUDPC (%)	
	O	P	O	P	O	P
1*	18.5	18.3	23.2	28.8	20.7	10.4
2*	21.5	21.8	27.5	33.0	10.6	6.5
3	14.4	12.9	22.4	21.6	36.2	36.6
4	21.1	14.7	28.7	26.3	18.1	25.2
5	21.5	15.2	28.9	28.0	17.7	22.1
6	19.3	14.3	26.7	26.9	22.2	24.4
7	21.0	16.3	26.2	34.0	13.7	14.7
8	14.1	12.5	22.0	20.4	38.5	40.0
9	19.0	16.0	27.9	33.0	21.5	15.7
10	19.8	15.8	27.8	32.0	20.5	16.8
11	19.7	16.7	24.5	23.3	15.9	19.6
12*	26.1	26.7	-	-	0.6	0.2
13	17.8	16.1	23.0	21.8	22.1	24.5
14	23.2	20.9	28.8	27.9	4.6	8.3
15	22.5	21.1	27.4	28.2	7.6	7.8
16	22.5	21.4	27.1	28.9	8.2	6.9
17	23.3	20.3	28.1	25.1	5.1	13.6
18	17.3	17.8	22.6	26.2	23.2	12.9
19*	20.5	20.6	23.3	27.6	13.5	5.0
20	19.4	19.0	23.9	20.2	18.1	30.7

^a Code used to identify the epidemic. Epidemics are described in Table 3. The same code is used in Fig. 4.

* In epidemics 1, 2, and 19, predicted disease progress curves failed to reach 50 % disease severity therefore observed and predicted t_{25} values (time until 25 % severity is reached) are given for comparison. In epidemic 12, predicted and observed disease was limited and t_1 values (time until 1 % severity is reached) are given for comparison.

points (Table 6). Both these values were within the predefined threshold criterion of 3 days, therefore the model is judged to be valid in terms of correctly predicting the timing of observed disease progress. Further examination of summary measures reveals that there is no significant bias in model predictions ($\bar{P} \approx \bar{O}$), and that the model is able to predict the variability contained in the observations ($s_p \approx s_o$). $RMSE_u$ is close in value to $RMSE$, and the proportion of $RMSE$ that can be attributed to systematic errors ($RMSE_s^2/RMSE^2$) is very low at 0.01, confirming that the model is able to predict most of the major trends and patterns in observed RAUDPC. A value of 0.6 was obtained for Turchin's coefficient of prediction, C_p (Table 6). This fell within

Table 6. Quantitative measures of model performance

Summary univariate statistics ^a						OLS coeff. ^b		Difference measures ^c				
MD ₅	MD ₅₀	\bar{O}	\bar{P}	s _o	s _p	a	b	MAE	RMSE	RMSE _s	RMSE _u	C _p
2.3	2.7	16.9	17.1	9.6	10.7	0.9	1.5	4.6	5.9	0.7	5.8	0.6

^a Mean absolute deviation, MD (days), calculated using equation A1 in the appendix. MD₅ and MD₅₀ give the mean deviation between observed and predicted t_5 and t_{50} values respectively (time until 5 and 50 % severity). \bar{O} and \bar{P} (%) are the mean observed and predicted RAUDPC (%), and s_o and s_p (%) are the standard deviations for observed and predicted RAUDPC. Observed and predicted t_5 and t_{50} values and RAUDPC are given in Table 5 (n = 20).

^b Ordinary least squares regression of predicted on observed RAUDPC, where a = y-intercept of the linear regression (%) and b = slope of the linear regression (-).

^c Mean absolute error, MAE (%); root mean square error, RMSE (%); systematic root mean square error, RMSE_s (%); unsystematic root mean square error, RMSE_u (%); and Turchin's coefficient of prediction (Turchin, 2003), C_p (-), calculated on observed and predicted RAUDPC using equations A2 to A6 in the appendix.

the range defined as a second performance criterion ($0.4 \leq C_p \leq 0.9$), therefore overall model performance was judged to be acceptable.

Discussion

A spatio-temporal model of the potato late blight pathosystem was updated with cultivar-isolate specific parameters, environment-pathogen relations, and a new analytical equation describing lesion expansion and associated necrosis. These modifications were made to in order to extend the domain of applicability of the model from theory development to more applied questions. Sensitivity analyses with the updated model revealed a dichotomy in the epidemiological effects of fitness parameters of *P. infestans*, providing two useful reference curves with which to diagnose epidemics. The model predicted rates of focal expansion that closely approximated observed values in the literature and also predicted disease progress curves that closely matched observational data for a number of cultivar-isolate combinations. Thus, the model is able to translate measured resistance components, weather data and initial conditions into realistic epidemics, confirming its utility as a tool in the analysis and diagnosis of epidemics.

Simulation experiments to improve understanding about the effect of model parameters and initial conditions on the shape of disease progress curves revealed that each separate resistance component does not provide a unique mechanism for influencing the shape of disease progress curves; the six parameters (δ , γ , ι , λ , ρ , σ) used in this study present only four alternatives for altering the shape of curves (Fig. 1). Furthermore, it is apparent that a fixed latent period for all cultivar-isolate interactions is a useful simplifying assumption as disease progress was relatively insensitive to changes in its value. Separation of the epidemic processes of lesion expansion and lesion propagation provided two useful reference curves (Fig. 2) with which to formulate hypotheses regarding observed and predicted epidemics. Using these reference curves, it would appear that observed epidemics in 2004 were dominated to a greater degree by lesion propagation, relative to epidemics in 2002 (Fig. 4). The model predicted 3 blight days (days that are suitable for infection) during the course of the 2002 experiments, and 7 blight days over the duration of the 2004 field experiments, therefore it seems plausible that this effect is weather related.

The dispersal kernel used in the model has exponentially bounded tails and as such is said to be “thin-tailed.” Integrodifference equations that use thin-tailed kernels typically possess “traveling wave” solutions, where spread occurs in a wave like manner and a constant rate of expansion is approached (Kot et al., 1996). A second class of disease expansion has dispersive epidemic waves; i.e., a wave with an ever-increasing frontal velocity. Dispersive waves can be produced when dispersal kernels are “fat-tailed,” i.e., when the kernel does not have exponentially bounded tails (e.g., Minogue, 1989; Ferrandino, 1993). Mechanistic, statistical and meteorological arguments have been proposed for both types of disease expansion and it is common in plant pathology and epidemiology to fit both fat-tailed (e.g., negative power law) and thin-tailed (e.g., negative exponential) kernels to dispersal data. With specific regard to potato late blight, Minogue and Fry (1983) found that spread velocity was constant over time therefore the traveling wave concept and the use of thin tailed kernels seems appropriate for the model described in this study. This observed constancy could, however, be related to the limited temporal and spatial scales of their experiments (Madden et al., 2007). Kot et al. (1996) provide an excellent overview on the use of dispersal kernels to describe spatial population expansion.

Empirical data on the survival of detached sporangia reveal that most spores are killed within 1 hour on sunny days, but many survive for several hours on cloudy days (Mizibuti et al., 2000; Sunseri et al., 2002). Such information suggests a wide range of

possible dispersal distances. The only study in the literature that provides hard evidence of long-distance dispersal is by Zwankhuizen (1998), who established that *P. infestans* sporangia from a refuse pile infected potato fields up to 900 m away. This suggests that it would be of relevance, and interest, to simulate potato late blight in interconnected networks of host fields. A long-distance spore dispersal and deposition submodel has recently been added to the model presented here, in addition to host growth, fungicide and spore survival submodels, creating a spatially explicit, multi-scale model of the pathosystem. It is our intention that this model will be used to identify and evaluate promising new management strategies for the regional management of potato late blight. The development and validation of the long distance spore dispersal and deposition model is the subject of a future paper.

Appendix

Mean absolute deviation between predicted and observed t_5 and t_{50} points is given by:

$$MD = \frac{1}{n} \sum_{i=1}^n |P_i - O_i| \quad (A1)$$

where P_i and O_i are the predicted and observed t_5 or t_{50} points for the i th epidemic.

For the following statistics, P_i and O_i are the predicted and observed RAUDPC for the i th epidemic. The summary statistics mean prediction and mean observation, \bar{P} and \bar{O} , and the standard deviations of predictions and observations, s_p and s_o , are calculated according to formulae found in any standard statistics book. The MAE is calculated as:

$$MAE = \frac{1}{n} \sum_{i=1}^n |P_i - O_i| \quad (A2)$$

The RMSE is given by:

$$RMSE = \left[\frac{1}{n} \sum_{i=1}^n (P_i - O_i)^2 \right]^{0.5} \quad (A3)$$

MAE and RMSE provide a measure of the total deviation of predicted RAUDPC from observed RAUDPC.

Ordinary least squares regression of P_i on O_i is used to calculate $RMSE_s$ and $RMSE_u$ as follows:

$$RMSE_s = \left[\frac{1}{n} \sum_{i=1}^n (\hat{P}_i - O_i)^2 \right]^{0.5} \quad (A4)$$

$$RMSE_u = \left[\frac{1}{n} \sum_{i=1}^n (P_i - \hat{P}_i)^2 \right]^{0.5} \quad (A5)$$

where $\hat{P}_i = a + bO_i$ and $a = y$ -intercept of the linear regression and $b =$ slope of the linear regression. The $RMSE_s$ is a measure of the deviation of the linear regression line from the one to one line and therefore indicates systematic bias. The $RMSE_u$ is a measure of the random deviation around the regression line. Since the system is conservative for the squared values of these measures (i.e., $RMSE^2 = RMSE_s^2 + RMSE_u^2$), they can be used to calculate the proportions of the RMSE arising from systematic and unsystematic errors.

Turchin's coefficient of prediction, C_p (-), is used to assess overall model performance (2003):

$$C_p = 1 - \frac{\sum_{i=1}^n (P_i - O_i)^2}{\sum_{i=1}^n (\bar{O} - O_i)^2} \quad 0 \leq C_p \leq 1 \quad (A6)$$

C_p describes how much better a model does compared with using the mean observation as a simple forecaster. The closer C_p is to one, the higher the accuracy of the prediction.

Acknowledgements

Funding for this study was provided by the Dutch Ministry of Agriculture, Nature Management and Fisheries through the Umbrella Plan Phytophthora (DWK 427). We thank Wilbert Flier, Trudy van den Bosch, Petra van Bekkum and Henry van Raaij from PRI for their various roles in planning and executing the field and laboratory experiments. Thanks also to Jacques Withagen from PRI for his help in all matters statistical.

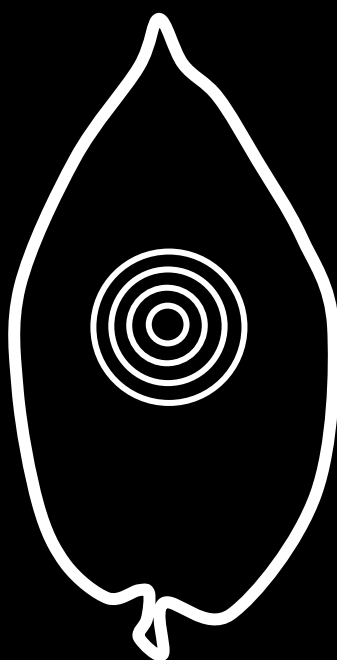
References

- Aylor, D.E. 1999. Biophysical scaling and the passive dispersal of fungal spores: relationship to integrated pest management strategies. *Agr. Forest Meteorol.* 97:275-292.
- Andrade-Piedra, J.L., Hijmans, R.J., Juarez, H.S., Forbes, G.A., Shtienberg, D., and Fry, W.E. 2005. Simulation of potato late blight in the Andes. II: Validation of the LATEBLIGHT model. *Phytopathology* 95:1200-1208.
- Black, W., Mastenbroek, C., Mills, W.R., and Peterson, L.C. 1953. A proposal for an international nomenclature of races of *Phytophthora infestans* and of genes controlling immunity in *Solanum demissum* derivatives. *Euphytica* 2:173-240.
- Campbell, C.L., and Madden, L.V. 1990. Introduction to plant disease epidemiology. John Wiley & Sons, New York.
- de Jong, M.D., Bourdôt, G.W., Powell, J., and Goudriaan, J. 2002. A model of the escape of *Sclerotinia sclerotiorum* ascospores from pasture. *Ecol. Model.* 150:83-105.
- Ferrandino, F.J. 1993. Dispersive epidemic waves: I. focus expansion within a linear planting. *Phytopathology* 83:795-802.
- Ferrandino, F.J., and Aylor, D.E. 1985. An explicit equation for deposition velocity. *Boundary. Meteorol.* 31:197-201.
- Flier, W.G., and Turkensteen, L.J. 1999. Foliar aggressiveness of *Phytophthora infestans* in three potato growing regions in the Netherlands. *Eur. J. Plant Pathol.* 105:381-388.
- Forster, M., and Sober, E. 1994. How to tell when simpler, more unified, or less ad-hoc theories will provide more accurate predictions. *Brit. J. Philos. Sci.* 45:1-35.
- Gregory, P.H. 1973. The microbiology of the atmosphere. Wiley, pp. 377.
- Goedhart, P.W., and Thissen, J.T.N.M. 2006. Biometris Genstat Procedure Library Manual 9th edition. PRI Biometris, the Netherlands.
- Hirst, J.M. 1953. Changes in atmospheric spore content: Diurnal periodicity and the effects of weather. *T. Brit. Mycol. Soc.* 36:375-393.
- Hyre, R.A. 1950. Spore traps as an aid in forecasting several downy mildew type diseases. *Plant Dis. Rep., Supplement* 190:14-18.
- James, C. 1971. A manual of assessment keys for plant diseases. Canada Department of Agriculture. Publication No. 1458.
- Kot, M., Lewis, M.A., and van den Driessche, P. 1996. Dispersal data and the spread of invading organisms. *Ecology* 77:2027-2042.
- Lannou, C., de Vallavieille-Pope, C., and Goyeau, H. 1994. Host mixture efficacy in disease control: Effects of lesion growth analyzed through computer-simulated epidemics. *Plant Pathol.* 43:651-662.
- Madden, L.V., Hughes, G., and van den Bosch, F. 2007. The study of plant disease epidemics. The American Phytopathological Society, St. Paul, Minnesota, USA.

- Malcolmson, J.F., and Black, W. 1966. New R genes in *Solanum demissum* Lindl. and their complementary races of *Phytophthora infestans* (Mont.) de Bary. *Euphytica* 15:199-203.
- Minogue, K.P. 1989. Diffusion and spatial probability models for disease spread. In: Jeger, M.J. (Ed.), *Spatial components of plant disease epidemics*. Prentice Hall, Englewood Cliff, NJ, pp. 127-143.
- Minogue, K.P., and Fry, W.E. 1983. Models for the spread of plant disease: some experimental results. *Phytopathology* 73:1173-1176.
- Mizubuti, E.S.G., Aylor, D.E., and Fry, W.E. 2000. Survival of *Phytophthora infestans* sporangia exposed to solar radiation. *Phytopathology* 90:78-84.
- Neubert, M.G., Kot, M., and Lewis, M.A. 1995. Dispersal and pattern formation in a discrete-time predator-prey model. *Theor. Popul. Biol.* 48:7-43.
- Paysour, R.E., and Fry, W.E. 1983. Interplot interference: A model for planning field experiments with aerially disseminated pathogens. *Phytopathology* 73:1014-1020.
- Rotem, J., Cohen, Y., and Putter, J. 1970. Relativity of limiting and optimum inoculum loads, wetting durations, and temperatures for infection by *Phytophthora infestans*. *Phytopathology* 61:275-278.
- Skelsey, P., Rossing, W.A.H., Kessel, G.J.T., Powell, J., and van der Werf, W. 2005. Influence of host diversity on development of epidemics: an evaluation and elaboration of mixture theory. *Phytopathology* 95:328-338.
- Sunseri, M.A., Johnson, D.A., and Dasgupta, N. 2002. Survival of detached sporangia of *Phytophthora infestans* exposed to ambient, relatively dry atmospheric conditions. *Am. J. Potato Res.* 79:443-450.
- Swallow, W.H. 1987. Relative mean squared error and cost considerations in choosing group size for group testing to estimate infection rates and probabilities of transmission. *Phytopathology* 77:1376-1381.
- Turchin, P. 2003. *Complex population dynamics: a theoretical/empirical synthesis*. Princeton University Press, Princeton.
- van der Plank, J.E. 1963. *Plant diseases: epidemics and control*. Academic Press Inc, New York.
- van Oijen, M. 1992a. Evaluation of breeding strategies for resistance and tolerance to late blight in potato by means of simulation modeling. *Neth. J. Plant Pathol.* 98:3-11.
- van Oijen, M. 1992b. Selection and use of a mathematical model to evaluate components of resistance to *Phytophthora infestans* in potato. *Eur. J. Plant Pathol.* 98:192-202.
- Willmott, C.J. 1981. On the validation of models. *Phys. Geog.* 2:184-194.
- Zaag, D.E. van der. 1956. Overwintering en epidemiologie van *Phytophthora infestans*, tevens enige nieuwe bestrijdingsmogelijkheden. Ph.D. thesis, Landbouwhogeschool Wageningen.
- Zwankhuizen, M.J. 1998. Development of potato late blight epidemics: disease foci, disease gradients, and infection sources. *Phytopathology* 88:754-763.

Zwankhuizen, M.J., and Zadoks, J.C. 2002. *Phytophthora infestans's* 10-year truce with Holland: a long-term analysis of potato late-blight epidemics in the Netherlands. *Plant Pathol.* 51:413-423.

CHAPTER 4



Scenario Approach for Assessing the Utility of Dispersal Information in Decision Support for Aerially Spread Plant Pathogens, Applied to *Phytophthora infestans*

P. Skelsey¹, W.A.H. Rossing², G.J.T. Kessel³, and W. van der Werf¹

¹ Wageningen University, Department of Plant Sciences, Crop and Weed Ecology Group, P.O. Box 430, 6709 RZ Wageningen, The Netherlands.

² Wageningen University, Department of Plant Sciences, Biological Farming Systems Group, P.O. Box 9101, 6709 PG Wageningen, The Netherlands.

³ Plant Research International, P.O. Box 16, 6700 AA Wageningen, The Netherlands.

Phytopathology (*in press*)

Abstract

Opportunities exist to improve decision support systems through the use of dispersal information gained from epidemiological research. This may lead to a reduced and more targeted chemical input. Dispersal and demographical information is, however, often fragmentary in plant pathology, and this uncertainty creates a risk of inappropriate action whenever such information is used as a basis for decision making. In this paper a scenario based simulation approach is used to evaluate where the use of dispersal information in decision making could be beneficial, and where it carries greatest risk of crop and economic losses to the farmer. The potato late blight pathosystem (*Phytophthora infestans* - *Solanum tuberosum*) was used as a case study. A recently validated spatio-temporal potato late blight model was coupled to submodels for crop growth, tuber dry matter production and fungicide efficacy. The yield response of a range of management scenarios to a single influx of primary inoculum (the initial spore load) was calculated. Damage curves (relative yield loss versus initial spore load) were produced for four potato varieties, representing extremes of resistance/susceptibility and early/late maturity types, in conjunction with four fungicide management regimes and two different spatial distributions of initial spore load. These curves were used to classify the various management scenarios as either sensitive to initial spore load or tolerant to initial spore load, thus identifying where a high degree of accuracy would be required in dispersal information for appropriate decision making, and where a greater degree of uncertainty could be tolerated.

General epidemics, resulting from spatially homogeneous initial spore loads, responded more strongly to the size of the initial spore load than focal epidemics, resulting from an initial spot infection. Susceptible varieties responded with sizeable yield losses even at low levels of initial spore

load, regardless of the fungicide management regime used. These results indicated that for susceptible varieties (late varieties in particular), the degree of accuracy that would be required in dispersal information for appropriate decision making is unlikely to be practically attainable. The results also indicated that contrary to “folk wisdom,” spore loads of a few hundred spores m^{-2} do not lead to appreciable crop loss in resistant cultivars, and are therefore acceptable. We conclude that scope exists for including dispersal information in decision making for potato late blight with resistant potato cultivars, but not for susceptible cultivars. The modeling framework used in this study can be extended to investigate the scope for inclusion of dispersal information in decision support for other aerially transmitted pathogens.

Additional keywords: crop loss assessment, dispersal models, decision support systems

Introduction

The study of botanical epidemics has burgeoned over the last few decades, in part because of the many costs attributed to plant disease. Crop loss assessment, more specifically the study of reduction in quantity of yield in relation to disease development, has accordingly become a common theme in plant pathology. Van der Plank (1963) already clearly identified the importance of the disease:yield relationship in evaluating the consequences of plant disease epidemics, and recent decades have seen the formulation of many models of the underlying processes (e.g., James, 1974; Madden et al., 1981; Teng, 1987; Ferrandino, 1989). Most commonly studied is the relationship between disease intensity (e.g., severity, area under the disease progress curve) and yield. Less common is to relate primary inoculum to yield. The reason for doing so is intuitive; it is the exponential part of epidemic progress that is relevant for disease management, and this early phase is strongly linked to initial levels of disease and inoculum. Nonetheless, despite the documented evidence that dispersal of inoculum is a key factor in epidemics, knowledge of dispersal has scarcely been used in the development of practical decision support systems (DSS) (Jeger, 1999). This is in part due to the difficulty of collecting empirical data, and the mathematical complexity of dispersal models, but especially to prediction uncertainties stemming from the stochastic nature of dispersal processes, as a result of the idiosyncrasies of the weather and the difficulty of knowing the whereabouts of disease sources. Dispersal and demography information is therefore often fragmentary in plant pathology, creating a risk of inappropriate action whenever such information is used as a basis for decision making.

It is a common perception amongst many farmers and farm advisors that the economic threat posed by certain aerially transmitted plant diseases, e.g., potato late blight, (causal agent *Phytophthora infestans*), is so great that no disease or infection risk at all should be tolerated. “Folk wisdom” often regards that a single spore is enough to destroy a crop, but is this really the case? The damage that can be caused by arriving inoculum depends on complex interactions between source and target characteristics and environmental conditions. Key factors affecting the arrival of inoculum at a target crop include: source size, strength and location, and the weather conditions that affect release, escape, transport, deposition and survival of inoculum. Key factors affecting the degree of damage caused by this inoculum include: the amount and spatial distribution of arriving spores, weather conditions, variety properties, and the level of chemical protection at the target crop. A large number of field experiments would be required to define the relationship between primary inoculum and yield loss but epidemiological models are well suited to investigate the interaction of these risk factors.

The objective of this paper is to provide a simulation approach that can be used to assess *ex ante* if dispersal information can add value to practical DSSs for aerially transmitted pathogens. This is done by first focusing on the question of how risk from aerially transmitted pathogens depends on the amount of primary inoculum (the initial spore load) that is deposited on the target crop, using potato late blight as a model pathosystem. Risk is assessed in a series of steps. First, the expected epidemic development after deposition of a range of spore loads is calculated. Epidemic development depends on the weather, the resistance level of the cultivar, on the fungicide regime, and on the spatial distribution of initial inoculum: spot (focal epidemic) or homogeneous (general epidemic). Yield reduction is then calculated by considering the loss of light interception on healthy green foliage throughout the duration of the crop. A distinction is therefore drawn between early and late maturing cultivars, because they differ substantially in the seasonal patterns of light interception and yield formation; while early maturing varieties have a growing season of only three to four months, after which the foliage senesces naturally, late maturing varieties grow for up to seven months, giving a disease epidemic much more time to claim the foliage and cause damage. Thus, we are able to highlight the yield response to a range of spore inputs, for a given choice of cultivar resistance, maturity type, chemical protection scheme and spatial distribution of initial spore load.

Once yield reduction data are determined for a range of management scenarios, we then focus on the question of how the scope for inclusion of dispersal information in practical DSSs depends on the potential consequences of uncertainty in that dispersal information. This is achieved by presenting yield reduction data in the form of damage curves (relative yield loss versus initial spore load). The basic shape of the damage curve is used to indicate where a high degree of accuracy would be required in dispersal information and when a greater degree of uncertainty could be tolerated (Fig. 1). When the damage curve is steep, or has a discontinuity (step), uncertainties in dispersal information could result in inappropriate management decisions with sizeable consequences. When the damage curve is initially flat or very shallow, the risk from aerially transmitted pathogens is low, the consequences that may arise from uncertainties in dispersal information and subsequent inappropriate management decisions are minimal, and scope exists for inclusion of dispersal information in decision-making. Thus, using a scenario based approach, the risk from

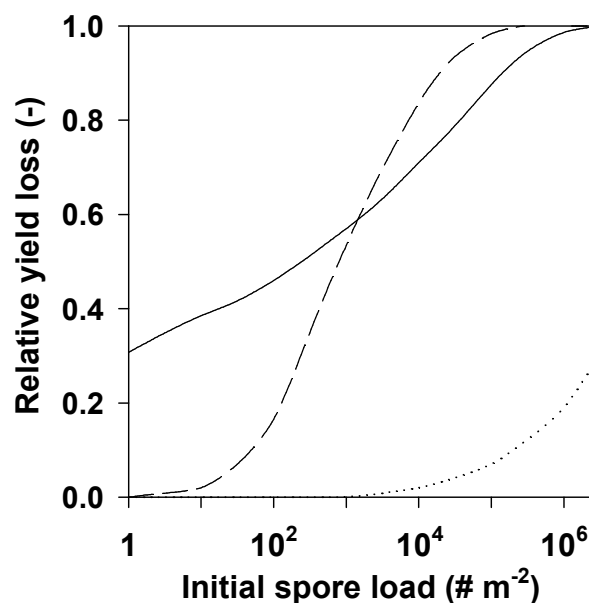


Fig. 1. A simple classification scheme for plant disease management strategies based upon the shape of damage curves. Damage curves show the relationship between yield loss (relative to final yield in a disease free crop) and primary inoculum (initial spore load) in simulated potato late blight epidemics. All epidemics were initiated with a single influx of spores. The solid line shows a sensitive response to initial spore load, where the damage curve has a large initial step. The dashed line also shows a sensitive response to initial spore load; there is no large initial step but the slope of the curve is steep. The dotted line shows a tolerant response to initial spore load, because the damage curve is initially flat over a wide range of spore loads.

aerially transmitted pathogens can be determined for a given choice of cultivar resistance, maturity type, chemical protection scheme and spatial distribution of initial spore load, and management conditions can be identified where there is scope for the inclusion of dispersal information in decision making.

Theory and approaches

The spatio-temporal/integrodifference equation model of the potato late blight pathosystem developed by Skelsey et al. (2005) simulates the life cycle of the pathogen, as well as the temporal and spatial development of general and focal late blight epidemics for various scales and patterns of host genotypes. The novel contribution of this model is its ability to capture spatial relationships in the potato late blight pathosystem, and Fig. 2 illustrates how the spatial development of potato late blight epidemics can be classified on a scale ranging from focal to general depending on the spatial distribution of primary infections. Spatial relationships are implemented in the model using a radial Laplace kernel (Skelsey et al., 2005) for the dispersal of spores. Parameter values for the kernel used here were taken from Paysour and Fry (1983), where experimental data were used to develop and validate a negative exponential kernel for the dispersal of *P. infestans* sporangia. The model is intended as a research tool and was designed for generating and testing hypotheses relating to epidemiological theory; more specifically the influence of host diversity on the development of epidemics. Recently, the original model was extended with weather relationships and laboratory experiments were used to derive quantitative components of resistance for a number of potato cultivar-isolate combinations (Skelsey et al., *in press*). The model was then validated against data from field trials in 2002 and 2004 with five potato cultivars and two isolates in Wageningen, the Netherlands (Skelsey et al., *in press*).

In this study the model is extended to include the growth of the potato host plant and the influence of fungicide applications. As a research tool, the primary value of this model is heuristic, therefore, based on the principles of parsimony (e.g., Turchin, 2003) and transparency, simple logistic-type equations are implemented as models for foliage growth and fungicide use, and a simple linear function of light interception describes tuber dry matter production. The most important extensions to the model are described below. Table 1 provides a summary of symbol definitions and units.

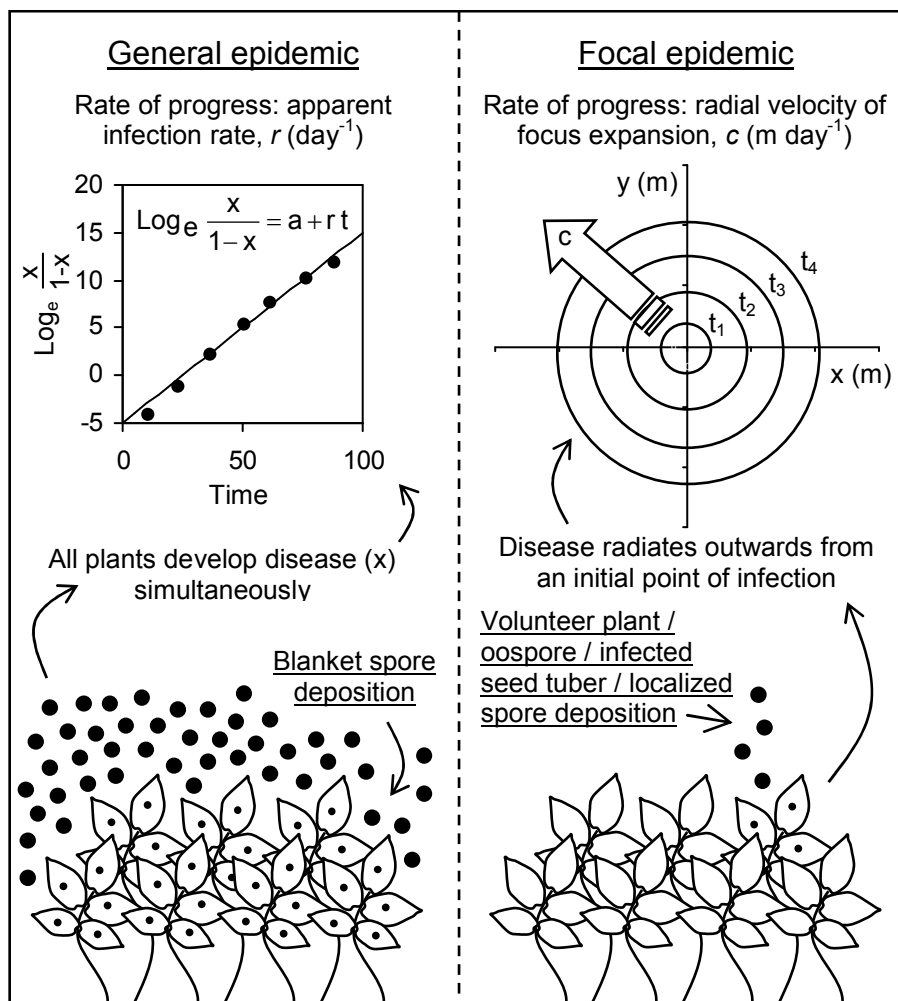


Fig. 2. Illustration of the differences between general and focal potato late blight epidemics.

Weather data

In this study, historical weather data from the Wageningen University Meteorostation in Wageningen, the Netherlands are used. These data-sets cover a ten year span: 1994 and 1996-2004 (data for 1995 were incomplete). The influence of climatic conditions on the pathosystem is characterized with hourly measurements of the following meteorological variables: temperature ($^{\circ}\text{C}$), global radiation, i.e., the sum of direct and diffuse shortwave radiation ($\text{MJ m}^{-2} \text{h}^{-1}$), and relative humidity (%).

Crop model

In this study, two levels of cultivar resistance are combined with two types of maturity class. Resistance level affects the growth rate of epidemics, while maturity class determines the growth duration of the crop and hence the period of time the

Table 1. Symbols used in this study

Symbol	Units	Description
f_e	-	Escape fraction
f_h	- ^a	Fraction of healthy tissue
k_l	-	Light extinction coefficient
l	-	Relative yield loss
LAI	-	Leaf area index
LAI_m	-	Maximum attainable leaf area index
r_d	(°C day) ⁻¹	Relative death rate
r_g	(°C day) ⁻¹	Relative growth rate
R_g	MJ m ⁻²	Daily amount of incoming global radiation
R_L	MJ m ⁻²	Daily amount of global radiation intercepted by green foliage
$R_{L,c}$	MJ m ⁻²	Cumulative global radiation intercepted by green foliage since the moment of tuber initiation
t	days	Time
t_a	days	Time of the last fungicide application
t_d	°C days	Growing degree days
t_{50}	days	Time after a fungicide application at which l reaches half of its maximum value
u	m s ⁻¹	Wind speed
v_d	m s ⁻¹	Deposition velocity
Y	tons (DM) ha ⁻¹	Final yield
Y_0	tons (DM) ha ⁻¹	Final yield in a disease free crop
α	-	Shape factor
β	-	Shape factor
δ	-	Deposition efficiency
l	-	Infection efficiency
l_{max}	-	Maximum infection efficiency
l_{min}	-	Minimum infection efficiency
I	days	Infectious period
κ	-	von Kármán constant (0.35)
λ	days	Latent period
ρ	m day ⁻¹	Radial growth rate of lesions
σ	# m ⁻²	Sporulation intensity
U	g MJ ⁻¹	Light use efficiency

^a - signifies that the defined quantity is dimensionless.

epidemic can grow. General growth characteristics of early and late maturing cultivars were described using parameter values that lie well within the generally accepted range for these variety types. Although late maturing cultivars are generally more resistant in practice than early maturing cultivars, resulting in a confounding of the effects of maturity type on epidemic development and time available for the pathogen to cause damage, the effects of maturity type and resistance level can be

studied in isolation in a modeling framework. This separation of resistance level and growth duration in the scenario studies allows greater insight into which factors are responsible for crop response to variety traits in relation to infection by *Phytophthora infestans*. Cultivar-isolate specific interactions are characterized in the model using three quantitative components of resistance: infection efficiency (ι , -), radial lesion growth rate (ρ , m day⁻¹), and sporulation intensity (σ , # m⁻²). These were measured on potato leaflets in the laboratory, providing parameter values for a susceptible and resistant cultivar (Skelsey et al., *in press*). The latent period (λ , days) is fixed at 5 days and the infectious period (l , days) at 1 day for all cultivars. The model has been validated against observed epidemics using these parameter values (Skelsey et al., *in press*). Early maturing and late maturing cultivars have a different maximum leaf area index, LAI_m (-), but the same relative growth and death rates. A complete listing of model parameters for simulation of different cultivars is given in Table 2.

Leaf area development is simulated through thermal time accumulation, by computing the growing degree days, t_d (°C days), as the positive difference between the (average daily) temperature and a base temperature of 2°C below which leaf growth stops (van Keulen and Stol, 1995). Leaf area is initialized at 155 cm² plant⁻¹ (Spitters et al., 1989), and leaf area expansion is calculated as a function of t_d according the Richards equation (Richards, 1959):

Table 2. Model parameters for potato variety types distinguished in this study

Maturity class	Early	Late
Date of emergence	May 1	May 1
Date of harvest	July 31	Sep 30
Onset of leaf shedding (°C days)	500.00	1000.00
Tuber initiation (°C days)	150.00	350.00
LAI_m (-) ^a	3.00	6.00
α (-)	1.00	0.60
r_g (°C day) ⁻¹	0.02	0.02
r_d (°C day) ⁻¹	0.01	0.01
ν (g MJ ⁻¹)	1.10	1.00
Level of partial resistance	Susceptible	Resistant
ι (-)	3.12×10^{-2}	1.00×10^{-2}
l (days)	1.00	1.00
λ (days)	5.00	5.00
ρ (m day ⁻¹)	4.76×10^{-3}	1.70×10^{-3}
σ (# m ⁻²)	4.55×10^8	1.64×10^8

^a - signifies that the defined quantity is dimensionless.

$$\frac{dLAI}{dt_d} = r_g LAI \left[1 - \left(\frac{LAI}{LAI_m} \right)^\alpha \right] \quad (1)$$

where r_g ($^{\circ}\text{C day}^{-1}$) is the relative leaf growth rate during exponential growth, LAI (-) is the leaf area index, LAI_m (-) is the maturity class specific maximum attainable leaf area index, and α (-) is a shape factor used to control the speed at which the function approaches its plateau, and thus, the shape of the growth curve. The shape parameter is used to ensure that both early and late maturing cultivars require the same amount of time to reach a fully developed canopy. Parameter r_g is set to 0.02 ($^{\circ}\text{C day}^{-1}$) for all cultivars.

Degree days accumulate over time to provide a temperature sum and leaf area will continue to grow until the temperature sum reaches a maximum cultivar specific value (estimated as 500°C days for early maturing cultivars and $1000^{\circ}\text{C days}$ for late maturing cultivars), at which point net leaf growth becomes net leaf death and the shedding of leaves follows a logistic function of t_d :

$$\frac{dLAI}{dt_d} = -r_d LAI \left(1 - \frac{LAI}{LAI_m} \right) \quad (2)$$

where r_d ($^{\circ}\text{C day}^{-1}$) is the relative leaf death rate, set to 0.01 ($^{\circ}\text{C day}^{-1}$) for all cultivars. Leaf area index is maintained near its maximum value for some time before leaf shedding begins, as is typical of growth patterns occurring in the field. Shedding affects all tissue types equally, i.e., shedding results in equal, proportional loss of healthy, latent, infectious, and necrotic areas. Green leaf area duration is reduced not only by the coverage of leaf area by lesions, but also because lesions can “girdle” stems and cause additional necrotic areas in non-infected leaf tissue; during the epidemic, an increase in latent area is assumed to cause an equal increase in the loss of the non-lesion covered leaf area (Skelsey et al., *in press*; van Oijen, 1992). Leaf lesion coverage and areas of necrotic leaf tissue caused by *P. infestans* are assumed to be distributed homogeneously throughout the canopy.

Early and late maturing varieties also differ in the moment of tuber initiation (estimated as 150°C days for early maturing cultivars and 350°C days for late maturing cultivars). Concomitant to tuber initiation, under the assumption of equal profiles of healthy and blighted leaf tissue over canopy depth, the interception of solar radiation is calculated using Lambert-Beer’s law:

$$R_L = f_h R_g [1 - \exp(-k_l LAI)] \quad (3)$$

where R_L (MJ m^{-2}) is daily intercepted radiation, f_h (-) is the fraction of healthy tissue, R_g (MJ m^{-2}) is the daily incoming global radiation, and k_l (-) is the light extinction coefficient, set to 1 (Haverkort and Kooman, 1997). R_L is integrated over the time and multiplied with the average light use efficiency for tuber dry matter production to give the tuber dry weight of the crop (Haverkort and Harris, 1987):

$$Y = \nu R_{L,c} \times 10^{-2} \quad (4)$$

where Y (tons (DM) ha^{-1}) is tuber yield, ν (g MJ^{-1}) is the light use efficiency for tuber dry matter and global radiation, $R_{L,c}$ (MJ m^{-2}) is the cumulative intercepted global radiation since tuber initiation, and the final term is a conversion factor. On the basis of experimental results, early varieties were assigned light use efficiencies of 1.1 g MJ^{-1} and late varieties 1.0 g MJ^{-1} (van Oijen, 1992).

Leaf area index also determines the fraction of spores that can escape the potato canopy and be made available for long range transport; the remaining fraction is assumed to be deposited back onto the crop to contribute to local epidemic development. The mechanistically derived model of de Jong et al. (2002) is used to provide an estimate of the escape fraction, f_e (-), as a function of LAI , the deposition velocity of *P. infestans* sporangia, v_d (m s^{-1}), and wind speed, u (m s^{-1}). The remaining fraction is used to define the deposition efficiency, δ (-), of spores back onto the crop:

$$\delta = 1 - f_e = 1 - \exp \left[-LAI \sqrt{v_d / (\kappa u)} \right] \quad (5)$$

where κ (-) is the von Kármán constant (0.35). According to Gregory (1973), a settling velocity for *P. infestans* sporangia of 0.0085 m s^{-1} and a deposition velocity equal to three times the settling velocity is assumed, giving a fixed value of 0.0255 m s^{-1} for v_d . A constant wind speed of 2 m s^{-1} is also assumed to be representative of wind speed at crop height (during dispersal events) in the Netherlands.

Fungicide model

Late blight management is simulated with protectant fungicides, which decrease the infection efficiency, ι (-), of sporangia. As an alternative to modeling the concentration of the active ingredient on the leaf, a Weibull function is used to simulate the application and decay of fungicides via their effect on ι :

$$\iota = \iota_{\min} \quad t = t_a$$

$$l = l_{\min} + \frac{l_{\max} - l_{\min}}{1 + [t_{50} / (t - t_a)]^\beta} \quad t > t_a \quad (6)$$

where l_{\min} (-) is the value l drops to immediately after an application, t (days) is time, t_a (days) is the time of the last fungicide application, l_{\max} (-) is the maximum value for the cultivar, t_{50} (days) is the time after application at which l is halfway restored after the drop caused by the application, and β (-) is a shape factor. Parameter values were chosen so as to represent the effects (level of protection, typical decay rate) of Shirlan (active ingredient fluazinam) on the leaves: l_{\min} is set to 1 % of l_{\max} , t_{50} is set to 9 days and β is set to 20 (H.T.A.M. Schepers, *personal communication*). The infection efficiency calculated with equation 6 is then adjusted to account for the growth of new, unprotected leaves which further reduce the efficacy of the fungicide treatment:

$$l = \min \left\{ l_{\max}, \frac{LAI \ l + \Delta LAI \ l_{\max}}{LAI + \Delta LAI} \right\} \quad (7)$$

where ΔLAI (-) is the increase in leaf area index since the last application of fungicides.

Simulation

Space is represented explicitly as a two-dimensional grid, in which each cell represents a potato plant. Based upon planting patterns in the Netherlands, the length of the side of a compartment cell is set at 0.75 m (distance between rows) and the width of each compartment cell at 0.3 m (distance between plants). In each simulation experiment the field size is fixed at 76.8 x 48 m, and contains a pure-line population of one of the four variety types. Host plants are linked through dispersal of spores and we describe where spores land with a 2-dimensional radial Laplace dispersal kernel, which describes the probability distribution of landing locations of spores in the two-dimensional plane (Skelsey et al., 2005). As described in Skelsey et al. (2005), spatial phenomena in the model are solved by performing convolutions between spatial distributions of spores and dispersal kernels. Convolutions are implemented in the model via fast Fourier transforms; a technique that greatly enhances the speed and accuracy of the numerical solution of the model. Spatial distributions (i.e., a kernel and a spore distribution) are transformed into the Fourier domain, multiplied, and the result is back-transformed into the spatial domain. This solution method requires periodic boundary conditions, therefore Fourier domain

arrays are duplicated an infinite number of times to the left, right, top and bottom. This means that each edge of the array is connected to the opposite edge of an identical array, leading to “wrap-around” effects, whereby any spore dispersing outside of the field’s borders will “reappear” on the opposite edge of the field when spatial distributions are back-transformed into the spatial domain. This artifact of the solution methodology can be used to provide a representation of high background inoculum levels (Skelsey et al., 2005) or interplot interference (Skelsey et al., *in press*). Alternatively, isolated fields can be simulated by “zero-padding” spatial distributions with a large border of “non-crop” area prior to convolution (Skelsey et al., 2005). Spores that are redistributed by the kernel into the non-crop area do not contribute to epidemic development. This prevents wrap-around effects and facilitates spore loss from the system. In this study, all simulated fields are isolated in this manner. Thus, apart from the initial inoculum, there is no further influx of spores into the field. Simulations are stopped when the overall percentage of visibly diseased (sporulating plus necrotic) foliage reaches 5 %, in order to simulate compulsory destruction of the haulm according to Dutch directives for *Phytophthora* control.

Final yield is chosen as the model output of relevance in this study because it is the relevant criterion in decision support. Unfortunately, it was not possible to incorporate tuber infection in this study as there is insufficient data with which to model the process. In order to assess the influence of spore load on final yield, general and focal epidemics are simulated in each of the four variety types, and for four different fungicide regimes. The number of spores that arrive at a target crop and initiate an epidemic depends on several factors, such as distance and air flow between source and target, the number of spores released at the source, the dilution of the spore cloud by the combined effects of advection and turbulence, and the loss of spores by deposition and death during flight (Aylor, 1986). Fifteen different levels of initial spore load are used as input data: 0, 1×10^0 , 3×10^0 , 1×10^1 , 3×10^1 , 1×10^2 , 3×10^2 , 1×10^3 , 3×10^3 , 1×10^4 , 3×10^4 , 1×10^5 , 3×10^5 , 1×10^6 , and 3×10^6 spores m^{-2} . Logarithmic series are used as the relevant range of spore loads is large. These densities are translated to an equivalent spore dose per plant; general inoculation proceeds with the application of the appropriate spore dose to each plant in the field, whereas for focal inoculation, only a central 3 x 3 block of nine plants in the field receives this dose. Inoculation occurs once, on the first suitable day for potato late blight as determined by the weather relationships in the model. In this study, the initial spore load is assumed to come from a distant source of infection; thus, each simulation experiment begins with a non-diseased crop. In order to demonstrate that

the selected range of initial spore loads used lies within the realm of possible spore fluxes that occur in nature, data from field experiments (Aylor, 2001) were considered; aerial concentrations of *P. infestans* sporangia were measured directly above infected potato canopies and a maximum total value of approximately 35,000 sporangia m⁻³ was recorded. Assuming a worst case scenario, in which all these spores were viable, this value can be considered to lie at the extreme limit of possible aerial concentrations of viable spores arriving at a target field, and after multiplication with the settling velocity of *P. infestans* sporangia, 0.0085 m s⁻¹ (Gregory, 1973), a flux density of around 2.5 x 10⁷ spores m⁻² day⁻¹ is arrived at, slightly higher than the highest value of initial spore load used in this study. The four variety types used as target crops in this study are: (1) early/resistant, (2) early/susceptible, (3) late/resistant, and (4) late/susceptible. The fungicide regimes are as follows: (A) no applications; (B) an adaptive regime based on the suitability of the weather for late blight, where fungicides can be applied immediately prior to any infection event, with a restriction that the minimum interval between designated applications is 5 days; (C) an adaptive regime, as in (B) but the first application is missed; and (D) a fixed schedule, where fungicides are applied every 7 days. This makes a total of 16 different management scenarios (4 cultivars x 4 fungicide regimes) and 480 epidemic scenarios (16 management scenarios x 15 spore fluxes x 2 epidemic types: general and focal). In order to investigate the influence of variation in climatic conditions on model results, each epidemic scenario is repeated using a different meteorological data-set from the 10 years available. This makes a total of 4800 simulation experiments (480 epidemic scenarios x 10 years of meteorological data).

Data treatment

Model predictions for final yield in each of the 480 epidemic scenarios are averaged over the 10 years of meteorological input data. The resultant (averaged) final yields, Y (tons (DM) ha⁻¹), are used to calculate the loss in yield relative to the disease free yield:

$$\ell = \frac{Y_0 - Y}{Y_0} \quad (8)$$

where ℓ (-) is the relative yield loss and Y_0 is the (average) final yield obtained with a disease free crop. These data are presented on semi-log plots of relative yield loss against log of initial spore load (damage curves).

Results

Three example epidemics, differing only in the initial amount of inoculum, are used in order to illustrate the mechanism by which an increase in initial spore load results in a reduction in final yield (Fig. 3). Lesions act independently of one another in the exponential phase of an epidemic therefore an increase in initial spore load only affects the starting density of the disease; it does not alter the relative growth rate of the epidemic or the shape of the disease progress curve. The increased spore input thus shifts the disease progress curve to the left on the time-axis (Fig. 3A). As earlier epidemic onset means that (according to Dutch regulations) farmers must destroy the haulm earlier in the season, there is less time available for foliage growth (Fig.

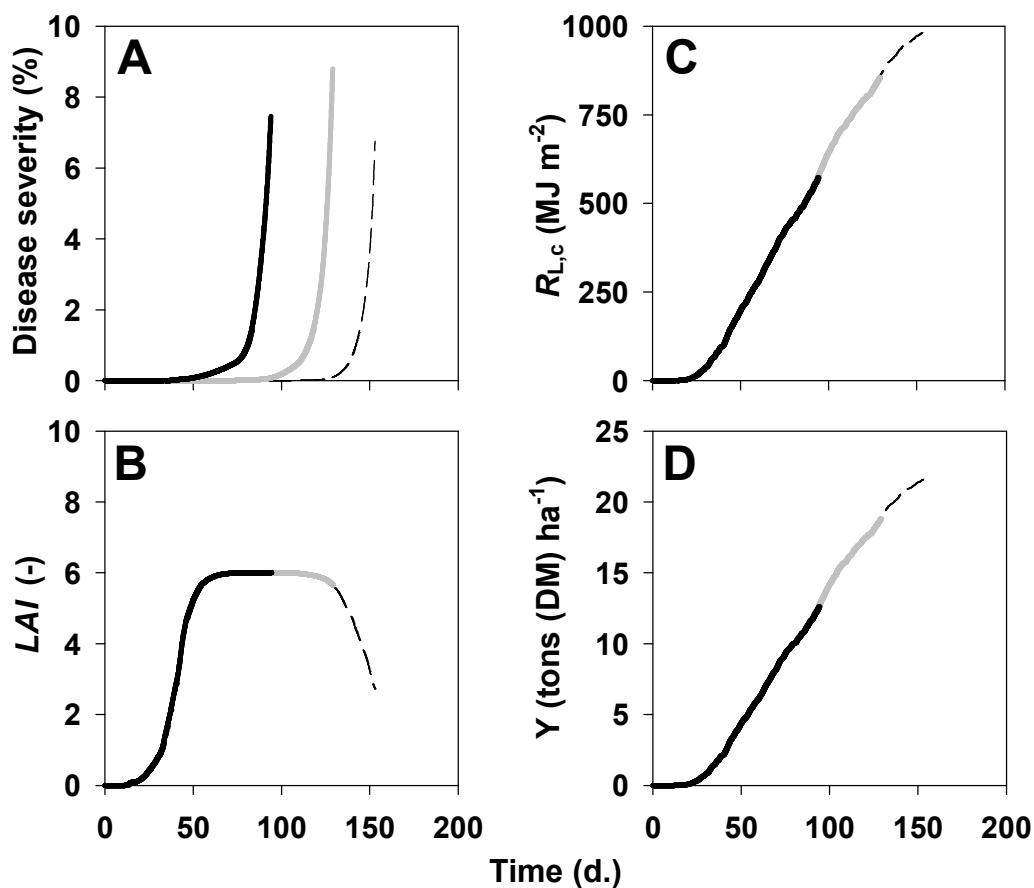


Fig. 3. Mechanism by which an increase in initial spore load (three line types) results in a decrease in final yield in the spatio-temporal model of the potato late blight pathosystem: A = epidemic increase; B = leaf area index dynamics; C = cumulative radiation interception by foliage; and D = dry matter accumulation in tubers. Higher levels of initial spore load are indicated by lines of increasing intensity.

3B). Less foliage means that less light can be intercepted (Fig. 3C) resulting in a decrease in the production and allocation of photosynthetic products to the tubers (Fig. 3D).

A frequency histogram is given to show the number of infection events in each of the 10 growing seasons, as determined by observed weather in Wageningen (1994, 1996 to 2004) in combination with the weather relationships (Fig. 4). Also shown is the number of fungicide applications under fungicide regime B (adaptive) in each growing season. The highest number of infection events in any year was 23 (1994 and 2001), the lowest number was 7 (1996) and the average over the 10 years was 15. It can be seen that the number of infection events differs widely between years, illustrating the importance of epidemic simulation over a wide and representative diversity of conditions. The maximum number of fungicide applications in any year was 12 (1994 and 2000), the minimum number was 5 (1996) and the average number of applications per growing season was 9. This is in stark contrast to the 20 applications that are simulated under the 7 day fixed spray schedule (regime D).

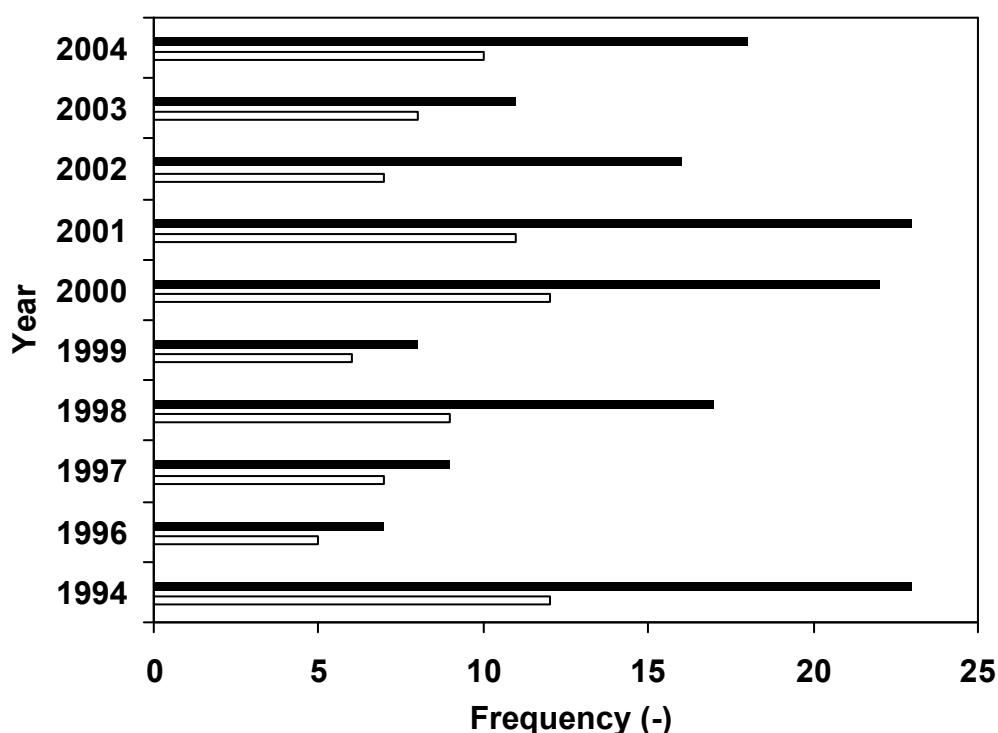


Fig. 4. Number of Infection events (solid bars) and fungicide applications (open bars) under an adaptive spray regime (regime B) in 10 growing seasons (May 1st to Sep 30th), as calculated by the spatio-temporal model of the potato late blight pathosystem using weather data from Wageningen University Meteorstation in Wageningen.

Predicted damage curves are grouped for resistant and susceptible cultivars (Figs. 5 & 6 respectively). Relative yield loss increased more rapidly in response to changes in initial spore load when the spatial distribution of initial inoculum was homogeneous (general epidemic) as opposed to focal (focal epidemics). This is because few plants are acting as initial sources of infection in the field in a focal epidemic, in contrast to general epidemics where every plant in the crop is an initial source. A focal epidemic must therefore progress in time and space before the entire field is infected whereas in a general epidemic, increase in disease is essentially temporal. Early variety types were less responsive to changes in initial spore load than late variety types, as early maturing cultivars escape part of the epidemic by

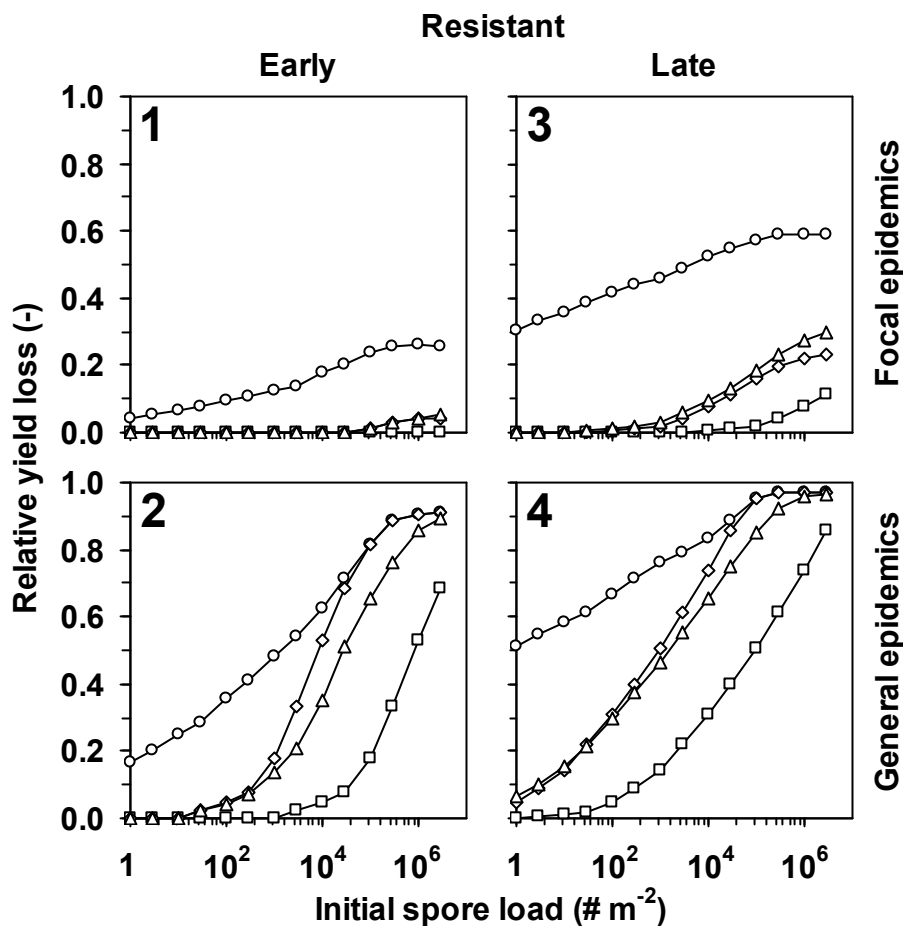


Fig. 5. Relationship between yield loss (relative to final yield in a disease free crop) and primary inoculum (initial spore load) in simulated potato late blight epidemics in resistant cultivars. Panels 1 and 3 indicate focal epidemics, while panels 2 and 4 indicate general epidemics. Panels 1 and 2 are for an early maturing cultivar, while panels 3 and 4 are for a late maturing cultivar. In each panel, four fungicide regimes are compared: \square = adaptive; \diamond = adaptive with the first spray missed, \triangle = 7 day fixed schedule; and \circ = no applications.

completing a greater fraction of their tuber filling before the disease causes premature net foliage death. Susceptible varieties responded with greater yield losses than resistant varieties, and an initial spore load of 1 spore m⁻² was enough to result in yield loss in all susceptible management scenarios. The slope of the damage curve was generally shallower for susceptible varieties as a result of relatively large initial yield losses at the lowest level of spore input tested. A further explanation is that initial differences in resistance level and yield response diminished as spore loads became increasingly overwhelming. Fungicide regime B (adaptive) was always the most effective of the four simulated regimes as applications always occurred

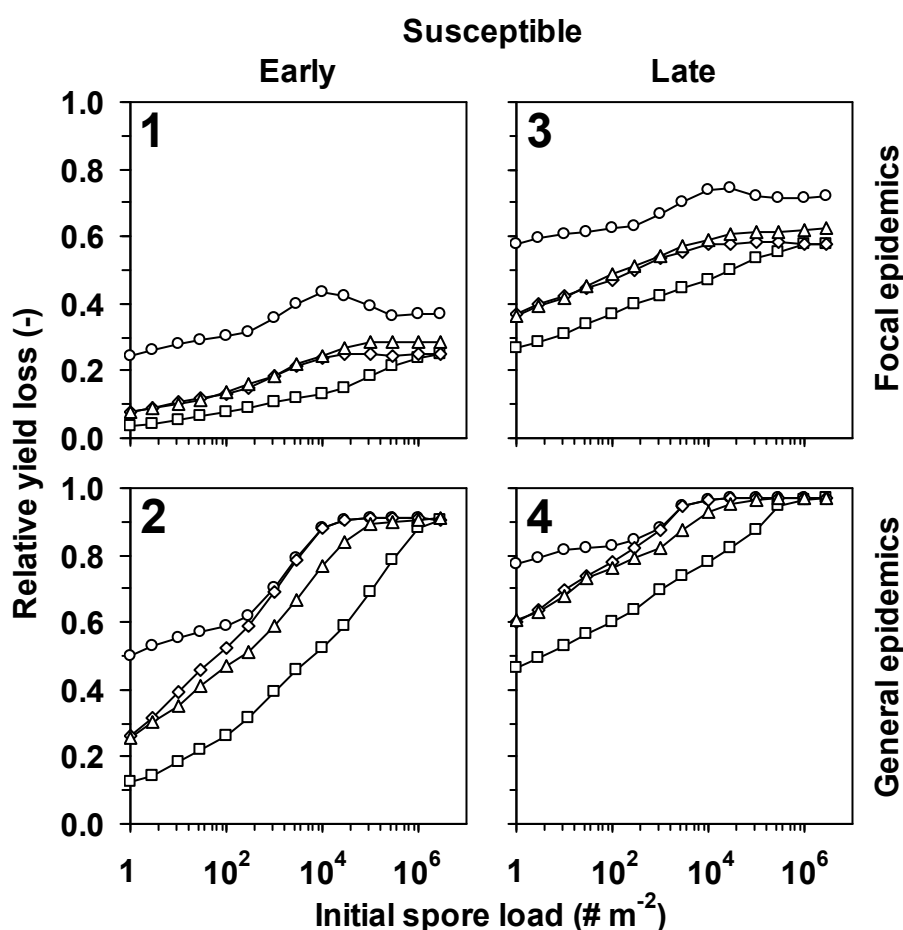


Fig. 6. Relationship between yield loss (relative to final yield in a disease free crop) and primary inoculum (initial spore load) in simulated potato late blight epidemics in susceptible cultivars. Panels 1 and 3 indicate focal epidemics, while panels 2 and 4 indicate general epidemics. Panels 1 and 2 are for an early maturing cultivar, while panels 3 and 4 are for a late maturing cultivar. In each panel, four fungicide regimes are compared: □ = adaptive; ◇ = adaptive with the first spray missed, △ = 7 day fixed schedule; and ○ = no applications.

immediately prior to the deposition of primary inoculum (and any subsequent infection event, provided the minimum spray interval had been exceeded). However, the adaptive regime was not capable of preventing yield loss under high initial spore loads, as fungicide protection is not absolute. Under focal inoculation (Figs. 5 & 6; Panels 1 & 3), an adaptive fungicide regime with the first spray of the season missed (fungicide regime C) always provided a higher level of protection than a weekly spray regime (fungicide regime D). The reverse was true under general inoculation as every plant in the crop left unprotected subsequently became infected (Figs. 5 & 6; Panels 2 & 4).

Interestingly, under focal inoculation, an increase in initial spore load did not always lead to an increase in relative yield loss. This is a demonstration of non-linear effects in the onset of epidemics and their interaction with weather in the model; primary foci can “burn out” if the weather prevents propagation of lesions and all available healthy tissue is consumed by lesion expansion.

The steepness of the damage curves indicate the degree of importance that would be attached to obtaining accurate knowledge on dispersal for a practical DSS (Figs. 5 & 6). Whenever fungicides were used in conjunction with a resistant cultivar, damage curves were generally flat up to a level of several hundred spores m^{-2} , sometimes as high as tens of thousands of spores m^{-2} for focal epidemics. This lack of response to spore input indicates resilience to inaccuracies in forecasts of spore inputs, suggesting dispersal information could be used in decision support where resistant cultivars are concerned, without an undue increase in the risk of yield loss to the grower if the potential for spore dispersal between fields was underestimated. Susceptible varieties, and especially susceptible late varieties, suffered sizeable yield losses even at the lowest tested spore input of 1 spore m^{-2} . This indicates that it would be risky to place a heavy emphasis on dispersal information or dispersal models for management decisions with susceptible varieties, as an unrealistic level of accuracy would be required.

Discussion

The scenario based approach presented in this manuscript was used to determine the scope for inclusion of spatial information (i.e., dispersal information, dispersal modeling) in DSSs for aerially transmitted pathogens. With specific regard to the model pathogen (*P. infestans*), the results of this study provide valuable information

for potato late blight initiatives such as the Umbrella Plan Phytophthora in the Netherlands, which is part of a covenant between the Dutch Ministry of Agriculture and a grower organization LTO (Land- en Tuinbouw Organisatie). The aim of this particular initiative is to diminish the dependency on fungicides in the short-term via an increase in the efficacy of chemical treatments and improvements in DSSs, and in the long term via the development of resistant cultivars. One of the objectives of our research is to determine if atmospheric dispersion and spore survival models could be used to modify the spray recommendations of existing DSSs. Currently, almost all DSSs work on the assumption that conducive weather for disease equates to the arrival of viable inoculum at all target crops. It is possible that new decision rules that consider the effects of weather on long distance dispersal and survival of spores could prove to be effective in reducing the number of chemical applications in a growing season. This study indicates that for susceptible varieties, any DSS that places emphasis on the dispersal capabilities of the pathogen would require dispersal information at a level of accuracy that is unlikely to be practically attainable. The probability of making an inappropriate spray decision would be high and the consequences to the grower could be formidable. In contrast, the relative tolerance of resistant cultivars to primary inoculum means that there is room for uncertainty in dispersal information and the probability of making an inappropriate spray decision (with consequences) is greatly decreased. These results indicate that there exists scope for including spore load estimations in DSSs for potato late blight for resistant potato cultivars, but not for susceptible cultivars.

The contribution of this paper is to present a scenario based simulation approach that can be used to assess *ex ante* the use of dispersal information in the development and evaluation of DSSs for aerially transmitted pathogens. This approach was used with a model pathogen (*P. infestans*) to evaluate the range of spore loads that pose a threat to potato crops. Model results demonstrated an important effect of cultivar x management decisions on yield loss associated with a particular spore load, and enabled an evaluation of the potential for inclusion of dispersal information in decision support for potato late blight, in terms that matter to growers. The development and experimental validation of a DSS for potato late blight that has a field to field dispersal component is the subject of a future study.

Acknowledgements

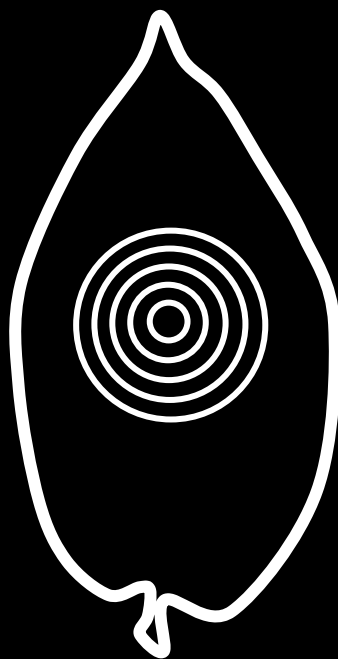
Funding for this study was provided by the Dutch Ministry of Agriculture, Nature Management and Fisheries through the Umbrella Plan *Phytophthora* (DWK 427).

References

- Aylor, D.E. 1986. A framework for examining inter-regional aerial transport of fungal spores. *Agr. Forest Meteorol.* 38:263-288.
- Aylor, D.E. 2001. Quantifying the rate of release and escape of *Phytophthora infestans* sporangia from a potato canopy. *Phytopathology* 91:1189-1196.
- de Jong, M.D., Bourdôt, G.W., Powell, J., and Goudriaan, J. 2002. A model of the escape of *Sclerotinia sclerotiorum* ascospores from pasture. *Ecol. Model.* 150:83-105.
- Ferrandino, F.J. 1989. A distribution-free method for estimating the effect of aggregated plant damage on crop yield. *Phytopathology* 79:1229-1232.
- Gregory, P.H. 1973. *The microbiology of the atmosphere*. 2nd edition. John Wiley & Sons, New York.
- Haverkort, A.J., and Harris, P.M. 1987. A model for potato growth and yield under tropical highland conditions. *Agr. Forest Meteorol* 39:271-282.
- Haverkort, A.J., and Kooman, P.L. 1997. The use of systems analysis and modeling of growth and development in potato ideotyping under conditions affecting yields. *Euphytica* 94:191-200.
- James, W.C. 1974. Assessment of plant diseases and losses. *Annu. Rev. Phytopathol.* 12:27-48.
- Jeger, M.J. 1999. Improved understanding of dispersal in crop pest and disease management: current status and future directions. *Agr. Forest. Meteorol.* 97:331-349.
- Madden, L.V., Pennypacker, S.P., Antle, C.E., and Kingsolver, C.H. 1981. A loss model for crops. *Phytopathology* 71:685-689.
- Paysour, R.E., and Fry, W.E. 1983. Interplot interference: A model for planning field experiments with aerially disseminated pathogens. *Phytopathology* 73:1014-1020.
- Richards, F.J. 1959. A flexible growth function for empirical use. *J. Exp. Bot.* 10:290-300.
- Skelsey, P., Rossing, W.A.H., Kessel, G.J.T., Powell, J., and van der Werf, W. 2005. Influence of host diversity on development of epidemics: an evaluation and elaboration of mixture theory. *Phytopathology* 95:328-338.
- Skelsey, P., Kessel, G.J.T., Rossing, W.A.H., and van der Werf, W. Parameterization and evaluation of a spatio-temporal model of the late blight pathosystem. *Phytopathology*, *in press*.

- Spitters, C.J.T., van Keulen, H., and van Kraalingen, D.W.G. 1989. A simple and universal crop growth simulator: SUCROS87. In: Rabbinge, R., Ward, S.A., van Laar, H.H., (Eds.), Simulation and systems management in crop protection. Simulation monographs, Pudoc, Wageningen, The Netherlands, pp. 147-181.
- Teng, P.S. 1987. Quantifying the relationship between disease intensity and yield loss. In: Teng, P.S. (Ed.), Crop loss assessment and pest management. APS Press, St Paul, MN, pp. 105-113.
- Turchin, P. 2003. Complex population dynamics: a theoretical/empirical synthesis. Princeton University Press, Princeton, New Jersey, 450 pp.
- van der Plank, J.E. 1963. Plant diseases: epidemics and control. Academic Press Inc, New York, 349 pp.
- van Keulen, H., and Stol, W. 1995. Agro-ecological zonation for potato production. In: Haverkort, A.J., and Mackerron, D.K.L. (Eds.), Ecology and modeling of potato crops under conditions limiting growth. Kluwer, Dordrecht, The Netherlands, pp. 357-372.
- van Oijen, M. 1992. Evaluation of breeding strategies for resistance and tolerance to late blight in potato by means of simulation modelling. Neth. J. Plant Pathol. 98:3-11.

CHAPTER 5



Development and Validation of a Quasi-Gaussian Plume Model for the Transport of Botanical Spores

P. Skelsey¹, W. van der Werf¹, and A.A.M. Holtslag²

¹ Wageningen University, Department of Plant Sciences, Crop and Weed Ecology Group, P.O. Box 430, 6709 RZ Wageningen, The Netherlands.

² Wageningen University, Meteorology and Air Quality Group, P.O. Box 47, 6700 AA Wageningen, the Netherlands.

Agricultural and Forest Meteorology 148:1383-1394

Abstract

Aerial dispersal of inoculum is the primary means of movement for many plant diseases. One of the challenges of modern decision support for plant health is to provide predictions of the influx of viable pathogen inoculum from sources outside a crop. Such prediction in a practical setting requires prediction tools that have modest computing and input requirements, yet provide sufficiently accurate predictions. In this paper a hybrid dispersion model was developed, combining Taylor's statistical theory of diffusion for horizontal dispersal with the eddy diffusion theory as implemented in the Lagrangian similarity diffusion model of Van Ulden (1978) and Gryning et al. (1983). The model was extended with a dry deposition method and an effective source strength. Model results were compared with experimental data for the transport of artificially released spores of *Lycopodium clavatum* above a potato canopy. The numerical results were in close agreement with the experimental data, which covered distances up to 100 m. Numerical predictions were compared to those produced by two alternative model versions and a previously published Gaussian plume model for the transport of spores above potato canopies. The potential for practical implementation of atmospheric dispersion models in plant disease decision support systems is discussed.

Keywords: spore dispersal, plant disease, *Lycopodium clavatum*, decision support systems

Introduction

The spread of pathogen inoculum to uninfected hosts is critical to the spatio-temporal development of plant disease epidemics. Improved computer simulation of

spore transport in heterogeneous landscapes could lead to an increased understanding of the epidemiology of many aerially transmitted diseases. An increased understanding could in turn lead to new plant disease management strategies that rely more on information and less on insurance sprays. It is the long term aim of our research to develop and use a multiple scale epidemiological model for potato late blight (causal agent *Phytophthora infestans*) to investigate (in a spatial context) operational and strategic issues pertaining to disease management. Dispersal modeling is of particular interest to potato late blight epidemiologists as empirical data on the survival of detached sporangia reveal that most spores are killed within 1 hour on sunny days, but many survive for several hours on cloudy days (Mizubuti et al., 2000; Sunseri et al., 2002). Such information suggests a wide range of possible dispersal distances. However, as the dispersal of viable inoculum depends on a complex interplay of population biological, atmospheric and spore survival processes, it is difficult to simulate.

Atmospheric dispersion models from the meteorological sciences are available as potential tools to provide a physically realistic description of the effects of atmospheric conditions on spore transport and deposition. Their use in plant pathology is not new and a number of researchers have developed spore dispersion models and validated them against experimental data (e.g., Aylor, 1989; Aylor and Flesch, 2000; Aylor et al., 2001; de Jong et al., 2002; Spijkerboer et al., 2002; Aylor, 2005; Aylor and Boehm, 2006; Bourdôt et al., 2006). The majority of this work involved validation against experimental data for the escape of spores above the canopy or for dispersal over very short distances only. The scarcity of larger scale spore dispersal data sets means that validation of spore dispersion models over distances more relevant for between-field spread of disease is relatively rare (e.g., Spijkerboer et al., 2002; Aylor and Boehm, 2006).

Gaussian plume models are immediately attractive as a simple, analytical means to describe the transport of spores; they are currently the most commonly used dispersion models to estimate the downwind impact of emission sources and are extensively tested around the world. They have modest computing and input requirements, and thus seem well suited to play a role as dispersal components in epidemiological simulation models. The Gaussian formula is derived under certain idealized conditions (steady state, horizontal homogeneity, constant wind speed, and constant eddy diffusivity) from the advection-diffusion equation for a passive scalar emitted from a point source (e.g., Pasquill and Smith, 1983; Seinfeld and Pandis, 1998). However, it was recognized as early as the 1960's by Gifford (1968), Pasquill

(1974) and others that the conventional Gaussian formula is not always applicable for low level releases. Due to the presence of a dynamically and thermodynamically active surface, the lower atmosphere, or surface layer, is a region of strong wind-shear and inhomogeneous turbulence. This means that constant wind speeds and eddy diffusivities are not realistic in the surface layer, which weakens the assumptions used to derive the Gaussian plume formula. This presents a problem for the application of Gaussian plume models in plant pathology (and other applications).

A number of researchers have investigated non-Gaussian diffusion models and compared their predictions with those of Gaussian models and experimental data (e.g., Elliot, 1961; Malhotra and Cermak, 1964; Huang and Drake, 1977; van Ulden, 1978; Nieuwstadt and van Ulden, 1978; Gryning et al., 1983; Hinrichson, 1986; Brown et al., 1992). Vertical distributions of tracer materials were observed to be of an exponential as opposed to a Gaussian form in the famous diffusion experiments of the Prairie Grass Project (Barad, 1958), the Green Glow Program (Barad and Fuquay, 1962) and the Hanford 67 diffusion experiments (Nikola, 1977). It is also not difficult to find examples in plant pathology that suggest the use of non-Gaussian diffusion models may be more appropriate for spore transport: McCartney (1990) measured exponential vertical profiles of *Pyrenopeziza brassicae* ascospores; Aylor and Qui (1996) and de Jong et al. (2002) observed vertical profiles of *Venturia inaequalis* spores that were exponential in shape; and Aylor et al. (2001) measured vertical profiles of *Phytophthora infestans* spores which were also of an exponential form.

A better description of low-level, vertical diffusion in a turbulent shear flow is given by allowing mean wind velocity and vertical eddy diffusivity to vary with height. Solution of the advection-diffusion equation with the gradient-transfer assumption requires specification of the spatial distribution of wind and eddy diffusivity, and realistic distributions of these variables generally require solution by a numerical method. However, such realistic solutions, due to their complexity and input requirements, are unsuitable as components in larger epidemic simulators. A more analytical approach is therefore necessary, where the intention is to parameterize eddy diffusivities as a function of the flow. Monin-Obukhov similarity relations provide the best means to describe the variation of eddy diffusivity with height and atmospheric stability; however, their use to represent wind speed and eddy diffusivity profiles prevents analytical solution of the advection-diffusion equation (Arya, 1999).

As early as the 1920's, the advection-diffusion equation for a ground level source was solved analytically with power laws inserted for the profiles of wind speed and

eddy diffusivity. These plume dispersion models yield vertical concentration profiles of a general exponential form. Van Ulden (1978) took such an approach, but then rewrote the power law solutions in terms of Monin-Obukhov similarity functions, giving a physically realistic description of the effect of stability on the structure of turbulence in the surface-layer. By comparing numerical results with data from the Prairie Grass experiments (Barad, 1958), he showed that vertical concentration profiles at a distance of 100 m can be well described with an exponential function of height raised to a power, s . A follow-up study by Gryning et al. (1983) yielded analytical expressions for s for both stable and unstable conditions, giving numerical predictions that compared well with the Prairie Grass experiments at distances from 50 to 800 m. The Lagrangian similarity diffusion model of Van Ulden (1978) and Gryning et al. (1983) currently still provides one of the best analytical descriptions of diffusion from a low-level source (see also Gryning et al., 1987).

In this paper we develop a hybrid, or quasi-Gaussian plume model for the dispersal of spores. The model combines Taylor's statistical theory of diffusion for horizontal dispersal with the Lagrangian similarity diffusion model of van Ulden (1978) and Gryning et al. (1983) for vertical dispersal. The potential of a non-Gaussian model for predicting and describing spore transport between fields is investigated through validation against the spore dispersal data of Spijkerboer et al. (2002). These data are particularly useful as dispersal is measured over distances up to 100 m from the source of spores. Numerical predictions are compared to two alternative model versions, and the Gaussian plume model of Spijkerboer et al. (2002) which was originally developed with these data.

Theory and approaches

Field data used for model validation

The ability of the quasi-Gaussian and Gaussian plume models to predict spore plumes was tested by calculating expected spore concentrations and assessing goodness of fit with the experimental data of Spijkerboer et al. (2002). These spore dispersal experiments were carried out in a 200 x 200 m field of potatoes in Wageningen (latitude 51°58' N, longitude 5°40' E), the Netherlands, in the summer of 1997. Spore concentrations were measured above the potato crop at up to 100 m from a point source of *Lycopodium clavatum* spores during fifteen 10 minute release sessions.

During each measurement session sporangia were released from an Erlenmeyer flask placed at crop height (0.7 m). The top of the flask was sealed and spores were released from a small aperture in the side by blowing compressed air in through a hole in the opposite side. The flask was weighed before and after each release session, and the number of spores released was calculated from the weight loss using the average number of 1.36×10^8 spores gram^{-1} (*unpublished data*).

Ten Rotorod model 20 spore traps (Sampling Technologies Inc., Minnetonka, MN, USA) were used in each session. Moreover, in most sessions, two Burkhard volumetric spore traps (Burkhard Manufacturing Ltd, Rickmansworth, Hertfordshire, England) were additionally used. Spore traps were mounted on wooden masts that were placed in a grid system of pre-dug holes in such a way that they stood in a crosswind line as much as possible. Up to four spore traps were mounted per mast, at intervals of 2 m vertically. After each measurement session, sporangia from both the Rotorod and Burkhard spore traps were counted under a microscope (x 100) with the aid of a counting reticule. These data were transformed into aerial concentrations following procedures outlined in the Rotorod and Burkhard user manuals.

Over the 15 measurement sessions, temperatures ranged from approximately 14 to 26°C, wind speeds from 2 to 8 m s^{-1} , friction velocity, u_* (calculated), from 0.1 to 0.5 m s^{-1} , and Monin-Obukhov length, L (calculated), from -1 to -520 m. Wind direction was measured on site in all fifteen measurement sessions, but wind speed and the measured temperature profiles required to calculate L were available for only three of these sessions. Measured wind speeds and temperature gradients (over grass) were available for all fifteen measurement sessions from the nearby Wageningen University weather station (Haarweg; <http://www.met.wau.nl>), 2 km southwest of the potato field. In using these data, an assumption is made that the meteorology is the same at the Haarweg site as it is at the potato field. This assumption was tested by using the models presented below to produce two sets of output data. Predictions were first made for the three measurement sessions for which on-site weather data were available; wind speeds were measured at 2 m and temperatures were measured at 4.5 and 2 m from the surface at the experimental site. Predictions were then made for all fifteen measurement sessions using wind speeds measured at 2 m and temperatures measured at 1.5 and 0.1 m at the nearby Haarweg weather station. The weather data measured on-site were fifteen minute averages whereas the off-site measurements were one hour averages.

As a reminder to the reader, the primary objective of this study is to develop and validate a spore transport model that will be used to investigate spatial aspects of the

potato late blight pathosystem (*Phytophthora infestans* - *Solanum tuberosum*). It should be noted that *L. clavatum* is a species of clubmoss that produces roughly spherical sporangia approximately 40 μm in diameter. In contrast, *P. infestans* produces “lemon-shaped” sporangia that are slightly smaller at around 30 μm . It should be expected that the aerodynamic properties of the two sporangia will therefore differ slightly. Nonetheless, *L. clavatum* sporangia are a useful substitute for dispersal experiments as they are readily available in large quantities commercially.

Dispersion models

Predictions of spore concentration were made with the following models: (1) a quasi-Gaussian plume model with no dry deposition; (2) the quasi-Gaussian plume model with the source-depletion method of Chamberlain (1953) for the dry deposition of spores; (3) the quasi-Gaussian plume model with a calibrated source-depletion method; and (4) the Gaussian plume model of Spijkerboer et al. (2002). Table 1 provides a summary of symbol definitions and dimensions.

Quasi-Gaussian plume model (QG)

In general, aerial concentration, \bar{c} ($\# \text{m}^{-3}$), at a receptor point (x, y, z) downwind from a source with an emission strength Q ($\# \text{s}^{-1}$) at $x = 0$, $y = 0$, and $z = h$ can be written as:

$$\bar{c}(x, y, z) = \frac{Q}{\bar{u}} D_y(x, y) D_z(x, z) \quad (1)$$

where h (m) is the height of the source, \bar{u} (m s^{-1}) is the mean transport velocity across the depth of the plume and D_y (m^{-1}) and D_z (m^{-1}) are the horizontal and vertical dispersion functions respectively.

Horizontal concentration distributions are assumed to be Gaussian and the crosswind dispersion function is given by:

$$D_y(x, y) = \frac{1}{\sqrt{2\pi}\sigma_y} \exp\left(-\frac{y^2}{2\sigma_y^2}\right) \quad (2)$$

where σ_y (m) is the standard deviation of concentration in the crosswind direction. This dispersion coefficient was parameterized using the Taylor (1921) model, which is widely regarded as giving the best estimation of σ_y (e.g., Arya, 1999):

Table 1. Symbols used in this study

Symbol	Units	Description
a	$\# \text{ m}^{-3}$	y-intercept of a linear regression of predicted on observed values
a_1	-	Constant in functions for dispersion parameters
a_2	-	Constant in functions for dispersion parameters
A	$-^a$	Function of shape parameter, s
b	-	slope of the linear regression of predicted on observed values
b_1	-	Constant in functions for dispersion parameters
b_2	-	Constant in functions for dispersion parameters
B	-	Function of shape parameter, s
c	-	Constant in functions for dispersion parameters
\bar{c}	$\# \text{ m}^{-3}$	Spore concentration
d	m	Displacement height
D	-	Modified index of agreement
D_y	m^{-1}	Horizontal dispersion function
D_z	m^{-1}	Vertical dispersion function
f_y	-	Function of the dimensionless travel time
F_d	$\# \text{ m}^{-2} \text{ s}^{-1}$	Dry deposition flux
g	m s^{-2}	Acceleration due to gravity (9.8)
h	m	Height of the source
K	-	Correction in σ_y and σ_z for effects of surface roughness
l	m	Particle length
L	m	Monin-Obukhov length scale
MAE	$\# \text{ m}^{-3}$	Mean absolute error
n	#	Number of observations
O	$\# \text{ m}^{-3}$	Observed spore concentration
\bar{O}	$\# \text{ m}^{-3}$	Mean observed spore concentration
p	-	Constant in functions for dispersion parameters
P	$\# \text{ m}^{-3}$	Predicted spore concentration
\bar{P}	$\# \text{ m}^{-3}$	Mean predicted spore concentration
Q	$\# \text{ s}^{-1}$	Source strength
RMSE	$\# \text{ m}^{-3}$	Root mean square error
RMSE _s	$\# \text{ m}^{-3}$	Systematic root mean square error
RMSE _u	$\# \text{ m}^{-3}$	Unsystematic root mean square error
s	-	Vertical concentration profile shape parameter
s_o	$\# \text{ m}^{-3}$	Standard deviation of observed spore concentration
s_p	$\# \text{ m}^{-3}$	Standard deviation of predicted spore concentration
t	s	Time
T_L	s	Lagrangian time scale
\bar{T}	K	Mean temperature
\bar{u}	m s^{-1}	Mean wind speed across the depth of the plume
u^*	m s^{-1}	Friction velocity
v_d	m s^{-1}	Deposition velocity
v_s	m s^{-1}	Stokes settling velocity
w	m	Particle width

Table 1 continued

Symbol	Units	Description
x	m	Downwind distance from source
x_0	m	Integration constant
y	m	Horizontal distance from plume centerline
z	m	Height above the surface
z_0	m	Surface roughness length
\bar{z}	m	Mean height of the plume
α	-	Constant in function for σ_y
β	-	Constant in function for σ_y
γ	-	Constant in function for σ_z
ε	-	Constant in function for σ_z
ϑ	K	Potential temperature
ϑ^*	-	Surface-layer temperature scale
κ	-	von Kármán constant (0.41)
π	-	Mathematical constant (3.14)
σ_u	m s^{-1}	Standard deviation of longitudinal velocity fluctuations
σ_v	m s^{-1}	Standard deviation of horizontal velocity fluctuations
σ_w	m s^{-1}	Standard deviation of vertical velocity fluctuations
σ_y	m	Standard deviation of spore concentration (crosswind direction)
$\sigma_y(t)$	m	Standard deviation of spore concentration for an averaging time, t (crosswind direction)
$\sigma_y(600)$	m	Standard deviation of spore concentration for an averaging time of 600 seconds (crosswind direction)
σ_z	m	Standard deviation of spore concentration (vertical direction)
τ	s	Travel time
φ_h	-	Non-dimensional temperature gradient
φ_m	-	Non-dimensional momentum gradient
ψ_h	-	Stability correction function for heat
ψ_m	-	Stability correction function for momentum

^a - signifies that the defined quantity is dimensionless.

$$\sigma_y = \sigma_v t f_y \left(\frac{\tau}{T_L} \right) \quad (3)$$

with the empirical formulation proposed by Draxler (1976) for f_y :

$$f_y = \frac{1}{1 + 0.9 \left(\frac{\tau}{1000} \right)^{0.5}} \quad (4)$$

where σ_v (m s^{-1}) is the standard deviation of velocity fluctuations in the horizontal direction, calculated using formulae from Arya (1999) (Table 2), τ (s) is the travel time

($\tau = x/\bar{u}$), and T_L is the Lagrangian time scale, which represents the characteristic time scale of turbulent eddies.

As there is a difference in the averaging time of meteorological input data (one hour or fifteen minute averages) and the sampling period of field measurements of spore concentration (ten minutes), the following empirical relation is used to correct σ_y in the model (Turner, 1970; KNMI, 1979):

$$\frac{\sigma_y(t)}{\sigma_y(600)} = \left(\frac{t}{600}\right)^{0.2} \quad (5)$$

where $\sigma_y(t)$ is the standard deviation for horizontal (y) dispersion and averaging time t (s), $\sigma_y(600)$ is the standard deviation for horizontal dispersion and an averaging time of 600 seconds, and t is the averaging time in seconds.

The Lagrangian similarity diffusion model of Van Ulden (1978) and Gryning et al. (1983) provides the vertical dispersion function for equation 1:

$$D_z(x,z) = \frac{A}{\bar{z}} \exp\left[-\left(B\frac{z}{\bar{z}}\right)^s\right] \quad (6)$$

where \bar{z} is the mean height of the plume, and A and B are functions of the shape parameter s , which is itself a function of stability and downwind distance. Under neutral conditions s approaches 1 far downwind from the source, under stable conditions s has an asymptotic limit of 3, and the convective limit of s is around 0.5. The dependence of s on x is implicit through \bar{z} . Substitution of equations 2 and 6 into equation 1 gives the full hybrid model:

Table 2. Monin-Obukhov similarity relations for the turbulence quantities σ_u , σ_v , and σ_w as suggested by Arya (1999)

$\frac{\sigma_{u,v}}{u_*} = (12 - 0.5 h/L)^{0.33}$	for $\frac{h}{L} < 0$
$\frac{\sigma_w}{u_*} = 1.3 (1 - 3 z/L)^{0.33}$	for $\frac{z}{L} < 0$
$\frac{\sigma_u}{u_*} \approx 2.5; \quad \frac{\sigma_v}{u_*} \approx 1.9; \quad \frac{\sigma_w}{u_*} \approx 1.3$	for $\frac{z}{L} \geq 0$

$$\bar{c}(x, y, z) = \frac{Q}{\bar{u}} \frac{A}{\sqrt{2\pi\sigma_y^2 z}} \exp\left(-\frac{y^2}{2\sigma_y^2}\right) \exp\left[-\left(B\frac{z}{\bar{z}}\right)^s\right] \quad (7)$$

An operational scheme to derive \bar{z} , \bar{u} , A , B , and s is provided in the appendix.

As most of the parameters in the Lagrangian similarity diffusion model are dependent on atmospheric stability in the form of z/L , surface-layer similarity theory is used to calculate the Monin-Obukhov length, L (m), which has become an important measure of atmospheric stability in the surface layer (e.g., Arya, 1999). Two scaling variables are required, the friction velocity, u_* (m s^{-1}), and the surface-layer temperature scale, ϑ_* (K):

$$u_* = \frac{\kappa \bar{u}}{\ln\left(\frac{z}{z_0}\right) - \psi_m\left(\frac{z}{L}\right) + \psi_m\left(\frac{z_0}{L}\right)} \quad (8)$$

$$\vartheta_* = \frac{\kappa(\bar{\vartheta}_2 - \bar{\vartheta}_1)}{\ln\left(\frac{z_2}{z_1}\right) - \psi_h\left(\frac{z_2}{L}\right) + \psi_h\left(\frac{z_1}{L}\right)} \quad (9)$$

where κ is the von Kármán constant (0.41), z_0 (m) is the surface roughness length, and $\bar{\vartheta}_1$ and $\bar{\vartheta}_2$ are potential temperatures, derived from temperature measurements taken at heights z_1 and z_2 (see Stull, 1988). The functions ψ_h (-) and ψ_m (-) are given in Table 3. The Monin-Obukhov length is then defined as:

$$L = \frac{\bar{T} u_*^2}{\kappa g \vartheta_*} \quad (10)$$

where \bar{T} (K) is the mean temperature and g is acceleration due to gravity (9.8 m s^{-2}). Equations 8 to 10 must be solved iteratively.

Quasi-Gaussian plume model with dry deposition of spores (QG_{dep})

The quasi-Gaussian plume model is applied over short distances ($\Delta x = 1 \text{ m}$), and for each step, material is removed from the plume by dry deposition. Chamberlain (1953) introduced the concept of “effective source strength,” whereby the reduction in plume concentration due to deposition at the surface is modeled at each Δx by reducing the strength of the source. The effective source strength depends on the amount of material already removed from the plume and therefore decreases with

downwind distance. The dry deposition flux, F_d ($\# \text{ m}^{-2} \text{ s}^{-1}$) at any point on the surface is given by:

$$F_d(x, y, 0) = v_d \bar{c}(x, y, 0) \quad (11)$$

The deposition velocity, v_d (m s^{-1}), is estimated according to Gregory (1973) as being three times the settling velocity, v_s (m s^{-1}):

$$v_d = 3 v_s = 3 (25 \times 10^6 / w) \quad (12)$$

where l and w are the length and width of the particle (m). Assuming a diameter of $40 \mu\text{m}$ for *L. clavatum* spores (e.g., Wanner and Pusch, 2000) gives a value of 0.12 m s^{-1} for v_d . Deposition is assumed to be constant over a short distance, Δx , and the change in source strength, Q , is given by:

$$Q_{x+\Delta x} - Q_x = -\Delta x F_d(x, 0) = -\Delta x v_d \int_{y=-\infty}^{\infty} \bar{c}(x, y, 0) dy \quad (13)$$

Thus, the source strength Q at $x+\Delta x$ can be calculated for the quasi-Gaussian model using:

$$Q_{x+\Delta x} = Q_x - \Delta x v_d \frac{Q_x A}{u z} \quad (14)$$

Starting at $x = 1 \text{ m}$, equation 14 is used repeatedly to provide the (effective) source

Table 3. The φ_h and φ_m functions adapted from Businger-Dyer relations (Arya, 1999), and the corresponding ψ functions.

<u>For $z/L \leq 0$</u>		
$\varphi_m = (1 - 15 z / L)^{-0.25}$	$\varphi_h = (1 - 15 z / L)^{-0.5}$	
$\psi_m = 2 \ln [(1 + x) / 2] + \ln [(1 + x^2) / 2] - 2 \tan^{-1} x + \pi / 2$		
$\psi_h = 2 \ln [(1 + x^2) / 2]$		
where $x = (1 - 15 z / L)^{0.25}$		
<u>For $z/L > 0$</u>		
$\varphi_m = 1 + 5 z / L$	$\varphi_h = 1 + 5 z / L$	$\psi_{m,h} = -5 z / L$

strength, Q , for equation 7, for any downwind distance x .

Quasi-Gaussian plume model with calibrated deposition (QG_{cal})

A weighted least squares parameter estimation method was used to determine if goodness of fit could be improved via adjustment of the deposition velocity, v_d ($m\ s^{-1}$), which was originally calculated using an approximation formula (equation 12).

Gaussian plume model (GPM)

The Gaussian plume model of Spijkerboer et al. (2002) provides a logical standard for cross-comparisons as it is the only dispersal model tested against the *L. clavatum* data used in this study. This model was also developed for spore dispersal above potato canopies. Readers are directed to their publication for a full description of the model but the main formula will be given below. It utilizes discrete stability classes (KNMI, 1972), as opposed to Monin-Obukhov similarity theory, to characterize atmospheric stability. The basic formula is:

$$\bar{c}(x, y, z) = \frac{Q}{2\pi\bar{u}\sigma_y\sigma_z} \exp\left(-\frac{y^2}{2\sigma_y^2}\right) \left\{ \exp\left[-\frac{(z-h)^2}{2\sigma_z^2}\right] + \exp\left[-\frac{(z+h)^2}{2\sigma_z^2}\right] \right\} \quad (15)$$

The dispersion coefficients were calculated using formula from de Jong (1988):

$$\sigma_y = K(z_0) 10^\alpha x^\beta \quad (16)$$

$$\sigma_y = K(z_0) \varepsilon x^\gamma \quad (17)$$

where α , β , ε , and γ are dimensionless empirical constants and $K(z_0)$ is calculated as:

$$K(z_0) = (10z_0)^{0.53} x^{-0.22} \quad (18)$$

For each measurement session, atmospheric stability is empirically classified into one of six discrete classes, which in turn affects the value of α , β , ε , and γ , and thus the shape of the plume. This model is used in conjunction with the source-depletion method of Chamberlain (1953) for the dry deposition of spores (equations 11 to 14).

In all model calculations the vertical coordinates of all source and receptors, h and z , were adjusted by the displacement height, d (m). The displacement height, sometimes known as the zero plane displacement length, describes the effect of the crop (here, a potato crop) on the wind profile. It is the level between the top and bottom of the roughness elements (i.e., the crop) above which the logarithmic wind

profile applies, i.e., tightly packed elements can act as a displaced surface and the displacement height is the level at which the mean drag on the surface appears to act. The displacement height was calculated according to Jacobs and Boxel (1991) as 0.43 m for a potato crop 0.7 m in height, i.e., 0.43 m was assumed to be the effective height of the surface in this study. Surface roughness length, z_0 , was calculated according to Jacobs and Boxel (1991) as 0.007 m for the Haarweg weather station and 0.1 m for the experimental site.

Model performance

According to the criteria of Willmott (1981), a complement of summary and difference statistics were used to evaluate model performance. The performance of each model was assessed on the basis of five characteristics: the mean absolute error (MAE), the root mean square error (RMSE), the systematic root mean square error ($RMSE_s$), the unsystematic root mean square error ($RMSE_u$), and Willmott's modified index of agreement (D). Formulae for these statistics are given in the appendix. As an accompaniment to the quantitative indices, log-log plots of predicted versus measured spore concentrations were made.

Results

Comparisons of measured vertical concentration profiles with predicted profiles are given in Fig. 1. All of the measured profiles were better approximated by a model that produces vertical concentration profiles of a general exponential form (QG_{dep}). Unfortunately, measured vertical profiles with sufficient data points to further test this conclusion were lacking in these data.

Fig. 2 shows the change in (normalized) effective source strength that results from application of the source-depletion method of Chamberlain (1953) with the quasi-Gaussian model (QG_{dep}). The steepness of the exponential decrease of effective source strength with distance depends on the level of atmospheric stability. Increased atmospheric stability means less turbulence to mix and dilute the spore plume (the atmosphere becomes more stable) therefore it lies closer to the surface, leading to heavier deposition and a faster decrease in effective source strength.

Model performance for the three measurement sessions in which on-site meteorological input data were available is compared in the first half of Table 4 and in Fig. 3. The basic quasi-Gaussian plume model, QG , is the least accurate of the four tested. This is not a surprising result as this was the only model that did not include dry deposition of spores. The importance of dry deposition is demonstrated by the marked improvement in all performance indices between QG and QG_{dep} . However, panel 2 of Fig. 3 reveals that the source-depletion method of QG_{dep} is slightly overpredicting the dry deposition of spores. This is confirmed in Table 4 ($\bar{P} < \bar{O}$). The proportion of RMSE that can be attributed to systematic errors ($RMSE_s^2/RMSE^2$) in QG_{dep} is high at 0.81. Since differences described by $RMSE_s$ can be described with a linear function, they are fairly easy to dampen with a new parameterization of the

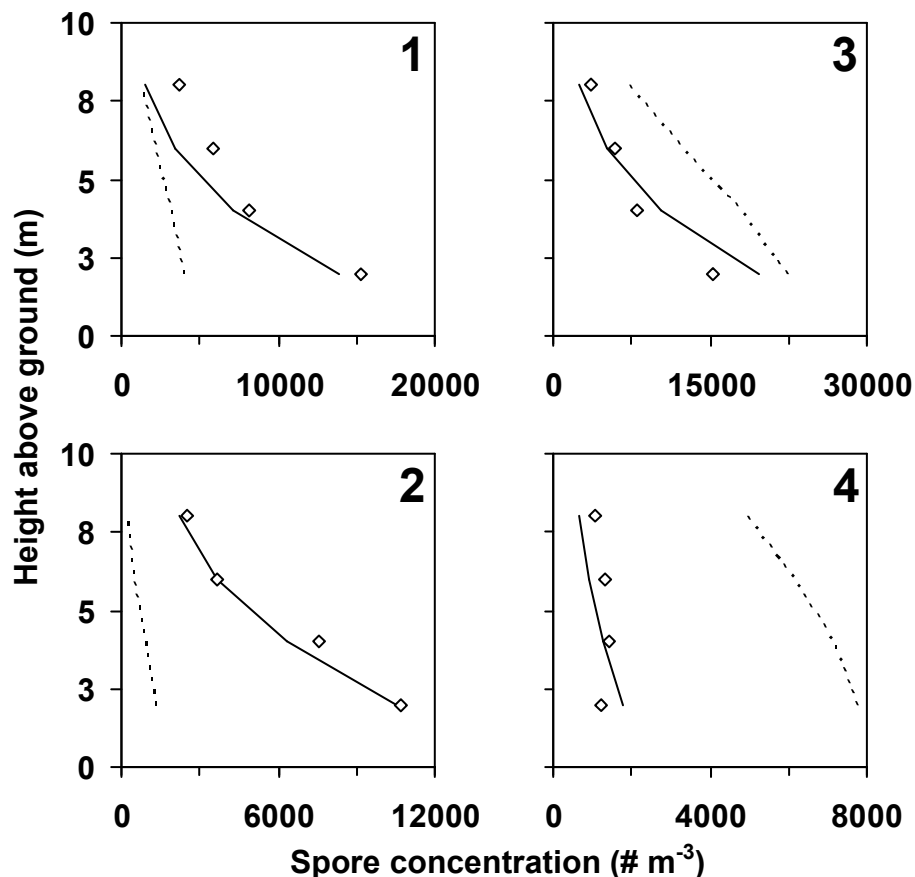


Fig. 1. Comparison between the measured vertical spore concentration profiles of Spijkerboer et al. (2002) and those predicted by a Gaussian and a quasi-Gaussian plume model: (1 and 2) $x = 35$ m, $y = 5$ m; (3) $x = 50$ m, $y = 10$ m; and (4) $x = 90$ m, $y = 10$ m distance from the source of spores. Diamonds represent measured values of spore concentration, solid lines show predicted values from the quasi-Gaussian plume model (QG_{dep}), and dotted lines predictions from the Gaussian plume model (GPM).

model, or by calibration. Calibration of v_d in QG_{cal} does give a slight improvement in performance over QG_{dep} . The value of v_d that gave the best fit between model predictions and field observations was 0.09 m s^{-1} , 25 % less than the original calculated value of 0.12 m s^{-1} . Calibration decreases the proportion of RMSE that can be attributed to systematic errors from 0.81 in QG_{dep} to 0.27 in model QG_{cal} , \bar{P} approaches \bar{O} , and improvements in MAE, RMSE and D are realised. Overall, QG_{dep} performs better than the Gaussian model (*GPM*). MAE and RMSE for *GPM* are approximately 30 % higher than for QG_{dep} . The relative and bounded measure, D, also indicates a significant advantage of the quasi-Gaussian approach over *GPM*.

Model performance for all fifteen measurement sessions, using temperature gradients and wind speeds measured off-site, is compared in Fig. 4 and the second half of Table 4. The inclusion of dry deposition in QG_{dep} again results in a large improvement in predictive accuracy, which is clearly evident when panels 1 and 2 (*QG* and QG_{dep}) in Fig. 4 are compared. Notably, the degree of overprediction of the deposition method is more profound in these data, which is apparent when the value of $\bar{P}-\bar{O}$ is compared for *QG* and QG_{dep} . Calibration of v_d (to 0.08 m s^{-1}) in QG_{cal} again results in an improvement in performance over QG_{dep} ; MAE drops by 20 %, RMSE by

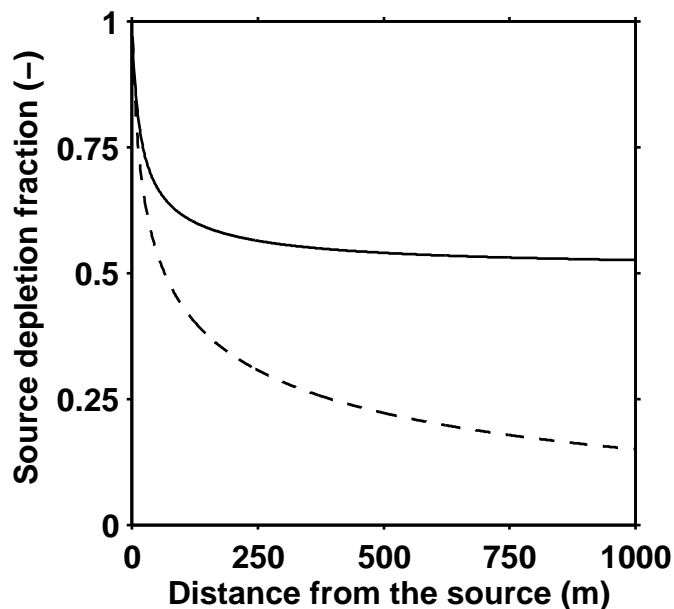


Fig. 2. Ratio of the depleted source strength to the original strength as a function of distance from the source, according to the source-depletion method of Chamberlain (1953), for two levels of atmospheric stability: solid line = unstable ($L = -10 \text{ m}$); and dashed line = stable ($L = 10 \text{ m}$). Both curves were produced using the quasi-Gaussian plume model (QG_{dep}).

35 % and the proportion of RMSE that can be attributed to systematic errors decreases from 0.92 in QG_{dep} to 0.12 in QG_{cal} . The reason that calibration is marginally more effective in this data set is perhaps statistical as this data set comprises all 15 measurement sessions. A two-fold difference in MAE and RMSE between models QG_{dep} and GPM indicates the advantage of the quasi-Gaussian approach in predicting spore plumes, at least within the confines of this study.

It is also of interest to use the two sets of results to test the assumption of homogeneous meteorology between the off-site weather station and the experimental site, i.e., to test the importance of using on-site meteorological data to characterize atmospheric turbulence. Willmott’s modified index of agreement, D , was calculated for the second set of results (off-site input data) using only data for the corresponding three measurement sessions that constitute the first set of results (on-site input data). The result for QG_{dep} is 0.7; showing no difference from D calculated

Table 4. Quantitative measures of model performance

Model ^d	Summary univariate statistics ^a				OLS coeff. ^b		Difference measures ^c				
	\bar{O}	\bar{P}	s_o	s_p	a	b*	MAE	RMSE	RMSE _s	RMSE _u	D*
<u>On-site meteorological input data (n = 33)</u>											
<i>QG</i>	2.3	8.6	3.1	9.1	2.2	3.4	6.6	9.3	7.3	5.7	0.2
<i>QG_{dep}</i>	2.3	1.3	3.1	1.8	0.5	0.2	1.3	2.1	1.9	0.9	0.7
<i>QG_{cal}</i>	2.3	2.1	3.1	2.7	0.7	0.4	1.1	1.7	0.9	1.4	0.7
<i>GPM</i>	2.3	1.8	3.1	1.4	0.2	1.2	1.6	2.7	2.5	1.2	0.5
<u>Off-site meteorological input data (n = 148)</u>											
<i>QG</i>	3.0	12.9	5.0	21.2	3.5	2.6	9.9	19.9	15.8	12.1	0.3
<i>QG_{dep}</i>	3.0	1.4	5.0	2.3	0.4	0.2	1.8	3.5	3.3	1.0	0.7
<i>QG_{cal}</i>	3.0	3.0	5.0	4.8	0.9	0.5	1.4	2.3	0.8	2.1	0.8
<i>GPM</i>	3.0	3.9	5.0	9.9	0.8	0.8	4.1	7.9	1.2	7.8	0.5

^a \bar{O} is the mean observed spore concentration; \bar{P} is the mean predicted spore concentration; s_o is the standard deviation of observed spore concentrations; s_p is the standard deviation of predicted spore concentrations; n is the number of observations. Individual Rotorod spore samplers are the basic units of observation.

^b a and b are the slope and intercept of linear ordinary least squares regressions of predicted on observed values

^c MAE (equation A6) is the mean absolute error; RMSE (equation A7) is the root mean square error. RMSE_s (equation A8) is the systematic root mean square error; RMSE_u (equation A9) is the unsystematic root mean square error; and D (equation A10) is Willmott’s modified index of agreement (Willmott et al., 1985).

^d *QG* = quasi-Gaussian; *QG_{dep}* = quasi-Gaussian with dry deposition; *QG_{cal}* = quasi-Gaussian with calibrated dry deposition; and *GPM* = Gaussian plume model.

* b and D are dimensionless whilst the other statistics have the units ($\# m^{-3}$) $\times 10^3$.

using on-site meteorological input data. This result indicates that the assumption of homogeneous meteorology between the two sites was valid; however, the small size of the data set used in this part of the study ($n = 33$) makes it difficult to draw any firm conclusions.

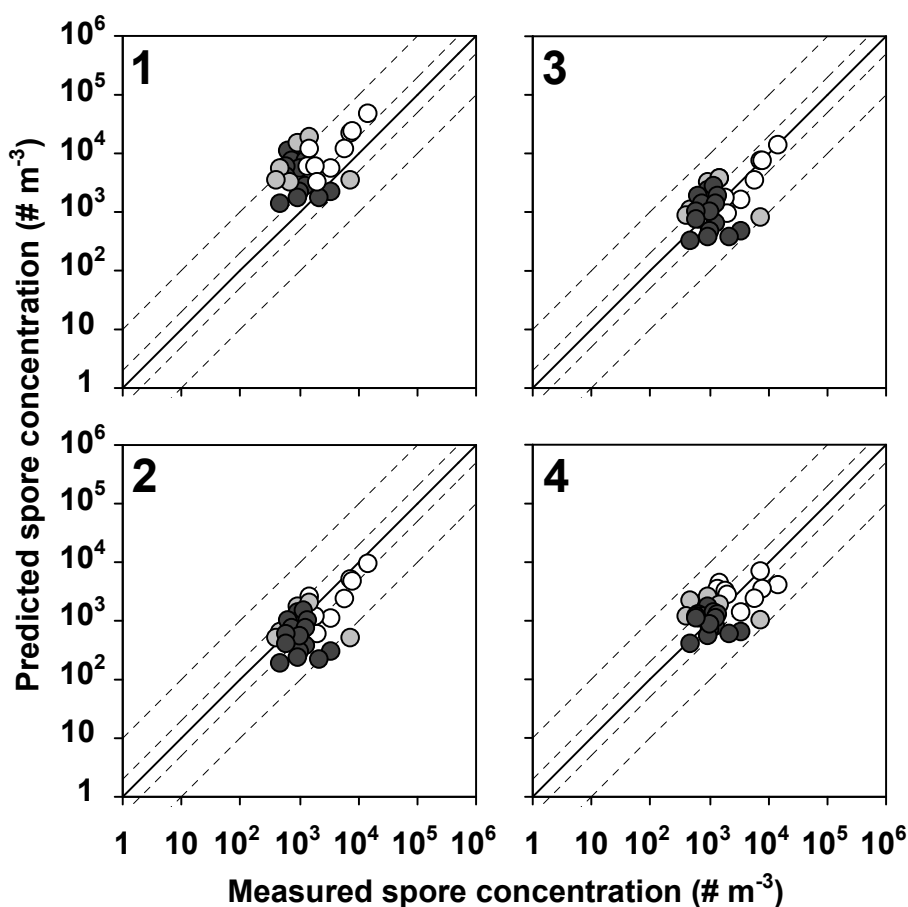


Fig. 3. Predicted versus measured spore concentrations for 3 measurement sessions: (1) quasi-Gaussian plume model, QG ; (2) quasi-Gaussian plume model plus the source depletion method of Chamberlain (1953) for dry deposition of spores, QG_{dep} ; (3) quasi-Gaussian plume model with source depletion method calibrated for deposition velocity, QG_{cal} ; and (4) Gaussian plume model of Spijkerboer et al. (2002), GPM . Downwind distance, x , of spore traps from the source of spores ranged from 25 to 110 m: $\circ = 25 < x \leq 50$ m, $\odot = 50 < x \leq 75$ m, $\bullet = x > 75$ m. Crosswind distances, y , ranged from - 50 to + 50 m. The inner dashed lines mark the boundary of a prediction error of factor two, the outer dashed lines mark the boundary of a prediction error of factor ten and the solid line represents a 1:1 line. All input meteorological data for the dispersion models were collected on-site.

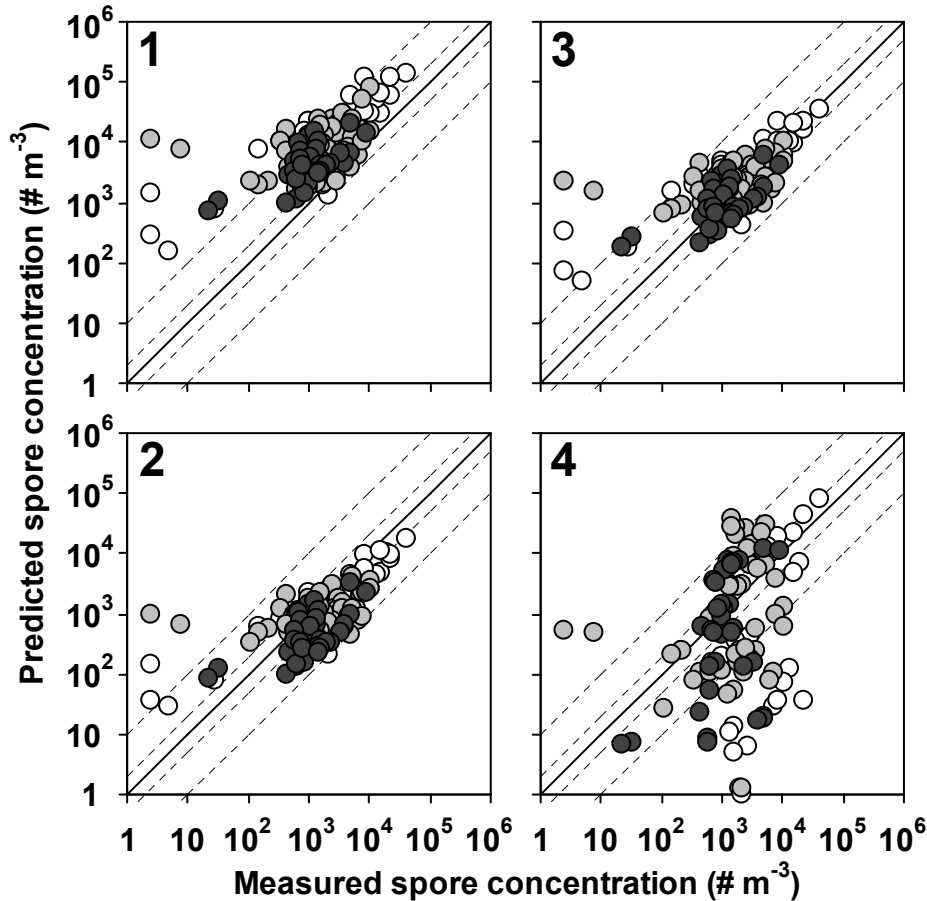


Fig. 4. Predicted versus measured spore concentrations for 15 measurement sessions: (1) quasi-Gaussian plume model, QG ; (2) quasi-Gaussian plume model plus the source depletion method of Chamberlain (1953) for dry deposition of spores, QG_{dep} ; (3) quasi-Gaussian plume model with source depletion method calibrated for deposition velocity, QG_{cal} ; and (4) Gaussian plume model of Spijkerboer et al. (2002), GPM . Downwind distance, x , of spore traps from the source of spores ranged from 25 to 110 m: $\circ = 25 < x \leq 50$ m, $\odot = 50 < x \leq 75$ m, $\bullet = x > 75$ m. Crosswind distances, y , ranged from -50 to +50 m. The inner dashed lines mark the boundary of a prediction error of factor two, the outer dashed lines mark the boundary of a prediction error of factor ten and the solid line represents a 1:1 line. All input meteorological data for the dispersion models, barring the wind direction, were collected off-site at a nearby agricultural meteorological station.

Discussion

Evaluation of model performance

In this paper, a transparent and parsimonious, yet physically realistic, and if possible, analytical approach to dispersion modeling of low-level releases of spores was sought. A non-Gaussian or exponential description of vertical concentration

distribution was shown to be advantageous since measured vertical profiles of spores at distances of up to nearly 100 m were better approximated by an exponential distribution. The addition of the source depletion model was highly effective in reducing overpredictions by the basic quasi-Gaussian model, and whilst more physically realistic deposition models exist, e.g., the surface depletion method of Horst (1977), this technique was preferable due to its simplicity. Overall, the predictive accuracy of the quasi-Gaussian approach was shown to exceed that of the previously published Gaussian diffusion model of Spijkerboer et al. (2002), over dispersal distances of up to 100 m. Collection of spore dispersal data sets over larger distances is unfortunately very difficult, but the benefits of such a data set to studies such as these would be considerable. Nonetheless, numerical results compared favorably with observations over distances that could account for the between-field transport of spores

The quasi-Gaussian approach outlined in this study does have its limitations. For example, the use of gradient transport theory becomes questionable in highly unstable conditions when turbulent eddies may transport material up or down irrespective of mean concentration gradients. In addition, surface layer similarity theories of diffusion can only be applied to near-surface releases and relatively short travel times so that the plume remains in the surface layer. Whilst these shortcomings could present problems for the applicability of this approach over long dispersal distances, they are not likely to be a limiting factor in the simulation of (early morning) dispersal of *P. infestans* spores over short distances between neighboring fields. Indeed, many other studies (e.g., Brown et al., 1993; Arya, 1999) in addition to this one, have concluded that gradient transport models offer a significant improvement over the Gaussian diffusion model due to the improved description of vertical dispersion. Gaussian diffusion models are, however, conceptually appealing and continue to play a role in plant pathology (e.g., de Jong et al., 2002; Spijkerboer et al., 2002; Bourdôt et al., 2006). Lagrangian stochastic (LS) simulation models have also been used recently in plant pathology. These are a class of models based on stochastic ordinary differential equations that describe the motion of single tracer particles in turbulent flows. LS models have been the subject of a large body of research on the release and dispersal of pollen and spores (e.g., Aylor, 1989; Aylor and Flesch, 2000; Aylor et al., 2001; Aylor, 2005; Aylor and Boehm, 2006). The Lagrangian stochastic approach is widely regarded as offering improvements in dispersion theory, but it suffers from two major disadvantages; increased computing time and more complex requirements in terms of input data

than simpler dispersion models. When viewed together, these factors could serve to limit the usefulness of LS models as components in disease risk warning systems, i.e. in decision support systems (DSS) for aerially transmitted plant pathogens.

Implications for decision support systems

The fundamental problem in any transport and dispersion exercise is that the turbulence must somehow be parameterized. In this study, the majority of the meteorological input data came from Wageningen University weather station (Haarweg; <http://www.met.wau.nl>). This attaches a degree of uncertainty to these data as the experiments of Spijkerboer et al. (2002) were conducted over a ten minute time interval whereas Haarweg weather data are one-hour averages. For this reason, equation 5 was used to convert horizontal dispersion coefficients from an hourly to a 10 minute averaging time. Issues of time averaging were not the only problems that had to be addressed with respect to the off-site meteorological input data, there was also a spatial problem as the Haarweg data is collected approximately 2 km southwest of the potato field and there may of course be differences in weather conditions between the two sites. Furthermore, Haarweg is primarily an agricultural weather station, therefore it measures temperature at standard heights of 1.5 and 0.1 m, which are not ideal heights for obtaining gradients for use in the calculation of surface-layer parameters such as u_* and L . For the calculation of surface-layer parameters, measurements must be taken within the surface-layer and temperature measurements taken at a height of 0.1 m are actually obtained within the “roughness sub-layer,” where sensors can be affected by local obstacles, such as small patches of bare soil, and the measurements obtained are therefore not necessarily representative of the whole field. Turbulence is required to “blend” these local effects and as a rule of thumb it is better to obtain the lower temperature measurements at a height of 3 x crop height. At the experimental site, temperature measurements were made at heights of 2 and 4.5 m above the potato canopy therefore an improvement in model results was expected. The reason that this improvement was not realized could be statistical; it is unfortunate that on-site meteorological data were only available for three of the fifteen measurement sessions. We would of course recommend the use of on-site weather data whenever possible in experiments.

In practical applications of dispersal models, most often, predictions will have to be made with off-site weather forecast data (e.g., Holtslag and van Ulden, 1983; de Rooy and Holtslag, 1999). It has been demonstrated that accurate predictions can be

obtained with the quasi-Gaussian plume approach using measurements over grass from a more distant meteorological station, provided the assumption of homogeneous meteorology holds true. This is of particular relevance to the providers of agricultural DSSs in large growing regions; it should be possible to obtain good predictions of spore dispersal with a relatively simple dispersion model using good quality forecast weather data for the region of interest.

If sophisticated DSSs based on dispersion models are to be developed, then a question arises as to the influence of uncertainty in dispersal model predictions on decision making. In a decision support setting, the correctness of dispersal model predictions would essentially be a classification issue, i.e., it is not *per se* required that the exact amount of arriving inoculum is predicted correctly as long as the resulting spray decision is appropriate. Risk, therefore, is the probability of making an incorrect spray recommendation due to uncertainty in dispersal model predictions. If the predicted spore load is high, while the true spore load is low, an unnecessary spray is indicated, with environmental consequences and attendant small private costs. On the other hand, if the predicted spore load is low, while the true spore load is high, the crop may be left unprotected when a chemical treatment should have been prescribed, with potentially large yield losses. In order to determine the degree of predictive uncertainty that could be tolerated in dispersal models, without undue risk of inappropriate action, one would first need to determine the risk posed to target crops by distant sources of inoculum. To give a simple example, higher levels of spore deposition are required to initiate disease in resistant as opposed to susceptible cultivars. This means that the risk of inappropriate action due to uncertainty in dispersal model predictions is lower for resistant as opposed to susceptible cultivars. The reality of the matter is far more complicated, as the risk posed by distant sources of inoculum is dependent on complex interactions between source and target characteristics and environmental conditions. A large number of field experiments would be required to define the relationship between arriving inoculum and crop loss, but epidemiological models are well suited to investigate the interaction of these risk factors. This is the subject of a previous study, where a scenario based simulation approach was used to evaluate where the use of dispersal information in decision making could be beneficial, and where it carries greatest risk of crop and economic losses to the farmer (Skelsey et al., *in press*).

This paper presents a quasi-Gaussian plume model for the dispersal of spores from a low-level release. It offers advantages over the Gaussian diffusion model as it provides a more physically realistic representation of vertical diffusion. Computed

results compare very favorably with experimental data over distances that could account for the between-field transport of spores. It is therefore anticipated that the model will prove attractive as a research tool for investigating the spatial spread of plant disease epidemics, and also as an operational decision support tool to aid in quantifying the risk of disease spread from external sources of inoculum. Incorporation of the model into a DSS for potato late blight, and validation of the system as a means of reducing fungicide applications is the subject of a future paper.

Appendix

Dispersion parameters

The mean height of the plume, \bar{z} , depends on travel distance, x , roughness length, z_0 , and Obukhov length, L . Their relation is approximated by (van Ulden, 1978):

$$x + x_0 = \left(\frac{\bar{z}}{\kappa}\right)^2 \left[\ln\left(\frac{c\bar{z}}{z_0}\right) - \psi_m\left(\frac{c\bar{z}}{L}\right) \right] \left[1 - \frac{\rho a_1 \bar{z}}{4L} \right]^{-0.5} \quad L < 0 \quad (\text{A1a})$$

$$x + x_0 = \left(\frac{\bar{z}}{\kappa}\right)^2 \left\{ \left[\ln\left(\frac{c\bar{z}}{z_0}\right) + \frac{2b_2 \rho \bar{z}}{3L} \right] \left[1 + \frac{b_1 \rho \bar{z}}{2L} \right] + \left[\frac{b_1}{4} - \frac{b_2}{6} \right] \frac{\rho \bar{z}}{L} \right\} \quad L > 0 \quad (\text{A1b})$$

where κ is the von Kármán constant (0.41), and x_0 is an integration constant that accounts for the height of the source. The coefficients ρ and c in (A1a,b) depend on s . For practical applications, Holtslag (1984) and Gryning et al. (1987) propose $\rho = 1.55$ and $c = 0.6$. The remaining constants and the ψ functions are related to the actual choice of φ_h and φ_m functions. Gryning et al. (1983) and Holtslag (1984) used the φ_h and φ_m functions suggested by Dyer (1974) with $a_1 = a_2 = 16$, $b_1 = b_2 = 5$ and $\kappa = 0.41$. However, the ψ functions they recommend for use with these coefficients were found to be numerically unstable in very unstable conditions; better results were obtained here with the adapted Businger-Dyer relations recommended by Arya (1999) and listed in Table 3. First, x_0 is computed by putting \bar{z} equal to the source height and x equal to zero (for a ground level source $x_0 = 0$). Then, \bar{z} is determined iteratively from (A1) for any downwind distance, x .

With \bar{z} , we can solve for the shape parameter, s , and the mean transport velocity, \bar{u} . Gryning et al. (1983) provide approximation formulae for s :

$$s = \frac{1 - a_1 c\bar{z}/(2L)}{1 - a_1 c\bar{z}/L} + \frac{(1 - a_2 c\bar{z}/L)^{-0.25}}{\ln(c\bar{z}/z_0) - \psi_m(c\bar{z}/L)} \quad L < 0 \quad (\text{A2a})$$

$$s = \frac{1 + 2b_1 c\bar{z}/L}{1 + b_1 c\bar{z}/L} + \frac{1 + b_2 c\bar{z}/L}{\ln(c\bar{z}/z_0) + b_2 c\bar{z}/L} \quad L > 0 \quad (\text{A2b})$$

The mean transport velocity, \bar{u} , is given by (van Ulden, 1978):

$$\bar{u} = \frac{u_*}{\kappa} \left[\ln\left(\frac{c\bar{z}}{z_0}\right) - \psi_m\left(\frac{c\bar{z}}{L}\right) \right] \quad L < 0 \quad (\text{A3a})$$

$$\bar{u} = \frac{u_*}{\kappa} \left[\ln\left(\frac{c\bar{z}}{z_0}\right) + \frac{b_2 \bar{z}}{L} \right] \quad L > 0 \quad (\text{A3b})$$

The functions A and B are given by (Pasquill and Smith, 1983):

$$A = \frac{s\Gamma(2/s)}{[\Gamma(1/s)]^2} \quad (\text{A4})$$

$$B = \frac{\Gamma(2/s)}{\Gamma(1/s)} \quad (\text{A5})$$

Performance indices

The MAE was calculated as:

$$\text{MAE} = \frac{1}{n} \sum_{i=1}^n |P_i - O_i| \quad (\text{A6})$$

where P_i are model predictions, O_i are observations and n is the number of observations.

The RMSE is given by:

$$\text{RMSE} = \left[\frac{1}{n} \sum_{i=1}^n (P_i - O_i)^2 \right]^{0.5} \quad (\text{A7})$$

Ordinary least squares regression of P_i on O_i is used to calculate RMSE_s and RMSE_u as follows:

$$\text{RMSE}_s = \left[\frac{1}{n} \sum_{i=1}^n (\hat{P}_i - O_i)^2 \right]^{0.5} \quad (\text{A8})$$

$$\text{RMSE}_u = \left[\frac{1}{n} \sum_{i=1}^n (P_i - \hat{P}_i)^2 \right]^{0.5} \quad (\text{A9})$$

where $\hat{P}_i = a + bO_i$ and $a = y$ -intercept of the linear regression and $b =$ slope of the linear regression. The RMSE is a measure of the total deviation of predicted spore concentration from observed spore concentration. The RMSE_s is a measure of the deviation of the linear regression line from the one to one line and therefore indicates systematic bias. The RMSE_u is a measure of the random deviation around the regression line. Since the system is conservative for the squared values of these measures (i.e., $\text{RMSE}^2 = \text{RMSE}_s^2 + \text{RMSE}_u^2$), they can be used to calculate the proportions of the RMSE arising from systematic and unsystematic errors.

Willmott et al. (1985) define the modified index of agreement as:

$$D = 1 - \left[\frac{\sum_{i=1}^n |P_i - O_i|}{\sum_{i=1}^n (|P_i'| + |O_i'|)} \right] \quad 0 \leq D \leq 1 \quad (\text{A10})$$

where $P_i' = P_i - \bar{O}$ and $O_i' = O_i - \bar{O}$. The value of D is a measure of how well the observed deviations about the observed mean value match the predicted deviations about the same observed mean value. A value of 1 denotes perfect correspondence between predictions and observations.

Acknowledgements

Funding for this study was provided by the Dutch Ministry of Agriculture, Nature Management and Fisheries through the Umbrella Plan Phytophthora (DWK 427). Thanks to Peter Hofschreuder, Adrie Jacobs and Jordi Vilá-Guerau de Arellano for their support and assistance, and Bert Heusinkveld for his help with the meteorological input data. We also thank Diedert Spijkerboer for his assistance with the field data.

References

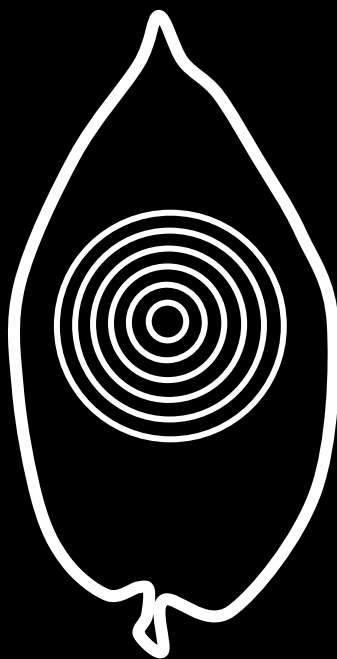
Arya, S.P. 1999. Air pollution meteorology and dispersion. Oxford university press, New York, NY.

- Aylor, D.E. 1989. Aerial dispersal close to a focus of disease. *Agr. Forest Meteorol.* 47:109-122.
- Aylor, D.E. 2005. Quantifying maize pollen movement in a maize canopy. *Agr. Forest Meteorol.* 131:247-256.
- Aylor, D.E., and Boehm, M.T. 2006. Quantifying aerial concentrations of maize pollen in the atmospheric surface layer using remote-piloted airplanes and Lagrangian stochastic modeling. *J. Appl. Meteorol. Clim.* 45:1003-1015.
- Aylor, D.E., and Qui, J. 1996. Micrometeorological determination of release rate of *Venturia inaequalis* ascospores from a ground-level source during rain. *Agr. Forest Meteorol.* 81:157-178.
- Aylor, D.E., and Flesch, T.K. 2000. Estimating spore release rates using a lagrangian stochastic simulation model. *J. Appl. Meteorol.* 40:1196-1208.
- Aylor, D.E., Fry, W.E., Mayton, H., and Andrade-Piedra, J.L. 2001. Quantifying the rate of release and escape of *Phytophthora infestans* sporangia from a potato canopy. *Phytopathology* 91:1189-1196.
- Barad, M.L. 1958. Project prairie grass, a field program in diffusion. Geophysical Research Papers, No. 59, Vols. 1 and II. Report AFCRC-TR-58-235, U.S. Air Force Cambridge Research Center.
- Barad, M.L., and Fuquay, J.J. 1962. The Green Glow diffusion program, Vol. 1. Geophysical Research Papers, No. 73. Hanford Report HW 71400, Geophysics Research Directorate, U.S. Air Force Cambridge Research Center.
- Bourdôt, G.W., Baird, D., Hurrell, G.A., and de Jong, M.D. 2006. Safety zones for a *Sclerotinia sclerotiorum*-based mycoherbicide: accounting for regional and yearly variation in climate. *Biocont. Sci. Technol.* 16:345-358.
- Brown, M.J., Arya, S.P., and Snyder, W.H. 1993. Vertical dispersion from surface and elevated releases: an investigation of a non-Gaussian plume model. *J. Appl. Meteorol.* 32:490-505.
- Chamberlain, A.C. 1953. Aspects of travel and deposition of aerosol and vapor clouds. Report No. A.E.R.E HP/R1261. Her Majesty's Stationery Office, London.
- de Jong, M.D. 1988. Risk to Fruit Trees Due to Control of Black Cherry (*Prunus serotina*) by Silver Leaf Fungus (*Chondrostereum purpureum*). PhD thesis, Wageningen Agricultural University, Wageningen, The Netherlands.
- de Jong, M., Bourdôt, G.W., Powell, J., and Goudriaan, J. 2002. A model of the escape of *Sclerotinia sclerotiorum* ascospores from pasture. *Ecol. Model.* 150:83-105.
- Draxler, R.R. 1976. Determination of atmospheric diffusion parameters. *Atm. Environ.* 10:99-105.
- Dyer, A. J. 1974. A review of flux-profile relationships. *Bound. Layer Meteorol.* 7:363-372.
- Elliot, W.P. 1961. The vertical diffusion of gas from a continuous source. *Int. J. Air Water Poll.* 4:33-46.

- Gifford, F.A. 1968. An outline of theories of diffusion in the lower layers of the atmosphere. In: Slade, D.H. (Ed.), *Meteorology and Atomic Energy*. U.S. Department of Energy, Technical Information Center, Oak Ridge, TN, pp. 65-116.
- Gregory, P.H. 1973. *The microbiology of the atmosphere*. Wiley, pp. 377.
- Gryning, S.E., van Ulden, A.P., and Larsen, S.E. 1983. Dispersion from a continuous ground-level source investigated by a *K* model. *Q. J. Roy. Meteor. Soc.* 109:355-364.
- Gryning, S.E., Holtslag, A.A.M., Irwin, J.S., and Sivertsen, B. 1987. Applied dispersion modelling based on meteorological scaling parameters. *Atmos. Environ.* 21:79-89.
- Hinrichson, K. 1986. Comparison of four analytical dispersion models for near-surface releases above a grass surface. *Atmos. Environ.* 20:29-40.
- Holtslag, A.A.M. 1984. Estimates of vertical diffusion from sources near the ground in strongly unstable conditions. In: de Wispelaere, C. (Ed.), *Air Pollution Modeling and its Application III*. Plenum Press, New York, pp. 619-630.
- Holtslag, A.A.M., and van Ulden, A.P. 1983. A simple scheme for daytime estimates of the surface fluxes from routine weather data. *J. Clim. Appl. Meteorol.* 22:517-529.
- Horst, T.W. 1977. A surface depletion model for deposition from a Gaussian plume. *Atmos. Environ.* 11:41-46.
- Huang, C.H., and Drake, R.L. 1977. Validation of Gaussian and non-Gaussian diffusion models for a point source. *Joint Conference on Applications of Air Pollution Meteorology*, Salt Lake City, Amer. Met. Soc. 299-303.
- Jacobs, A.F.G., and Boxel, J.H. 1991. Horizontal and vertical distribution of wind speed in a vegetation canopy. *Neth. J. Agric. Sci.* 39:165-178.
- KNMI. 1972. *Klimatologische gegevens van Nederlandse stations. Frequentietabellen van de stabiliteit van de atmosfeer*. No. 150-158.
- KNMI. 1979. *Luchtverontreiniging en weer*. Staatsuitgeverij/KNMI.
- Malhotra, R.C., and Cermak, J.E. 1964. Mass diffusion in neutrally and unstably stratified boundary-layer flows. *Int. J. Heat Mass Tran.* 7:169-186.
- McCartney, H.A. 1990. The dispersal of plant pathogen spores and pollen from oilseed rape crops. *Aerobiologia* 6:147-152.
- Mizubuti, E.S.G., Aylor, D.E., and Fry, W.E. 2000. Survival of *Phytophthora infestans* sporangia exposed to solar radiation. *Phytopathology* 90:78-84.
- Nieuwstadt, F.T.M., and van Ulden, A.P. 1978. A numerical study on the vertical dispersal of passive contaminants from a continuous source in the atmospheric surface layer. *Atmos. Environ.* 12:2119-2124.
- Nikola, P.W. 1977. *The Hanford 67-series: a volume of atmospheric field diffusion measurements*. PNL-2433, Battelle, Pacific Northwest Laboratories.
- Pasquill, F. 1974. *Atmospheric Diffusion*, 2d ed. Ellis Horwood Ltd., Chichester, England.
- Pasquill, F., and Smith, F.B. 1983. *Atmospheric diffusion*, 3rd ed. Ellis Horwood Ltd., Chichester, England.

- Rooy, W.C. de, and Holtslag, A.A.M. 1999. Estimation of surface radiation and energy fluxes from routine weather data. *J. Appl. Meteorol.* 38:526-540.
- Seinfeld, J.H., and Pandis, S.N. 1998. *Atmospheric Chemistry and Physics*. John Wiley and Sons, Inc., New York.
- Skelsey, P., Kessel, G.J.T., Rossing, W.A.H., and van der Werf, W. Scenario approach for assessing the utility of dispersal information in decision support for aerially spread plant pathogens, applied to *Phytophthora infestans*. *Phytopathology*, *in press*.
- Spijkerboer, H.P., Beniers, J.E., Jaspers, D., Schouten, H.J., Goudriaan, J., Rabbinge, R., and van der Werf, W. 2002. Ability of the Gaussian plume model to predict and describe spore dispersal over a potato crop. *Ecol. Model.* 155:1-18.
- Stull, R.B. 1988. *An introduction to boundary layer meteorology*. Kluwer Academic Publishers, Dordrecht, the Netherlands, 666 pp.
- Sunseri, M.A., Johnson, D.A., and Dasgupta, N. 2002. Survival of detached sporangia of *Phytophthora infestans* exposed to ambient, relatively dry atmospheric conditions. *Am. J. Potato Res.* 79:443-450.
- Taylor, G.I. 1921. Diffusion by continuous movements. *Proc. London Math. Soc.* 20:196-211.
- Turner, D.B. 1970. *Workbook of atmospheric dispersion estimates*. Public Health Service Pub. No. 999-AP-26, US Department of Health, Education and Welfare, 84 pp.
- van Ulden, A.P. 1978. Simple estimates for vertical diffusion from sources near the ground. *Atmos. Environ.* 12:2119-2124.
- Wanner, S.C., and Pusch, M. 2000. Use of fluorescently labeled Lycopodium spores as a tracer for suspended particles in a lowland river. *J. N. Am. Benthol. Soc.* 19:648-658.
- Willmott, C.J. 1981. On the validation of models. *Phys. Geogr.* 2:184-194.
- Willmott, C.J., Ackleson, S.G., Davis, R.E., Feddema, J.J., Klink, K.M., Legates, D.R., O'Donnell, J., and Rowe, C.M. 1985. Statistics for the evaluation and comparison of models. *J. Geophys. Res.* 90:8995-9005.

CHAPTER 6



Regional Spore Dispersal as a Factor in Disease Risk Warnings for Potato Late Blight: a Proof of Concept

P. Skelsey¹, G.J.T. Kessel², A.A.M. Holtslag³, A.F. Moene³, and W. van der Werf¹

¹ Wageningen University, Department of Plant Sciences, Crop and Weed Ecology Group, P.O. Box 430, 6709 RZ Wageningen, The Netherlands.

² Plant Research International, P.O. Box 16, 6700 AA Wageningen, The Netherlands.

³ Wageningen University, Meteorology and Air Quality Group, P.O. Box 47, 6700 AA Wageningen, the Netherlands.

Agricultural and Forest Meteorology (*in press*)

Abstract

This study develops and tests a novel approach for including regional spatial risk factors in operational disease risk warnings against potato late blight. The central premise is that fungicide inputs can be reduced by omitting applications on days when conditions are unsuitable for the atmospheric transport of viable sporangia. The decision support system first decides whether a specific day is “high risk” (suitable for disease development *in planta*) and a chemical treatment is required. Simulation studies revealed that on such high risk days, the capacity of the atmosphere to transport sporangia viably over relevant distances varies widely. An additional rule assesses this capacity, which is high when weather conditions allow a large numbers of spores to be released from the canopy and transported viably over long distances. When this capacity is high the original spray advice is followed, and when it is low a no-spray advice is given.

The concept was implemented using the published decision support system SIMCAST complemented with aerobiological models for spore release from sporangiophores, spore escape from the canopy, a newly developed model for spore dispersal, dry deposition of spores, spore survival during transportation, and weather forecast data from the meso-scale meteorological model MM5. Cultivar resistance was also incorporated into spray advice.

The concept was tested in a field experiment in 2007 with three cultivars, representing a range in resistance to potato late blight from susceptible to highly resistant, and compared to a “stand-alone” version of SIMCAST. In a period with normal “infection pressure” (risk of disease) one third of the spray recommendations made by SIMCAST alone were modified and negated by the new system

for the highly resistant cultivar. These savings came on top of a reduced, resistance-level dependent, dose rate of Shirlan (a.i. Fluazinam).

The results demonstrate the feasibility of including dispersal modeling and forecasted meteorology in disease warnings against *Phytophthora infestans*, even if the whereabouts of sources are unknown. The principles can be used in many decision contexts, but further work is needed to test and refine the method before it can be used in practice.

Keywords: inoculum dispersal, spatial risk factors, supplementary spatial component, distance-weighted infection pressure, disease management.

Introduction

Phytophthora infestans (causal agent of tomato and potato late blight) is a persistent and pervasive pathogen. Far from being limited to a single host species, *P. infestans* is aggressive on many tuber and non-tuber bearing species of the genus *Solanum* (e.g., Erwin and Ribeiro, 1996). It has enormous potential for asexual spore production and rapid destruction of host foliage. Detached sporangia have been observed to survive ambient environmental conditions for several hours (Minogue and Fry, 1981; Mizubuti et al., 2000; Sunseri et al., 2002) and can cause infections several kilometers from their original source (Hyre et al., 1950; van der Zaag, 1956; Zwankhuizen et al., 1998). The pathogen is also able to reproduce sexually; giving rise to aggressive new strains and hardy oospores that can survive in soil for years (e.g., Drenth et al., 1995; Turkensteen et al., 2000). Potato late blight is an ongoing problem in the global potato industry (Hijmans et al., 2000), demanding grower attention from day to day, and still causing losses despite this attention. The costs of losses to potato late blight, and of controlling it, are enormous; it is estimated that *P. infestans* is responsible for multi-billion dollar losses annually in global tomato and potato production (Duncan 1999; Birch and Whisson, 2001, Haverkort et al., *in press*). Chemical control is still the most important measure used, and many growers anticipate that disease control requires regular applications of fungicides at high rates and short intervals throughout the growing season. This is an unsustainable situation that is now being questioned, in part due to an increase in environmental awareness and public concern about the negative side effects of fungicide use in agriculture, and in part due to concerns over the development of pathogen resistance to (liberally applied) chemical products. Efforts to reduce the environmental impact of potato cultivation

are now driving exploration into new options to reduce the number of sprays, and/or the dosage, while ensuring crop health.

The strong weather dependency of potato late blight has been used as a basis for different types of models to make a prediction of whether or not crop protection measures are required. There are many examples of models that have been successful in rationalizing fungicide inputs (e.g., Smith, 1956; Ullrich and Schrödter, 1966; Krause et al., 1975; Hansen et al., 1995; Hansen and Andersson., 1996; Hadders, 1999; Nugteren, 2004). When disease prediction calculations are carried out by means of dedicated software, the term “decision support system” (DSS) is sometimes used (Madden et al., 2007). DSSs attempt to target chemical applications to moments when genuine risk is present. Historical, and often forecasted weather conditions are considered in terms of their suitability for the development of new infections. In some DSSs the extent to which a crop canopy is likely to be unprotected is also estimated, both in terms of the growth of new leaves and the wear-off and degradation of previous chemical applications.

It is important to realize that almost all DSSs that offer day-to-day spray advice (operational decision support) form diagnoses at the individual plant/field-scale. Little or no consideration is given to the wider spatial environment. Spatial aspects of the disease cycle, such as inoculum dispersal and survival during transportation, are not considered as risk influencing factors and such information has been scarcely used in DSS development. This is despite the fact that recent decades have seen growth in the development of mathematical models to predict the dispersal of airborne inoculum (e.g., de Jong, 1988; Aylor, 1989; Aylor and Flesch, 2000; Aylor et al., 2001; de Jong et al., 2002; Spijkerboer et al., 2002; Aylor, 2005; Aylor and Boehm, 2006; Bourdôt et al., 2006). The choice not to include daily predictions of spore dispersal and survival in operational decision support is in part due to a lack of empirical dispersal data with which to validate dispersal models, but especially to prediction uncertainties stemming from the highly variable nature of dispersal processes. These problems are compounded by the difficulty of knowing the whereabouts of disease sources; it is a seemingly impossible task to include models of spore transport and survival in an operational (day-to-day) decision making process when inoculum sources are unknown or knowledge of their whereabouts is incomplete. Moreover, dispersal models are based on complicated environmental physics and they are often embedded in unwieldy computer code that is impenetrable to non-experts.

In this study a novel approach is developed for predicting and including regional spore dispersal as a spatial risk factor in operational decision support. A previously validated spore dispersal and deposition model (Skelsey et al., 2008) is combined with models for spore release, spore escape from the canopy and spore survival to create a supplementary spatial component for DSSs. Whereas a (non-spatial) DSS characterizes risk as the susceptibility of the crop to infection, given the weather conditions and the current level of chemical protection, the supplementary spatial component characterizes risk as the likelihood that viable spores will be imported into the crop. This supplementary component is parameterized for potato late blight, but could also be parameterized for other airborne pathogens if sufficient empirical data exist. It works by using weather forecast data to modify the spray recommendations of existing DSSs according to the risk of long distance transport of viable spores. High risk days are those on which weather conditions allow a large numbers of spores to be released from infected canopy and transported viably over relevant distances between inoculum sources and targets. In this process, the geographic locations of actual disease sources and target crops need not be considered and do not form part of the decision making process. Some important questions this study attempts to address are: (1) is such a concept feasible for implementation; (2) can it reduce the number of sprays; and (3) would such a system provide robust control? In the sections that follow, this novel new system is described, in addition to a field trial in which the ability of the system to reduce fungicide inputs and maintain control of potato late blight is tested. The implications for the future of decision support are discussed.

Theory and approaches

The new system is designed to be used as a supplementary spatial component for existing non-spatial DSSs. The (standard) DSS will operate as normal and determine, generally on the basis of historical and forecasted weather data and an estimate of the current level of chemical protection on target crops, whether a specific day is “high risk” and a chemical application is required. The supplementary spatial component can then be used to potentially modify that decision if atmospheric conditions render substantial long distance transport of viable spores unlikely. Two fundamental assumptions are made: (i) target crops are disease-free and “threatened” by an upwind source of inoculum, the size and distance of which are

unknown; and (ii) the capacity of the atmosphere to transport viable spores over distance is highly variable. Models for spore release from sporangiophores, escape of spores from the canopy, dispersal, deposition and survival are used in conjunction with a hypothetical source of spores to provide a quantitative estimate of the capacity of the atmosphere to release and disperse viable sporangia over relevant distances. A new indicator variable, the distance-weighted infection pressure, is calculated and compared to a threshold value in order to assess if the original spray advice from the DSS can be negated or not. The threshold value was determined by running ten years of historical weather data and three potato cultivars through the system. This provided a range of values for the new indicator variable, produced under a variety of different atmospheric conditions and cultivar susceptibility. The threshold value was then set such that in the long term over a population of potato varieties, a reduction of one third of spray recommendations would be obtained. This operational assumption is arbitrary and can be relaxed without affecting the conceptual approach.

An overview of the concept described above is given in Fig. 1. In this example a DSS for potato late blight is using historical weather data as input for models that determine the suitability of the weather for disease development, and the degree of fungicide weathering since the last application. This is very similar to the non-spatial DSS used in the field trial described below. Together, these models provide input data for a decision algorithm that quantifies the risk of disease development *in planta*, and formulates a decision regarding the need for chemical protection. If a spray is recommended, the supplementary spatial component is used to potentially modify that decision. Weather forecast data and models describing the aerobiological aspects of the disease cycle are used to provide input data for a decision algorithm that quantifies the risk of viable spore transport over relevant distances. If the risk is high the original spray advice is followed, otherwise the decision is overruled. The spatial component thus makes a spray decision contingent to the co-occurrence of conditions suitable for infections and conditions suitable for field-to-field spread of substantial numbers of viable spores.

In the following sections the spore release, escape, dispersal, deposition and survival models that form the core of the system are described. There then follows a description of the risk algorithm used as a diagnostic test to make yes-or-no decisions on the need for chemical applications. It should be pointed out that several simplifying assumptions are made with regards to meteorology. As this is a proof of concept study, such simplifications are considered to be acceptable. These are

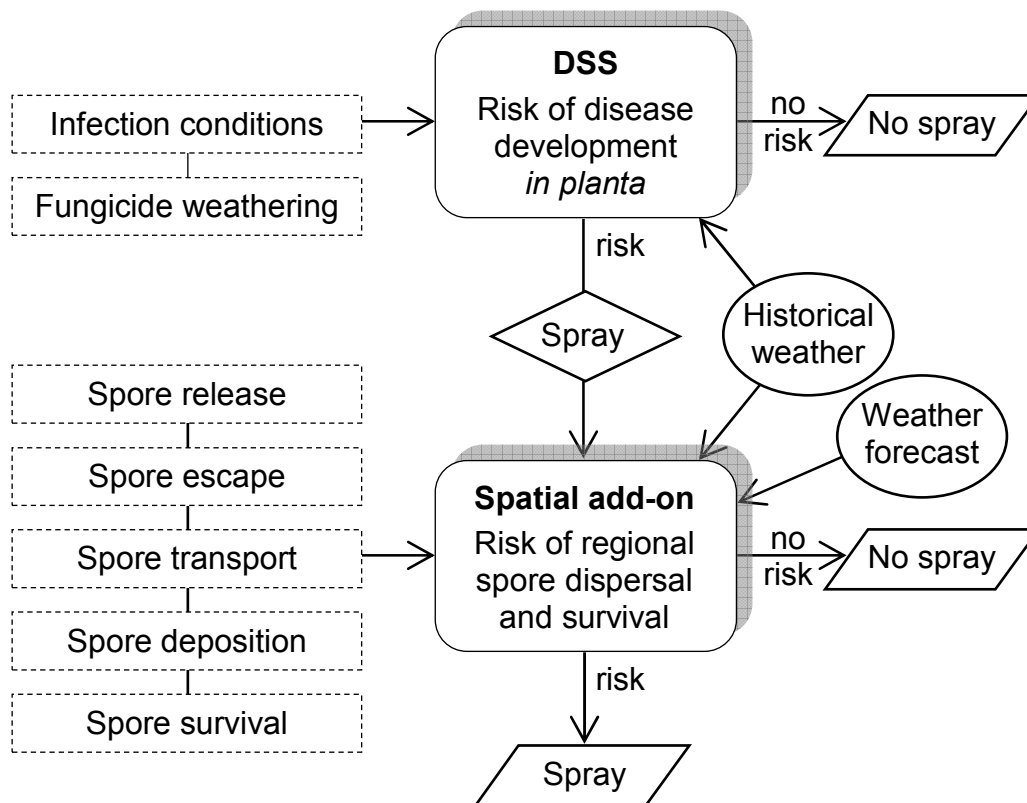


Fig. 1. Schematic overview of how a supplementary spatial component can be integrated into existing (non-spatial) operational decision support systems (DSS).

indicated in the following text. Table 1 provides a summary of symbol definitions and units.

Aerobiological models

Source strength - spore release and escape models

A standing spore crop of 1×10^9 spores is available for dispersal each day in the model. This figure represents the extreme end of Dutch regulations concerning unacceptable levels of late blight in a 1 ha. crop. A specific source strength is assumed to facilitate explanation of the approach; the assumed value of source strength does not affect the decision outcome, however, because the final evaluations of the need for spray are made on a relative, comparative scale (see below). The fraction of spores released, f_r (-), every hour from sporangiophores, and thus from the standing spore crop, is inversely related to the humidity level below 90%:

Table 1. Symbols used in this study

Symbol	Units	Description
A	- ^a	Function of shape parameter, s
B	-	Function of shape parameter, s
\bar{c}	# m ⁻²	Crosswind integrated aerial spore concentration
D_z	m ⁻¹	Vertical dispersion function
DWIP	lesion m	Distance-weighted infection pressure
DWIP ₃₃	lesion m	Threshold value for distance-weighted infection pressure
f_e	-	Fraction of spores that escape the canopy
f_r	-	Fraction of spores released from sporangiophores
f_s	-	Fraction of spores that survive
F_d	# m ⁻¹ s ⁻¹	Crosswind integrated dry deposition flux
h	m	Effective height of a potato crop / source height
L	m	Monin-Obukhov length scale
LAI	-	Leaf area index
Q	# s ⁻¹	Source strength
RH	%	Relative humidity
s	-	Vertical concentration profile shape parameter
$s_p(x)$	# m ⁻¹	Spore pressure
u	m s ⁻¹	Wind speed
\bar{u}	m s ⁻¹	Mean wind speed across the depth of the plume
v_d	m s ⁻¹	Deposition velocity
v_s	m s ⁻¹	Stokes settling velocity
x	m	Downwind distance from source
z	m	Height above the surface
z_i	m	Boundary layer height
\bar{z}	m	Mean height of the plume
l	-	Infection efficiency (cultivar specific)
K	-	von Kármán constant (0.41)
φ	MJ m ⁻²	Dose of global radiation

^a - signifies that the defined quantity is dimensionless.

$$f_r = \begin{cases} 0 & RH \geq 90 \\ \frac{1}{RH - 91} + 1 & RH < 90 \end{cases} \quad (1)$$

where RH (%) is the relative humidity. Spores that are released into the air then need to escape the canopy to be made available for long distance dispersal. The fraction of released spores that escape the canopy, f_e (-), is dependent on wind speed, u (m s⁻¹) and the leaf area index, LAI (-), of the canopy (de Jong et al., 2002):

$$f_e = \exp \left[-LAI \sqrt{v_d / (ku)} \right] \quad (2)$$

where κ is the von Kármán constant (0.41), u (m s^{-1}) is the wind speed at a characteristic height within the canopy, and v_d (m s^{-1}) is the dry deposition velocity, estimated according to Gregory (1973) as being three times the settling velocity, v_s (m s^{-1}), for *P. infestans* sporangia:

$$v_d = 3 v_s = 3 \times 0.0085 = 0.026 \text{ m s}^{-1} \quad (3)$$

Growth of the crop was not simulated and *LAI* was assumed to be fixed at 5 in equation 2. The characteristic height at which wind speed is calculated for equation 2 is assumed to be the canopy top (0.7 m), giving maximum escape. This wind speed was calculated from forecasted wind speeds, relative to a displacement height (describes the effect of the crop surface on the wind profile), using a standard logarithmic wind profile with stability correction (e.g., Arya, 1999). Displacement height was calculated according to Jacobs and Boxel (1991) as 0.43 m. It should be noted that a standard logarithmic wind profile is not strictly valid for wind speeds at and just above the top of the canopy; however, use of this formula is considered to be a desirable model simplification for an initial proof of the concept outlined in this manuscript.

Dispersal model

The dispersal model is an adaptation of the quasi-Gaussian dispersal model developed by Skelsey et al. (2008). One of the key assumptions of this model is that during each time step, steady-state conditions exist with regard to meteorological driving forces. This limits the model to short dispersal episodes and local scales. For this reason we implement a time step of 1 hour and limit the spatial extent of the model to distances of 10 km from the source. All dispersion parameters are calculated using weather conditions for the region of interest, provided by the MM5 weather forecast model (e.g., Dudhia, 1993; Grell et al., 1995).

Crosswind (horizontally) integrated aerial concentration, \bar{c} ($\# \text{ m}^{-2}$), at a receptor point (x, z) downwind from a source with emission strength Q ($\# \text{ s}^{-1}$) at $x = 0$, and $z = h$ can be written as:

$$\bar{c}(x, z) = \frac{Q}{\bar{u}} D_z(x, z, h) \quad (4)$$

where h (m) is the effective height of the source (canopy top - displacement height), \bar{u} (m s^{-1}) is the mean transport velocity across the depth of the plume and D_z (m^{-1}) is

the vertical dispersion function. Vertical concentration distributions are assumed to be non-Gaussian and D_z is given by the Lagrangian similarity diffusion model of van Ulden (1978) and Gryning et al. (1983):

$$D_z = \frac{A}{\bar{z}} \exp \left[- \left(B \frac{z}{\bar{z}} \right)^s \right] \quad (5)$$

where \bar{z} (m) is the mean height of the plume and A and B are functions of the shape parameter s , which is itself a function of atmospheric stability (the turbulent state of the atmosphere) and downwind distance. Since the primary interest in this study is dry deposition of spores at the surface ($x,0$), equation 5 is reduced to:

$$D_z = \frac{A}{\bar{z}} \quad (6)$$

The dispersion parameters \bar{z} , \bar{u} , and A are all dependent on atmospheric stability in the form of z/L , where L (m) is a characteristic length scale of the surface layer (lower 10 % of the atmospheric boundary layer). This limits the applicability of the model to near-surface releases and relatively short travel times. For operational procedures to obtain L , see Stull (1988) or Skelsey et al. (2008), and for \bar{z} , \bar{u} , and A , see Gryning et al. (1987) or Skelsey et al. (2008).

When a spore cloud is sufficiently far from the source, it will become well mixed in the boundary layer due to turbulence. For a well mixed situation, the dispersion function becomes:

$$D_z = \frac{1}{z_i} \quad (7)$$

where z_i (m) is the depth of the atmospheric boundary layer. Equation 6 is replaced by equation 7 when $\bar{z} \geq 2.5 z_i$. It should be pointed out that plume rise above the height of the boundary layer is not physically realistic as a temperature inversion at the top of the boundary layer acts as a lid preventing further upward movement from the turbulent "mixing-layer" below. This serves to further homogenize the vertical distribution in the plume. Substitution of equation 7 for equation 6 provides a means to approximate the change from limited vertical mixing to full mixing in the plume. Note that equation 6 gives the same result as $1/z_i$ within 4 % for the entire vertical distribution within the mixing layer when $\bar{z} \geq 2.5 z_i$, so a gradual change from limited vertical mixing to full mixing at larger distances is obtained.

Dry deposition model

The dispersion model is applied over long distances using small spatial steps ($\Delta x = 1$ m), and for each step material is removed from the plume by dry deposition. Chamberlain (1953) introduced the concept of “effective source strength,” whereby the reduction in plume concentration due to deposition at the surface is modeled at each Δx by reducing the strength of the source. The effective source strength depends on the amount of material already removed from the plume and therefore decreases with downwind distance. The (crosswind integrated) dry deposition flux, F_d ($\# \text{ m}^{-1} \text{ s}^{-1}$) at any point on the surface is given by:

$$F_d(x,0) = v_d \bar{c}(x,0) \quad (8)$$

Deposition is assumed to be constant over a short distance, Δx , and the change in source strength, Q , is given by:

$$Q_{x+\Delta x} - Q_x = -\Delta x F_d(x,0) = -\Delta x v_d \bar{c}(x,0) \quad (9)$$

Thus, the source strength Q at $x+\Delta x$ can be calculated using:

$$Q_{x+\Delta x} = Q_x - \Delta x v_d \frac{Q_x A}{\bar{u} \bar{z}} \quad \bar{z} < 2.5 z_i \quad (10a)$$

$$Q_{x+\Delta x} = Q_x - \Delta x v_d \frac{Q_x 1}{\bar{u} z_i} \quad \bar{z} \geq 2.5 z_i \quad (10b)$$

Starting at $x = 1$ m, equation 10 is iterated to provide the (effective) source strength, Q , for equation 4, for any downwind distance x .

Spore survival model

The experimental results of Mizubuti et al. (2000) are used to determine the fraction of deposited spores that remain infective. Survival of spores during transportation is dependent on the dose, φ (MJ m^{-2}), of global radiation received (direct plus diffuse shortwave radiation) during spore flight:

$$f_s = 0.79 \exp(-1.21\varphi) \quad (11)$$

where f_s (-) is the fraction of deposited spores that survive. In order to calculate φ , information regarding the time spent in the air and the flux of incoming global radiation is required. According to the results of Mizubuti et al. (2000), a one hour exposure on a sunny day was enough to inactivate 95 % of the sporangia of a *P. infestans* isolate belonging to the US-1 clonal lineage.

Weather forecast data - MM5 model.

The forecast data required as input by the above models are provided by The Pennsylvania State University /National Center for Atmospheric Research mesoscale model version 3.6 (e.g., Duda, 1993; Grell et al., 1999), as ran by the Meteorology and Air Quality group at Wageningen University. MM5 is a limited-area, nonhydrostatic, terrain-following sigma-coordinate model designed to simulate or predict mesoscale atmospheric circulation. The model is supported by several pre- and post-processing programs, which are referred to collectively as the MM5 modeling system. A number of processes cannot be resolved explicitly by the model, and need to be parameterized. MM5 provides a number of options for each process. For this study, the following parameterizations are relevant: (i) the interaction of the land surface with the atmosphere is described using the Noah land surface model (Ek et al., 2003); (ii) turbulent transport in the boundary layer is described using the eddy diffusivity formulation by Hong and Pan (1996); and (iii) radiation is treated using the cloud radiation scheme. The MM5 forecasts are initialized using output of the Global Forecasting System (GFS) model from the National Centers for Environmental Prediction (NCEP) in the US. GFS runs initiated at 00 GMT are used. The MM5 forecasts are run for a period of 48 hours. Two nested computational grids are used, with grid sizes of 27 and 9 kilometers, respectively, and domain sizes of 2295 x 2295 km, and 333 x 306 km. The domains are centered on Wageningen (latitude 51°58' N, longitude 5°40' E). In total, MM5 provides 7 meteorological variables for input and parameterization of the aerobiological models described above: sea level air pressure, temperature, specific humidity at 2 m height, incoming shortwave radiation, sensible heat flux, boundary layer height, and wind speed at 10 m.

Risk algorithm

On any day in which a spray is recommended by a DSS, the above models for spore release, escape, dispersal, deposition and survival are combined with the MM5 weather forecast model to make a quantitative estimate of the risk of infection from a hypothetical, distant source of inoculum. This estimate is compared to a threshold value in order to make a yes-or-no decision regarding modification of that original advice. MM5 forecast data between the hours of 7 am and 4 pm are used as input for the models as these are the hours when spore release and dispersal are most likely. Either data from the 1 day or the 2 day forecast can be used, depending on how much advance time is required to implement the decision.

The first step is to use the spore release model (equation 1) to calculate the hourly release of spores from the hypothetical source, which has a standing spore crop of 1×10^9 spores, which is refreshed each day. Next, the spore escape model (equations 2 and 3) is used to determine the fraction of the released spores that escape the source canopy and are made available for long distance transport. These two models provide the source strength, Q , for the dispersal model. Equations 4 to 7 are used to calculate aerial (crosswind integrated) spore concentrations at downwind distances of 1 to 10,000 m (every meter), and the deposition (equations 8 to 10) and spore survival models (equation 11) are used to provide a prediction of the downwind viable spore deposition gradient. Hourly deposition gradients are summed over the course of the day (from 7 am till 4 pm) to give the total number of viable spores deposited per meter (spore pressure) at each distance, x (m), from the hypothetical source (Fig. 2A).

Next, this gradient is summarized using the following statistic, DWIP (lesion m), which is the distance-weighted infection pressure (Fig. 2B):

$$\text{DWIP} = \iota \int_{x=0}^{\infty} x s_p(x) dx \quad (12)$$

where ι (-) is the cultivar specific infection efficiency, x (m) is the distance from the source, and $s_p(x)$ ($\# \text{ m}^{-1}$) is the crosswind integrated spore pressure at distance x . DWIP is therefore a cultivar specific statistic that attaches weight to high values of infection pressure, and to distant values of infection pressure, i.e., high risk days are those in which a lot of spores are released and escape the canopy, and/or those in which spores can travel and survive over long distances. DWIP can also be interpreted as the total number of new infections caused downwind from a standard source of one billion spores, multiplied by the average distance to the source, assuming a landscape covered entirely with potatoes and optimal conditions for infection at the target sites. Each cultivar specific DWIP value is then compared to a pre-calculated threshold level in order to make a yes-or-no decision regarding modification of the original spray advice for that particular cultivar (Fig. 2C).

The threshold level was determined by calculating a range of DWIP values using epidemiologically relevant weather conditions. First, critical late blight periods (days conducive to potato late blight development in the field) were selected from a 10 year (1997 to 2006) historical weather data set provided by the Wageningen University weather station (Haarweg; <http://www.maq.wur.nl>). Critical periods were determined using environment-pathogen relations from the potato late blight model

of Skelsey et al. (*in press*) and weather data pertaining to the potato growing season (May to September) in each year. This gave a total of 140 critical late blight periods for the 10 year historical weather data set. Next, DWIP values were calculated for those critical periods using ι values for the three potato cultivars used in the field

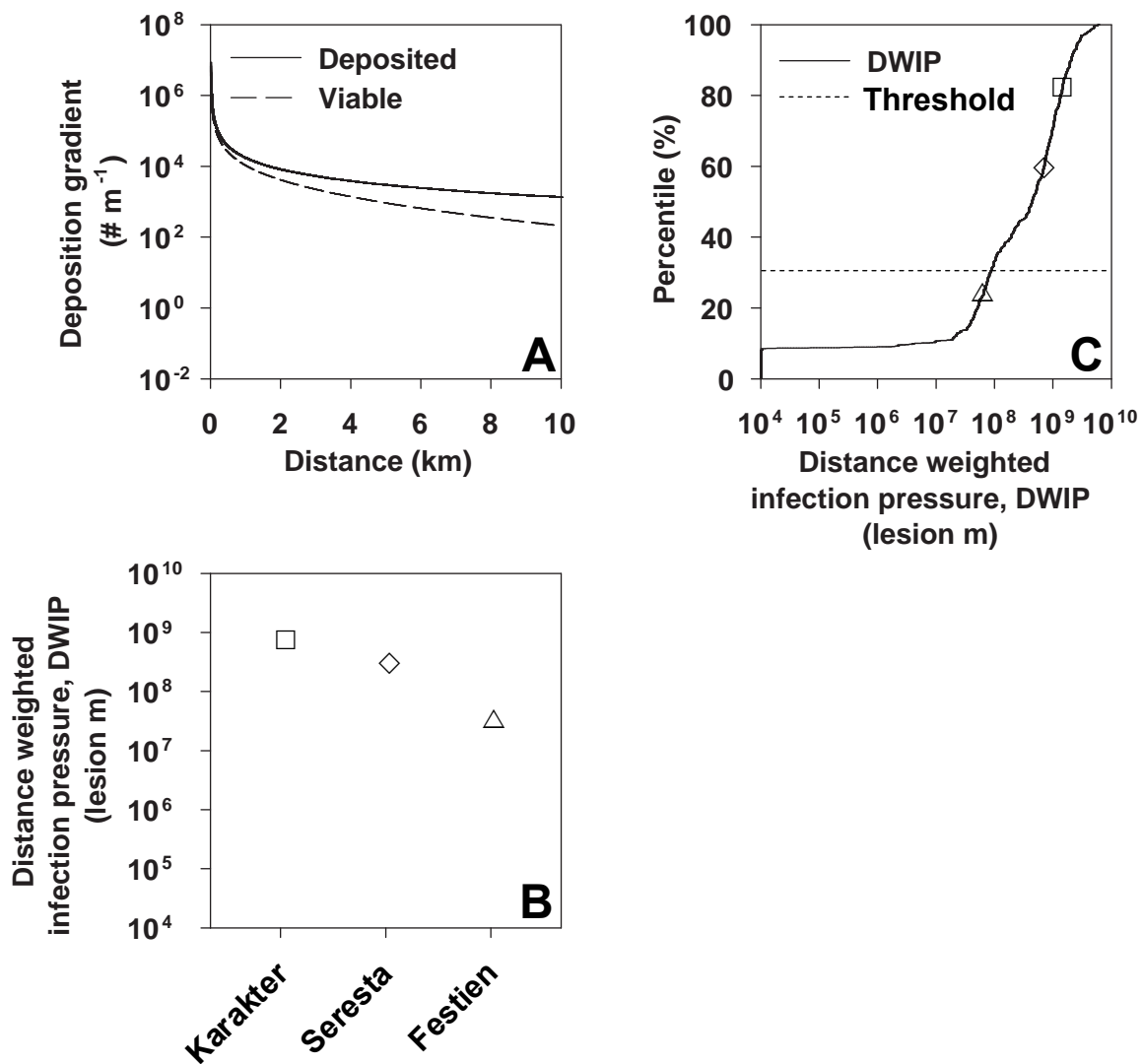


Fig. 2. Graphical portrayal of the calculation steps contained in the risk algorithm of a supplementary spatial component for potato late blight decision support systems: (A) a spore deposition gradient is produced for the day of interest using weather forecast data and the models for spore release, escape, dispersal and deposition - this gradient is then modified to produce a deposition gradient of viable spores using the spore survival model; (B) the viable deposition gradient is summarized using a new statistic, the cultivar specific distance-weighted infection pressure, DWIP (lesion m; equation 12); and (C) DWIP is compared to a threshold value, derived from historic weather data, in order to make a decision on the need for crop protection measures.

trials described below. These were determined experimentally following the procedures outlined in Skelsey et al. (*in press*); giving values of 0.0025, 0.025, and 0.05 for cultivars Festien (highly resistant), Seresta (moderately resistant) and Karakter (susceptible) respectively. This gave a total of 420 historical DWIP values (140 critical periods x 3 cultivars). All DWIP values were then ranked and the value of the 33rd percentile was chosen as the threshold level, DWIP₃₃, for all decisions regarding modification of spray recommendations (Fig 2C). Thus, on any day that a spray is recommended by a DSS, DWIP values are calculated for each cultivar of interest and compared to the threshold value, DWIP₃₃. If the predicted value from the risk algorithm is greater than DWIP₃₃ then the risk of infection from distant sources of inoculum is deemed to be high enough to warrant crop protection measures for that particular cultivar, otherwise, no action is required and the original spray advice is overruled.

As described previously, this system is intended to operate as a supplementary spatial component for existing DSSs. The intent in choosing the 33rd percentile to determine the threshold level for spray recommendations is to reduce the number of recommendations of a “standard” DSS by one third. This is an arbitrary choice for an experimental system, and by constructing the risk algorithm in this way, an implicit assumption is made that days conducive for disease development in the field are only risky for dispersal to distant “clean crops” on an average of 2 out of 3 occasions. Furthermore, the threshold value, DWIP₃₃, is (by nature of the calculation steps described above) strictly only valid for modifying spray recommendations made on the three potato cultivars used in this study. As an experimental system, these simplifications are regarded as being conducive to a proof of concept. The reader should refer to Fig. 2C for the distribution of DWIP, calculated on the basis of 10 years historical weather data and three cultivars. It can be seen that this distribution extends over 7 orders of magnitude. Approximately 10 % of DWIP values were zero as humidity levels did not drop sufficiently to result in spore release on those days (not plotted).

Field evaluation

A field experiment was conducted in 2007 in Valthermond (latitude 52°53' N, longitude 6°57' E), the Netherlands, in the center of the Dutch Northeastern starch potato growing area (which continues into Germany to the east of Valthermond). A randomized, split-plot design was used, with three potato cultivars, two late blight management systems, and four replications. Potato cultivars were used as main plots

and potato late blight management systems as sub-plots. Each sub-plot measured 6 x 12 m. As mentioned previously, the potato cultivars were Festien (highly resistant), Seresta (moderately resistant), and Karakter (susceptible); all starch potato cultivars. They were planted on 4th May 2007, and two Curzate treatments were applied on the 1st and 11th of June to eliminate latent tuber infections. From 11th of June onwards, spray decisions were based on historical and predicted weather and the remaining level of protection from previous sprays using one of two DSSs: SIMCAST (Grünwald et al., 2000; Grünwald et al., 2002) or SIMCAST-plus.

The experiment took place in the summer of 2007, which was a warm and wet summer (Fig. 3). According to KNMI (the Royal Dutch Meteorological Society; <http://www.knmi.nl/>), this period saw the second wettest July on record since 1901. Continual rain and high levels of humidity meant that conditions for potato late blight during the first half of the field experiment were extremely favorable. Consequently, natural disease pressure was high providing exacting test conditions for the new system. Potato fields bordering the experimental site were observed to be heavily infected (and were subsequently desiccated) and on the 30th June and 3rd July, two eradivative treatments (2.5 kg Curzate M + 0.4 l Shirlan per ha) were applied to eliminate low levels of infection in some of the experimental plots. Conditions became drier from the end of July onwards and the level of disease pressure subsequently decreased.

In SIMCAST, “blight units” are calculated each day using temperature and humidity data, and these accumulate over time to provide an estimate of the risk of disease development in the field. The remaining level of protection on the crop is also estimated and “fungicide units” are calculated based on precipitation and the number of days since the last spray. A spray is recommended whenever the number of blight units or fungicide units is greater than 15; the threshold value for susceptible cultivars. Total blight and fungicide units are reset after fungicide is applied and new totals begin to accumulate. SIMCAST-plus consisted of SIMCAST and the supplementary spatial component described above.

The threshold values for blight and fungicide units used in SIMCAST (and therefore SIMCAST-plus) are the threshold values for susceptible cultivars. SIMCAST also includes a possibility to delay sprays on more resistant cultivars by using a higher threshold for blight and fungicide units. Use of the lower threshold values creates a margin of protection for resistant cultivars that is subsequently exploited here to reduce the Shirlan dose rate according to the resistance level of the cultivar. Shirlan dose rates were 0.4, 0.2 and 0.1 l ha⁻¹ for cultivars Karakter, Seresta and Festien

respectively; by default, Karakter receives a full dose, Seresta a half dose and Festien a quarter dose of Shirlan, which is recommended (full dose) at 0.4 l ha^{-1} .

SIMCAST recommendations were followed according to certain practical restrictions: chemical applications were not applied when it was raining, and were also not applied on Sundays. Expert judgment was used to apply fungicides one day early if it was expected that the threshold value for a spray recommendation would

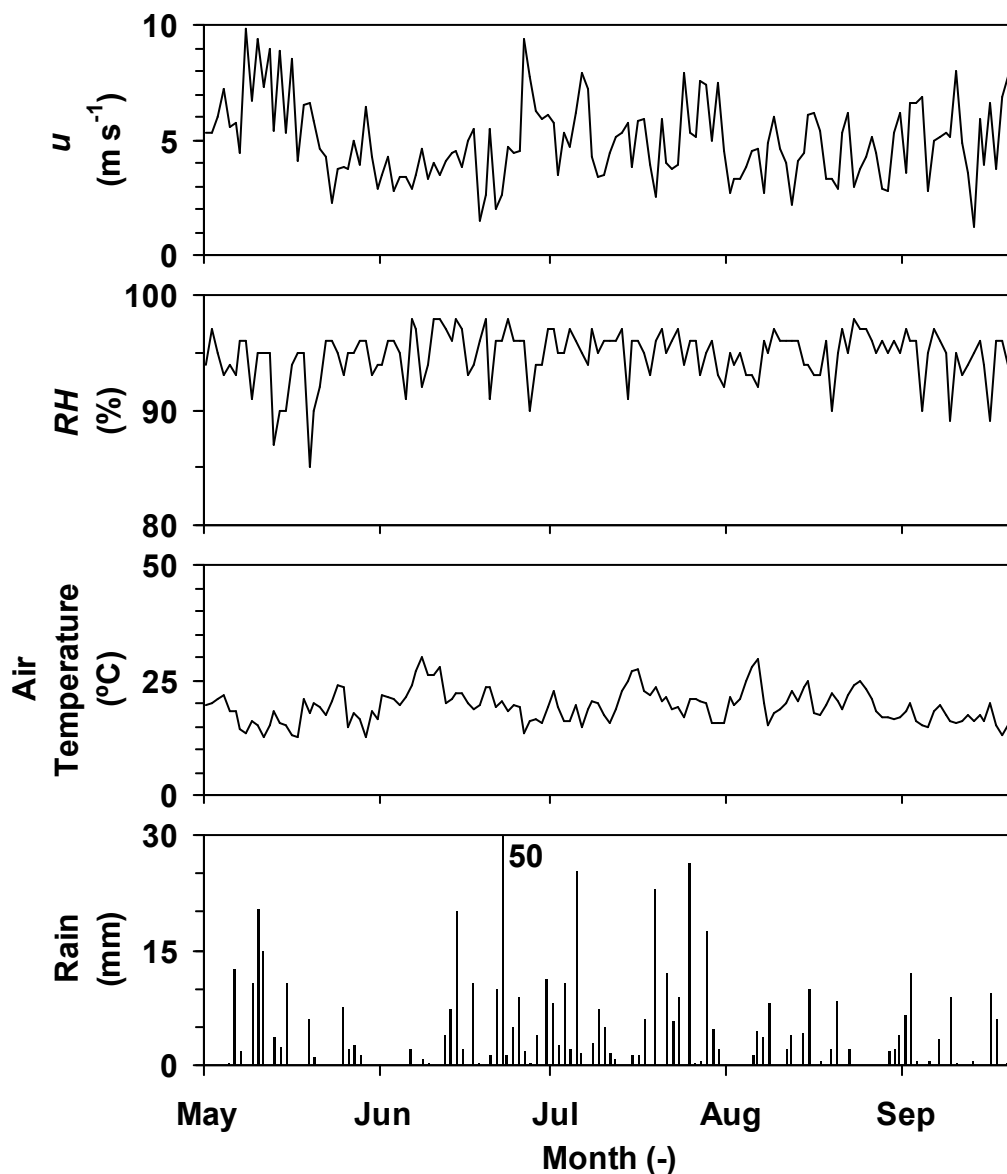


Fig. 3. On site meteorological measurements for the 2007 Valthermond field trials provided by a commercial standard agricultural meteorological weather station exploited by Dacom PLANT Service (Emmen, the Netherlands). Panels from top to bottom show the maximum wind speed, relative humidity and air temperature (hourly averages) and the total precipitation on each day.

be breached on a Sunday. Historical weather data (temperature, precipitation, humidity) for SIMCAST calculations were provided by a commercial standard agricultural weather station exploited by Dacom PLANT Service (Emmen, the Netherlands), which was adjacent to the experimental site. Disease severity was assessed once or twice per week using the PD scale (de Visser and Meier, 2000). Following completion of the cropping cycle, the plots were desiccated with Reglone on September 18th.

Results

One of the aforementioned assumptions upon which the supplementary spatial component for DSSs operates is that “the capacity of the atmosphere to transport viable spores over distance is highly variable.” The validity of this assumption is demonstrated by showing the extreme ends of the range of spore deposition and survival gradients that were used to determine DWIP values and the threshold for yes-or-no spray decisions in the risk algorithm (Fig. 4). These two sets of curves were both produced on separate days that were identified as being of high risk for disease development in the field, i.e., on days in which a chemical application would normally be recommended by a DSS. A comparison of the two spore survival gradients reveals that at a distance of 1 km from the hypothetical source, the number of viable spores depositing per meter differs by three orders of magnitude. At a distance of 10 km, this difference increases to four orders of magnitude. This figure graphically portrays the wide variation in dispersal conditions on “high risk” days that gave rise to the large range of DWIP values shown in Fig. 2. It also serves to illustrate the margin within which the supplementary spatial component operates to modify spray recommendations according to the level of risk from distant sources of inoculum.

A sensitivity analysis is used to demonstrate the effects of different weather conditions on the shape of spore deposition and survival gradients predicted by the supplementary spatial component (Fig. 5). It can be seen that when levels of solar radiation are higher, spore survival decreases according to the spore survival model. Higher levels of radiation also create more “vertical mixing” in the spore dispersal model. As the level of radiation increases, so does the heat flux from the surface, creating more and larger eddies of turbulent air that serve to mix the spore cloud in the vertical direction. This means that spore clouds become deeper and more dilute as turbulent eddies of air lift spores upwards away from the surface. Thus, when

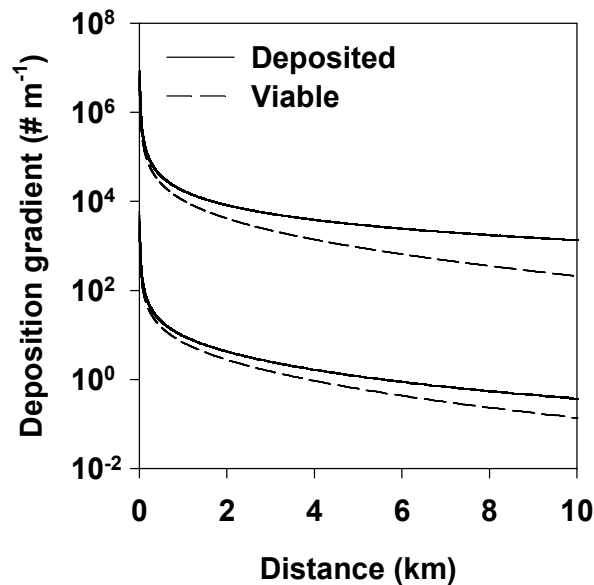


Fig. 4. Variation in the ability of the atmosphere to transport viable spores over distance. The upper two curves show the maximum deposition gradient of spores (solid line) and viable spores (dashed line) and the lower two curves the minimum deposition and survival gradients, as calculated by a supplementary spatial component for potato late blight decision support systems, using input weather data for every “high risk” day (days conducive to disease development) over a 10 year period (1997 to 2006 inclusive). Hourly weather data were provided by the Wageningen University weather station (Haarweg; <http://www.maq.wur.nl>).

conditions are more turbulent (unstable), surface deposition of viable spores decreases, which tends to decrease the risk for substantial long distance transport of viable spores. Stronger winds serve to transport spores to their destination at greater speeds. Shorter travel times mean that less radiation is absorbed and spore survival increases. With stronger winds there is less vertical mixing and spore deposition gradients flatten. Strong winds thus tend to increase the risk of substantial long distance transport of viable spores.

Over the course of the field experiment, SIMCAST recommended a total of 14 fungicide applications (Fig. 6). These recommendations were based on calculated fungicide units, as their threshold value was always reached before the threshold for blight units. Whilst this is not strictly relevant for the operation of the system, it does indicate an interesting trade off. Fungicide weathering was, according to SIMCAST, contributing more to risk than the warm, humid conditions conducive for disease development.

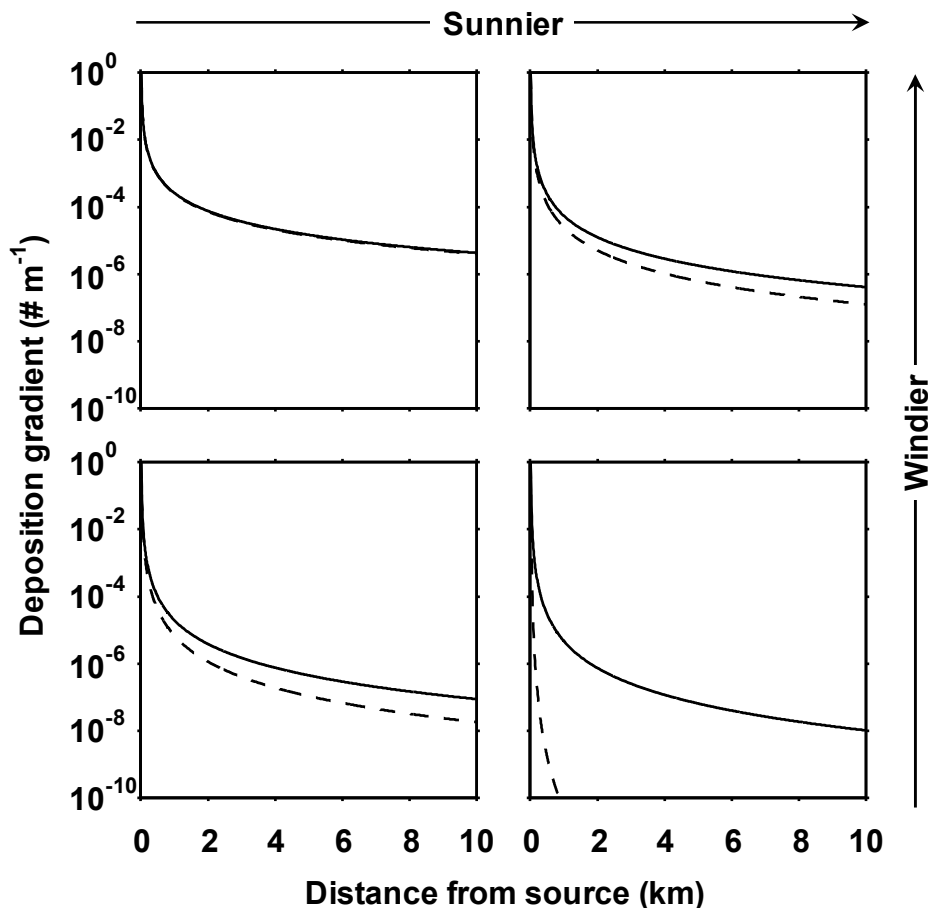


Fig. 5. Influence of weather conditions on the shape of spore deposition and survival gradients predicted by a supplementary spatial component for potato late blight decision support systems. Global radiation was varied between 100 and 1000 W m^{-2} , and wind speed between 1 and 10 m s^{-1} .

The supplementary spatial component incorporated in SIMCAST-plus modified a total of three of the 14 spray recommendations for the cultivar Festien (Fig. 6). On these occasions, cultivars Karakter and Seresta were sprayed whereas cultivar Festien was left untreated. The negated spray recommendation was kept in memory and if in the following days the risk of viable spore transport was high (according to the supplementary spatial component) then fungicides were applied to the untreated plots. This was the case on the day following the first modified spray recommendation, and fungicides were accordingly applied to the untreated Festien plots. On the second and third occasions where a spray decision was modified, conditions continued to be unsuitable for transport of viable spores over distance (according to the supplementary spatial component) and as a result, both chemical treatments were avoided altogether.

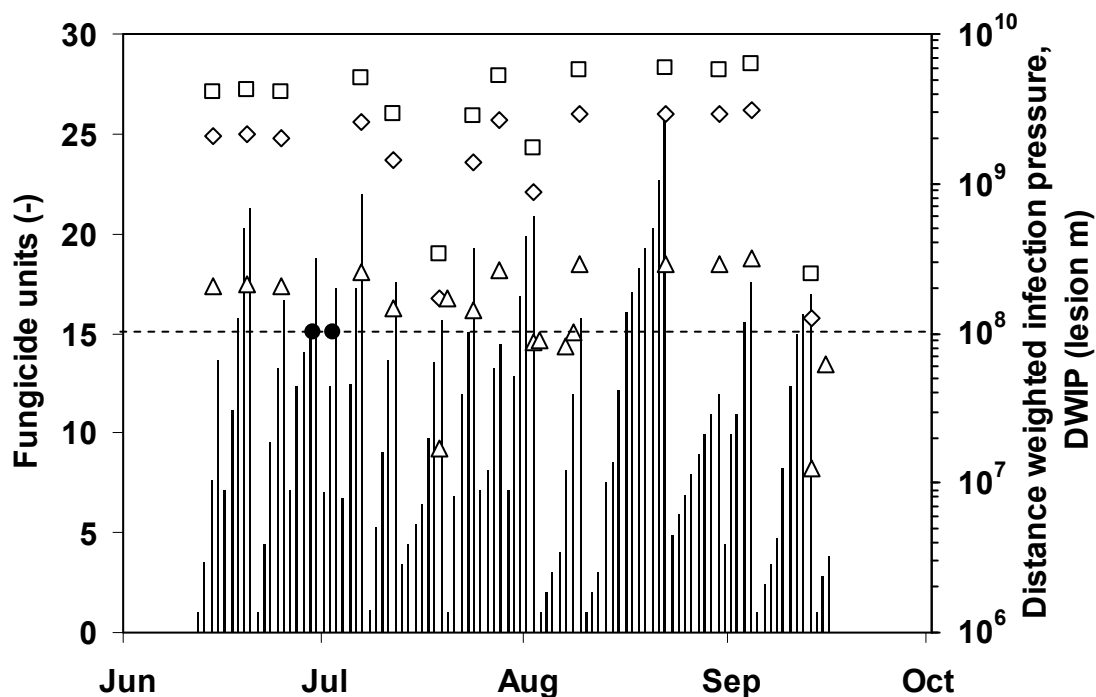


Fig. 6. Output from the two decision support systems for potato late blight used in the 2007 Wageningen field trials. Solid lines show calculated SIMCAST fungicide units (left hand y-axis). Data markers show calculations of distance-weighted infection pressure, DWIP (lesion m), (right hand y-axis) by a supplementary spatial component incorporated into SIMCAST-plus, for cultivars Karakter (\square ; susceptible), Seresta (\diamond ; moderately resistant), and Festien (\triangle ; highly resistant). These calculations (of DWIP) are initially made only if cumulated fungicide units in SIMCAST exceed a threshold. Solid data markers show the application of two Curzate treatments to eliminate low levels of infection in some of the plots. The two y-axes have been scaled so that the dashed line shows the threshold value for spray recommendations for both SIMCAST fungicide units and DWIP.

A high level of disease control was achieved by both DSSs (Fig. 7) despite (very) favorable conditions for potato late blight and high disease pressure from the direct surroundings of the experiment during large parts of the growing season. Reducing the fungicide dose rates according to resistance level of the cultivar proved to be an effective strategy as there was almost no difference in final disease levels between cultivars. Similarly, the difference in the level of disease control afforded by the two DSSs was miniscule and not significant. This serves to demonstrate that the supplementary spatial component for DSSs can reduce the number of sprays recommended in a growing season and maintain adequate levels of crop protection.

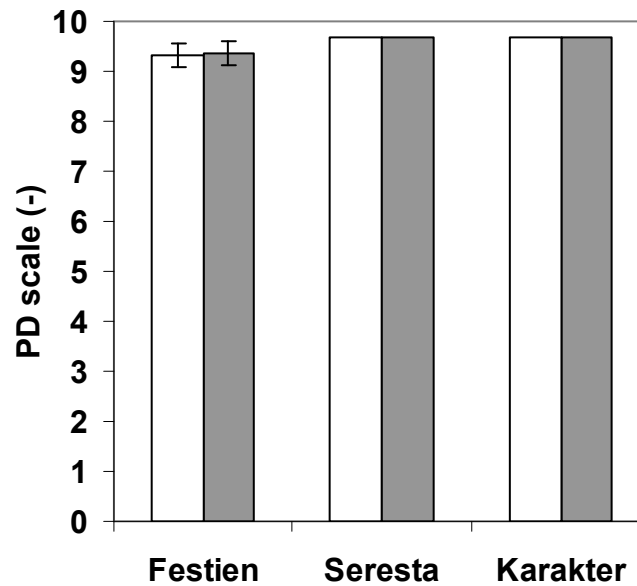


Fig. 7. Final disease severity in the 2007 Valthermond field trials. Columns show disease severity according to the PD scale for experimental plots protected by the decision support systems SIMCAST (white bars), and SIMCAST-plus (grey bars), for each of the three cultivars used in the field trials. The PD scale estimates potato late blight severity from 0 (crop completely dead) to 10 (no disease). Each bar is an average over four replicate plots. Error bars show +/- one standard deviation.

Discussion

Fundamentally, this study is concerned with including more meteorological information in operational decision support. Given the strong weather dependency of plant pathogens such as *P. infestans*, it is natural to question if a more detailed consideration of meteorology could lead to improvements in practical disease management. Spatial epidemiology has been scarcely used in operational decision support, and the development of spatial risk factors for regional spore dispersal from aerobiological models offers a new approach for manipulation of spray intervals in such systems. Previously, the influx component of the infection risk was largely ignored because it is difficult to handle. Instead it was assumed that spore influx always takes place at significant levels so that decisions come to depend on local conditions only. One of the strengths of the approach outlined in this manuscript therefore lies in the comprehensive use of forecast data already incorporated in many DSSs; here, we used sophisticated MM5 forecast data but meteorological forecast data are routinely purchased and used by providers of DSSs, so here may be

a feasible opportunity for enhancing use of meteorological information in disease decision support. A further advantage is the applicability of this concept to a range of similar pathosystems characterized by airborne dispersal of inoculum. It has been demonstrated here that spatial risk algorithms are easily incorporated into existing frameworks in the form of a supplementary spatial component, with model results conveniently expressed in the form of a yes-or-no spray modification decision. Results from the field trials showed that in the period of normal disease pressure (the drier half of the field trial, from the end of July onwards), a total of 2 out of the 6 remaining fungicide applications were saved for the most resistant of the three cultivars tested, which was otherwise sprayed with only 25 % of the recommended dose rate of Shirlan. The total reduction of fungicide input for the resistant cultivar (Festien) was high at almost 80 %: the ratio of active ingredient applied to maximum possible used = $(1/4 \text{ dose} \times 12 \text{ sprays}) / (\text{full dose} \times 14 \text{ sprays}) = 0.2$. A high level of protection was maintained throughout the season, even in plots that received a reduced number of sprays. This demonstrates that the supplementary spatial component can provide robust control. These results suggest potential for this approach and further field trials are planned for system development and validation. Total reduction in fungicide input over the whole field trial was also high at 43 %: the ratio of active ingredient applied to maximum possible used = $(8 \text{ plots of cv. Karakter} \times \text{full dose} \times 14 \text{ sprays} + 8 \text{ plots of cv. Seresta} \times 1/2 \text{ dose} \times 14 \text{ sprays} + 8 \text{ plots of cv. Festien} \times 1/4 \text{ dose} \times 12 \text{ sprays}) / (24 \text{ plots total} \times \text{full dose} \times 14 \text{ sprays}) = 0.57$.

There is currently much interest in the inclusion of spatial information in decision support. Advances in geographic information systems (GIS) have provided exciting new opportunities. For example, SIMBLIGHT1 is a potato late blight DSS that uses GIS to interpolate weather forecast data and produce maps showing “hot spots” of maximum risk (Kleinhenz and Zeuner, 2006). By incorporating GIS technology, this system is able to improve the quality of historical meteorological input data for disease prediction models, and produce vivid map representations that make decision support results easier to understand. In contrast to the concept outlined in this study, the predictive emphasis of this GIS based system is on mapping of weather conditions that facilitate the development of disease *in planta*, as opposed to a quantification of the physical dispersal of viable inoculum between fields. More akin to the current approach is an innovative example of aerobiological modeling in the United States Department of Agriculture Soybean Rust Coordinated Framework (Isard et al., 2004; Isard et al., 2007). An integral component of this framework, the Soybean Rust Aerial Prediction System (SRAPS), combines models for spore

production, spore escape, spore transport, deposition and survival and runs several different overwintering scenarios in order to predict likely large-scale (state by state) spread for the upcoming growing season. Although similar to the concept outlined in this study, SRAPS attempts to predict long-term spatial invasion patterns based on assumptions regarding the initial distribution of disease. As an early warning system, output from SRAPS is used in a strategic sense, to guide rust monitoring strategies and provide advanced warning to extension specialists concerning possible spread to their state. In contrast, the supplementary spatial component described here produces location specific output (by virtue of location specific weather forecasts) that is designed to be used by growers on a day-to-day basis for operational decision making. There are many more examples of innovative use of spatial information in decision support. Another exciting new development is the use of a network of spore traps as part of the early warning Syntinel RustTracker system (von Qualen, 2006). Spore traps (around 2 per soybean growing state) are monitored in an attempt to warn growers that spores are in their area. This of course does not equate to disease being present in the area, and this information is again used to direct scouting efforts. Even with these few examples, it becomes clear that a number of different strategies exist for the inclusion of spatial context in decision support. With spatial decision support receiving more and more attention, the use of spatial tools to solve spatial problems and meet desired spatial goals seems set to continue in integrated crop protection strategies.

The contribution of this paper is to present a novel approach for including regional spore dispersal as a spatial risk factor in operational disease risk warnings for potato late blight when the location of sources is not known. The supplementary spatial component for DSSs provides a quantification of the risk of viable spore dispersal over relevant distances, and represents a low cost method for including regional dispersal modeling in operational decision support. An initial proof of concept has been presented. Further field trials are required before definitive conclusions can be drawn as to the utility of this approach. The approach is not limited to potato late blight and the method developed here could prove to be useful in a decision context for other pathosystems.

Acknowledgements

Funding for this study was provided by the Dutch Ministry of Agriculture, Nature Management and Fisheries through the Umbrella Plan *Phytophthora* (DWK 427), and the Umbrella Plan *Phytophthora* II (BO06-08).

References

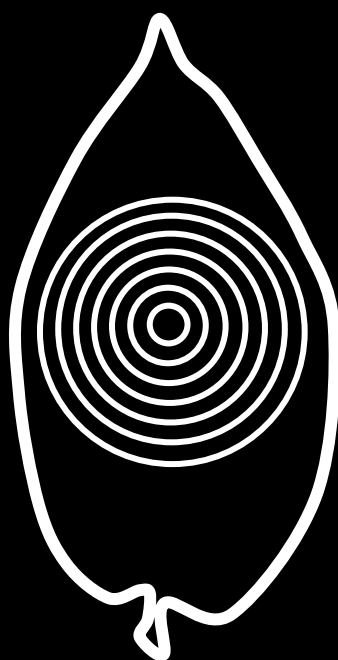
- Arya, S.P. 1999. Air pollution meteorology and dispersion. Oxford university press, New York, NY, 310 pp.
- Aylor, D.E. 1989. Aerial dispersal close to a focus of disease. *Agr. Forest Meteorol.* 47:109-122.
- Aylor, D.E. 2005. Quantifying maize pollen movement in a maize canopy. *Agr. Forest Meteorol.* 131:247-256.
- Aylor, D.E., and Boehm, M.T. 2006. Quantifying aerial concentrations of maize pollen in the atmospheric surface layer using remote-piloted airplanes and Lagrangian stochastic modeling. *J. Appl. Meteorol. Clim.* 45:1003-1015.
- Aylor, D.E., and Flesch, T.K. 2000. Estimating spore release rates using a lagrangian stochastic simulation model. *J. Appl. Meteorol.* 40:1196-1208.
- Aylor, D.E., Fry, W.E., Mayton, H., and Andrade-Piedra, J.L. 2001. Quantifying the rate of release and escape of *Phytophthora infestans* sporangia from a potato canopy. *Phytopathology* 91:1189-1196.
- Birch, P.R.J., and Whisson, S.C. 2001. *Phytophthora infestans* enters the genomics era. *Mol. Plant Pathol.* 2:257-263.
- Bourdôt, G.W., Baird, D., Hurrell, G.A., and de Jong, M.D. 2006. Safety zones for a *Sclerotinia sclerotiorum* -based mycoherbicide: Accounting for regional and yearly variation in climate. *Biocont. Sci. Technol.* 16:345-358.
- Chamberlain, A.C. 1953. Aspects of travel and deposition of aerosol and vapor clouds. Report No. A.E.R.E HP/R1261. Her Majesty's Stationery Office, London.
- de Jong, M.D. 1988. Risk to Fruit Trees Due to Control of Black Cherry (*Prunus serotina*) by Silver Leaf Fungus (*Chondrostereum purpureum*). PhD thesis, Wageningen Agricultural University, Wageningen, The Netherlands.
- de Jong, M., Bourdôt, G.W., Powell, J., and Goudriaan, J. 2002. A model of the escape of *Sclerotinia sclerotiorum* ascospores from pasture. *Ecol. Model.* 150:83-105.
- de Visser, C.L.M., and Meier, R. 2000. Field evaluation of four decision support systems for potato late blight in the Netherlands. In: Schepers, H. (Ed.), Proceedings of the Workshop

- on the European network for development of an integrated control strategy of potato late blight, Oostende, Belgium. PAV Special Report no. 6:137-155.
- Dudhia, J. 1993. A nonhydrostatic version of the Penn State - NCAR mesoscale model: Validation tests and simulation of an Atlantic cyclone and cold front. *Mon. Weather. Rev.* 121:1493-1513.
- Drenth, A., Janssen, E.M., and Govers, F. 1995. Formation and survival of oospores of *Phytophthora infestans* under natural conditions. *Plant Pathol.* 44:86-94.
- Duncan, J.M. 1999. *Phytophthora* - an abiding threat to our crops. *Microbiol. Today* 26:114-116.
- Ek, M.B., Mitchell, K.E., Lin, Y., Grunmann, P., Rogers, E., Gayno, G., and Koren, V. 2003. Implementation of the upgraded Noah land-surface model in the NCEP operational mesoscale Eta model. *J. Geophys. Res.* 108:8851.
- Erwin, D.C., and Ribeiro, O.K. 1996. *Phytophthora infestans* (Mont.) de Bary (1876). *Phytophthora Diseases Worldwide*. St. Paul, Minnesota, APS Press, 562 pp.
- Gregory, P.H. 1973. *The microbiology of the atmosphere*. Wiley, 377 pp.
- Grell, G.A., Dudhia, J., and Stauffer, D.R. 1995. A description of the fifth-generation Penn State/NCAR Mesoscale Model (MM5), NCAR Tech. Note, NCAR/TN-398 + STR, 122 pp.
- Grünwald, N.J., Rubio-Covarrubias, O.A., and Fry, W.E. 2000. Potato late-blight management in the Toluca Valley: Forecasts and resistant cultivars. *Plant Dis.* 84:410-416.
- Grünwald, N.J., Cadena-Hinojosa, M.A., Rubio-Covarrubias, O., Rivera-Pena, A., Niederhauser, J.S., and Fry, W.E. 2002. Potato cultivars from the Mexican national potato program: Sources and durability of resistance against late blight. *Phytopathology* 92:688-693.
- Gryning, S.E., van Ulden, A.P., and Larsen, S.E. 1983. Dispersion from a continuous ground-level source investigated by a *K* model. *Quart. J. R. Met. Soc.* 109:355-364.
- Gryning, S.E., Holtslag, A.A.M., Irwin, J.S., and Sivertsen, B. 1987. Applied dispersion modelling based on meteorological scaling parameters. *Atmos. Environ.* 21:79-89.
- Hadders, J. 1999. Experiences with Plant-Plus in 1998. In: Schepers, H., and Bouma, E. (Eds.), *Proceedings of the Workshop on the European network for development of an integrated control strategy of potato late blight*, Uppsala, Sweden. PAV Special Report no. 5:194-200.
- Hansen, J.G., Andersson, B., and Hermansen, A. 1995. NEGFY - A system for scheduling chemical control of late blight in potatoes. In: Dowley, L.J., Bannon, E., Cooke, L.R., Keane, T., and O'Sullivan, E. (Eds.), *Phytophthora 150: EAPR conference proceedings*. EAPR, Boole Press, Dublin, Ireland, pp. 201-208.
- Hansen, J.G., and Andersson, B. 1996. Development and practical implementation of a system for potato late blight forecasting in potatoes. In: Dalezios, N.T. (Ed.), *International Symposium on Applied Agrometeorology and Agroclimatology*. European Commission. Cost 77, 79, 711, pp. 251-258.

- Haverkort, A.J., Boonekamp, P.M., Hutten, R., Jacobsen, E., Lotz, L.A.P., Kessel, G.J.T., Visser, R.G.F., and van der Vossen, E.A.G. 2008. Societal costs of late blight in potato and prospects of durable resistance through cisgenic modification. *Pot. Res.*, *in press*.
- Hijmans, R.J., Forbes, G.A., and Walker, T.S. 2000. Estimating the global severity of potato late blight with GIS-linked disease forecast models. *Plant Pathol.* 49:697-705.
- Hong, S.Y., and Pan, H.L. 1996. Nonlocal boundary layer vertical diffusion in a medium-range forecast model. *Mon. Weath. Rev.* 124:2322-2339.
- Hyre, R.A. 1950. Spore traps as an aid in forecasting several downy mildew type diseases. *Plant Dis. Rep., Suppl.* 190:14-18.
- Isard, S.A., Russo, J.M., and Ariatti, A. 2007. The Integrated Aerobiology Modeling System applied to the spread of soybean rust into the Ohio River valley during September 2006. *Aerobiologia* 23:271-282.
- Isard, S.A., Gage, S.H., Comtois, P., and Russo, J.M. 2004. Principles of the atmospheric pathway for invasive species applied to soybean rust. *BioScience* 55:851-861.
- Jacobs, A.F.G., and Boxel, J.H. 1991. Horizontal and vertical distribution of wind speed in a vegetation canopy. *Neth. J. Agric. Sci.* 39:165-178.
- Kleinhenz, B., and Zeuner, T. 2006. Introduction of GIS in decision support systems for plant protection. In: Alford, D.V., Feldmann, F., von Hasler, J., and Tiedemann, A. (Eds.), *Best practice in disease, pest and weed management: the state of the art*, Humboldt University, Berlin, Germany. *Symposium proceedings no. 82*:28-30.
- Krause, R.A., Massie, L.B., and Hyre, R.A. 1975. BLITECAST: a computerized forecast of potato late blight. *Plant Dis. Rep.* 59:95-98.
- Madden, L.V., Hughes, G., and van den Bosch, F. 2007. *The study of plant disease epidemics*. The American Phytopathological Society, St. Paul, Minnesota, USA, pp. 421.
- Minogue, K. P., and Fry, W.E. 1981. Effect of temperature, relative humidity and rehydration rate on germination of dried sporangia of *Phytophthora infestans*. *Phytopathology* 71:1181-1184.
- Mizubuti, E.S.G., Aylor, D.E., and Fry, W.E. 2000. Survival of *Phytophthora infestans* sporangia exposed to solar radiation. *Phytopathology* 90:78-84.
- Nugteren, W. 2004. ProPhy advice in the Netherlands: what's new? In: Westerdijk, C.E., and Schepers, H.T.A.M. (Eds.), *Proceedings of the eighth workshop of an European network for development of an integrated control strategy of potato late blight*, Jersey, England-France. *PAV Special Report no. 10*:27-34.
- Skelsey, P., Kessel, G.J.T., Rossing, W.A.H., and van der Werf, W. Parameterization and evaluation of a spatio-temporal model of the late blight pathosystem. *Phytopathology*, *in press*.
- Skelsey, P., van der Werf, W., and Holtslag, A.A.M. 2008. Development and validation of a quasi-Gaussian plume model for the transport of botanical spores. *Agr. Forest. Meteorol.* 148:1383-1394.

- Smith, L.P. 1956. Potato late blight forecasting by 90 % humidity criteria. *Plant Pathol.* 5:83-87.
- Spijkerboer, H.P., Beniers, J.E., Jaspers, D., Schouten, H.J., Goudriaan, J., Rabbinge, R., and van der Werf, W. 2002. Ability of the Gaussian plume model to predict and describe spore dispersal over a potato crop. *Ecol. Model.* 155:1-18.
- Stull, R.B. 1988. An introduction to boundary layer meteorology. Kluwer Academic Publishers, Dordrecht, the Netherlands, 666 pp.
- Sunseri, M.A., Johnson, D.A., and Dasgupta, N. 2002. Survival of detached sporangia of *Phytophthora infestans* exposed to ambient, relatively dry atmospheric conditions. *Am. J. Potato Res.* 79:443-450.
- Turkensteen, L.J., Flier, W.G., Wanningen, and R. Mulder, A. 2000. Production, survival and infectivity of oospores of *Phytophthora infestans*. *Plant Pathol.* 49:688-696.
- Ullrich, J., and Schrödter, H. 1966. Das Problem der Vorhersage des Auftretens der Kartoffelkrautfäule (*Phytophthora infestans*) und die Möglichkeit seiner Lösung durch eine "Negativprognose". *Nachrichtenblatt Deutsch. Pflanzenschutzdienst (Braunschweig)* 18:33-40.
- van Ulden, A.P. 1978. Simple estimates for vertical diffusion from sources near the ground. *Atm. Environ.* 12:2119-2124.
- von Qualen, R. 2006. Spore traps help researchers watch for soybean rust. *Integrated Crop Management* 496:185.
- Zaag, D. E. van der. 1956. Overwintering en epidemiologie van *Phytophthora infestans*, tevens enige nieuwe bestrijdingsmogelijkheden. Ph.D. thesis, Landbouwhogeschool Wageningen.
- Zwankhuizen, M.J., Govers, F., and Zadoks, J.C. 1998. Development of potato late blight epidemics: disease foci, disease gradients, and infection sources. *Phytopathology* 88:754-763.

CHAPTER 7



Invasion of a Virulent *Phytophthora infestans* Genotype at the Landscape Level; Does Spatial Heterogeneity Matter?

P. Skelsey¹, G.J.T. Kessel², W.A.H. Rossing³, and W. van der Werf¹

¹ Wageningen University, Department of Plant Sciences, Crop and Weed Ecology Group, P.O. Box 430, 6709 RZ Wageningen, The Netherlands.

² Plant Research International, P.O. Box 16, 6700 AA Wageningen, The Netherlands.

³ Wageningen University, Department of Plant Sciences, Biological Farming Systems Group, P.O. Box 9101, 6709 PG Wageningen, The Netherlands.

Abstract

Proper landscape-scale deployment of disease resistant genotypes of agricultural crop species could make those crops less vulnerable to invasion by resistance breaking genotypes. Here we develop a multi-scale, spatio-temporal model of the potato late blight pathosystem (*Phytophthora infestans* - *Solanum tuberosum*) to investigate spatial strategies for the deployment of host resistance. The model comprises a landscape generator, a potato late blight model, and a suite of aerobiological models, including an atmospheric dispersion model. Spatial phenomena are solved using Fast Fourier transforms.

Increasing the number of host genotypes caused the greatest reduction in epidemic extent, followed by reduction of the proportion of potato in the landscape, lowering the clustering of host fields, and reducing the size of host fields. Simulation results showed that spatial spread through short-distance “island hopping” is not a prerequisite for *P. infestans* invasions, and it appeared not possible to generate host free zones at the landscape level that were large enough to provide worthwhile levels of resilience against disease invasion from one host area to another. Deployment of host resistance in genotype mixtures had a large effect on disease invasion. A new functional connectivity parameter, characterizing the probability of successful infection following spore dispersal, proved to be useful in interpreting these results.

Variation in simulation results revealed the importance of using an atmospheric dispersion model for dispersal, with large weather data sets, and many random landscape iterations. The specific coincidence in time and space between weather conditions and the geographic locations of source and target sites defined true landscape connectivity and determined model results regarding inoculum exchange between fields.

Given the apparent capacity of *P. infestans* for long distance transport of viable inoculum, it can be concluded that spatial resistance deployment strategies that center on the creation of spatial barriers to disease at scales up to several kilometers may not be effective in mitigating invasions of

virulent pathogen strains. Strategies that induce finer-grained spatial and genotypic heterogeneities in host populations are more limiting to epidemic spread. Genotype mixing was an effective option for generating agricultural landscapes that are comparatively resilient to disease invasion.

Keywords: *Solanum*, invasion, Gaussian plume model, functional connectivity, landscape design

Introduction

Phytophthora infestans is a plant pathogen that has shaped nations. In Europe in the mid-nineteenth century, potato late blight disease (caused by *P. infestans*) spread like wildfire. Crop losses were most severe in Ireland, where the notorious “Irish potato famine” resulted in the death of 1 million people and the displacement of 1.5 million more (Large, 1940). Undoubtedly, this is still the most striking example of the damage that can be wrought on plants and human society through invasion of a virulent plant pathogen. Since those dark days *P. infestans* has been the subject of intense academic interest, but despite this attention it continues to be a problem today. Currently, *P. infestans* is responsible for multi-billion dollar losses annually in global tomato and potato production (Birch and Whisson, 2001). This truly is a potent, persistent and pervasive plant pathogen.

There is no single, simple solution to the global late blight problem. Host resistance is almost unanimously viewed as the most cost-effective and sustainable form of management, but counteractive to this form of management are a number of societal, economic and market forces that determine what is grown and where. There is hope that genetic engineering technologies will yield improved variants of currently used varieties that show far greater levels of resistance, but this is still a work in progress. Fungicides can provide effective protection but their applicability can be compromised by adverse environmental effects, by the emergence of resistant pathogen strains and by faltering public support for frequent use of biocides in agriculture, especially in the western world. Nonetheless, the efficacy of fungicides is appealing to farmers in developed and developing economies alike, and fungicide use is a common practice throughout the world (Forbes, 2004). Thus, it appears that the sensible short-, medium- and perhaps long-term approach to the potato late blight problem is to continue to develop and improve integrated late blight management strategies.

Crop heterogeneity can profoundly affect epidemics caused by the transmission of infectious agents (e.g., Zhu et al., 2000). Landscape design and strategic

deployment of host resistance therefore emerge as a means to spatially separate aggressive pathogen genotypes from other local host and pathogen populations. The efficacy of such strategies is likely to be dependent, however, on the scale of pathogen dispersal processes relative to the scale of (induced) heterogeneities in host populations. Detached *P. infestans* sporangia are killed within 1 hour on sunny days, but many survive for several hours on cloudy days (Mizubuti et al., 2000; Sunseri et al., 2002). Such information suggests a wide range of possible dispersal distances. The only study in the literature that provides hard evidence of long-distance dispersal is by Zwankhuizen et al. (1998), who used DNA fingerprinting to establish that infested crops led to the dispersal of at least two *P. infestans* genotypes over an area of 25 km² in a period of 2 weeks. In one instance, sporangia of *P. infestans* from a refuse pile were found/inferred to infect potato fields up to 900 m away. This apparent capacity for long-distance dispersal gives a mixed review on the likelihood that spatial resistance deployment strategies will be effective in controlling potato late blight invasions. Evidence of the beneficial effects of host diversity in reducing the spread of potato late blight have been found in field studies (e.g., Garrett and Mundt, 2000; Andrivon et al., 2003), but we are unaware of any information about the role that resistance deployment strategies may play in potato late blight management at a regional-scale. This raises an important question regarding the spatial epidemiology of *P. infestans* - does spatial heterogeneity in host populations matter, and if so, what scale is relevant?

We describe a simulation framework to investigate which spatial strategies reduce the development of epidemics when a breakthrough of resistance occurs in a proportion of the host population, i.e., when a new, aggressive strain of the pathogen evolves. The framework comprises a recently validated potato late blight model (Skelsey et al., *in press* b) and a suite of aerobiological models, including a long range atmospheric spore dispersion model. Invasion opportunities of virulent pathogen genotypes are assessed under a variety of weather conditions and landscape configurations. The effects of landscape design are studied using scenarios that vary the potato landscape using a limited set of design parameters: (1) less or more potatoes; (2) few or many host genotypes; (3) large or small fields; (4) spatial clustering or maximal spreading over the landscape; and (5) genotype mixing *within* a field or *among* fields. Genotype mixtures serve to reduce disease in three basic ways, known collectively as a “mixing effect”: (a) resistance induction, by avirulent spores preventing or delaying infection by adjacent virulent spores; (b) barrier effects, with resistant plants acting as barriers to pathogen spread and (c) dilution of susceptibles,

where there is an increased distance between plants of the most susceptible genotype (Philips et al., 2005). It should be noted that pathogen population genetics are not considered and that our aim is to identify the spatial parameters that have most influence on the rate and extent of invasion of a new, resistance breaking pathogen genotype. Of particular interest is the interplay between weather variability and landscape design. Weather determines the release and escape of spores from the canopy, the direction and extent of spore dispersal, the survival and deposition of spores, and the ability of spores to infect. Weather thus affects the whole chain of events that spores go through to cause infections somewhere in the landscape after production in another place. As weather has the potential to modify the effects of landscape design on disease invasion, we raise a second question regarding the spatial epidemiology of potato late blight - do weather conditions exert a strong influence on the magnitude of spatial parameter effects? The implications of simulation results are discussed in terms of the spatial parameters that have most influence on the rate and extent of invasion of a new, resistance breaking pathogen genotype, and in relation to strategic deployment of current and future potato varieties at field and landscape-scale.

Theory and approaches

Simulation framework

Host and pathogen life cycles, host-pathogen interactions, and fungicide applications are simulated on gridded (raster) landscapes composed of potato and non-potato areas. An adaptation of the spatio-temporal/integrodifference equation model of the potato late blight pathosystem originally developed by Skelsey et al. (2005) is used to provide field-scale dynamics. This model was recently validated using data from field trials on the temporal development of two genotypes of *P. infestans* in five potato cultivars in the Netherlands (Skelsey et al., *in press b*). Individual fields in the landscape are linked through models describing spore release from sporangiophores, escape from the canopy, dispersal, deposition and survival during transportation. Within this modeling framework, the composition, configuration and connectivity of host populations are manipulated in order to reveal their influence on epidemic progress. The results of these manipulations are used to develop spatial strategies for the deployment of resistance genes. A schematic overview of the framework is given in Fig. 1. A brief description of the components is given here, and these are described

in more detail in subsequent sections. Table 1 provides a summary of symbol definitions and units.

The landscape generator creates a landscape grid with potato and non-potato areas according to a variety of spatial parameters: proportion of potato, field size, number of varieties, clustering of fields, and deployment of varieties in genotype mixtures, or non-mixtures. In each simulated landscape, a certain fraction of the potato population is designated as being vulnerable to invasion by an aggressive pathogen strain. The remaining potato varieties are classified as (partially) resistant.

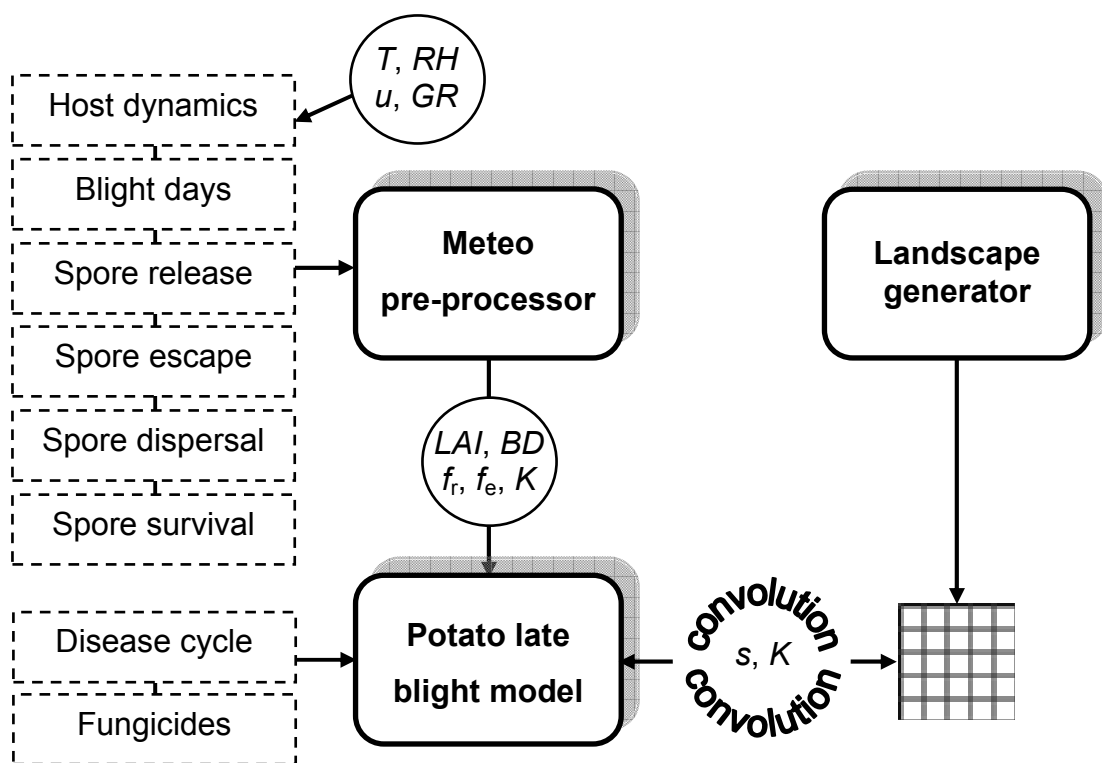


Fig. 1. Schematic overview of the simulation framework. Solid boxes show main model components. Dashed boxes show submodels. Circles show input variables: T = temperature ($^{\circ}\text{C}$) measured at 2 heights (0.1 and 1.5 m); RH = relative humidity (%); u = wind speed (m s^{-1}) measured at 10 m, and wind direction; GR = global radiation (W m^{-2}); LAI = leaf area index (-); BD = blight days (-), a discrete “on-off switch” for disease dynamics, as determined by a set of environment-pathogen relations; f_r = release fraction (-), the fraction of spores that are released into the atmosphere; f_e = escape fraction (-), the fraction of spores that escape the canopy and are made available for long-distance transport; K = dispersal kernel ($\# \text{ m}^{-2}$), a spatial footprint (distribution) of viable sporangia deposition flux values that is used to redistribute spores; and s = spores ($\#$), a spatial distribution of (escaped) spores. The “convolution” symbol indicates a spatial convolution, which is performed using fast Fourier transforms.

Table 1. Symbols used in this study

Symbol	Units	Description
BD	$-^a$	Blight days (conducive to development of disease <i>in planta</i>)
\bar{c}	$\# m^{-3}$	Aerial concentration of spores
\bar{c}_0	$\# m^{-3}$	Concentration of spores at the surface
D	-	Modified index of agreement
f	-	Fraction of potato acreage that is susceptible
f_e	-	Fraction of spores that escape the canopy
f_r	-	Fraction of spores released from sporangiophores
f_s	-	Fraction of spores that survive transportation
F_d	$\# m^{-2} s^{-1}$	Dry deposition flux
GR	$W m^{-2}$	Global radiation (short wave direct plus diffuse)
h	m	Effective height of the source
H	-	Heaviside function
k	-	Factor of (artificially induced) predictive error
K	$\# m^{-2}$	Dispersal kernel: distribution of viable spore deposition flux values
\bar{K}	$\# m^{-2}$	Average dispersal kernel
L	m	Monin-Obukhov length scale
LAI	-	Leaf area index
n	$\#$	Number of observations
O	$\# m^{-3}$	Observed spore concentration
\bar{O}	$\# m^{-3}$	Mean observed spore concentration
P	$\# m^{-3}$	Predicted spore concentration
\bar{P}	$\# m^{-3}$	Mean predicted spore concentration
q	-	Host connectivity (equation 13a)
q_p	-	Pathogenic connectivity (equation 13b)
Q	$\# s^{-1}$	Source strength
RH	%	Relative humidity
s	$\#$	Spores
s_L	$\#$	Total number of successfully deposited spores in the landscape
s_v	$\# m^{-2}$	Variety specific spore density
t	s	Time
T	$^{\circ}C$	Temperature
T_L	s	Lagrangian time scale
u	$m s^{-1}$	Wind speed
\bar{u}	$m s^{-1}$	Mean wind speed at effective source height, h
u^*	$m s^{-1}$	Friction velocity
v_d	$m s^{-1}$	Deposition velocity
v_s	$m s^{-1}$	Stokes settling velocity
x	m	Coordinate
x_G	m	Distance at which the image source streamline cuts the ground plane
y	m	Coordinate
z	m	Coordinate
α_0	-	Reflection coefficient
l	-	Infection efficiency

Table 1 continued

Symbol	Units	Description
κ	-	von Kármán constant (0.41)
π	-	Mathematical constant (3.14)
ρ	m day^{-1}	Radial growth rate of lesions
σ	$\# \text{m}^{-2}$	Sporulation intensity (per unit infectious leaf tissue)
σ_v	m s^{-1}	Standard deviation of horizontal wind velocity fluctuations
σ_w	m s^{-1}	Standard deviation of vertical wind velocity fluctuations
σ_y	m	Standard deviation of spore concentration in the crosswind direction
σ_z	m	Standard deviation of spore concentration in the vertical direction
τ	s	Travel time
φ	MJ m^{-2}	Dose of global radiation (direct plus diffuse shortwave radiation)
ψ	-	Cultivar specific resistance component

^a - signifies that the defined quantity is dimensionless.

A meteorological pre-processor is used to provide time series of all weather dependent calculations for the period of interest. These are calculated in advance and used as required during dynamic epidemic simulation. This greatly enhances the speed at which multiple model iterations (using the same weather data on different landscapes) are performed. The pre-processor uses five (hourly) weather variables: temperature at two heights (T , °C), relative humidity (RH , %), wind speed (u , m s^{-1}) and wind direction, and global radiation (GR , W m^{-2}). Various component submodels are used to create time series for host dynamics, i.e., leaf area index (LAI , -), the fraction of spores that are released from sporangiophores (f_r , -), and the fraction of spores that escape the canopy (f_e , -). These are aggregated to a daily time step for later use in the late blight model. The pre-processor also calculates a time series of “blight days” (BD , -). These are based on pathogen-environment relations (Skelsey et al., *in press* b,c) and are used in the late blight model to “switch” the epidemic on or off depending on the suitability of the weather for disease development during a day. The pre-processor also contains a long-range atmospheric dispersion and deposition model, and a spore survival model. These use hourly weather data to calculate “dispersal kernels,” (K , $\# \text{m}^{-2}$) characterizing the spatial “footprint” or pattern of viable spore deposition flux values for each hour. These are aggregated to a daily time step and used to calculate dispersal and survival of spores each day. It is assumed that the kernels are spatially invariant, i.e., the same kernel is used for each source location in the landscape.

The integrated model then works as follows. At the start of each growing season, the landscape generator creates a gridded landscape composed of susceptible and (partially) resistant potato fields, and non-potato areas. The potato late blight model simulates host, disease and fungicide dynamics on the gridded landscape, using pre-calculated time series from the meteorological pre-processor for all weather-dependent variables. Each (daily) time step, a spatial convolution is performed between the pre-calculated dispersal kernel and the spatial distribution of (produced, released and) escaped spores for that day. This results in a spatial distribution of deposited, viable spores. At the end of the growing season, a new landscape can be generated, or the same landscape can be reused to simulate a different growing season.

There now follows a more detailed description of the simulation framework and the solution methodology for spatial phenomena. This is followed by a description of two functional landscape connectivity measures. These measures are used during the generation of random landscapes with given connectivity for disease spread, and to interpret the results of epidemic simulations. In the next section the spatial scenarios used to develop resistance deployment strategies are described. Finally, model output is defined.

Meteorological pre-processor

The meteorological pre-processor is composed of a series of submodels that provide all weather dependent host and epidemic dynamics as far as it is spatially invariant. Hourly weather data were provided by the Wageningen University “Haarweg” weather station (<http://www.maq.wur.nl>), latitude 51° 58' N, longitude 5° 38' E. The growing season is assumed to last from May to September, and a total of 10 years of weather data are used (1997 to 2006). Daily time series of weather dependent variables are calculated for each growing season and stored for later use as input data for the potato late blight model. There now follows a description of each component submodel.

Host dynamics

The submodel for host dynamics is described in full in Skelsey et al. (*in press c*) therefore only a summary is given here. Leaf area development is simulated through thermal time accumulation, by computing the growing degree days as the positive difference between the (average daily) temperature and a base temperature (2°C) below which leaf growth stops. Leaf area index, *LAI*, is initialized at 0.05, and increase

in *LAI* is modeled as a logistic function of growing degree days. *LAI* is increased until the temperature sum reaches a maximum cultivar specific value (estimated as 1000°C days), at which point net leaf growth becomes net leaf death. Shedding of leaves is also calculated as a logistic function of growing degree days.

Blight days

A simplifying assumption is made that development of disease *in planta* is independent of weather conditions, and that only germination of dispersed sporangia is weather dependent. Two simple rules are used to analyze hourly weather data and determine if the conditions during the subsequent 24 hour period are suitable for sporangia to cause infection. The first rule determines if the temperature and humidity each hour are suitable for the germination process to take place. The second rule determines the number of consecutive conducive hours required to allow germination to reach completion in a 24 hour period. If the conditions of these rules are not met, then infection does not take place and the parameter ι (infection efficiency, -) is set to 0 for that 24 hour period. These rules therefore act as a “switch” with new infection only occurring when conditions are conducive, and not at all if it is not. Spores older than 24 hours are no longer viable and cannot germinate. The 24 hour periods run from 4 pm on each day till 4 pm the next day, ensuring that the cut-off between these intervals is made during the “dry time” of the day, when lack of leaf wetness is hampering infection. These rules are described in detail in Skelsey et al. (*in press b*).

Spore release

The fraction of spores that can be released, f_r (-), every hour from sporangiophores is inversely related to the humidity level below 90 % (Skelsey et al., *in press a,c*):

$$f_r = \begin{cases} 0 & RH \geq 90 \\ \frac{1}{RH - 91} + 1 & RH < 90 \end{cases} \quad (1)$$

This relationship is assumed rather than derived from experimental fitting. It is based on the observation that most *P. infestans* sporangia are released at the first humidity drop in the early hours of the day (e.g., Nielsen et al., 2007), and an assumed 90 % humidity criteria for leaf wetness.

Spore escape

The fraction of released spores that can escape the canopy, f_e (-), is dependent on wind speed, u (m s^{-1}) and the leaf area index, LAI (-), of the canopy (de Jong et al., 2002; Skelsey et al., *in press* a-c):

$$f_e = \exp \left[-LAI \sqrt{v_d / (\kappa u)} \right] \quad (2)$$

where κ is the von Kármán constant (0.41), u (m s^{-1}) is the wind speed at a characteristic height within the canopy, and v_d (m s^{-1}) is the dry deposition velocity. Dry deposition velocity is estimated according to Ferrandino and Aylor (1985) as:

$$v_d = (1 + LAI) v_s \quad (3)$$

where v_s is the settling velocity (m s^{-1}), given by Gregory (1973) as 0.0085 m s^{-1} for *P. infestans* sporangia. The characteristic height at which wind speed is calculated for equation 2 is assumed to be the canopy top (0.7 m). This wind speed is calculated from measured wind speeds (10 m height), relative to a displacement height using a standard logarithmic wind profile with stability correction (e.g., Arya, 1999). Displacement height is calculated according to Jacobs and Boxel (1991) as 0.43 m. Atmospheric stability is characterized in this study using Monin-Obukhov similarity theory via the “profile method” (e.g., Stull, 1988; Skelsey et al., 2008). The profile method uses a single measured value of wind speed and measured values of temperature at two heights to characterize the turbulent state of the atmosphere via two parameters: the friction velocity, u_* (m s^{-1}), and the Monin-Obukhov length, L (m).

Spore dispersal

The partial reflection Gaussian plume model of Overcamp (1976) is used to compute spore transportation and deposition as it is a fully analytical atmospheric dispersion model. It should be noted that many applications of the Gaussian plume formula apply a mathematical device known as an “image source.” The image source is used to satisfy a boundary condition of complete reflection of material at the surface, i.e., diffusion of material through the surface does not take place. The image source has the same strength as the real source and its location is the mirror image of the real source (below the surface). This means that any portion of the plume that extends below the surface is instantaneously replaced (reflected) by the image source. In the model by Overcamp (1976), the contribution from the image source is reduced by a

factor, α (-), to account for removal of material from the lower part of the plume by dry deposition. This factor is known as the reflection coefficient. The reflection coefficient is not a constant; it is a function of the deposition velocity of spores, spread of the plume in the vertical direction, and downwind distance. It can be shown that Overcamp's solution satisfies an integral mass conservation equation specifying that the decrease in airborne flux equals the deposition (Overcamp, 1976). The basic formula is (Arya, 1999):

$$\bar{c}_0(x, y, 0) = \frac{Q[1 + \alpha_0(x)]}{2\pi\bar{u}\sigma_y\sigma_z} \exp\left(-\frac{y^2}{2\sigma_y^2}\right) \exp\left(-\frac{h^2}{2\sigma_z^2}\right) \quad (4)$$

where \bar{c}_0 (# m⁻³) is the concentration of spores at the surface ($z = 0$ m), x (m) and y (m) are coordinates in the downwind and crosswind directions respectively, Q (# s⁻¹) is the source emission strength, $\alpha_0(x)$ is the reflection coefficient for calculating ground level concentrations, \bar{u} (m s⁻¹) is wind speed, σ_y (m) and σ_z (m) are the standard deviations of concentration in the crosswind and vertical directions respectively, and h (m) is the effective height of the source (canopy height minus the displacement height).

Overcamp (1976) derived the following expression for the (partial) reflection coefficient:

$$\alpha_0(x) = 1 - \frac{2v_d}{\left(v_d + \frac{\bar{u}h}{\sigma_z} \frac{d\sigma_z}{dx}\right)} \quad (5)$$

It can be seen from equation 5 that α_0 varies between -1 and 1. Close to the source, the vertical extent of the plume is small, $d\sigma_z/dx$ is large, and $\alpha_0 \approx 1$. At large downwind distances turbulence has mixed the plume well in the vertical direction, therefore $d\sigma_z/dx \approx 0$ and $\alpha_0 \approx -1$. It therefore follows from equation 5 that ground level concentrations are at first large as there is a large contribution from the image source, then as downwind distance increases the ground level concentration will eventually approach 0 as the entire plume is deposited.

The dispersion coefficients, σ_y and σ_z , in equation 4 describe the shape of the plume in the crosswind and vertical directions. They are functions of downwind distance from the source and atmospheric turbulence, i.e., as downwind distance increases, turbulent eddies of air cause the plume to expand outwards and upwards and σ_y and σ_z increase. These coefficients were parameterized using the Taylor (1921)

model, which is widely regarded as giving the best estimation of σ_y and σ_z (e.g., Arya, 1999):

$$\sigma_y = \sigma_v t f_y(\tau/T_L) \quad (6a)$$

$$\sigma_z = \sigma_w t f_z(\tau/T_L) \quad (6b)$$

with empirical formulations proposed by Draxler (1976):

$$1/f_y = \begin{cases} 1 + 0.9(\tau/300)^{0.5} & L < 0 \\ 1 + 28/\tau^{0.5} & L > 0 \end{cases} \quad (7a)$$

$$1/f_z = \begin{cases} 1 + 0.9(\tau/500)^{0.5} & L < 0 \\ 1 + 0.9(\tau/50)^{0.5} & L < 0 \end{cases} \quad (7b)$$

where σ_v and σ_w (m s^{-1}) are the standard deviations of wind velocity fluctuation (turbulence intensities) in the horizontal and vertical directions, τ (s) is the travel time ($\tau = x/\bar{u}$), and T_L is the Lagrangian time scale, which represents the characteristic time scale of turbulent eddies of air. Formulae for the turbulence intensities, σ_v and σ_w , are given by Arya (1999).

The dry deposition flux, F_d ($\# \text{ m}^{-2} \text{ s}^{-1}$), at any point on the surface is given by:

$$F_d(x, y) = v_d \bar{c}_0(x, y) \quad (8)$$

where $\bar{c}_0(x, y)$ is the concentration of spores at the surface, as defined in equation 4.

The ability of the partial reflection model to predict spore plumes is tested by calculating expected spore concentrations and assessing goodness of fit with the experimental spore dispersal data of Spijkerboer et al. (2002). Details of these experiments and of model performance are given in the appendix.

Spore survival

The experimental results of Mizubuti et al. (2000) are used to determine the fraction of deposited spores that remain infective. Survival of spores during transportation is dependent on the dose, φ (MJ m^{-2}), of global radiation received (direct plus diffuse shortwave radiation) during transportation:

$$f_s = 0.79 \exp(-1.21\varphi) \quad (9)$$

where φ is the product of the travel time, τ , and the flux of incoming global radiation, GR . According to the results of Mizubuti et al., (2000), a one hour exposure on a

sunny day was enough to inactivate 95 % of the sporangia of a *P. infestans* isolate belonging to the US-1 clonal lineage.

Landscape generation

Neutral landscapes (not shaped by biotic or abiotic processes) are generated on two-dimensional grids comprised of random associations of two habitat types: potato and non-potato area. The number, size, aggregation and classification of potato fields can be varied. Two potato phenotypes are represented: susceptible and (partially) resistant. The susceptible phenotype represents the genotype with broken resistance, while the other phenotype represents all other genotypes. A proportion $1/k$ of the potatoes in the landscape is susceptible, while the remainder is (partially) resistant, representing a situation in which the region was planted with k potato genotypes, one of which has had its resistance broken. The $k-1$ (partially) resistant varieties are all modeled using the same parameter set, i.e., they are the same phenotype. Partially resistant varieties can still become infected, although the rate of infection is far reduced in comparison to the “broken” or susceptible genotype.

The two phenotypes are mixed at either regional level, with each field consisting of a single potato phenotype, or at field level, where each field is planted with a mixture of k varieties, each with a different genetic background for resistance to potato late blight.

Host-pathogen interactions are characterized in the model using three quantitative components of resistance: infection efficiency, ι (-), radial lesion growth rate, ρ (m day⁻¹), and sporulation intensity per unit of infectious tissue, σ (# m⁻²). These were measured in the laboratory on potato leaflets of two cultivars, providing parameter values for a highly susceptible (Bintje/isolate IPO82001) and a partially resistant (Agria/isolate IPO82001) interaction (Table 2). Latency and infectious

Table 2. Empirically determined quantitative components of resistance used to define host-pathogen interactions in the model^a

Cultivar	Infection efficiency (-)	Lesion growth rate (m day ⁻¹)	Sporulation intensity (# m ⁻²)	Latent period (days)	Infectious period (days)
Agria	0.01	0.002	1.6×10^8	5	1
Bintje	0.03	0.005	4.6×10^8	5	1

^a Infection efficiency (ι), radial lesion growth rate (ρ), and sporulation intensity (σ) were determined experimentally (Skelsey et al., *in press* b).

periods are assumed to remain fixed regardless of the cultivar-isolate interaction, as the model is not sensitive to these parameters (Skelsey et al., *in press b*). The potato late blight model (described below) has previously been validated for these and other cultivar-isolate combinations by comparison of predicted epidemics with independent data from field trials (Skelsey et al., *in press b*).

Each landscape measures 6.4 x 6.4 km and is surrounded by a buffer of “empty space” to facilitate spore loss from the system and represent a 6.4 x 6.4 km potato growing area that is embedded in a greater landscape without potatoes. The whole area is subdivided into 100 x 100 m grid cells and individual plants are not simulated. Potato fields are simulated either as single grid cells (100 x 100 m) or - if larger fields of 4, 16 or 64 ha are considered - as assemblies of 2 x 2, 4 x 4 or 8 x 8 potato cells. Different levels of clustering of 100 x 100 m potato fields are created from an initial random allocation of potato cells in the total landscape. Potato fields with the lowest number of potato neighbors are swapped with non-potato fields with the highest number of potato neighbors, until a predetermined level of connectivity is achieved. The neighborhood structure of the landscape is assessed using the “queen’s adjacency” system (set of all touching fields, including fields on the diagonal), and connectivity is assessed using the “host connectivity” parameter, q (-) (Skelsey et al., 2005), which is described below.

To study the effect of fine-scale within-field mixing of genotypes, simulated landscapes are generated with the same design parameters as described above, but now with the genotype mixing conducted within field, instead of among fields. As individual plants are not simulated, field-scale genotype mixtures are approximated by weighting the resistance components with f (-), the fraction of the landscape classified as susceptible:

$$\psi_{\text{mix}} = \psi_{\text{sus}} f + \psi_{\text{res}} (1 - f) \quad (10)$$

where ψ represents one of the three cultivar specific resistance components described above (sporulation intensity, infection efficiency, lesion growth rate; Table 2). The subscripts stand for “mixture”, “susceptible” and “resistant.”

The motivation for the 6.4 x 6.4 km extent of the simulated landscapes was entirely pragmatic. Larger simulated landscapes greatly increased the execution time of the model and became limiting to the number of simulations that could be performed. The ramifications of this modeling choice are discussed in relation to simulation results in the discussion section.

Potato late blight model

The potato late blight model is comprised of two submodels; a model of the disease cycle and a model for fungicide management. Both submodels generate state variable values for each cell in the gridded landscape. The model for the disease cycle makes use of pre-calculated time series of weather dependent variables, as provided by the meteorological pre-processor. The model for the disease cycle is described in Skelsey et al. (2005; *in press* b,c) and the fungicide management model in Skelsey et al. (*in press* c). A short description of these models is given below.

Disease cycle

The *Phytophthora* population in the model is age- and spatially-structured and keeps track for every grid cell in the landscape of the number of lesions according to the day of establishment; thus, after t days of simulation there will be t age classes of lesions. Lesions are assumed to be circular and grow radially (ρ), producing a new ring of growth (annulus) each day. New lesion annuli are latent for a period of time known as the latency period, after which they become infectious and produce spores. During each successive day, as another annulus of daily radial growth reaches the end of the latency period, this annulus will sporulate with intensity σ . The proportion of spores released from sporangiophores into the air each time step is provided by pre-calculated time series of spore release fractions (f_r). Similarly, the fraction of spores that escapes the canopy and is made available for long distance transport is provided by pre-calculated time series of spore escape fractions (f_e). Spores that do not escape the canopy autodeposit and contribute to epidemic development within the source cell. The percentage of spores (originating from within the grid cell and from neighboring grid cells) that deposit on the canopy is equivalent to the percentage of ground cover, which is calculated for potato canopies according to Haverkort and Harris (1987). Leaf area dynamics are provided by the pre-calculated time series of LAI . Time series for f_r , f_e , and LAI are not spatially indexed, i.e., the same dynamics are used for each host cell in the landscape.

After sporulation (lasting one day), infectious areas are classed as necrotic. Necrosis also occurs due to “girdling” of leaves and stems by lesions, which proceeds at a rate equal to the calculated rate of increase in latent area (van Oijen, 1992). Total latent, infectious and necrotic lesion area in each grid cell is calculated by summing over age classes the number of lesions in each age class, multiplied by the age-specific area of latent, infectious and necrotic tissue per lesion. Under the assumption that leaf lesion coverage and areas of girdled leaf tissue caused by *P. infestans* are

distributed homogeneously over the canopy profile, shedding of leaves (decrease in LAI) affects all tissue types equally, i.e., shedding results in equal, proportional loss of healthy, latent, infectious, and necrotic areas. The age-structured population model for lesions is updated daily by “aging” the existing lesions by 1 day, and starting new lesions at a rate calculated as the product of the number of landed spores per m² leaf area in a day, the infection efficiency (ι), and the fraction of area not yet occupied by colonies of *P. infestans*.

The major difference between the current model version and previous versions is that the basic spatial unit for host and pathogen dynamics is 1 ha (100 x 100 m grid cell). Dispersal of inoculum from plant to plant is therefore not simulated. This is in contrast to previous model versions where the basic spatial unit was an individual plant and spread of disease through a crop was simulated with statistical contact distributions (Skelsey et al., 2005; *in press* b,c). In this study the spatial scale of interest lies beyond the plant level; rather, our primary interest is in movement of the pathogen between fields. This also means that the areal expansion of lesions is affected by competition for available space at the scale of 1 ha, whilst in previous model versions, competition for space was at the single plant level.¹

Fungicide management

To obtain realistic results, fungicide protection of potato crops is included in the modeling framework. Protectant sprays are applied once per week. A Weibull function is used to simulate the decay of protectant fungicides via their effect on the infection efficiency, ι , of sporangia (Skelsey et al., *in press* c). Eradicant sprays are applied on an individual grid cell basis (1 ha) when disease severity (including latent, infectious, and necrotic areas) in the grid cell reaches or exceeds 1 %. For fields larger than 1 ha, this is akin to applying an eradicant spray to a “hot-spot” or focus (100 x 100 m) of late blight within the field. The minimum interval between consecutive eradicant sprays in a grid cell is set to 10 days. Eradicant sprays kill 99 % of lesions and also have protectant properties. Thus when an eradicant spray is applied, a protectant spray is assumed and the weekly spray schedule for that individual cell is adjusted.

¹ This means that lesions can grow to be larger than the average size of a leaflet. This is a justifiable assumption as potato late blight lesions can grow through petioles and stems to claim plant area exceeding a single leaflet. It was found that after removal of the upper and lower 5 % of lesion sizes, the trimmed mean lesion size seldom exceeded that of 2 or 3 times the average size of a leaflet.

Solution of dispersal phenomena

Spatial dispersal processes are accounted for by conducting convolutions between dispersal kernels ($\# \text{ m}^{-2}$) and spatial distributions of inoculum ($\#$). The dispersal kernels, or spore deposition footprints, are calculated in the weather preprocessor and they are spatially invariant, i.e., the same dispersal kernel is applied to each cell in the landscape during convolution.

Whilst the overall model operates at a 1 day-time step and 100 x 100 m grid cell resolution, spore dispersal is first calculated at an hourly basis and 10 x 10 m resolution, to account for weather variability (notably wind direction) within a day, and potentially steep dispersal gradients. Ten hourly spore dispersal kernels (see below) are calculated and added, and subsequently aggregated to 100 x 100 m grid cell resolution to obtain the daily spore deposition footprints.

For each hour of meteorological input data, a refined 10 x 10 m grid of coordinates is defined that spans the extent of the landscape in both positive and negative x and y directions. A rotation of the axes is performed to align the x axis with the downwind direction for that hour. A single source is located at the origin, and dispersal is simulated using weather data from 7 am till 4 pm, as release and dispersal of spores of *P. infestans* is assumed to be most likely during these hours (e.g., Nielsen et al., 2007). A total of 1 spore is released over the course of each day, therefore 0.1 spores are released each hour (7 am till 4 pm inclusive) and the source strength, Q , in equation 4 is set at $0.1/3600 \text{ s}^{-1}$ or $2.78 \times 10^{-5} \text{ s}^{-1}$. Equations 4 to 9 are used as described above to produce a two-dimensional distribution of viable, spore deposition flux values ($\# \text{ m}^{-2}$) for that hour. Hourly distributions are added together over the course of the 10 hour dispersal period, and the final daily distribution is aggregated spatially from a 10 x 10 m grid to a 100 x 100 m grid to match the grid resolution of other model components. This is the daily “viable spore dispersal kernel,” K ($\# \text{ m}^{-2}$), or spatial footprint of viable spore deposition flux values. Some example kernels are given in Fig. 2.

Convolutions are implemented at a daily time step in the model via fast Fourier transforms. Spatial distributions (i.e., a daily dispersal kernel and a distribution of escaped spores) are transformed into the Fourier domain, multiplied, and the result is back-transformed into the spatial domain, giving the spatial distribution of dispersed spores. This solution method requires periodic boundary conditions, therefore Fourier domain arrays are duplicated an infinite number of times to the left, right, top and bottom. Thus, each edge of the array is connected to the opposite edge of an identical array. This leads to “wrap-around” effects, whereby any spore

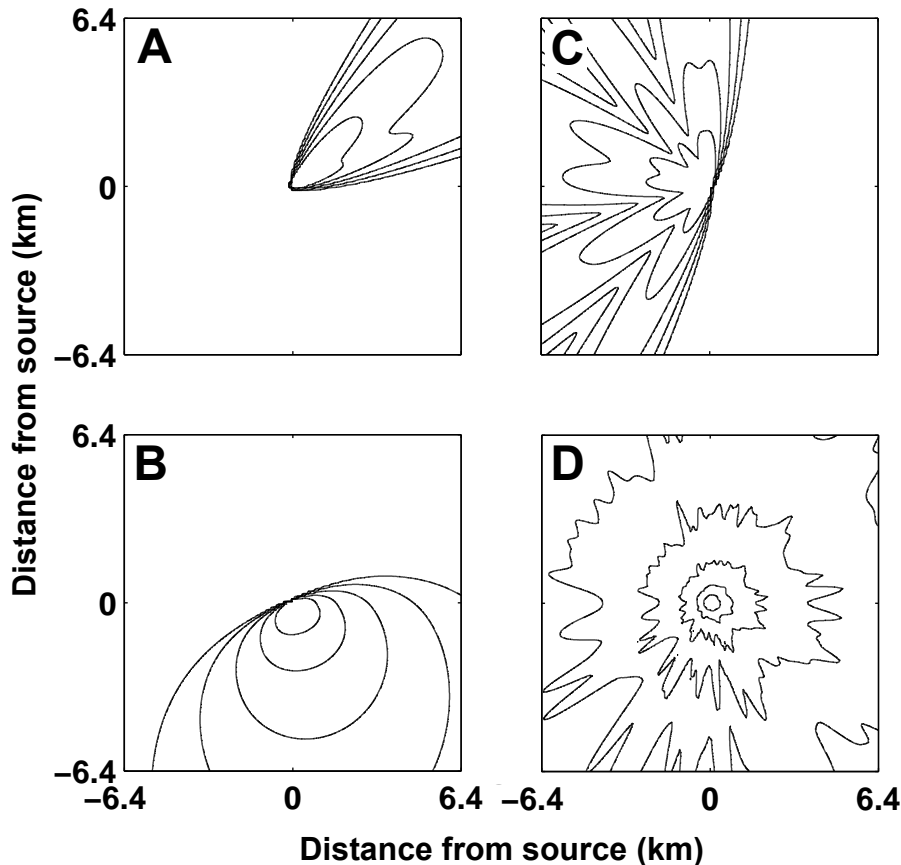


Fig. 2. Example daily viable spore deposition kernels for *Phytophthora infestans* sporangia, as calculated by the dispersal, deposition and survival models: (A) stable conditions (non-turbulent, $L = 10$ m) with a constant wind direction; (B) unstable conditions (turbulent, $L = -10$ m) with a slowly meandering wind direction; and (C) variable wind direction. Contours show the deposition flux of viable sporangia ($\# \text{ m}^{-2}$), ranging from 10^{-10} (inner contour) to 10^{-14} (outer contour), with an interval of factor 10. Panel D shows a normalized dispersal kernel that is used to represent the “average” daily dispersal event over 10 growing seasons. This was calculated by accumulating hourly spore deposition fluxes over 10 growing seasons, then dividing by the total mass under the kernel. Contours show the deposition flux of viable sporangia, ranging from 10^{-7} (inner contour) to 10^{-11} (outer contour), with an interval of factor 10. In all panels, the outer contour delineates an area containing 99.9 % of the total deposition flux.

dispersing outwith the boundaries of the landscape will “reappear” on the opposite edge of the landscape when spatial distributions are back-transformed into the spatial domain. In this study, spatial distributions are “padded” with a large border of “non-host space” prior to convolution (“zero-padding”). Spores that are redistributed by the kernel into the non-host space are lost from the system, thereby preventing wrap-around effects. Thus, the simulations represent a potato growing area surrounded by space without potatoes.

Functional connectivity measures

Connectivity is considered a vital element of landscape structure (e.g., Levins, 1970; Fahrig and Merriam, 1985; Taylor et al., 1993). The difficulty lies in quantifying *functional* connections between host areas. Functional connections depend on the interaction between landscape characteristics and the biological process of interest, e.g., host areas that are connected for bird flight might not be connected for pathogen dispersal. Key to the quantification of functional connectivity, therefore, is consideration of the scale and nature of the dispersal process relative to the scale of heterogeneities in the landscape. In this study, two different (non-temporal) measures of functional landscape connectivity are developed to aid in both landscape generation and the interpretation of simulation results. Both measures make use of dispersal kernels, calculated as described above. A cumulative distribution of viable deposition flux was calculated using every blight day from the entire 10 year weather data set (using only the hours between 7 am and 4 pm). This distribution was normalized by division with the total mass under the kernel to provide an “average” viable spore dispersal kernel for the entire period of interest (10 growing seasons). This kernel shall henceforth be referred to as the average dispersal kernel, \bar{K} . This is an alternative, and at landscape-scale, more realistic approach than using a radially symmetric dispersal kernel, such as the 2D radial Laplace kernel (Skelsey et al., 2005). It can be seen in Panel D of Fig. 2 that \bar{K} is not radially symmetric; such an approach can therefore be used to produce dispersal kernels that reflect prevalence in weather conditions for any area and time span.

The host connectivity parameter, q (-), expresses the overall probability that a propagule produced in a host field, when dispersed according to the average dispersal kernel, will be deposited within (upon) a host field (whether the same field or another field). In order to derive q , a spatial convolution is used to redistribute spores from each source location in the landscape to each target location. Let $s(x,y)$ express a density of spores (per unit ground area) at grid location (x,y) ; $s(x,y)$ is 1 m^{-2} if the grid cell is a potato field, and 0 m^{-2} otherwise. Let (x',y') denote source locations, and (x,y) target locations. Then we can write:

$$s(x,y) = \iint_{x'y'} s(x',y') \bar{K}(x-x',y-y') dy' dx' \quad (11)$$

where $\bar{K}(x-x',y-y')$ is the average dispersal kernel. The density of spores redistributed to each new location, $s(x,y)$ is then weighted with a Heaviside function, H (-), which is 1 if the target location contains host tissue, and 0 otherwise, i.e., the

Heaviside function is used to facilitate calculation of successful spore deposition in heterogeneous landscapes. Integration over the whole spatial domain then gives the total number of successfully redistributed spores, s_L (#), in the landscape:

$$s_L = \int \int_{x,y} H(s(x,y)) \int \int_{x',y'} s(x',y') \bar{K}(x-x',y-y') dy' dx' dy dx \quad (12)$$

To obtain the overall probability, q , that a spore produced somewhere in the landscape will land on a host tissue, equation 12 is divided by the total number of spores produced in the landscape:

$$q = \frac{\int \int_{x,y} H(s(x,y)) \int \int_{x',y'} s(x',y') \bar{K}(x-x',y-y') dy' dx' dy dx}{\int \int_{x',y'} s(x',y') dy' dx'} \quad (13a)$$

Parameter q describes connectivity from a physical dispersal and topographical perspective, through quantification of the scale of dispersal processes and the scale of heterogeneities in the landscape. It is a probability and cannot be smaller than 0 or greater than 1. Parameter q is used to provide a measure of clustering of potato populations and is used in landscape generation (as described above).

A second version of equation 13 can be defined that includes relevant pathogenic parameters at each source and receptor location. "Pathogenic connectivity," q_p (-), calculates the overall probability that spores produced somewhere in the landscape will deposit successfully and germinate:

$$q_p = \frac{\int \int_{x,y} \iota(x,y) \int \int_{x',y'} s_v(x',y') \bar{K}(x-x',y-y') dy' dx' dy dx}{\int \int_{x',y'} s_v(x',y') dy' dx'} \quad (13b)$$

where $\iota(x,y)$ is the variety specific infection efficiency at the target location, and $s_v(x',y')$ is the variety specific spore density at the source location. Parameter ι is zero for non-host locations. Parameter $s_v(x',y')$ is calculated assuming a fully mature potato canopy ($LAI = 5$) in each potato grid cell, 1 % of which is covered with sporulating lesions. Total (variety specific) spore density at each source location, $s_v(x',y')$, is therefore given by $LAI \times 0.01 \times \sigma(x',y')$, where $\sigma(x',y')$ is the variety specific sporulation intensity at that location. Calculation of q_p in landscapes composed of crop fields with genotype mixtures requires that $\iota(x,y)$ and $\sigma(x',y')$ are weighted according to equation 10. Variety specific parameters are given in Table 2. Again, as

q_p is a probability, it is bounded between 0 and 1. In order to reach the theoretical upper bound of 1, all redistributed spores would have to land on susceptible host tissue and cause an infection. If an area is planted entirely with a variety with infection efficiency ι , and no spores would be lost outside the area, q_p would equal ι , while q_p would theoretically be 0 if all spores were dispersed to non host sites. Parameter q_p is used to aid in the interpretation of simulation results, providing a static (non-temporal) measure of the impact of spatial heterogeneity on the processes of spore dispersal and infection at a landscape-scale.

The relative importance of within- and between-field dispersal in different landscapes can be determined by calculating autoinfections and alloinfections. Autoinfections are defined as those in which the donor field is the same as the recipient field. Alloinfections are those in which the donor (source) field is different from the recipient (infected) field. Both autoinfections and alloinfections are calculated in a similar way to q_p , i.e., by applying the average dispersal kernel, \bar{K} , to the landscape, without dynamic simulation of epidemics. Each field in the landscape is treated as a source in exactly the same manner as described for calculations of q_p . The average dispersal kernel is applied one field at a time (to every grid cell in that field), and the resultant number of infections that occur in the source field (autoinfections) and in other fields (alloinfections) is calculated using the appropriate variety specific ι . This process is repeated for each field in turn, and the total number of auto- and alloinfections in the landscape is calculated. The whole process is repeated for 10 different random landscapes for each scenario, and total auto- and alloinfections are averaged over the random landscape iterations.

Note that in dynamic simulation there are two forms of autodeposition. A fraction of the spores produced are released, and a fraction of those do not escape the canopy and autodeposit. According to \bar{K} (and K), which is calculated on a 10 x 10 m grid, some spores do not disperse farther than the confines of a 100 x 100 m grid cell, and also autodeposit within that cell. The former autodeposition component is not accounted for in the calculation of any of the functional connectivity measures described above, but the latter component is.

Spatial scenario analyses

To identify the spatial landscape parameters that have most influence on the rate and extent of invasion of a new, resistance breaking *P. infestans* genotype, four basic scenario analyses are made. These analyses address the influence of (1) the proportion of potato in the landscape, (2) the number of different resistant potato

genotypes, (3) the size of fields, and (4) the degree of spatial clustering of potato fields. Moreover, in each of these four scenario analyses, potato genotypes can be deployed at two spatial scales of mixing. Under the first scheme, designated “between-field diversity,” each individual field in the landscape contains a single host genotype; either resistant or susceptible. Under the second scheme, designated “within-field diversity,” each field contains a mixture of (partially) resistant and susceptible varieties, i.e., a genotype mixture. Table 3 specifies the range of parameter settings for each scenario analysis, while Fig. 3 depicts for the situation of between-field genotype mixing the landscape designs resulting from the lower and upper bounds of the range of parameter settings in each of the four basic scenario analyses. The parameter setting defining landscape maps as in Fig. 3, in combination with the spatial scale of mixing genotypes, defines a scenario.

In scenario analysis 1, the landscape is varied from a scenario with only 1/64th of the area planted with potatoes (Fig. 3A) to one in which the entire area is planted with potatoes (Fig. 3B). Under scenario analysis 2, a landscape with 1/4th potatoes is modified from being planted with 64 varieties, one of which has broken resistance (Fig. 3C), to one with only a single variety which has its resistance broken, so it is susceptible (Fig. 3D). Under scenario analysis 3, a landscape with 1/4th of potatoes is

Table 3. Spatial parameter values defining the four sets of spatial scenarios for the multi-scale simulator of the potato late blight pathosystem.

Scenario analysis	Proportion of potato fields in landscape (-)	Field size (ha)	Host connectivity, q^a (-)	Proportion of potato acreage that is susceptible (-)	Spatial pattern of fields (-)
Standard	1/4	1	0.5	1/4	Random
1	1/64, 1/16, 1/4, 1 ^b	1	0.3, 0.4, 0.5, 1.0	1/4	Random
2	1/4	1	0.5	1/64, 1/16, 1/4, 1	Random
3	1/4	1, 4, 16, 64	0.5, 0.7, 0.8, 0.9	1/4	Random
4	1/4	1	0.5, 0.7, 0.8, 0.9	1/4	Clustered

^a Host connectivity is defined using equation 13a.

^b Parameter settings for Fig. 4B, C, D and E are shown in bold.

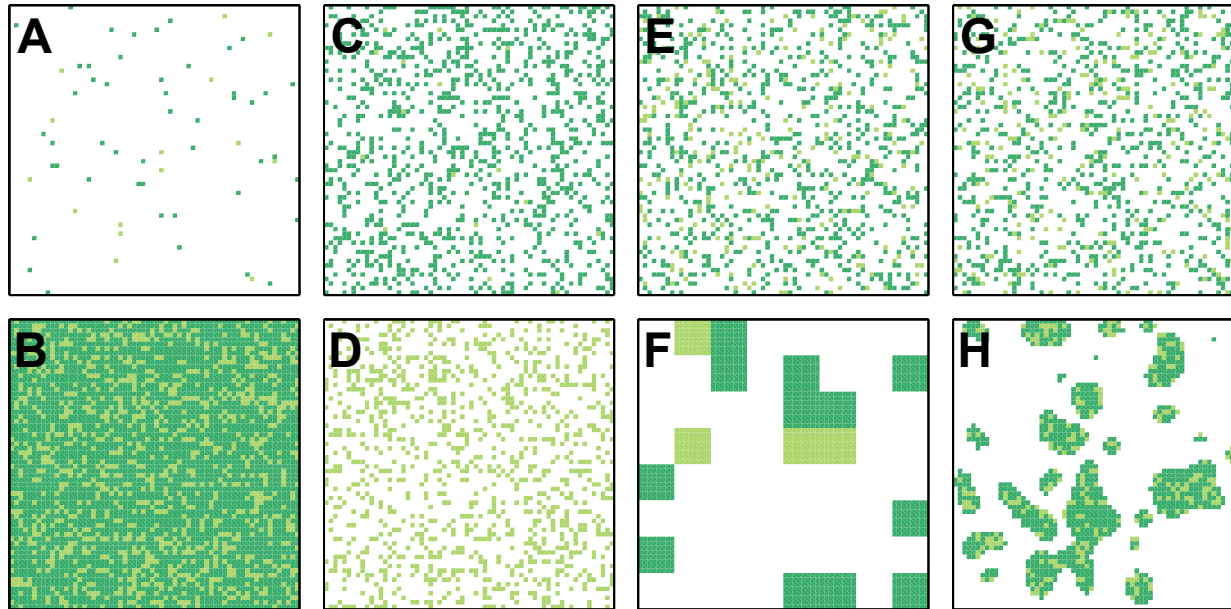


Fig. 3. Range of landscape designs used in this study. These are generated using the extreme spatial parameter settings from the four basic spatial scenarios analyses (Table 3). The first row shows the lower bound for the parameter value and the second row the upper bound. All simulated landscapes are 6.4 x 6.4 km, use 100 x 100 m potato fields, 1/4 of which are susceptible to disease, unless stated otherwise. One fourth of the landscape is planted with potato, unless stated otherwise. Light green fields are susceptible potatoes, dark green fields are partially resistant potatoes, and white area is non host to potato late blight. Scenario analysis 1: proportion of randomly distributed potato in the landscape varies from 1/64 (A) to 1 (B); scenario analysis 2: proportion of susceptible potatoes varies from 1/64 (C) to 1 (D); scenario analysis 3: field size varies from 1 (E) to 64 ha (F); and scenario analysis 4: clustering of fields varies from $q = 0.5$ (equation 13a) (G) to $q = 0.9$ (H). The map for the lower bound parameter setting under scenario analysis 3 (E) represents the “standard” landscape with 1/4 potato, 1/4 of which is susceptible, and 1 ha fields distributed at random.

constructed using different field sizes, from 1 ha (Fig. 3E) to 64 ha (Fig. 3F). The fourth scenario study spans landscapes ranging from one with a completely random distribution of potato fields ($q = 0.5$; Fig. 3G) to one with distinct clusters of potatoes and increased connectivity ($q = 0.9$; Fig. 3H). It should be noted that host connectivity q (Table 3; fourth column) is affected in scenario analyses 1 and 3, in which it was not the primary variable of interest. This is because alteration of separation distances and connectivity between fields is unavoidable when field number and size are manipulated. Connectivity is the parameter of interest in the fourth scenario analysis, in which separation distances are manipulated (without change in other spatial parameter values) by altering the degree of clustering of fields. As the value of q (host connectivity; equation 13a) is given for each parameter setting in Table 3, cross-comparisons can be made between all experiments.

The scenarios employing genotypic diversity of potatoes at the within-field level result in essentially the same maps as those represented in Fig. 3 for studying between-field diversity effects, the only difference being that all potato fields are identical under the within-field diversity scheme, with a proportion susceptible (resistance-broken) potatoes of $1/4^{\text{th}}$ under the default scenario or a varying proportion (from $1/64$ to $1/4$) in scenario study 2.

Example epidemics

Dynamic simulation results are introduced using a series of example epidemics. Spatio-temporal epidemic dynamics are presented in the form of a time-series of two-dimensional landscape maps showing spatial epidemic extent, thus visualizing the influence of spatial parameters settings on pathogen invasion prospects in time and space. In each example epidemic, a spatial parameter of the landscape is modified and an entire growing season is simulated (May 1st to September 30th, 2006). A single source of primary inoculum is simulated in each case; a single susceptible potato parcel of 1 ha is randomly selected under the between-field diversity resistance deployment scheme, whereas any potato grid cell is selected under the within-field diversity scheme. Epidemics are then initiated with 10 lesions m^{-2} ground area in the selected grid cell.

Dynamic simulation results

Ten random landscapes are generated for each scenario, and on each of these, ten different growing seasons are simulated. This gives a total of 200 simulations for each parameter setting: 10 random landscapes x 10 years of weather data x 2 spatial

scales of genotype mixing. The output variable of interest is incidence (-), which is defined as the number of infected potato hectares relative to the number of potato hectares in the landscape. A potato hectare is defined as being infected when the level of disease severity (sum of latent, infectious, and necrotic areas expressed as a percentage of total leaf area) $\geq 1\%$. This variable was found in pilot studies to be a good indicator of the speed and extent of invasions in heterogeneous potato landscapes. Incidence values are averaged over the 100 landscape and weather iterations per scenario. This makes a total of 8 sets of results: 4 scenario studies with 2 spatial scales of mixing each.

Uncertainty analysis

Relative standard errors of incidence (standard error expressed as a % of the mean incidence) are calculated between years within random landscape iterations (reps) for each scenario. These describe year to year variability in disease for the same random landscape, and thus indicate the influence of yearly variation in weather on disease invasion. Relative standard errors are also calculated for the average incidence over ten years of weather data per landscape in order to assess the degree to which the precision of simulation results are influenced by the number of random maps generated.

Perturbation analysis

The robustness of simulation results to parameters characterizing epidemic processes is investigated by means of a coarse perturbation analysis. A magnifying / minimizing perturbation is applied to the rate of lesion formation by multiplying the number of new lesions formed in each grid cell at each time step by an arbitrary constant, k (0.1, 1 or 10). Interpretation focuses on the effects of these perturbations on emergent model trends, i.e., qualitative as opposed to quantitative effects. By proceeding in this manner, emergent trends in the effects of spatial design on the rate and spatial extent of epidemics can be “checked” against consistent over- or under-prediction in model components. As 3 levels for k are introduced, there are 24 sets of model results in this analysis: 4 scenarios studies x 2 scales of mixing genotypes x 3 levels of perturbation.

Results

Example epidemics

Example epidemics demonstrate substantial effects of spatial design parameters and spatial scale of mixing genotypes (within- or between-fields) on invasion rates (Fig. 4). Incidence for the “standard” example epidemic (Fig 3E; Table 3) was 0.004, 0.016 and 0.062 for days 75, 100 and 125, respectively (Fig 4A). Increasing the proportion of potato in the landscape (Fig. 3B) caused a substantial increase in incidence (Fig. 4B) compared to the standard scenario, resulting in incidence values of 0.01, 0.063, and 0.144 for days 75, 100 and 125, respectively. In such a highly connected landscape as in Fig. 3B or Fig. 4B, there are no real barriers to spatial spread. This example hints at the dangers of growing potatoes in concentrated growing regions.

As expected, increasing the proportion of the potato population planted with a susceptible cultivar had a marked effect on the spatial extent of the epidemic (Fig 4C). In this monoculture scenario where each field is susceptible to disease, there are no real spatial barriers to dispersal as the pathogen can easily bridge the distances between susceptible host fields. In this example, where the landscape is 1/4th potato in 1 ha fields distributed at random, the average distance from a host field to its nearest neighbor is approximately 125 m. Incidence values were 0.014, 0.114, and 0.34 for days 75, 100 and 125, respectively. This example clearly highlights the dangers of monoculture, and hints at the benefits to be gained from planting a diversity of potato varieties.

Increasing the size of host fields from 1 to 64 ha resulted in a lesser increase in incidence over the standard scenario in comparison to the previous two examples (Fig. 4D). Incidence values were 0.004, 0.033, and 0.11 for days 75, 100 and 125, respectively. In this example the average distance from a host field to its nearest neighbor is approximately 1 km (from center-point to center-point). Here, the pathogen is able to bridge a distance of approximately 4 km to colonize a distant susceptible host field in the landscape. This indicates that it may be difficult to generate potato free zones at the landscape level that are large enough to provide worthwhile levels of resilience against disease invasion from one field to another. This result also suggests that spatial spread through short-distance “island hopping” is not a prerequisite for *P. infestans* invasions.

In the next example epidemic, small host fields are aggregated together into clusters (Fig 4E). This caused the smallest increase in incidence over the standard epidemic of all the examples thus far. Incidence values were 0.007, 0.035, and 0.089

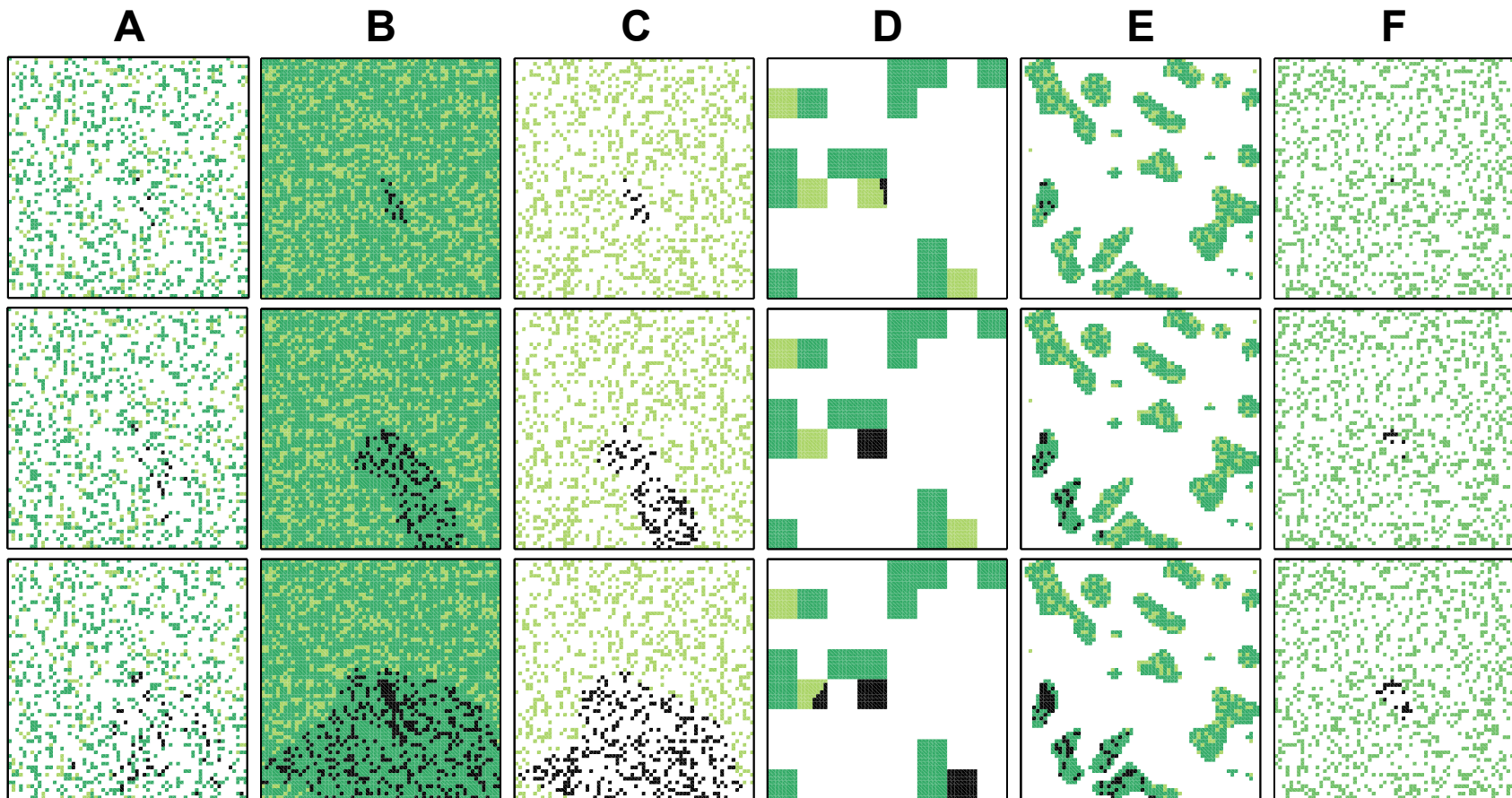


Fig. 4. Example epidemics of selected spatial scenarios (Table 3). All simulated landscapes are 6.4 x 6.4 km. Rows 1 to 3 show “snapshots” of the epidemics at 75, 100, and 125 days respectively. Column A provides a “standard” spatial scenario: proportion of potato acreage = 1/4; proportion susceptible = 1/4; deployment scheme = between-field diversity; and field area = 1 ha. Subsequent columns differ in terms of one spatial parameter: (B) proportion of potato acreage = 1; (C) proportion of the host population that is susceptible = 1; (D) field area = 64 ha; (E) distribution of fields is clustered until host connectivity, $q = 0.9$; and (F) as A, but each field contains a genotype mixture. Light green = susceptible, dark green = partially resistant, intermediate shade = genotype mixtures, black = infected areas.

for days 75, 100 and 125, respectively. In this example all potato fields (bar 2) had an adjacent neighboring potato field, and the average distance from a cluster of fields to its nearest neighboring cluster (center-point to center-point) was approximately 1 km, similar to the distance between fields in the previous example epidemic. Values of q were also similar between these two examples, at around 0.9 in both cases. Again, it appears that increasing separation distances is not a worthwhile strategy if it comes at the expense of creating larger contiguous potato areas. The ease at which disease can spread to neighboring fields in an infected cluster outweighs any suppressive effects caused by increasing distances between clusters. Nonetheless, the increase in incidence over the standard example is slightly less than the increase caused by enlarging field size. This is despite the similarity in the size and separation of contiguous potato areas in the two examples. The reason for this is that a mixing effect has occurred in each infected cluster, i.e., spores are lost from the system due to deposition on neighboring resistant fields in the cluster.

In the final example epidemic, each field contains a mixture of host genotypes (Fig 4F). One quarter of the host population is susceptible to disease therefore each host field also contains three partially resistant varieties. This is the only scenario where a decrease in disease was realised in comparison to the standard scenario; incidence values were 0.001, 0.009, and 0.02 for days 75, 100 and 125, respectively. It appears that fine-grain mixing of potato varieties could be a worthwhile strategy for suppression of late blight invasions.

Dynamic simulation results

Now that we have exemplified the influence of the various spatial parameters on pathogen invasion prospects, we provide an assessment of the efficacy of the various landscape designs under a variety of weather conditions and random map configurations. Results for the full set of simulation experiments, averaged over the 10 random landscape iterations and 10 growing seasons, are given in Fig. 5. Here, the steepness of the incidence response curve is used as a measure of the capacity of the spatial parameter for influencing pathogen invasion.

In confirmation of the example epidemic results, modification of the proportion of potato acreage had a substantial effect (Fig. 5A) on epidemic extent. For the between-field diversity scheme (open data markers in Fig. 5), incidence increased by a factor of 5 over the range of spatial parameter settings in this scenario (Table 3; Scenario analysis 1). There was a marked effect of genotype mixtures (closed data markers in Fig. 5) in suppressing pathogen invasion; incidence increased by a factor of

3 over the range of spatial parameter settings. This indicates that there may be substantial benefit in planting genotype mixtures in areas where a high density of potato is unavoidable.

Manipulation of the susceptible fraction had a large effect on epidemic extent (Fig. 5B). Incidence increased by a factor of 23 over the range of spatial parameter settings for both resistance deployment schemes. Increasing the diversity of potato genotypes in the landscape therefore emerges as a worthwhile spatial strategy for suppression of epidemics. Disease levels were once again substantially lower for the within-field diversity scheme, until the susceptible proportion is 1 and both resistance

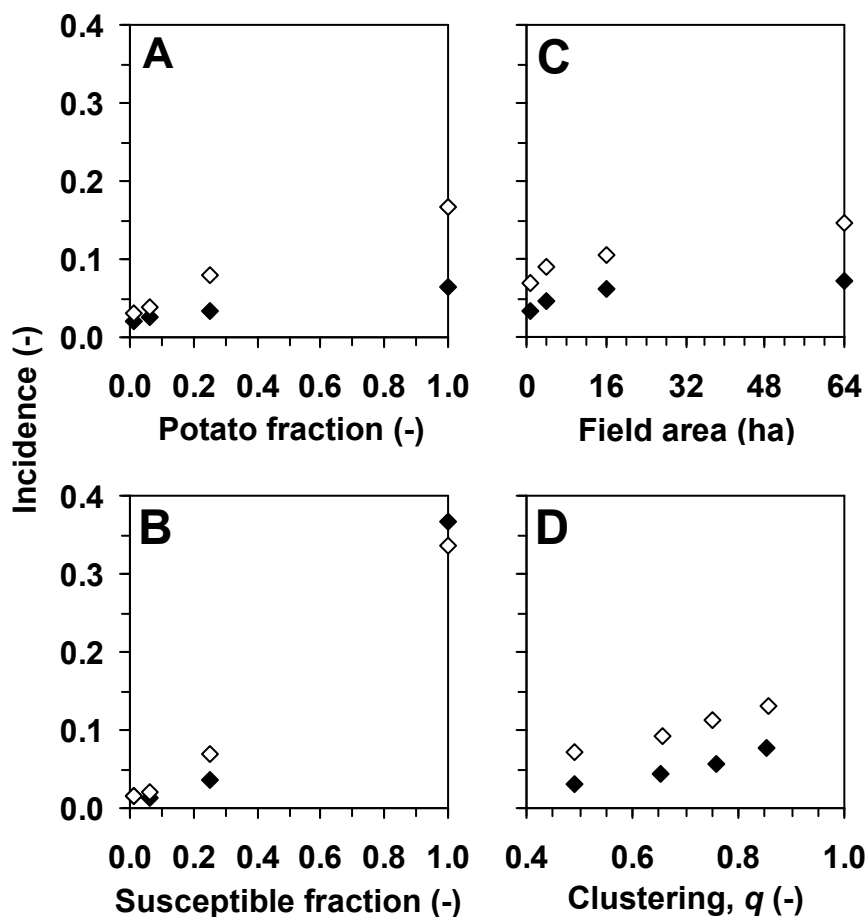


Fig. 5. Influence of spatial host population characteristics on the spatial extent of simulated potato late blight epidemics. Panels A to D correspond to the four basic spatial scenario analyses outlined in the text. Parameter settings (x-axes) for the spatial scenario analyses are given in Table 3. Incidence is defined as the number of potato hectares infected (disease severity ≥ 1 %) relative to the number of potato hectares in the landscape. Open data markers show predictions for the between-field diversity resistance deployment scheme, and closed data markers for the within-field diversity scheme.

deployment schemes are equivalent. Note the superproportional increase in disease as the proportion of susceptible tissue in each genotype mixtures increases. This is in accordance with Leonard's classic model of host diversity effects on disease (Leonard, 1969), which predicts that disease severity will increase exponentially as susceptible plants are added to a mixture.

Manipulation of field area had a minimal impact on epidemic extent (Fig. 5C). Incidence increased by a factor of 2 over the range of spatial parameter settings for both resistance deployment schemes. The effectiveness of genotype mixtures in suppressing pathogen invasion is clear over the whole range of field sizes used, indicating that deployment of genotype mixtures would be a particularly useful strategy if reduction in field size is problematic.

Level of field aggregation had a comparatively modest influence on epidemic extent (Fig. 5D). Incidence increased by a factor of 1.8 and 2.5 over the range of spatial parameter settings for the within- and between-field diversity schemes, respectively. Similar to the previous scenario (manipulation of field area), the creation of large separation distances between contiguous potato areas (clusters) did not limit pathogen invasion. Values of q were also similar between the two scenario studies (Table 3). The difference in disease levels for the between-field diversity scheme for these two scenario studies is less than the difference that occurred in the single example epidemics (Fig 4E) in the previous section. In contrast to the example epidemics, this result indicates a negligible mixing effect within infected clusters.

Uncertainty analysis

Relative standard errors between years and within random landscape iterations (describing the influence of the number of years of weather data on incidence) ranged from 8 to 20 % (across all parameter value manipulations), with a mean value of 13 %. Relative standard errors for rep averages (describing the influence of the number of random landscape iterations on incidence) ranged from 4 to 15 %, with a mean value of 7 %. These percentage standard errors indicate that substantial variability in model outcomes is generated both by weather variability and by randomness in landscape maps for the same design parameters. The remaining noise in simulation outcomes does not obscure emergent patterns, and the level of replication is deemed adequate, though greater precision could be reached by increasing the number of replications. This was not practically feasible.

Perturbation analysis

Perturbation of the number of new lesions formed at each time step resulted in a significant change in the level of incidence on the y-axis, but no change in the shape of the response to variables on the x-axis (Fig. 6). The exception was manipulation of potato fraction under a minimizing perturbation (Fig. 6A; lower 2 curves). It can be seen that incidence can decrease with an increase in the amount of potato in the landscape. The absolute number of hectares infected actually increases for both

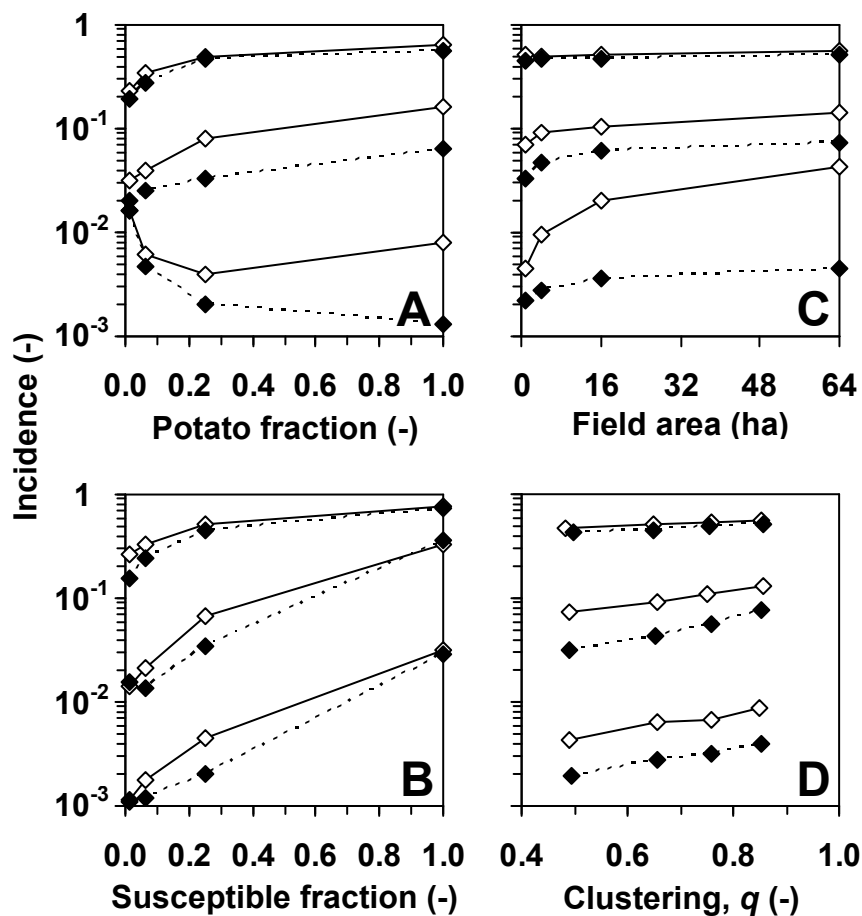


Fig. 6. Robustness of simulation results under an artificial magnifying/minimizing perturbation, whereby the number of new lesions formed in each grid cell at each time step is multiplied by a constant, k (-). Panels A to D correspond to the four basic spatial scenarios analyses outlined in the text. Parameter settings (x-axes) for the spatial scenario analyses are given in Table 3. Incidence is defined as the number of potato hectares infected (disease severity ≥ 1 %) relative to the number of potato hectares in the landscape. Results in each panel are divided under the between-field diversity scheme (solid lines with open data markers) and the within-field diversity scheme (dotted lines with closed data markers). For each paired set of results, the value of k is: upper set, $k = 10$; middle set, $k = 1$; and lower set, $k = 0.1$.

resistance deployment schemes (*unpublished data*), but when incidence is expressed as a proportion of the number of hectares of potato in the landscape, then this increase is masked. This is not an unexpected result, given the combination of a low proportion of susceptible host in the landscape and an artificial reduction in the number of new lesions that can form. Thus, emergent trends in simulation results are generally preserved even if processes are simulated with an order of magnitude error.

Functional connectivity

The influence of scenarios on the relative contributions of between- and within-field dispersal are revealed through a comparison of total autoinfections and total alloinfections (Fig. 7). As described in the methodology section, these results are for a single dispersal event only, and all spores produced are assumed to be made available for dispersal.

Focusing first on a comparison of the two spatial scales of genotype deployment, it appears that the major effect of within-field mixtures on epidemic development is to reduce the total number of autoinfections, i.e., infections within the same field. Host diversity within crops does not serve to markedly limit alloinfections, i.e., infections caused in other fields. This finding, in combination with the finding that genotype mixing within crops has a large effect on rate of disease invasion, indicates that the rate of disease invasion at the landscape scale can be substantially affected by efforts to reduce the local increase of disease in individual potato fields.

In the first spatial scenario analysis, autoinfections increase linearly with the proportion of potato acreage, as each field contributes an equal (variety specific) amount of self-infection (Fig 7A & B). Alloinfections show a more than proportional increase with potato fraction. As potato density increases, colonization of new host areas becomes progressively easier as separation distances between fields become smaller and smaller. As the limit of potato acreage is approached, alloinfections dominate in both genotype mixing schemes, as the distance between fields progressively becomes non-limiting to inoculum exchange.

Similar to the previous scenario analysis, autoinfections increase linearly with the susceptible fraction (Fig. 7C & D). This is because each susceptible field contributes a higher amount to the autoinfection total than a resistant field, and the contribution of each susceptible field is equal. Alloinfections also increase linearly with the susceptible fraction. Unlike the previous set of scenarios, colonization of new host

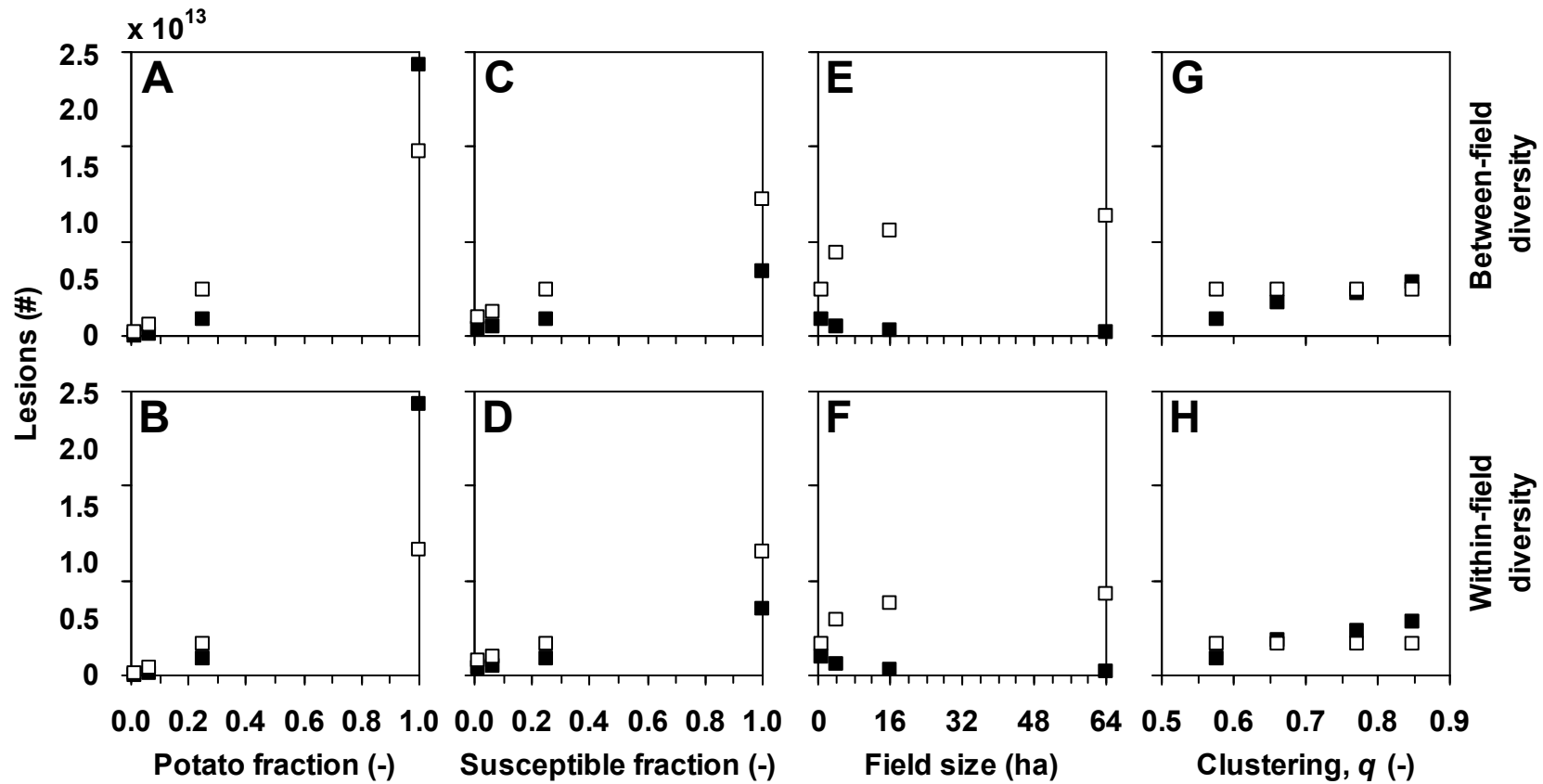


Fig. 7. Influence of spatial host population characteristics on autoinfections and alloinfections. Open data markers show predicted autoinfections and closed data markers show predicted alloinfections. Figure panels correspond to the spatial scenario analyses outlined in the text: (A&B) = scenario analysis 1; (C&D) = scenario analysis 2; (E&F) = scenario analysis 3; and (G&H) = scenario analysis 4. Spatial parameter settings (x-axes) for the four basic scenario analyses are given in Table 3. The top row shows predictions for the between-field diversity scheme and the bottom row the within-field diversity scheme.

areas does not appear to become progressively easier as the limit of susceptible fraction is approached. This is because the landscape is only 1/4th potato in this analysis, therefore host fields, susceptible or otherwise, are well separated in space (approximately 200 m apart).

In the third spatial scenario analysis, a less than proportional increase in autoinfections is observed with an increase in field area (Fig 7E & F). An increase in field area means that spores have, on average, further to travel before reaching the edge of the field, and are therefore more likely to autodeposit. As fields become larger, the response curve begins to plateau as the proportion of spores that autodeposit approaches an asymptotic limit of 1. Larger fields also act as larger sources of inoculum, which increases the likelihood of spore transport to distant fields. This latter effect is more than offset, however, by increased separation distances between fields as their size is increased (and their number decreased). The net effect on alloinfection is a slight decrease with increased field size.

In the fourth scenario analysis, increasing the spatial clustering of fields had no impact on autoinfections, while it resulted in an increase in alloinfections, due to the increased proximity of neighboring fields in each cluster (Fig. 7G & H). The increase in alloinfection within clusters is only partially offset by a decrease in alloinfection between clusters, i.e. as the level of aggregation increases, the number of individual clusters decreases and they become further apart. The net effect of clustering is therefore an increase in alloinfections. Similar to the first set of scenarios, at the limit of aggregation alloinfections dominate due to the close proximity of a large number of potato fields. This effect is slightly more pronounced for the within-field diversity scheme, as each field contains susceptible host tissue.

The influence of spatial parameter settings and resistance deployment scheme on functional connectivity, q_p , is given in Fig. 8.

In the first set of scenarios, a linear increase in q_p with the potato fraction is observed (Fig 8A). In other words, the ratio of total infections (auto- and alloinfections) to total spore production is proportional to the potato fraction. Alternatively, the probability that a spore will encounter a host and germinate is proportional to the potato fraction. Clearly, genotype mixtures at crop level reduce connectivity compared to the deployment of the same number of different cultivars at landscape level. A linear relationship is also observed in the second set of scenarios (Fig. 8B), indicating that pathogenic connectivity is also proportional to the susceptible fraction in the potato population. In the third scenario analysis (Fig 8C), the increase in q_p with field size mirrors the increase of autoinfections with field area

(Fig 7E & F). This is due to the almost negligible contribution of alloinfection to q_p that results from the large separation distances between fields. The difference between the two genotype mixing schemes is quite pronounced in this scenario analysis. This is because genotype mixtures have a large impact on autoinfection, and increasing field size results in a large increase in autoinfection (see Fig. 7). In the fourth scenario analysis (Fig 8D), the increase in q_p with clustering mirrors the increase in alloinfections with clustering (Fig. 7G & H). As explained above, this is because aggregation has no effect on autoinfection. Of course, a linear relationship may be expected in this analysis as clustering is quantified using the (similar) host connectivity parameter, q . This does not mean, however, that the extra biological

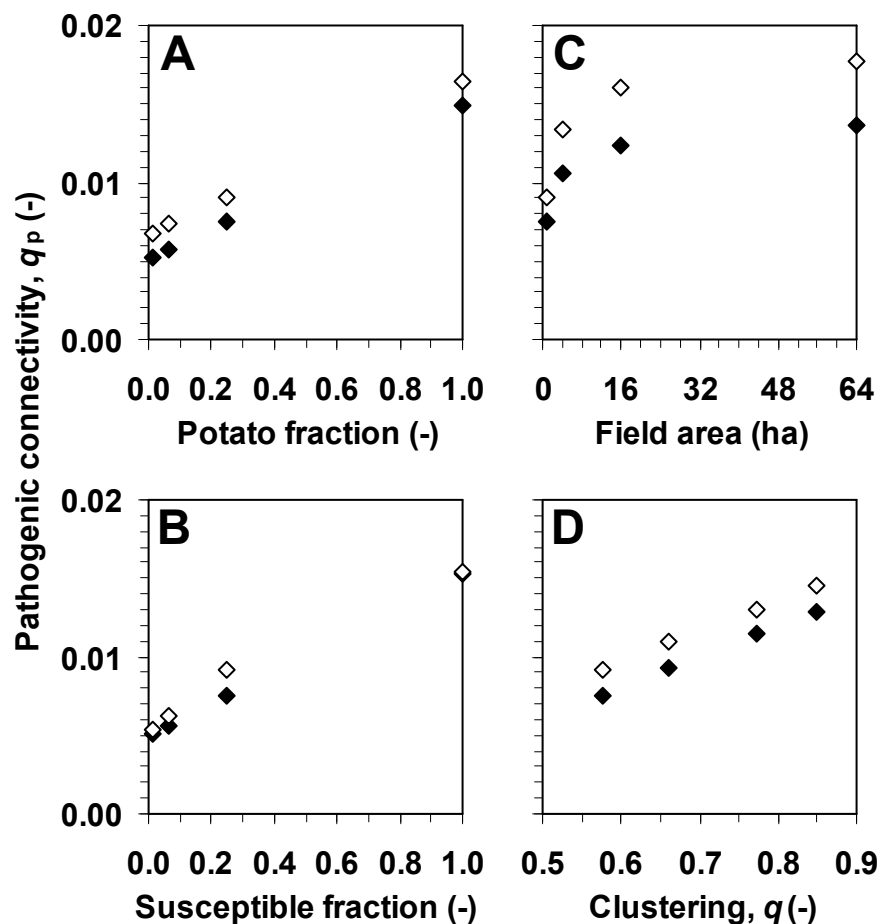


Fig. 8. Influence of spatial host population characteristics on pathogenic connectivity, q_p (equation 13b). Panels A to D correspond to the four basic spatial scenarios analyses outlined in the text. Parameter settings (x-axes) for the spatial scenario analyses are given in Table 3. Open data markers show predictions for the between-field diversity resistance deployment scheme, and closed data markers show predictions for the within-field diversity scheme.

information incorporated in q_p is unnecessary, and that q is as good a predictor of connectivity as q_p . Parameter q contains no variety specific information and is unable to differentiate between fields containing different cultivars, and between the two resistance deployment schemes.

The connectivity parameters, q and q_p , are defined using a single “average” dispersal event. Static (non-temporal) measures such as these do not fully capture the influence of landscape and meteorological heterogeneity, and fungicide management, on the polycyclic process of spatial epidemic expansion. Nonetheless, it is useful to look at the capacity of q_p as a predictor of spatio-temporal epidemic dynamics (Fig. 9).

It appears that the increase in the spatial extent of epidemics with q_p is more

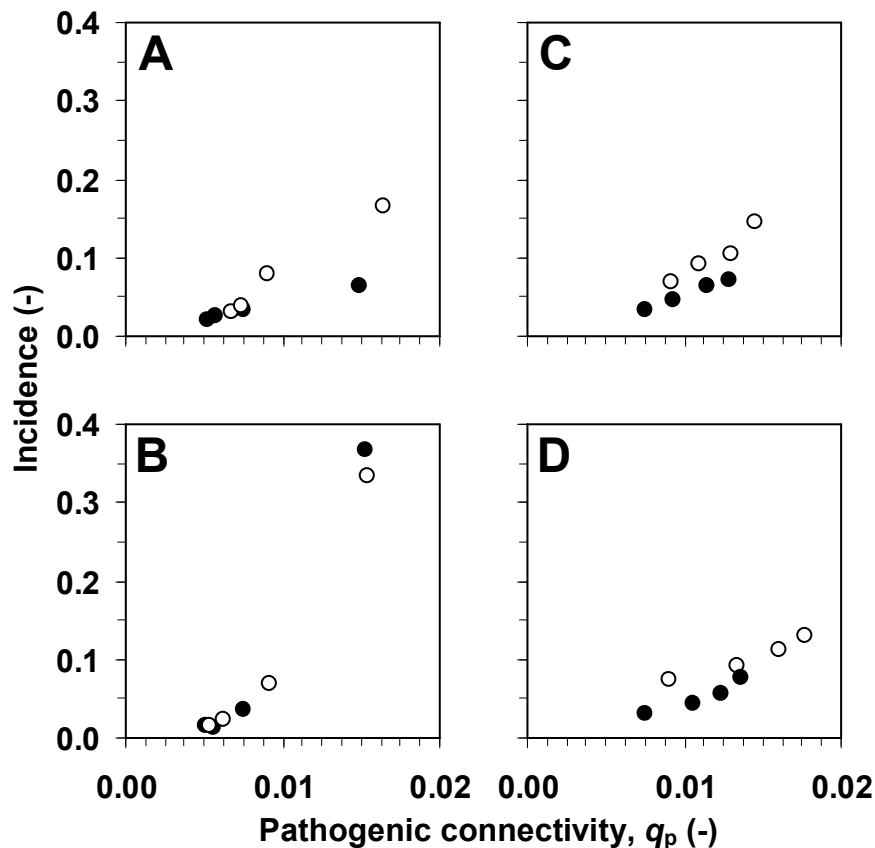


Fig. 9. Relationship between pathogenic connectivity, q_p (equation 13b), and final epidemic extent. Panels A to D correspond to the four basic spatial scenarios analyses outlined in the text. Parameter settings (x-axes) for the spatial scenario analyses are given in Table 3. Incidence is defined as the number of potato hectares infected (disease severity $\geq 1\%$) relative to the number of potato hectares in the landscape. Open data markers show predictions for the between-field diversity resistance deployment scheme, and closed data markers show predictions for the within-field diversity scheme.

than proportional under manipulation of all spatial parameters. An increase in connectivity means that a higher number of distant fields can be colonized by the pathogen. As each newly colonized field acts as a “stepping stone” for colonization of (a greater number of) other fields, an exponential type increase in epidemic extent with increased connectivity is observed. Note, however, that multiple values of incidence are possible for each value of q_p (Fig. 9A-D). It can therefore be concluded that q_p has no precise predictive power, but is useful in predicting trends in the effects of spatial manipulations on pathogen invasion, and in interpreting those results.

Discussion

The results of this study indicate that spatial heterogeneity in host populations does matter for *P. infestans*, and that landscapes can be designed that suppress invasions of virulent pathogen genotypes. The more effective of the spatial strategies tested concerned increasing the number of potato genotypes, decreasing the amount of potato, or increasing the degree of spatial mixing of genotypes. Landscape designs that focused on spatial isolation of aggressive pathogen strains through manipulation of field size and clustering of potato fields were found to have limited effect. There appeared to be little evidence of thresholds in the response of epidemics to manipulation of spatial landscape variables, i.e., in the calculated scenarios, no situations were identified in which spatial design had quantum effects on the prevalence of *P. infestans*. Simulation results also revealed a considerable influence of stochasticity in meteorological conditions and potato locations on predicted invasion prospects. A large number of combinations of source and target location and weather data were required to reduce noise and detect trends in model outcomes. An important conclusion follows from this finding; it is the specific coincidence in time and space between weather conditions and the geographic locations of source and target sites that defines true landscape connectivity and drives spatial epidemic expansion. In other words: under the same landscape design parameters, the rate of disease invasion may be very different from one year or spatial implementation to another, depending upon the vagaries of spore dispersal in relation to the placement of crop fields at the landscape level. Whereas incidence averaged over many random iterations and sets of weather data is meaningful, it is the variation in results that describes the range of possibilities that could occur in reality. It can be concluded that

in the simulation of (airborne) pathogen invasions, it is important to use an atmospheric dispersion model, large weather data sets that represent weather variability, and conduct many random landscape iterations.

It seems intuitive that the most effective landscape designs will be the ones that create the largest spatial barriers to spread. The results of this study indicate, however, that increasing the level of genetic diversity in host populations, and/or the degree of spatial mixing of host genotypes, could be more limiting to epidemic spread than manipulation of landscapes to produce large-scale (coarse-grained) spatial heterogeneities. This result can be explained with regard to the inordinately effective invasion strategy of *P. infestans*, which has two main components. The first component is a large capacity for rapid destruction of host foliage. Even if the distance from the donor to the recipient field is large, and the number of primary infections that results from a dispersal event is small, the highly effective asexual cycle of the pathogen can quickly lead to the production of large amounts of inoculum in the recipient crop. This leads to the second component of this invasion strategy, which is one of aerial bombardment of distant uninfected crops through massive deployment of asexual sporangia. This vastly increases the pathogens' chances of crossing large inhospitable areas of the landscape. Whether or not any particular landscape design or genotype mixing strategy will be effective in suppressing epidemics is dependent on how it affects both components of this invasion strategy. This concept can be explained in terms of an epidemiological trade off between the number of susceptible genotype units in the landscape, and the genotype unit area. Here, we define a genotype unit as a contiguous area containing a single host genotype. A genotype unit can therefore refer to a single plant, a row or patch of plants of the same genotype, or a field or group of fields of the same genotype. Genotype unit area is the ground area of a single genotype unit. The number of genotype units in the landscape affects pathogen invasion through its influence on alloinfection. Genotype unit area affects pathogen invasion through its influence on autoinfection, and thus the rate of disease progress within genotype units. Genotype unit area also affects the size of inoculum sources. It is the balance of advantage/disadvantage to the pathogen caused by this trade-off that determines whether or not a particular spatial strategy will be successful in buffering epidemic progress.

Decreasing the amount of potato grown in a region creates only disadvantage to the pathogen (Fig 5A). Genotype unit areas remain fixed and the number of susceptible genotype units in the landscape decreases. This was one of the more

effective of the landscape designs tested, but is perhaps the least pragmatic as it would affect productivity in the region.

In any landscape in which the amount of potato must remain fixed, it appears that spatial strategies that center on coarse-scale spatial mixing of host genotypes, i.e., the creation of large fields (Fig 5C) or clustering of host fields (Fig 5D), will not be effective. Between-field distances of the order of several kilometers did not prevent establishment of the pathogen over a wide geographical area. This finding acts to confirm the scant information in the literature on the capacity of *P. infestans* for long distance dispersal (e.g., Zwankhuizen et al., 1998; Mizubuti et al., 2000; Sunseri et al., 2002). Furthermore, increasing the density of potato in any given area can result in explosive localized epidemics upon the arrival of primary inoculum. It therefore appears that the advantage to the pathogen of a larger genotype unit area (resulting in higher autoinfection rates and larger sources of inoculum) outweighs the disadvantage to the pathogen of a decreased number of susceptible genotype units (resulting in larger separation distances and decreased alloinfection). This suggests that further strategies concerning geographic separation of growing areas according to potato genotype or farming technique (GM, conventional, organic) could also be risky.

By corollary, strategies that create fine-scale spatial mixing of host genotypes are effective in suppressing epidemics. This can be achieved by disaggregating potato production and redistributing fields across a wider area, or by planting potato in smaller, more numerous, separated fields. In both cases, the advantage to the pathogen of a larger number of genotype units (and increased alloinfection) is outweighed by the disadvantage of a decreased genotype unit area (and decreased autoinfection). An even more effective, and perhaps, pragmatic method to increase the degree of spatial mixing in the host population is to deploy host genotypes in mixtures. The results of this study show that this strategy is always effective in reducing pathogen invasion prospects regardless of the other spatial characteristics of the landscape (Fig 5A-D). The value of a fine-grain mixing strategy becomes more compelling given the apparent capacity of *P. infestans* for long distance dispersal of viable inoculum that has been suggested by this study.

The strategy that appears to work best, at least within the confines of this study, is to increase the level of genetic diversity in the host population (Fig 5B). Deployment of a greater number of host genotypes in the landscape creates only disadvantage to the pathogen; genotype unit areas remain fixed and the number of susceptible genotype units decreases. We can postulate at this point that if there

were no costs attached to the creation and deployment of large numbers of resistant genotypes, this would be the best strategy as invasions are suppressed whilst potato production is (relatively) unaffected. Genetic resistance resources for potato late blight are currently limited, however, and fears exist over the erosion of these resources. This point is addressed in more detail below.

In combining this knowledge, we arrive at a unified spatial strategy for deployment of host resistance, with a view to suppressing invasions of a virulent strain of *P. infestans*: region-wide, homogenous (non-aggregated) deployment of diverse genotype mixtures in small fields. Simulation results suggest that this strategy would be effective in reducing spatial increase in disease, and thus in minimizing the consequences of a breakthrough in resistance. Secondary effects could include an increase in the performance and durability of resistance, and a reduction in the need for plant protection products. There are, however, two major issues with this strategy that must be addressed. The first is operational, and concerns the fact that genotype mixtures can increase operational costs, as different mixture components with different traits for consumption and processing must be separated at harvest. Clearly, homogenous or random mixtures as simulated here would not be practical unless they consist of isogenic lines that are characterized by identical quality traits and differ only in the genetic basis of disease resistance. It would be better to plant different potato varieties in alternate rows to facilitate lifting and separation at harvest. The second issue concerns deployment of a larger number of potato varieties, and the aforementioned fears over the erosion of resistance gene resources due to pathogen evolution. There may be a future solution, as the possibility of building (cis)gene cassettes into existing potato varieties is investigated (Kessel et al., 2007). The rationale behind the stacking of major resistance (R) genes into individual plant lines is that the pathogen would require multiple independent mutations to become virulent. The concept and technology required are not yet fully developed but the eventual plan is to monitor *Phytophthora* populations and swap resistance cassettes when required. In this way directional selection in pathogen populations can be disrupted by temporal rotation of engineered plant lines. In addition, there would be no issues concerning separation of mixture components at harvest. A combination of strategic spatial deployment, monitoring of pathogen populations, and temporal rotation of new engineered lines is an exciting prospect as it will facilitate a dynamic engineered approach that combines the best attributes of the gene stacking and spatial deployment strategies. Several assumptions underlying this

strategy will have to be scrutinized however, e.g., would it be impossible for the pathogen to circumvent a resistance gene cassette with a single mutation?

It is useful at this point to review the modeling (dispersal) approach of other simulation studies concerning spatio-temporal epidemic development and resistance management: White and Gilligan (1998) utilized a reaction diffusion model to explore spatial pattern development in a three species host-pathogen-biological control agent system; Holt and Chancellor (1999) used a two-dimensional negative exponential function to model the spatial deployment of resistant rice varieties; Gilligan (2002) developed an epidemiological framework for disease management using cellular automata; Park et al. (2001; 2003) used a metapopulation framework to investigate the dynamics of plant-parasite interactions; Otten et al. (2004) used percolation theory to investigate strategies for the control of invasions of fungal parasites and saprotrophs; and Aubertot et al. (2006) used a displacement vector based on wind speed and direction to test strategies for the deployment of oilseed rape resistance. Further recent examples of landscape-scale modeling of spatio-temporal epidemic processes are few in the literature, but that is not surprising given the difficulties associated with simulation of large-scale epidemics using physically and biologically realistic, yet relatively simple models.

In comparison to these studies, the major strength of the approach presented here lies in the use of a physically realistic atmospheric dispersion and spore survival model. This facilitated an assessment of invasion opportunities under a wide range of weather conditions. A further unique point of this study is the novel application of Fast Fourier transforms (FFTs). FFTs are sometimes used in the simulation of dispersal processes to perform a spatial convolution between a statistical contact distribution (a spatial probability density function for dispersal distance) and a spatial distribution of population numbers. In this study, atmospheric dispersion modeling was integrated and applied in such a way that enabled the use of spatial convolutions and FFTs to solve spatial phenomena at each time step in the dynamic simulation using a temporally varying kernel, as dictated by the weather. The use of FFTs greatly enhanced the speed at which the atmospheric dispersion model could be applied, and the speed of dynamic epidemic simulations. The dispersion model and solution methodology used here therefore provides a more physically realistic (and fast) dispersal alternative to temporally fixed statistical contact distributions for long-term, large-scale simulation models. It should be noted that this technique would not be suitable if simulation of spatial heterogeneity in meteorological conditions is

required. This is because the convolution implies identical atmospheric conditions at each source location.

A new element in this study is the pathogenic connectivity measure, q_p . This parameter quantifies landscape connectivity from a physical dispersal, topographical, and biological infection perspective. This is in contrast to other more commonly used neighborhood/aggregation measures that consider only the geometric and (geo)statistical properties of landscapes. The resulting integrative parameter q_p was useful as a predictor and interpreter of the influence of spatial heterogeneity on spatio-temporal epidemic dynamics, without the need for dynamic simulation. Only a single spatial convolution is required to calculate q_p , thus it provides an almost instantaneous measurement of functional connectivity, even for very large landscapes. This parameter could also be used to assess pathogenic connectivity in similar pathosystems through incorporation of relevant pathogenic parameters and dispersal functions. Such an approach may be useful in other ecological applications, for example in assessing the connectivity of landscapes for gene flow from genetically engineered to conventional crops or wild relatives. A “pollen connectivity” parameter could be defined in the same vein as equation 13b through incorporation of a pollen dispersal kernel and parameters describing, e.g., selfing/outcrossing and pollen survival during transportation.

A further question that should be addressed concerns the influence of scale on model results; would different conclusions have been reached if landscapes were larger than the 6.4 x 6.4 km landscapes used in this study? Or more specifically, at what distance does spatial separation of potato areas become complete? Simulation results reveal a separation distance of approximately 4 km between each field would not be enough to ensure complete protection from inoculum exchange. This issue was investigated in a previous study with a numerical hybrid dispersion model (Skelsey et al., *in press a*). In this study the model was validated for the dispersal of botanical spores, and embellished with the same models for spore release, escape and survival described here. The integrated aerobiological model was used to investigate the capacity of the atmosphere to transport *P. infestans* inoculum viably on days that were classified as being of high risk for development of disease *in planta*. Simulation results revealed that a separation distance of 10 km from an inoculum source is still not enough to ensure complete protection from viable inoculum exchange. Implementing a separation distance this large between each potato field would be practically infeasible. It must be remembered that the objective of this study was to determine pragmatic spatial strategies for epidemic suppression.

Such a distance could be implemented between potato growing areas by aggregating production to certain zones, but simulation results show that that can lead to explosive localized epidemics, and is therefore extremely inadvisable. Overall, the results of this study indicate that strategies that induce finer-grained spatial and genotypic heterogeneities in host populations are more limiting to epidemic spread. It therefore seems unlikely that a different conclusion would be reached if a larger spatial domain had been used in conducting the scenario analyses.

In answer to our initial question, it appears that in the case of *P. infestans*, spatial heterogeneity does matter. Despite the large capacity of the pathogen for long distance dispersal of viable inoculum, significant reductions in epidemic development can be obtained through careful spatial management of host resistance. There are three potato landscape design parameters that seem to work best to make a potato region resilient to invasion by a resistance breaking genotype: (1) deploying a large number of resistance genes; (2) reducing the amount of host, i.e., one should not concentrate potato cultivation in certain regions; and (3) within-field genotype mixing. Of course, reducing the level of potato production in a region may not be pragmatic, and deployment of a large number of resistance genes is currently hard to realize and should be assessed/implemented with consideration of the evolutionary potential of the pathogen. It is hoped that the simulation framework presented here can be extended in future studies through the inclusion of pathogen population genetics. This would lead to a significant improvement in the utility of the model as landscape designs and genotype mixing strategies could be further assessed in relation to pathogen evolutionary potential and durability of host resistance.

Appendix

The spore dispersal experiments of Spijkerboer et al. (2002) were carried out in a 200 x 200 m field of potatoes in Wageningen (latitude 51°58' N, longitude 5°40' E), the Netherlands, in the summer of 1997. Aerial spore concentrations were measured using spore traps at distances of up to 100 m from a point source of *Lycopodium clavatum* spores. Data from a total of fifteen measurement sessions are used here. The partial reflection model of Overcamp (1976) as given in the text is used to calculate ground level concentrations, whereas these experimental data were measured at various heights above the surface. In order to make the partial reflection model height dependent, the basic equations must be reformulated. The

concentration at receptor point (x,y,z) has a contribution from the image source via a streamline that cuts through the ground plane at distance x_G (m):

$$\bar{c}(x,y,z) = \frac{Q[1+\alpha_0(x_G)]}{2\pi\bar{u}\sigma_y\sigma_z} \exp\left(-\frac{y^2}{2\sigma_y^2}\right) \left\{ \exp\left[-\frac{(z-h)^2}{2\sigma_z^2}\right] + \exp\left[-\frac{(z+h)^2}{2\sigma_z^2}\right] \right\} \quad (\text{A1})$$

with $\alpha_0(x_G)$ given by:

$$\alpha_0(x_G) = 1 - \frac{2v_d}{\left(v_d + \frac{\bar{u}h}{\sigma_z} \frac{d\sigma_z(x_G)}{dx}\right)} \quad (\text{A2})$$

An implicit equation for x_G is (Overcamp, 1976):

$$z+h = h \frac{\sigma_z(x)}{\sigma_z(x_G)} \quad (\text{A3})$$

A log-log plot of predicted versus measured spore concentrations reveals that the model had a tendency to underpredict observed aerial spore concentrations (Fig. A1).

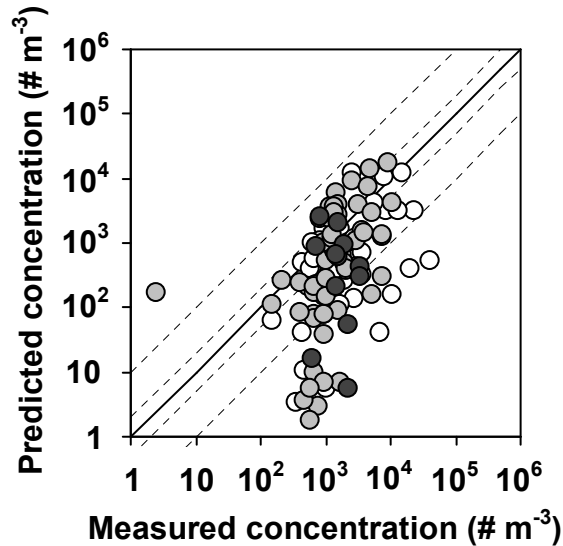


Fig. A1. Predicted versus measured spore concentrations. ○ = 25 < distance from source ≤ 50 m, ◐ = 50 < distance from source ≤ 75 m, ● = distance from source > 75 m. The inner dashed lines mark the boundary of a prediction error of factor two, the outer dashed lines mark the boundary of a prediction error of factor ten, and the solid line represents a 1:1 line.

Model performance was also evaluated using Willmott's (1985) modified index of agreement, D (-):

$$D = 1 - \left[\frac{\sum_{i=1}^n |P_i - O_i|}{\sum_{i=1}^n (|P_i'| + |O_i'|)} \right] \quad 0 \leq D \leq 1 \quad (\text{A4})$$

where P = prediction, O = observation, $P_i' = P_i - \bar{O}$ and $O_i' = O_i - \bar{O}$. The value of D is a measure of how well the observed deviations about the observed mean value match the predicted deviations about the same observed mean value. A score of 0.6 was achieved, where a value of 1 denotes perfect correspondence between predictions and observations. This is considered to be a satisfactory result for a fully analytical dispersal and deposition model.

Acknowledgements

Funding for this study was provided by the Dutch Ministry of Agriculture, Nature Management and Fisheries through the DuRPh project - theme: "Resistance management," project no. 3340043100. Thanks to Joost de Groot for his help with the computer cluster.

References

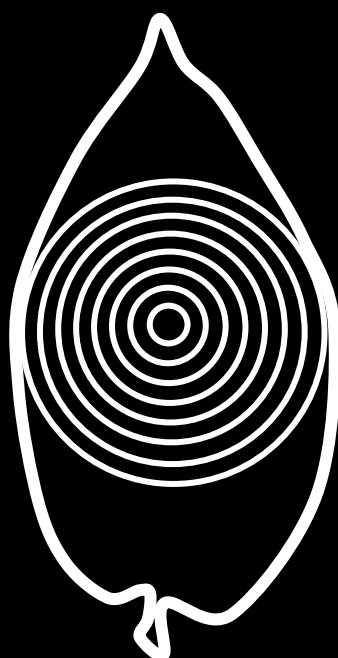
- Andrison, D., Lucas, J.M., and Ellisseche, D. 2003. Development of natural late blight epidemics in pure and mixed plots of potato cultivars with different levels of partial resistance. *Plant Pathol.* 52:586-594.
- Aubertot, J.N., West, J.S., Bousset-Vasline, M.U., Salam, M.J., Barbetti, M.J., and Diggle, A.J. 2006. Improved resistance management for durable disease control: a case study of Phoma stem canker of oilseed rape (*Brassica napus*). *Eur. J. of Plant Pathol.* 114:91-106.
- Arya, S.P. 1999. Air pollution meteorology and dispersion. Oxford university press, New York, NY.
- Birch P.R.J, and Whisson, S.C. 2001. *Phytophthora infestans* enters the genomic era. *Mol. Plant Pathol.* 2:257-63.
- de Jong, M., Bourdôt, G.W., Powell, J., and Goudriaan, J. 2002. A model of the escape of *Sclerotinia sclerotiorum* ascospores from pasture. *Ecol. Model.* 150:83-105.

- Draxler, R.R. 1976. Determination of atmospheric diffusion parameters. *Atm. Environ.* 10:99-105.
- Ferrandino, F.J., and Aylor, D.E. 1985. An explicit equation for deposition velocity. *Bound. Layer Meteorol.* 31:197-201.
- Fahrig, L., and Merriam, G. 1985. Habitat patch connectivity and population survival. *Ecology* 66:1762-1768.
- Forbes, G. 2004. Global overview of late blight. In: Lizarraga, C. (Ed.), *Proceedings of the regional workshop on potato late blight for East and Southeast Asia and the Pacific*. GILB, International Potato Center, Lima, Peru, pp. 3-10.
- Garrett, K.A., and Mundt, C.C. 2000. Host diversity can reduce potato late blight severity for focal and general patterns of primary inoculum. *Phytopathology* 90:1307-1312.
- Gilligan, C.A. 2002. An epidemiological framework for disease management. *Adv. Botanic. Res.* 38:1-64.
- Gregory, P.H. 1973. *The microbiology of the atmosphere*. Wiley, pp. 377.
- Haverkort, A.J., and Harris, P.M. 1987. A model for potato growth and yield under tropical highland conditions. *Agr. Forest Meteorol.* 39:271-282.
- Holt, J., and Chancellor, T.C.B. 1999. Modelling the spatio-temporal deployment of resistant varieties to reduce the incidence of rice tungro disease in a dynamic cropping system. *Plant Pathol.* 48:453-461.
- Jacobs, A.F.G., and Boxel, J.H. 1991. Horizontal and vertical distribution of wind speed in a vegetation canopy. *Neth. J. Agric. Sci.* 39:165-178.
- Kessel, G.J.T., Boonekamp, P.M., and Haverkort, A.J. 2007. Potato late blight in the Netherlands, a thing of the past? New frontiers in resistance breeding and disease. In: Hannukkala, A., and Segerstedt, M. (Eds.), *New and old pathogens of potato in changing climate: Proceedings of the EAPR Pathology Section seminar, Hatula, Finland*. Agrifood Research Working Papers 142:15.
- Large, E.C. 1940. *The advance of the fungi*. Jonathan Cape, London, pp. 488.
- Leonard, K.J. 1969. Factors affecting rates of stem rust increase in mixed plantings of susceptible and resistant oat varieties. *Phytopathology* 59:1845-1850.
- Levins, R. 1970. Extinction. In: Gerstenhaber, M. (Ed.), *Lectures on mathematics in the life sciences: Volume 2*. American Mathematics Society, Providence, Rhode Island, USA, pp. 77-107.
- Mizubuti, E.S.G., Aylor, D.E. and Fry, W.E. 2000. Survival of *Phytophthora infestans* sporangia exposed to solar radiation. *Phytopathology* 90:78-84.
- Nielsen, B.J., Hansen, J.G., Pinnschmidt, H., Narstad, R., Hermansen, A., Le, V.H., and Hannukkala, A. 2007. Studies of release and infectivity of *Phytophthora infestans* sporangia under field conditions. In: Schepers, H.T.A.M. (Ed.), *Proceedings of the tenth workshop of an European network for development of an integrated control strategy of potato late blight, Bolgna, Italy*. PAV Special Report no. 12:211-220.

- Otten, W., Bailey, D.J., and Gilligan, C.A. 2004. Empirical evidence of spatial thresholds to control invasion of fungal parasites and saprotrophs. *New Phytologist* 163:125-132.
- Overcamp, T.J. 1976. A general Gaussian diffusion-deposition model for elevated point sources. *J. Appl. Meteorol.* 15:1167-1171.
- Park, A.W., Gubbins, S., and Gilligan, C.A. 2001. Invasion and persistence of plant parasites in a spatially structured host population. *Oikos* 94:162-174.
- Park, A.W., Gubbins, S., and Gilligan, C.A. 2003. Extinction times for closed epidemics: The effects of host spatial structure. *Ecology Letters* 5:747-755.
- Philips, S.L., Shaw, M.W., and Wolfe, M.S. 2005. The effect of potato variety mixtures on epidemics of late blight in relation to plot size and level of resistance. *Ann. Appl. Biol.* 147:245-252.
- Spijkerboer, H.P., Beniers, J.E., Jaspers, D., Schouten, H.J., Goudriaan, J., Rabbinge, R., and van der Werf, W. 2002. Ability of the Gaussian plume model to predict and describe spore dispersal over a potato crop. *Ecol. Model.* 155:1-18.
- Skelsey, P., Holtslag, A.A.M., and van der Werf, W. 2008. Development and Validation of a Quasi-Gaussian Plume Model for the Transport of Botanical Spores. *Agr. Forest Meteorol.* 148:1383-1394.
- Skelsey, P., Kessel, G.J.T., Holtslag, A.A.M., Moene, A.F., and Werf, W. Regional spore dispersal as a factor in disease risk warnings for potato late blight: a proof of concept. *Agr. For. Meteorol., in press a.*
- Skelsey, P., Kessel, G.J.T., Rossing, W.A.H., and van der Werf, W. Parameterization and evaluation of a spatio-temporal model of the late blight pathosystem. *Phytopathology, in press b.*
- Skelsey, P., Kessel, G.J.T., Rossing, W.A.H., and van der Werf, W. Scenario approach for assessing the utility of dispersal information in decision support for aerially spread plant pathogens, applied to *Phytophthora infestans*. *Phytopathology, in press c.*
- Skelsey, P., Rossing, W.A.H., Kessel, G.J.T., Powell, J., and van der Werf, W. 2005. Influence of host diversity on development of epidemics: an evaluation and elaboration of mixture theory. *Phytopathology* 95:328-338.
- Stull, R.B. 1988. An introduction to boundary layer meteorology. Kluwer Academic Publishers, Dordrecht, the Netherlands.
- Sunseri, M.A., Johnson, D.A., and Dasgupta, N. 2002. Survival of detached sporangia of *Phytophthora infestans* exposed to ambient, relatively dry atmospheric conditions. *Am. J. Pot. Res.* 79:443-450.
- Taylor, G.I. 1921. Diffusion by continuous movements. *Proc. London Math. Soc.* 20:196-211.
- Taylor, P.D., Fahrig, L., Henein, K., and Merriam, G. 1993. Connectivity is a vital element of landscape structure. *Oikos* 68:571-573.
- van Oijen, M. 1992. Selection and use of a mathematical model to evaluate components of resistance to *Phytophthora infestans* in potato. *Eur. J. Plant Pathol.* 98:192-202.

- White, K. A. J., and Gilligan, C. A. 1998. Spatial heterogeneity in three-species, plant-parasite-hyperparasite, systems. *Phil. Trans. R. Soc. Lond. B* 353:543-557
- Willmott, C.J., Ackleson, S.G., Davis, R.E., Feddema, J.J., Klink, K.M., Legates, D.R., O'Donnell, J., and Rowe, C.M. 1985. Statistics for the evaluation and comparison of models. *J. Geophys. Res.* 90:8995-9005.
- Zhu, Y., Chen, H., Fan, J., Wang, Y., Li, Y., Chen, J., Fan, J., Yang, S., Hu, L., Leung, H., Mew, T. W., Teng, P.S., Wang, Z., and Mundt, C.C. 2000. Genetic diversity and disease control in rice. *Nature* 406:718-722.
- Zwankhuizen, M.J. 1998. Development of potato late blight epidemics: disease foci, disease gradients, and infection sources. *Phytopathology* 88:754-763.

CHAPTER 8



Introduction

The primary objective of this thesis was to quantify the spatial dimension of the potato late blight pathosystem and evaluate if knowledge of spatial epidemiology could contribute towards the development of more effective and eco-friendly late blight management strategies. This objective was pursued in a number of different steps that combined knowledge of plant pathology, epidemiology, meteorology, potato production systems and spatial modeling. Chapters 2 and 3 detail the development and validation of a spatio-temporal late blight model that is appropriate for simulating epidemic dynamics within potato fields. In Chapter 4 the model is extended and used to evaluate the risk of infection from distant sources of inoculum. Chapter 5 describes the development and validation of an atmospheric dispersion and deposition model that can be used to simulate transport of spores between fields. In Chapter 6 the dispersion model is combined with other aerobiological models to develop and test a new concept for inclusion of a spatial dimension in decision support systems (DSSs). In Chapter 7, a multi-scale epidemic simulator is created and used to test various landscape designs for suppression of potato late blight epidemics.

This chapter starts with a review of the main insights obtained into the spatial epidemiology of potato late blight. This is followed by an analysis of the strengths, weaknesses, validity and scope of the various modeling approaches developed and used in the thesis. Where relevant, suggestions for further improvement are given. The chapter ends with an outlook to the management implications of this thesis.

Spatial epidemiology

Although the spatial dimension of potato late blight epidemiology is widely acknowledged by researchers who study plant disease, the corresponding theoretical framework is underdeveloped. This is because epidemic patterning in space is the product of a complex interplay between meteorological driving forces, host resistance, chemical and cultural management, and the spatial characteristics of crops and landscapes. The results presented in this thesis illustrate how mathematical modeling and numerical simulation can be used to unravel some of this complexity, and enhance understanding of the spatial epidemiology of the disease.

Host diversity within crops

In Chapter 2, spatial increase of potato late blight disease within crops was abstracted to one of two extremes: general epidemics that develop from numerous, randomly dispersed infections, and focal epidemics that develop from localized spots of infection and radiate outwards. An analysis of life history theory (e.g., Keyfitz, 1985) and the theory of traveling waves (Van den Bosch et al., 1988a-c; 1990) revealed that a linear relationship must exist between the apparent infection rate of general epidemics, and the radial velocity of focus expansion in focal epidemics. This suggested that crop diversity effects on focal epidemics should also be realized in general epidemics. This hypothesis was confirmed by simulation results. An important effect of host diversity within crops was found for both general and focal epidemics across a range of patterns of genotype mixtures, and for several different statistical contact distributions. Theoretical predictions from ideal (homogenous) mixture theory were, in the most part, found to be valid also for non-ideal mixtures, such as row or strip crops. The extensive body of simulation work into the effectiveness of mixtures conducted by Mundt et al. (Mundt and Browning, 1985; Mundt and Leonard 1985 to 1986; Mundt et al., 1986) was replicated and given a simple mechanistic explanation based on spore loss from the simulated environments.

There is empirical evidence for a potentially beneficial effect of genotype mixtures in reducing potato late blight disease under both general and focal patterns of primary inoculum in temperate regions (Garrett and Mundt, 2000; Andrivon et al., 2003). Field trials in tropical regions do not, however, reflect these results (Garrett et al., 2001). It has been proposed that differences in inoculum dynamics in temperate and tropical regions are the cause of variation in empirical results (Garrett et al., 2001). The results of this modeling study indicate a beneficial effect of crop diversity when simulated fields are completely isolated, or part of a wider virtual environment of identical composition and infection level. This finding suggests that variation in empirical results is probably more related to aspects of experimental design (e.g., plot size, cultivar resistance levels, level of interplot interference), and location (e.g., close proximity to infected commercial fields) as opposed to any fundamental differences in potato late blight epidemiology, or in the response of potato late blight to crop diversity, in different agro-ecosystems.

Waggoner's (1952) statement "we shall find the real epidemic muddy and uncomfortable" certainly seems to apply to this topic and it is clear that further (consistent) research into the effects of crop diversity and disease pressure on

epidemic development is required in both temperate and tropical regions. These findings provide theoretical support for such endeavors, and for the future development of globally applicable management strategies based on diversified landscapes / mosaics.

Dichotomy in spatial epidemic processes

Spatial increase of potato late blight disease also arises from the expansion of foliar (and stem) lesions. Thus, in the potato late blight pathosystem, the disease cycle can be abstracted to a combination of two processes: lesion expansion and the polycyclic process of lesion propagation. In Chapter 3, a sensitivity analysis of the potato late blight model was used to elucidate the effect of these two spatial epidemic processes on the shape of disease progress curves. It was found that when only the consequences of lesion expansion are realized, a gentle s-shaped disease progress curve with a short lag period is produced. In contrast, when lesion growth is negligible and epidemics progress primarily through the propagation of new lesions, a steep s-shaped curve with a long lag period results.

This dichotomy in the contribution of these two spatial processes to disease progress provides two useful reference curves to help interpret observed and predicted epidemics. In Chapter 3 the curves were used to hypothesize that measured epidemics from the 2004 field trials were dominated to a greater degree by lesion propagation relative to the 2002 field trials. A further analysis of the field trial weather data revealed that conditions were less conducive for infection in 2002, so this mechanistic interpretation of the shape of the disease progress curve was congruent with the effect of weather on the infection process. This finding adds a new heuristic to the study of plant disease epidemics.

Risk of infection from external inoculum

In Chapter 4 the potato late blight model was used to analyze the yield response of potatoes to a single influx of primary inoculum under a range of disease management scenarios. General epidemics responded more strongly to initial spore load than focal epidemics. It was found that susceptible potato varieties, late maturing varieties in particular, were extremely sensitive to the amount of arriving inoculum, regardless of the degree of chemical protection. In contrast, the combination of a resistant cultivar with a good fungicide protection scheme provided a high degree of tolerance to the amount of arriving inoculum.

These results indicate that the influence of large-scale spatial epidemic processes cannot be considered separately from field-scale pathosystem processes. Quantification of spore dispersal from distant donor crops carries little epidemiological meaning without further detailed quantification of management practices at recipient crops. The results of Chapter 4 also serve to identify in which management situations a high degree of accuracy would be required in dispersal information for appropriate decision making, and where a greater degree of uncertainty could be tolerated.

Long distance transport of viable inoculum

There is a complete lack of information in the literature concerning the impact of variation in meteorology on the aerial component of the disease cycle as an integrated process (see Chapter 1, Fig. 2). This lack of information makes it impossible to draw conclusions concerning the capacity of the atmosphere to transport sporangia viably over distance. In Chapter 6, an aerobiological model of the aerial component of the disease cycle was used to produce a range of viable spore deposition gradients using real weather data pertaining to “high-risk” days for development of disease *in planta*. In the first instance, this analysis revealed that the fast inactivation of spores under radiation results in a substantial reduction of viable spore deposition, especially at greater distances from the source. Typically, at a distance of 1 km from the source, the spore survival model reduced deposition per meter by around 40 %, compared to an average reduction of 75 % at 10 km from the source. This analysis also revealed that at a distance of 10 km from the source, there could be as much as four orders of magnitude difference in the number of viable spores depositing per meter downwind from the source, depending on atmospheric transport conditions.

These results indicate that viable *P. infestans* inoculum can be transported over distances exceeding 10 km. Furthermore, they reveal a large degree of variation in the capacity of the atmosphere to transport viable *P. infestans* inoculum on days that are typically classified as being of high risk for disease; a finding that could be exploited for disease management.

Landscape design for epidemic suppression

Spatial increase in disease is also affected by spatial heterogeneity in host populations at the landscape level. Owing to the difficulties of measurement over such large scales, the influence of spatial heterogeneity on the development of

potato late blight epidemics at the landscape-scale has yet to be quantified. Chapter 7 detailed the integration of the field-scale potato late blight model with an aerobiological model of the aerial component of the disease cycle, and a landscape generator. The insights facilitated by this model represent a completely new chapter in the spatial epidemiology of potato late blight.

Simulation results showed that increasing the number of host genotypes caused the greatest reduction in epidemic extent, followed by reduction of the proportion of potato in the landscape, lowering the clustering of host fields, and reducing the size of host fields. Genotype mixtures proved to be effective in controlling disease in a single field (Chapter 2), and they were also effective in this multiple-source-multiple-target setting. When epidemic scenarios were repeated using genotype mixtures as opposed to 1 potato genotype per field, incidence levels were reduced by a factor of 2 on average.

One clear point that emerged time and time again throughout these analyses was the large capacity of *P. infestans* for long-distance transport of viable spores. These results indicate that increasing the level of genetic diversity in host populations, and/or the degree of mixing of host genotypes, could be more limiting to epidemic spread than manipulation of landscapes to produce large-scale (coarse-grained) spatial heterogeneities.

Methodological review

Spatially explicit modeling is the primary tool used in this thesis to obtain a better understanding of the epidemiology and options for management of potato late blight at a field and landscape level. One of the major challenges has been to combine knowledge about parts of the disease cycle (in isolation) in ways that integrate their interactions during an epidemic. A further challenge has been the creation and utilization of parsimonious but biologically realistic models that facilitate learning about epidemic processes. Ultimately, the end goal of improved potato late blight management required that the models developed herein be practically useful too. Thus, parsimony, realism, heuristic learning, and practicality were the features that set the criteria for the models developed and used in this thesis. The following sections provide an analysis of the validity, weaknesses, strengths and scope of each of the various models and modeling approaches used. Together, these sections detail a progression from the development, experimental parameterization, testing and

validation of models of pathosystem processes, through to the creation and application of integrated process models and scenario studies.

Theoretical version of the potato late blight model

Chapter 2 saw the first incarnation of a potato late blight model. This model was extended and altered throughout the first half of the thesis, but the core structure remained the same. The model of the potato late blight pathosystem combines individual based modeling (IBM) with an integrodifference equation (IDE) approach and epidemiological compartment modeling (ECM). IBM facilitates inclusion of a spatial dimension; space is modeled as a two-dimensional grid composed of individual potato plants. The IDE approach combines difference equations that describe pathogen dynamics during a sedentary stage, with redistribution kernels that characterize spore dispersal during a vagile stage. This format implies a mathematical convolution over space in each time step that can be solved quickly and accurately with Fast Fourier transforms (FFTs). Often, IDEs are used to describe populations with discrete, non-overlapping generations (e.g., Kot et al., 1996). In this model, the IDE approach is applied at a daily time step to an age-structured population of expanding lesions. This facilitates the simulation of overlapping lesion generations. ECM is used to simulate the progression of lesion areas from latent to infectious stages, through to necrosis.

The model was first used for development of epidemiological theory, as opposed to precise epidemic prediction (Chapter 2). For this reason, some strongly simplifying assumptions were made. In order to elucidate only the effects of spatial heterogeneity on epidemic progress, host dynamics (i.e., growth and shedding of foliage) were not simulated and weather conditions were assumed to be non-limiting to disease development. Furthermore, parameters describing host-pathogen interactions were not determined experimentally, rather, they were based on expert judgment. As the focus of this chapter was on inoculum exchange between crop elements, several different (empirically parameterized) dispersal kernels were tested for their influence on model results. Perhaps noteworthy in this model is the assumption that lesions can grow to be larger than the size of an average leaflet. Leaflets were not simulated and lesion growth rate was limited due to competition for space at the plant level. Sensitivity analyses with the model (*unpublished data*) revealed that this was of little importance to epidemic development, in this and in all other versions of the model. Furthermore, it was felt that this was a plausible

assumption as lesions can grow through petioles and stems to claim plant area exceeding a single leaflet.

In Chapter 2 the wrap-around effects of the solution methodology was used to simulate fields that are part of a wider environment of identical composition and infection level. It could be argued that the conclusions reached regarding the efficacy of genotype mixtures under such conditions may have been different if higher levels of background disease pressure were simulated. To give an example of the implications of the wrap-around effects, under general inoculation and using the wide Laplace kernel, approximately 5 % of all spores produced are dispersed outwith the boundaries of the field for any of the genotype mixtures shown in Fig. 3 of Chapter 2. The assumption that this inoculum loss is compensated by the surrounding environment actually equates to a very high level of background disease pressure.

This abstraction of the potato late blight pathosystem was used in Chapter 2 to replicate, interpret and enhance current knowledge concerning the spatial epidemiology of potato late blight in mixtures of potato genotypes. This model version may therefore prove to be useful in providing further theoretical support for development of crop diversification strategies.

Extension and validation of the potato late blight model

Modifications were required to use the potato late blight model for investigating operational and strategic management issues. In Chapter 3, new parameter values describing host-pathogen interactions (resistance components) were determined experimentally in the laboratory for a number of cultivar-isolate combinations. The heavy weather-dependence of the disease cycle also required that environment-pathogen interactions were included in the model. In order to maintain transparency of model results, a highly idealized set of environment-pathogen relations were developed using the experimental results of Zwankhuizen and Zadoks (2002) and Rotem et al. (1970). This increased level of detail and the applied nature of the research goals prompted an assessment of the quality of model predictions using real world data. Both temporal and spatial model predictions were in close agreement with observations, confirming the ability of the model to translate measured resistance components, weather data and initial conditions into realistic epidemics.

The data of Rotem et al. (1970) precede the migration of the A2 mating type into Europe, therefore it would be of benefit in the future to revamp the climatic relations using pathogenic data pertaining to the new, more aggressive *Phytophthora* population. It is also possible that predictive accuracy could have been improved

through a more detailed treatment of environment-pathogen interactions in the model. The goal in validation, however, was not to achieve or force a high level of predictive accuracy. As a tool for heuristic learning, it was deemed more important to be able to produce realistic epidemic dynamics using as simple and transparent a model as possible. For the same reason, model calibration was to be avoided if at all possible. The results of a sensitivity analysis proved to be useful in this respect. An emergent dichotomy in the effects of resistance components on disease progress was used to formulate a plausible hypothesis regarding differences in observed disease progress curves in different years. This somewhat unusual application of a sensitivity analysis demonstrates that transparency in model results facilitates an increased understanding of model behavior, which in turn leads to an improved understanding of system dynamics.

It would be of interest in the future to extend the scope of the potato late blight model through qualification with observational data from other climatic regions. This would greatly enhance the general applicability of the model.

Applied version of the potato late blight model

In Chapter 4 the potato late blight model was used to investigate the sensitivity of a number of different management scenarios to incoming inoculum. This information was then used to draw conclusions regarding the potential consequences of uncertainty in dispersal information in epidemiological prediction. Thus, a cautious approach towards the development and practical application of an atmospheric dispersion model was adopted in this thesis. This objective required that more detail be added to the model. Leaf area dynamics, tuber growth and fungicide dynamics were added using descriptive equations designed to maintain transparency of model results.

Perhaps the weakest part of this model version is the fungicide submodel. Unfortunately there is a paucity of information in the literature concerning the precise quantitative effects of fungicides on disease cycle processes. This meant that fungicide submodel parameters had to be based on expert judgment.

A plus-point of this model version is its flexibility. It includes host and pathogen life cycles, host- and pathogen-environment relations, and fungicide management practices within a spatial framework. It is therefore a useful research tool for investigating interactions between pathogen, host genotype, spatial crop characteristics, environment, and management.

Quasi-Gaussian plume model

One of the underlying aims of this study is to champion the cause for more meteorology in epidemiological prediction, through the development and utilization of practically useful aerobiological models. This was the key objective in Chapter 5, where a hybrid spore dispersion model was developed; combining a Gaussian plume model with the analytical Lagrangian similarity diffusion model (Van Ulden, 1978; Gryning et al., 1983) and a spore deposition model.

This choice of modeling approach was determined by a number of criteria. Prediction in a practical (operational) setting requires a model with modest computing and input requirements, yet sufficiently accurate predictions. A Gaussian plume model seemed the obvious first choice as they are widely used, well understood, easy to apply, and have received international approval. Incorporation of the Lagrangian similarity diffusion model added value as it facilitated a non-Gaussian description of vertical concentration distributions. The source depletion model of Chamberlain (1953) was preferred over other more physically realistic deposition models due to its relative simplicity.

In order to determine if the model was accurate enough to be useful in practical disease prediction, it was validated against spore dispersal data (Spijkerboer, 2002). Ultimately, these exercises proved the model to be a useful predictor of spore transport over distances that could account for the between-field transport of spores (Chapter 5).

Nonetheless, the quasi-Gaussian approach does have its limitations. The Lagrangian diffusion model is a solution of the diffusion equation that is formulated in terms of gradient transport theory, and surface layer similarity theory. Gradient transport theory becomes questionable in highly convective conditions when turbulent motions of air can transport material up or down irrespective of mean concentration gradients. In addition, surface layer similarity theories of diffusion should only be applied to near-surface releases and relatively short travel times so that the plume remains in the surface layer. This essentially means that the model is best suited to simulation of (early morning) dispersal of *P. infestans* spores between neighboring fields. This was not considered to be problematic, as most *P. infestans* sporangia are released at the first humidity drop in the early hours of the day (e.g., Nielsen et al., 2007), and most are deposited relatively close to the inoculum source (Fry and Mizubuti, 1998).

Overall, the predictive accuracy of the quasi-Gaussian approach was shown to exceed that of a previously published Gaussian diffusion model for transport of

P. infestans sporangia (Spijkerboer et al., 2002). Moreover, the model is not limited to *P. infestans* dispersal and is easily adapted for other pathosystems, e.g., via adjustment of the settling speed of particles, and the effect of canopy structure on wind profiles.

Supplementary spatial component for decision support systems

In Chapter 6 the quasi-Gaussian model was further developed into an integrated model of the aerial component of the disease cycle, and used to enhance knowledge of the regional epidemiology of the disease, and exploit that knowledge for improved late blight management. Additional submodels describing spore release from sporangiophores, spore escape from the canopy, and spore survival during transportation were added. These submodels were all single, descriptive equations that were designed to maintain transparency of results, and preserve the attractiveness of the integrated model to practitioners. Both the spore escape (de Jong et al., 2002) and spore survival (Mizubuti et al., 2000) submodels have been tested against experimental data.

The integrated aerobiological model was packaged as an “add-on” (supplementary) spatial component for existing non-spatial decision support systems (DSSs). It uses weather forecast data as input, and works by (potentially) modifying the spray recommendations of the DSS according to a quantification of the risk of infection from distant sources of inoculum (distance-weighted infection pressure). A field trial in the Netherlands in 2007 provided an initial proof of the concept, as the system was successful in further rationalizing the spray recommendations of a DSS.

There are weaknesses in the approach, however, and further refinement of the suite of models and the risk algorithm could improve the performance of the system. In particular, it is possible that the predictive accuracy of the system could be improved through incorporation of a more advanced dispersion model. On the counter-side, this could increase the complexity (and run-time) of the system, which may serve to decrease its attractiveness to practitioners. Already, running this integrated DSS including the spatial add-on is a complicated task as it entails the use of weather forecasts made with the MM5 meso-scale weather model. It is also likely that the risk algorithm could be improved through the incorporation of empirically determined cultivar specific action threshold values (for yes-or-no spray decisions). Currently, the system uses an arbitrarily chosen threshold value that was derived through simulation studies with historical weather data and parameters describing three potato cultivars. Field trials are planned in future growing seasons to test the

consequences of different variety specific thresholds, and to test the system using a wider range of non-spatial DSSs. This should provide a much more rigorous evaluation of the concept.

Nevertheless, the models and approaches used were deemed to be suitable for an initial proof of the concept. Notably, this represents a new application for the Lagrangian diffusion model, indeed for any atmospheric dispersion model, as existing DSSs for aerially transmitted plant pathogens do not utilize atmospheric dispersion models in the generation of their day-to-day spray advice. Furthermore, this approach is not limited to potato late blight and the method developed here could prove to be useful in a decision context for many other pathosystems.

Multi-scale epidemic simulator

The original intention in Chapter 7 was to integrate all the aforementioned models to produce a multi-scale epidemic simulator. Early on in the integration process, however, it became clear that serious steps would have to be taken to reduce the execution time of the model. It simply wasn't possible to use a numerical dispersion model to simulate dispersal to and from every plant in a suitably sized landscape, over the course of a growing season. Three main steps were taken to solve this problem: (i) the numerical quasi-Gaussian plume model was replaced by a fully analytical Gaussian plume dispersion and deposition model (Overcamp, 1976); (ii) the spatial resolution of simulated landscapes was decreased from individual plants to 100 x 100 m potato areas (grid cells); and (iii) dispersal to and from individual grid cells was conducted using spatial convolutions.

The first point required validation of the new dispersion and deposition model. The same spore dispersal data were used as for the quasi-Gaussian plume model in Chapter 5. Although numerical predictions were not as accurate as for the numerical model, the predictive accuracy was sufficient for the task at hand, i.e., to increase understanding of the regional dynamics of the disease, as opposed to precise epidemic prediction.

Decreasing the spatial resolution of simulated landscapes required some changes to the potato late blight model. Spore dispersal between plants obviously had to be dropped from the model. As the primary interest was inoculum exchange between fields, this was of little consequence. As an alternative to between-plant dispersal, autodeposition within the same (source) grid cell (100 x 100 m) was calculated as the difference between the number of spores that were released from sporangiophores and the number that escaped the canopy, multiplied by the percentage ground cover.

Furthermore, the coarser spatial resolution meant that the geometry of genotype mixture elements could not be simulated. Instead, region-wide homogenous (random) genotype mixtures were approximated by weighting the values of variety specific resistance components with the proportion of that variety in the landscape. The validity of this assumption was checked by comparing final disease levels in a 1 ha mixture against those produced in a similar homogenous mixture composed of individual plants (using the applied version of the model, without spore dispersal between plants). Although there was not a perfect correspondence, the temporal increase in disease produced by the two approaches was fairly close (*unpublished data*).

The final step taken to improve the speed of the model involved the use of fast Fourier transforms (FFTs) to perform convolutions between the output of the atmospheric dispersion and survival models and spatial distributions of inoculum sources. Spatial distributions were always padded with zeros prior to convolution to prevent wrap-around of spores, i.e., to facilitate spore loss outwith the boundaries of simulated landscapes. Application of this technique greatly enhanced the speed of the model. Without this approach, model execution times would have been too long to simulate epidemics with an atmospheric dispersion model (even a fully analytical one) over such large spatial and temporal scales.

Another point of interest in Chapter 7 concerns the methods used to interpret simulation results. Functional connectedness between host areas was quantified using a new parameter; pathogenic connectivity, q_p (-). This parameter calculates the overall probability that spores produced somewhere in the landscape will deposit successfully and germinate. It therefore quantifies landscape connectivity from a physical dispersal, topographical and biological infection perspective. Included in q_p are cultivar-isolate specific resistance components for spore production and infection efficiency, and a dispersal kernel that was produced using an integrated aerobiological model of the aerial component of the disease cycle. This parameter proved to be useful in interpreting complex simulation results. It can easily be adapted for any number of alternative pathosystems through incorporation of relevant pathogenic parameters and dispersal kernels. In a similar vein, it can easily be adapted for use in other ecological applications, for example in assessing viable pollen connectivity for gene flow applications, or even particulate connectivity in pollution studies.

It is worthwhile to reflect on the validation status of the multi-scale simulator. Although the potato late blight model and the atmospheric dispersion model were

individually validated (Chapters 3 and 7, respectively), and the spore escape and spore survival models have previously been tested against experimental data, it is unfortunate that suitable data were not available for validation of this framework as an integrated process model. Collection of empirical data over such large temporal and spatial scales would be extremely problematic, if not impossible. It is possible, however, that a spatially referenced database of inoculum sources of the type maintained by some DSS providers could be used for model evaluation. With such data it may be possible to reconstruct or reverse engineer the invasion history of a potato late blight epidemic on a field by field basis. It is highly unlikely that such data would be detailed (or complete) enough to facilitate a formal validation of this complex model, but a qualitative assessment of predicted invasion patterns could be realized.

Simulation of fungicide management is an unresolved issue in the model. As discussed previously, the submodel for protectant fungicides was parameterized using expert judgment. Early on in the development of the multi-scale simulator, it was found that epidemics quickly spanned the entire extent of simulated landscapes. This was not a realistic outcome. This led to the simulation of eradicant fungicide treatments; an added level of (operational) realism that was found to be important in producing realistic regional epidemic dynamics. Unfortunately, this again led to “guesstimation” of fungicide parameters as the literature proffered nothing of use. Clearly, for simulation purposes, there is a need for empirical data regarding the precise quantitative effects of fungicides on potato late blight disease cycle processes.

To conclude, the major strong point of the multi-scale epidemic simulator is its ability to simulate interactions between pathogen, host genotype, crop diversity, the spatial characteristics of landscapes, management, and the environment. The scope of this model is accordingly large and it is suited to the investigation of many ecological and epidemiological problems. For example, the model could be used to investigate the potential role of spore trap networks in disease risk warnings, and optimize their placement at landscape level. Furthermore, the results of the perturbation analysis show that emerging model trends are robust to order of magnitude changes in local epidemic rate. This suggests that conclusions from this study could hold for other diseases, as long as they have similar mechanisms for regional spread.

Implications for management

There is no single, simple solution to the global late blight problem in sight. Host resistance is almost unanimously viewed as the most cost-effective and eco-friendly form of management, but unfortunately breeding programs have not been able to markedly increase the level of resistance of commercially grown potato varieties. It is hoped that genetic engineering technologies will yield improved variants of currently used varieties that show far greater levels of resistance, but this is still a work in progress. Potato production today is therefore heavily reliant on the use of fungicides as a control strategy. Fungicides can provide effective protection, but their applicability can be compromised by adverse environmental effects and by the emergence of resistant pathogen strains. This strategy is not only expensive, it is inconsistent with worldwide efforts to reduce the environmental impact of food production systems. This unsustainable situation has been further exacerbated by recent migrations of the pathogen. Both the A1 and A2 mating types now have a global distribution on potato, leading to an increase in the diversity, virulence, and aggressiveness of pathogen populations around the world.

The sensible short-, medium- and perhaps long-term approach to the potato late blight problem is to continue to develop and improve integrated late blight management strategies. Integrated management of potato late blight is an amalgamation of techniques designed to improve the level of disease control and maintain the quality of the environment. The results presented in this thesis illustrate how a framework for quantifying spatio-temporal epidemic dynamics can contribute to integrated management strategies.

The supplementary spatial component for DSSs emerges as a potentially viable option for improving disease risk warnings for potato late blight, and reducing the environmental impact of potato production. It provides a quantification of the risk of viable spore transport without the need for a database containing spatially-referenced source and target crop information. It therefore represents a low-cost method for inclusion of aerobiological prediction in existing DSS. It utilizes the location-specific weather forecast data that many DSS providers already pay for and include in their systems. As it provides a more detailed treatment of that data, without any other significant running costs, it represents a cost-effective way to improve the performance of existing DSS. The supplementary spatial component can also be used to generate maps of predicted spore plumes, which provide a simplistic yet striking portrayal of infection risk in any locale. Such images could make decision

support results easier to understand for system subscribers, and perhaps compound the need for the system in non-subscribers. Improvements in system performance, cost-effectiveness and usability could help to achieve a more widespread adoption of DSS technology.

The results of this thesis also demonstrate that landscapes could be designed to minimize the rate of invasion of resistant breaking pathogen strains. Landscape design and genotype mixing strategies therefore emerge as a means to avert crop loss and minimize the consequences of a breakthrough in resistance. Suppression of pathogen invasion rates could also create a window of opportunity to implement appropriate control action. Secondary effects could include an increase in the performance and durability of host resistance through a reduction in the size of the pathogen's "genetic neighborhood." This in turn could lead to a reduction in the need for chemical inputs.

These two different strategies (improved disease prediction and landscape design) could be viewed as opposing flanks in a "pincer movement" on late blight. Alternatively, they can be used to complement each other, resulting in a "full frontal attack." This idea is developed further in the following section.

A strategy for more effective and eco-friendly potato late blight management

A dynamic approach towards spatial resistance deployment and epidemiological prediction could provide synergism in management outcomes:

Prevention

Potato late blight is a difficult disease to escape in space, but the results of this thesis show that landscapes can be designed to suppress spatial increase of disease. Region-wide deployment of genotype mixtures emerges as a spatial resistance deployment strategy that has a profound effect in suppressing regional epidemic dynamics, regardless of the other spatial characteristics of the landscape. This is a relatively pragmatic strategy as growers can continue to plant crops in locations that are optimal for growth, and are well supported by production chain infrastructure.

Protection

Use of plant protection products can be optimized through the use of spatial DSSs that target fungicide sprays to moment of genuine risk of viable spore influx. Risk can be determined using a standard DSS to predict development of disease *in planta*, and the supplementary spatial component to determine the risk of viable spore transport

over relevant distances. Knowledge of the potato varieties deployed in the mixtures could be incorporated in the supplementary spatial component, facilitating a quantification of the influx component of infection risk for specific mixture compositions, and a final determination of the need for protectant sprays.

Monitoring

Phytophthora populations and resistance performance could be monitored frequently throughout the growing season, and any instances of resistance breakthrough reported. This information could be used to update the spatial risk factors of the supplementary spatial component for DSSs on a continuous basis. This information may also be used to make recommendations on suitable mixture components for the following growing season. In this way directional selection in pathogen populations could be disrupted by temporal rotation of potato varieties, or by spatial rotation to different production areas.

Conclusions and perspective

The goal of this thesis was to enhance understanding of the spatial dimension of potato late blight epidemiology, and explore new options for local and regional management of the disease. This goal was achieved through a combination of epidemiological and aerobiological modeling. Explanatory models of pathosystem processes were developed, validated, integrated and manipulated to derive information about the spatial epidemiology of the disease that would be otherwise difficult to measure. This led to the development of two tools for management. An aerobiological model of the aerial component of the disease cycle was combined with an existing DSS to develop and test a novel concept for inclusion of regional aerobiological modeling in disease risk warning forecasts. This new system was able to reduce the use of plant protection products and provide adequate control in a field trial. It seems likely that DSSs will play an increasingly important global role to rationalize biocide usage in a more technologically based agriculture, therefore this thesis could contribute towards the development of a new generation of DSSs for aerially transmitted plant pathogens. The second management tool developed in this thesis was a comprehensive, multi-scale model of the potato late blight pathosystem. This tool was used to test various landscape designs and genotype mixing strategies for their ability to suppress regional potato late blight epidemics. Such spatially

informed strategies could serve to minimize the consequences of a breakthrough of host resistance, improve the durability of resistance resources, and further reduce the need for chemical applications. With the anticipated advent of widespread deployment of genetically engineered potato varieties, opportunities exist to use this tool to optimize strategies for proper landscape-scale deployment of engineered resistance. Collectively, the results of this thesis contribute towards the development of more effective and eco-friendly integrated late blight management strategies.

References

- Andrison, D., Lucas, J.M., and Ellisseche, D. 2003. Development of natural late blight epidemics in pure and mixed plots of potato cultivars with different levels of partial resistance. *Plant Pathology* 52:586-594.
- Chamberlain, A.C. 1953. Aspects of travel and deposition of aerosol and vapor clouds. Report No. A.E.R.E HP/R1261. Her Majesty's Stationery Office, London.
- de Jong, M., Bourdôt, G.W., Powell, J., and Goudriaan, J. 2002. A model of the escape of *Sclerotinia sclerotiorum* ascospores from pasture. *Ecol. Model.* 150:83-105.
- Fry, W.E., and Mizubuti, E.S. 1998. Potato late blight. In: Jones, D.G. (Ed), *The Epidemiology of Plant Disease*. Luwer Publishers, Dordrecht, Netherlands, pp. 371-388.
- Garrett, K.A., and Mundt, C.C. 2000. Host diversity can reduce potato late blight severity for focal and general patterns of primary inoculum. *Phytopathology* 90:1307-1312.
- Garrett, K.A., Nelson, R.J., Mundt, C.C., Chacon, G., Jaramillo, R.E., and Forbes, G.A. 2001. The effects of host diversity and other management components on epidemics of potato late blight in the humid highland tropics. *Phytopathology* 91:993-1000.
- Gryning, S.E., van Ulden, A.P., and Larsen, S.E. 1983. Dispersion from a continuous ground-level source investigated by a *K* model. *Q. J. Roy. Meteor. Soc.* 109:355-364.
- Keyfitz, N. 1985. *Applied Mathematical Demography*, 2nd Edition. Springer Verlag, New York, 441 pp.
- Kot, M., Lewis, M.A., and van den Driessche, P. 1996. Dispersal data and the spread of invading organisms. *Ecology* 77:2027-2042.
- Mizubuti, E.S.G., Aylor, D.E., and Fry, W.E. 2000. Survival of *Phytophthora infestans* sporangia exposed to solar radiation. *Phytopathology* 90:78-84.
- Mundt, C.C., and Browning, J.A. 1985. Development of crown rust epidemics in genetically diverse oat populations: effect of genotype unit area. *Phytopathology* 75:607-610
- Mundt, C.C., and Leonard, K.J. 1985. Effect of host genotype unit area on epidemic development of crown rust following focal and general inoculations of mixtures of resistant and susceptible oat plants. *Phytopathology* 75:1141-1145.

- Mundt, C.C., and Leonard, K.J. 1986. Analysis of factors affecting disease increase and spread in mixtures of resistant and susceptible plants in computer-simulated epidemics. *Phytopathology* 76:832-840
- Mundt, C.C., and Leonard, K.J. 1986. Effect of host genotype unit area on development of focal epidemics of bean rust and common maize rust in mixtures of resistant and susceptible plants. *Phytopathology* 76:895-900.
- Mundt, C.C., Leonard, K.J., Thal, W. M., and Fulton, J. H. 1986. Computerized simulation of crown rust epidemics in mixtures of resistant and susceptible oat plants with different genotype unit areas and spatial distributions of initial disease. *Phytopathology* 76:590-598.
- Nielsen, B.J., Hansen, J.G., Pinnschmidt, H., Narstad, R., Hermansen, A., Le, V.H., and Hannukkala, A. 2007. Studies of release and infectivity of *Phytophthora infestans* sporangia under field conditions. In: Schepers, H.T.A.M. (Ed.), Proceedings of the tenth workshop of an European network for development of an integrated control strategy of potato late blight, Bolgna, Italy. PAV Special Report no. 12:211-220.
- Overcamp, T.J. 1976. A general Gaussian diffusion-deposition model for elevated point sources. *J. Appl. Meteorol.* 15:1167-1171.
- Rotem, J., Cohen, Y., and Putter, J. 1970. Relativity of limiting and optimum inoculum loads, wetting durations, and temperatures for infection by *Phytophthora infestans*. *Phytopathology* 61:275-278.
- Spijkerboer, H.P., Beniers, J.E., Jaspers, D., Schouten, H.J., Goudriaan, J., Rabbinge, R., and van der Werf, W. 2002. Ability of the Gaussian plume model to predict and describe spore dispersal over a potato crop. *Ecol. Model.* 155:1-18.
- Van den Bosch, F., Frinking, H.D., Metz, J.A.J., and Zadoks, J.C. 1988a. Focus expansion in plant disease. III. Two experimental examples. *Phytopathology* 78:919-25.
- Van den Bosch, F., Verhaar, M.A., Buiel, A.A.M., Hoogkamer, W., and Zadoks, J.C. 1990. Focus expansion in plant disease. IV. Expansion rates in mixtures of resistant and susceptible hosts. *Phytopathology* 80:598-602.
- Van den Bosch, F., Zadoks, J.C., and Metz, J.A.J. 1988b. Focus expansion in plant disease. I. The constant rate of focus expansion. *Phytopathology* 78:54-8.
- Van den Bosch, F., Zadoks, J.C., and Metz, J.A.J. 1988c. Focus expansion in plant disease. II. Realistic parameter sparse models. *Phytopathology* 78:59-64.
- van Ulden, A.P. 1978. Simple estimates for vertical diffusion from sources near the ground. *Atmos. Environ.* 12:2119-2124.
- Waggoner, P.E. 1952. Distribution of potato late blight around inoculum sources. *Phytopathology* 42:323-328.
- Zwankhuizen, M.J., and Zadoks, J.C. 2002. *Phytophthora infestans's* 10-year truce with Holland: a long-term analysis of potato late-blight epidemics in the Netherlands. *Plant Pathology* 51:413-423.

Summary

Chapter 1

Phytophthora infestans, causal agent of potato late blight, is a highly aggressive plant pathogen that can decimate a potato crop in a matter of days. It is found in almost every corner of the globe, literally wherever potatoes are grown. *P. infestans* has two mating types (A1 and A2), and in recent years, upon the spread of the A2 mating type across the globe, the pathogen has developed sexually recombining populations in areas where it was previously reproducing asexually. As a result, there has been a dramatic increase in the genotypic diversity and aggressiveness of the pathogen in many areas, including Europe. There is no single solution to the late blight problem. Fungicides provide effective protection but their applicability can be compromised by adverse environmental effects and by the emergence of resistant pathogen strains. Genetic engineering of host resistance offers hope, but even that may not be a panacea. *P. infestans* has a large capacity for long-distance dispersal, and thus a large capacity for gene and genotype flow. A large “genetic neighborhood” also increases the probability that virulent mutations will be present, that recombination will occur, and that diversity will be maintained. This means that breakthrough of engineered resistance could simply be a matter of time. The best short-, medium-, and perhaps long-term solutions are to continue to develop and improve integrated late blight management strategies. The spatial dimension of potato late blight epidemiology, although widely recognized, has scarcely been incorporated into integrated management strategies. This is because spatial increase of potato late blight disease is the product of a complex interplay between host, pathogen, management, environment, and the spatial characteristics of crops and landscapes. As a result, the theoretical framework for the spatial dimension of this disease is underdeveloped and spatial data on disease occurrence are hard to obtain and seldom complete. This thesis describes experimental and simulation work aimed at enhancing our understanding of the spatial dimension of potato late blight epidemiology. The primary objective is to enhance understanding, with the ultimate objective of contributing towards the development of effective and eco-friendly late blight management strategies.

Chapter 2

One of several crop diversification strategies to limit spatial increase of disease is to grow mixtures of plants that differ in their resistance to the pathogen. Empirical

results show some variation in the success of genotype mixtures for control of potato late blight in different agro-ecosystems. This prompted a need for a detailed theoretical analysis of the influence of crop diversity on epidemic development. A spatio-temporal model of the potato late blight pathosystem was developed and utilized to study the effect of different scales and patterns of host genotypes on the development of general and focal potato late blight epidemics. The model combines individual based modeling with an integrodifference equation approach and epidemiological compartment modeling. Spore dispersal is provided by several different statistical contact distributions. A new analytical expression for the apparent infection rate of general epidemics is described. Also described is a new functional connectivity parameter. Both parameters were useful as predictors of epidemic progress. The relationship between the apparent infection rate and the radial velocity of focus expansion in focal epidemics was linear in accordance with epidemiological theory for homogeneous genotype mixtures. The findings indicate that the spatial arrangement of the host population impacts the development of general epidemics and the spread of focal epidemics by a common mechanism: spore loss on resistant plants. Genotype mixtures that are effective in reducing focal epidemics of *P. infestans* through this mechanism will likewise curtail general epidemics, and *vice versa*.

Chapter 3

In order to use the potato late blight model to investigate new strategies for local and regional management of late blight, it was necessary to extend the model from the theoretical domain to applied infectious disease modeling. It also became necessary to evaluate the quality of model predictions. The strong influence of weather on potato late blight required that environment-pathogen interactions were added. These were based on published epidemiological data. Cultivar-isolate specific interactions were characterized in the model using three quantitative components of resistance: infection efficiency, lesion growth rate, and sporulation intensity. These were measured on detached potato leaflets in the laboratory. A combination of five potato cultivars and two *P. infestans* isolates were used. A sensitivity analysis was conducted in order to illuminate the effects of these parameters, and others, on epidemic progress. A sensitivity analysis of the model resulted in a heuristic for distinguishing epidemics driven by lesion expansion from those driven by lesion propagation. Epidemics driven entirely by lesion expansion had a smooth very gradual s-shaped disease progress curve, whereas epidemics driven by lesion

propagation without lesion expansion were characterized by long lag times followed by a sudden disease explosion. The spatial component of the model produced focal expansion rates that compared well with published experimental data. Validation data for the temporal model came from 20 late blight epidemics observed in field trials conducted in the Netherlands in 2002 and 2004. Temporal model predictions were in close agreement with observational data, confirming the utility of the model as a tool in the analysis and diagnosis of epidemics.

Chapter 4

The relationship between arriving (primary) inoculum and crop damage is an essential component of the spatial epidemiology of potato late blight that is missing from the literature. Such knowledge could guide efforts to quantify the influx component of infection risk for improved epidemic prediction. The potato late blight model was coupled to submodels for crop growth, tuber dry matter production and fungicide efficacy. The yield response of a range of management scenarios to a single influx of primary inoculum was then calculated under different practically relevant scenarios for varieties, fungicide regime and disease initiation. The scenarios considered extremes of host resistance/susceptibility and maturity type, four fungicide management regimes, and two different spatial distributions of initial spore load. Simulation results were used to classify the various management scenarios as either sensitive to incoming inoculum or tolerant to incoming inoculum. General epidemics, resulting from spatially homogeneous initial spore loads, responded more strongly to initial spore load than focal epidemics, resulting from an initial spot infection. Susceptible varieties responded with sizeable yield losses even at low levels of initial spore load, regardless of the fungicide management regime used. These results indicate that for susceptible varieties (late varieties in particular) the degree of accuracy that would be required in dispersal information for appropriate decision making is unlikely to be practically attainable. In contrast, for resistant varieties, a greater degree of uncertainty in dispersal information could be tolerated, and there exists scope for the inclusion of dispersal information in epidemiological prediction and decision making.

Chapter 5

One of the challenges of modern decision support for plant health is to provide predictions of the influx of viable pathogen inoculum from sources outside a crop. A hybrid dispersion model was developed, combining Taylor's statistical theory of

diffusion for horizontal dispersal with eddy diffusion theory for vertical dispersal. A source depletion method was added for spore deposition. The model was validated using experimental data for the dispersal of *Lycopodium clavatum* spores over a potato canopy. Numerical predictions were in close agreement with experimental data, confirming the utility of this model as a tool for decision support.

Chapter 6

A novel approach for inclusion of regional spatial risk factors in operational disease risk warnings against potato late blight was developed and tested. The hybrid spore dispersion model was embellished with models describing spore release from sporangiophores, spore escape from the canopy, and spore survival during transportation. This suite of aerobiological models was used as a supplementary spatial component for an existing non-spatial DSS. The central premise was that fungicide applications could be reduced by omitting sprays on days when atmospheric conditions are unsuitable for the transport of viable inoculum over distance. The DSS first makes a spray recommendation according to the risk of disease development *in planta*. A risk algorithm assesses the capacity at any day for viable spore transport over distance, in comparison to a frequency distribution of this capacity over 10 years of historic weather data. If the risk is large the original spray advice is followed, otherwise a no-spray advice is given. The concept was tested in a field experiment with three potato cultivars in 2007. The spatial supplementary component was combined with the published DSS SIMCAST. The MM5 weather forecast model was used to provide input data for aerobiological prediction. System performance was compared to a stand-alone version of SIMCAST. A total of two fungicide applications were negated by the spatial supplementary component; representing one third of recommended sprays in a period of normal disease pressure. The same high level of disease control as with SIMCAST alone was achieved. These fungicide savings came on top of a reduced resistance level dependent dose rate of Shirlan (a.i. Fluazinam). These results provide an initial proof of concept, but further field trials are required to refine and test the method before it can be used in practice. This approach is not limited to potato late blight and the method developed here could prove to be useful in a decision context for many other pathosystems.

Chapter 7

Proper spatial deployment of disease resistant genotypes of agricultural crop species could make those crops less vulnerable to invasion by resistance breaking genotypes.

To enable model studies at a landscape-scale, a fully analytical Gaussian plume dispersal and deposition model was developed. This model was validated using experimental spore dispersal data and combined with the field-scale potato late blight model, a suite of aerobiological models (spore release, escape and survival), and a landscape generator. The resultant multi-scale simulator of the potato late blight pathosystem was used to investigate a number of pragmatic spatial strategies for deployment of host resistance. Simulation results showed that the spatial extent of epidemics is most affected by manipulation of the number of potato genotypes in the landscape, followed by manipulation of the amount of potato, the level of clustering of fields, and the size of individual fields. Region wide deployment of genotype mixtures had a large effect on epidemic extent regardless of other landscape characteristics. It was difficult to create potato free zones large enough to provide effective levels of resilience to disease invasion. Fine-scale spatial and genotypic fragmentation of host populations was therefore a more appropriate strategy.

Chapter 8

A summary of the main epidemiological insights is followed by a detailed review of the various models and modeling approaches developed and used in the thesis. The results of chapters 2-7 are then integrated and discussed with respect to late blight management. Spatial decision support emerges as a strategy to improve late blight control and reduce the environmental impact of potato production. The supplementary spatial component for decision support offers a way to improve the performance, cost-effectiveness and usability of DSSs. It can therefore help to achieve a more widespread use of DSS technology. Spatial resistance deployment strategies can be used to improve late blight control and minimize the consequences of a breakthrough in host resistance. Secondary effects could include an increase in the performance and durability of host resistance, and a reduction in the use of plant protection products. If the two approaches are combined within a framework of monitoring of resistance performance and pathogen population structures, a powerful dynamic spatial strategy for late blight management could be realized.

Samenvatting

Ruimtelijke modellering van epidemieën van de aardappelziekte

Phytophthora infestans, de veroorzaker van de aardappelziekte, is een agressief plantenpathogeen dat een aardappelgewas in enkele dagen kan verwoesten. Het pathogeen wordt wereldwijd, waar aardappels worden verbouwd, aangetroffen. *P. infestans* beschikt over twee “mating types” en sinds de wereldwijde introductie van het zogenaamde A2 mating type worden wereldwijd seksueel recombinerende populaties aangetroffen. Hierdoor is er in veel gebieden een enorme toename van de genetische diversiteit en agressiviteit van het pathogeen. Dit geldt ook voor Europa.

Er is geen eenvoudige oplossing voor de aardappelziekte. Fungiciden bieden effectieve bescherming, maar de toepassing hiervan heeft nadelige milieueffecten en kan het ontstaan van resistente genotypen van het pathogeen bevorderen. Genetische modificatie biedt perspectief voor ontwikkeling van waardplantresistentie, maar ook deze methode heeft nadelen. *Phytophthora* heeft een groot vermogen tot lange-afstands verspreiding, en daardoor voor “gene flow”. Een grote genetische variatie verhoogt ook de kans dat er virulente genotypen aanwezig zijn, dat er recombinatie zal optreden en dat diversiteit (in het pathogeen) gehandhaafd blijft of zelfs vergroot wordt. Daardoor zou doorbreking van resistentie in de aardappel slechts een kwestie van tijd zijn. De beste oplossing op de korte, midden en misschien ook lange termijn is daarom te blijven werken aan de ontwikkeling en verbetering van geïntegreerde strategieën voor ziektebeheersing.

De ruimtelijke dimensie van de epidemiologie van de aardappelziekte wordt breed onderkend, maar deze speelt nauwelijks of geen rol van betekenis in de huidige geïntegreerde beheersingsstrategieën. Dit komt doordat de ruimtelijke uitbreiding van de aardappelziekte het resultaat is van een complexe interactie tussen de waardplant, de ziekteverwekker, het gewasmanagement, de omgeving en de ruimtelijke kenmerken van gewassen en landschappen. Bovendien zijn ruimtelijke gegevens over het voorkomen van bronnen moeilijk te verkrijgen en zelden compleet. Het theoretische raamwerk voor de ruimtelijke dimensie van deze ziekte is onderontwikkeld.

Dit proefschrift beschrijft experimenteel en modelmatig werk dat erop gericht is het inzicht in de ruimtelijke aspecten van de epidemiologie van de aardappelziekte te vergroten en toe te passen. De lange termijn ambitie is om een bijdrage te leveren

aan de ontwikkeling van effectieve en milieuvriendelijke strategieën voor de beheersing van aardappelziekte.

Hoofdstuk 2

Een van de manieren waarop ruimtelijke diversificatie kan worden ingezet voor vermindering van ruimtelijke ziekteuitbreiding is de teelt van mengsels van rassen die verschillen in de genetische basis van resistentie. Empirische gegevens laten variatie zien in het effect van rassenmengsels op de aardappelziekte in verschillende agro-ecosystemen. Daarom is het onderzoek gestart met een theoretische analyse van het effect van gewasdiversiteit op de ontwikkeling van een epidemie. Er werd een spatiotemporeel model ontwikkeld voor het pathosysteem aardappel-*Phytophthora*. Met dit model werd onderzocht hoe menging van rassen in verschillende patronen en op verschillende schalen epidemieën van aardappelziekte beïnvloedt. De modelaanpak behelst een combinatie van individu-gebaseerd modelleren, integrodifferentievergelijkingen en modellering op basis van compartimenten. Verspreiding van sporen wordt in dit hoofdstuk gemodelleerd met behulp van statistische contactverdelingen. Er wordt een nieuwe analytische formule beschreven voor berekening van de relatieve groeisnelheid 'r' van een algemene epidemie, d.w.z. een epidemie die zich ruimtelijk (min of meer) homogeen in een perceel ontwikkelt. Bovendien wordt een nieuwe parameter beschreven die de mate van ruimtelijke verbinding voor *P. infestans* sporen tussen individuen van de waard karakteriseert. Beide parameters werden gebruikt om de voortgang van epidemieën te voorspellen. Er bleek een lineaire relatie te bestaan tussen de relatieve groeisnelheid van een algemene epidemie (r) en de ruimtelijke uitbreidingssnelheid van een focale, d.w.z. haardvormige, epidemie (c), zoals verwacht werd op basis van de wiskundige theorie van epidemieën in "ideale" mengsels. De resultaten geven aan dat de ruimtelijke structuur van de waardpopulatie de ontwikkeling van algemene en focale epidemieën beïnvloedt via hetzelfde mechanisme: verlies van sporen op resistente planten. Mengsels van genotypen die effectief zijn in het reduceren van focale epidemieën van *Phytophthora* remmen ook algemene epidemieën, en *vice versa*.

Hoofdstuk 3

Om nieuwe strategieën voor lokale en regionale ziektebeheersing te ontwikkelen, moest het model van een theoretisch instrument verder ontwikkeld worden tot een hulpmiddel voor het doen van praktische ziektevoorspellingen. De kwaliteit van de voorspellingen werd daartoe geëvalueerd met empirische gegevens. Omdat bekend

is dat de verspreiding van *Phytophthora* sterk door het weer wordt beïnvloed, werden weersinvloeden opgenomen in het model. Hiervoor werden literatuurgegevens over klimaatrelaties gebruikt. Cultivar-specifieke eigenschappen van *Phytophthora* isolaten werden gekarakteriseerd met drie kwantitatieve resistentiecomponenten: infectie-efficiëntie, lesiegroeisnelheid, en sporulatie-intensiteit. Deze werden gemeten op afgeknipte blaadjes in de klimaatkamer. Er werd een combinatie van twee isolaten en vijf aardappelrassen gebruikt. Een gevoeligheidsanalyse werd uitgevoerd om de effecten van deze en andere parameters op de voortgang van epidemieën te belichten. Deze analyse resulteerde in een heuristisch waarmee epidemieën die worden gedreven door lesie-expansie worden onderscheiden van epidemieën die worden gedreven door vermeerdering van het aantal lesies. Epidemieën die worden gedreven door lesie-expansie hebben een korte “lag period” gevolgd door een geleidelijke toename terwijl epidemieën die gedreven worden door vermeerdering van het aantal lesies een lange “lag period” hebben, gedurende welke men nagenoeg geen ziekteontwikkeling kan waarnemen, gevolgd door een plotselinge explosie van aantasting. Het model resulteerde in ruimtelijke uitbreidingsnelheden die goed overeen kwamen met gepubliceerde gegevens. Voor verdere validatie van het model werden gegevens gebruikt van 20 epidemieën die in 2002 en 2004 in veldproeven in Nederland werden vastgelegd. De temporele modelvoorspellingen waren in goede overeenstemming met de waarnemingen en bevestigen de bruikbaarheid van het model als een hulpmiddel voor de analyse en diagnose van echte epidemieën.

Hoofdstuk 4

De relatie tussen de hoeveelheid primair inoculum en opbrengstverlies als gevolg van dit inoculum is een essentiële component van de ruimtelijke epidemiologie van *Phytophthora*. Kennis hierover zou gebruikt kunnen worden om de mate van risico van een bepaalde influx van inoculum te schatten in het kader van beslissingsondersteuning. Het aardappelziektemodel werd gekoppeld met submodellen voor gewasgroei, droge stofproductie en fungicideneffectiviteit. Het effect van één enkele influx van primair inoculum op de aardappelopbrengst werd gekwantificeerd onder diverse scenario's die voor de praktijk relevant zijn. Deze scenario's hadden betrekking op extremen van waardplantresistentie of vatbaarheid, de vroegheid van het gewas, vier verschillende fungicidenregimes, en een focaal of perceelsgewijs verloop van de epidemie. Bij een focaal verloop verspreidt een aantasting zich vanuit één punt in een perceel. Bij een algemene epidemie, raakt in

het begin het hele perceel besmet, en neemt de ziekte over het hele perceel in de tijd toe. De simulatieresultaten werden gebruikt om de scenario's te classificeren als gevoelig of tolerant ten aanzien van inkomend inoculum. Algemene epidemieën reageerden sterker op de initiële sporendruk dan focale epidemieën. Vatbare aardappelrassen leden grote opbrengstverliezen onder elk van de getoetste fungicidenregimes, zelfs bij lage initiële sporendruk. Deze resultaten geven aan dat bijzonder nauwkeurige voorspellingen van sporendruk nodig zijn om deze te kunnen gebruiken in beslissingsondersteuning voor vatbare variëteiten. Dit geldt in het bijzonder voor late rassen omdat epidemieën in deze gewassen langer de tijd hebben zich te ontwikkelen. Nauwkeurige voorspellingen van sporendruk zijn echter in de praktijk waarschijnlijk niet haalbaar. Voor resistente variëteiten kon echter een grotere mate van voorspelonderzekerheid worden getolereerd. Er is daarom vooral voor resistente rassen potentieel voor het gebruik van informatie over sporenverspreiding in beslissingsondersteuning.

Hoofdstuk 5

Een van de uitdagingen in moderne beslissingsondersteuning voor gewasbescherming is het doen van voorspellingen over sporeninflux van bronnen buiten een gewas. Hiervoor werd een hybride atmosferisch verspreidingsmodel ontwikkeld. In dit model werd statistische diffusietheorie voor horizontale dispersie gecombineerd met een eddy-diffusie theorie voor verticale dispersie. Tevens werd een bron-depletiemodel toegevoegd voor de depositie van sporen. Het nieuwe verspreidingsmodel werd gevalideerd met experimentele meetgegevens over de dispersie van sporen van *Lycopodium clavatum* boven een aardappelgewas. De numerieke voorspellingen waren in goede overeenstemming met de experimentele gegevens, waardoor dit model gebruikt kan worden als component voor beslissingsondersteuning.

Hoofdstuk 6

In Hoofdstuk 6 wordt een benadering ontwikkeld en getoetst om influx van sporangia op regio niveau in te bouwen in operationele spuitadviezen voor beheersing van de aardappelziekte. Het hybride sporenverspreidingsmodel werd uitgebreid met modellen voor het vrijkomen van sporen van de sporendragers, voor ontsnapping van sporen uit het brongewas, en overleving van sporen tijdens transport in de atmosfeer. Deze combinatie van aerobiologische modellen werd als een extra module toegevoegd aan een bestaand niet-ruimtelijk beslissingsondersteunend

systeem. De centrale premisse was dat bespuitingen met fungiciden achterwege zouden kunnen blijven op dagen waarop de toestand van de atmosfeer niet geschikt is voor transport van sporen over grote afstanden of voor overleving van de sporen tijdens dit transport. Het beslissingondersteunend systeem bepaalt eerst of een bespuiting nodig is op basis van het risico op infectie. Dit risico hangt af van weersomstandigheden en de mate van resterende fungicidenbescherming. Vervolgens wordt de capaciteit van de atmosfeer voor transport van levende sporen over grote afstanden bepaald. Als deze geschiktheid groter is dan een vooraf bepaalde drempelwaarde wordt het oorspronkelijke spuitadvies gevolgd, maar indien de voorspelde capaciteit van de atmosfeer lager is dan de drempelwaarde wordt geadviseerd niet te spuiten. De drempelwaarde werd bepaald op basis van historische weersgegevens. De spuitdosering werd aangepast aan de mate van resistentie van de aardappelcultivar.

Dit concept werd in 2007 getoetst in een veldproef onder hoge infectiedruk met drie aardappelrassen. De ruimtelijke module werd gekoppeld aan het gepubliceerde beslissingondersteunende systeem SIMCAST. Het MM5 weersverwachtingsmodel werd gebruikt om de meteorologische invoer te genereren voor de aerobiologische modellen. De resultaten van het systeem werden vergeleken met SIMCAST zonder atmosferische verspreidingsmodule. Toepassing van de ruimtelijke module gaf een besparing van twee bespuitingen en leidde tot uitstel van één bespuiting. De mate van bescherming tegen *Phytophthora* werd niet verminderd.

Deze resultaten leveren een eerste bewijs dat het concept werkt. Er is verder onderzoek nodig om de methode te toetsen en verfijnen en geschikt te maken voor toepassing in de praktijk. Het ontwikkelde principe kan ook worden uitgewerkt voor andere plantenziekten.

Hoofdstuk 7

Slimme ruimtelijke allocatie van resistente genotypen van landbouwgewassen zou deze minder vatbaar kunnen maken voor invasie door resistentie-doorbrekende virulente genotypes van ziekteverwekkers. Er werd een volledig analytisch Gaussisch pluimmodel ontwikkeld om modelstudies op landschapsschaal mogelijk te maken. Dit model werd opnieuw gevalideerd met experimentele gegevens over sporenverspreiding boven een aardappelgewas. Vervolgens werd het model gecombineerd met een model voor de epidemiologie van aardappelziekte op veldschaal, met modellen voor aerobiologische processen, en met een landschapsgenerator. Het resulterende meerschelijke model voor het

aardappelziektesysteem werd gebruikt om een aantal pragmatische strategieën voor allocatie van resistente variëteiten te toetsen op hun weerbaarheid tegen invasie.

De resultaten tonen aan dat de mate van ziekteuitbreiding het meest wordt beïnvloed door het aantal verschillende resistenties, vervolgens door aanpassing van de fractie aardappelareaal in het landschap, gevolgd door clustering van percelen, en tenslotte de grootte van de percelen. Een regiobrede toepassing van mengsels van genotypen binnen percelen had een groter effect op regionale invasiesnelheid dan toepassing van verschillende genotypes in verschillende percelen. Op de getoetste schalen was het niet mogelijk om aardappelvrije zones te creëren die groot genoeg waren om een significante factor te zijn in de weerbaarheid tegen ziekte-invasie. Fijnschalige ruimtelijke en genotypische variatie bleek effectiever dan grootschalige variatie.

Hoofdstuk 8

In dit hoofdstuk passeren de voornaamste resultaten en inzichten van het onderzoek de revue. De verschillende modellen en modelbenaderingen worden in detail besproken. De resultaten van hoofdstuk 2 t/m 7 worden vervolgens besproken in het licht van het management van de aardappelziekte. Ruimtelijke beslissingsondersteuning komt naar voren als een levensvatbare optie voor ziektebeheersing en vermindering van milieubelasting door *Phytophthora* bestrijding. De ruimtelijke module voor beslissingsondersteuning biedt een mogelijkheid om de performance, kosteneffectiviteit en bruikbaarheid van beslissingsondersteunende systemen verder te verbeteren, en kan helpen om de toepassing van deze systemen in de praktijk te verbeteren. Ruimtelijke strategieën voor het inzetten van resistenties kunnen gebruikt worden om de beheersing van de aardappelziekte te verbeteren en om de consequenties van doorbreking van resistentie te verzachten. Deze strategieën kunnen potentieel bijdragen aan de performance en duurzaamheid van waardplantresistentie en een reductie in het gebruik van gewasbeschermingsmiddelen. Een combinatie van operationele en strategische toepassing van ruimtelijke strategieën, in combinatie met het monitoren van waardplantresistentie en populatiestructuur van de ziekteverwekker, kan bijdragen tot een dynamische ruimtelijke strategie voor beheersing van de aardappelziekte en verduurzaming van de aardappelteelt.

Publications

- Skelsey, P., Holtslag, A.A.M., and van der Werf, W. 2008. Development and validation of a quasi-Gaussian plume model for the transport of botanical Spores. *Agr. Forest Meteorol.* 148:1383-1394.
- Skelsey, P., Kessel, G.J.T., Holtslag, A.A.M., Moene, A.F., and van der Werf, W. Regional spore dispersal as a factor in disease risk warnings for potato late blight: a proof of concept. *Agr. For. Meteorol.*, *in press*.
- Skelsey, P., Kessel, G.J.T., Rossing, W.A.H., and van der Werf, W. Parameterization and evaluation of a spatio-temporal model of the late blight pathosystem. *Phytopathology*, *in press*.
- Skelsey, P., Kessel, G.J.T., Rossing, W.A.H., and van der Werf, W. Scenario approach for assessing the utility of dispersal information in decision support for aerially spread plant pathogens, applied to *Phytophthora infestans*. *Phytopathology*, *in press*.
- Skelsey, P., Rossing, W.A.H., Kessel, G.J.T., van der Werf, W., and Holtslag, A.A.M. 2007. Multi-scale modeling of infection pressure from *Phytophthora infestans*. In: Schepers, H.T.A.M. (Ed.), Proceedings of the tenth workshop of an European network for development of an integrated control strategy of potato late blight, Bologna, Italy. PAV Special Report no. 12:161-164.
- Skelsey, P., Kessel, G.J.T., Rossing, W.A.H., and van der Werf, W. 2007. Simulation of potato late blight in the Netherlands: validation of the BLIGHTSPACE model reveals dichotomy in the epidemiological effects of resistance components. In: Schepers, H.T.A.M. (Ed.), Proceedings of the tenth workshop of an European network for development of an integrated control strategy of potato late blight, Bologna, Italy. PAV Special Report no. 12:233-236.
- Skelsey, P. 2006. Multi-scale modeling of effective infection pressure from *Phytophthora infestans*. *Phytopathology* 96:S108.
- Rossing, W.A.H., Skelsey, P., Kessel, G.J.T., and van der Werf, W. 2006. Sensitivity of potato late blight epidemics and potato yield to variation in initial inoculum density: a model-based analysis with implications for predicting atmospheric transport of spores. In: Westerdijk, C.E., and Schepers, H.T.A.M. (Ed.), Proceedings of the ninth workshop of an European network for development of an integrated control strategy of potato late blight, Tallin, Estonia. PAV Special Report no. 11:35-39.

- Skelsey, P., Jacobs, A.F.J., Hofschreuder, P., Kessel, G.J.T., Rossing, W.A.H., and van der Werf, W. 2006. Multi-scale modeling of effective infection pressure from *Phytophthora infestans*. IOBC wprs Bulletin 29 (6): 661-662.
- Skelsey, P., Jacobs, A.F.J., Hofschreuder, P., and van der Werf, W. 2006. Comparison of atmospheric dispersion models for the short-range transport of *Lycopodium clavatum* spores above a potato canopy. In: Westerdijk, C.E., and Schepers, H.T.A.M. (Ed.), Proceedings of the ninth workshop of an European network for development of an integrated control strategy of potato late blight, Tallin, Estonia. PAV Special Report no. 11:101-105.
- Skelsey, P., Rossing, W.A.H., Kessel, G.J.T., and van der Werf, W. 2006. Influence of host diversity on development of epidemics: an evaluation and elaboration of mixture theory. In: Westerdijk, C.E., and Schepers, H.T.A.M. (Ed.), Proceedings of the ninth workshop of an European network for development of an integrated control strategy of potato late blight, Tallin, Estonia. PAV Special Report no. 11:217-223.
- Skelsey, P., Rossing, W.A.H., Kessel, G.J.T., Powell, J., and van der Werf, W. 2005. Influence of host diversity on development of epidemics: an evaluation and elaboration of mixture theory. *Phytopathology* 95:328-338.
- Rossing, W.A.H., Jellema, A., Skelsey, P., van Bruggen, A.H.C., Kessel, G.J.T., Opdam, P.F.M., van der Werf, W. 2004. Combining landscape ecology and production ecology: habitat networks and habitat connectivity as guiding principles for thinking about land use. In: Jacobsen, S.E., Jensen, C.R, and Porter, J.R. (Ed.), Book of Proceedings of the VIII ESA Congress: European Agriculture in a global context, Copenhagen, Denmark. Narayana Press, Gylling, Denmark, pp. 661-662.

Curriculum vitae

Peter Skelsey was born on August 4, 1972 in Glasgow, Scotland. In 2001, he graduated with a BSc in Environmental Protection and Management at the Scottish Agricultural College in Edinburgh, Scotland. During this time he completed a thesis on the epidemiology of Dutch elm disease (causal agent - *Ophiostoma ulmi*) in the Edinburgh area. For this study he received the Scottish Power Prize for the best dissertation, and also the Scottish Agricultural College Gold Medal for the best student. In 2002, he completed a 9 month Marie-Curie Research Fellowship at Wageningen University, the Netherlands. This provided training in the use of GIS and spatio-temporal epidemiological modeling, using potato late blight as a model pathosystem. In 2004, he was admitted into a PhD program at Wageningen University, funded by the Dutch Ministry of Agriculture, Nature Management and Fisheries through the Umbrella Plan Phytophthora. During his PhD studies he collaborated on two further research projects. The first was for the “Umbrellaplan Phytophthora II,” which concerned the practical implementation of newly gained knowledge on how to reduce the environmental impact of potato late blight management. During this project he developed and tested a novel concept for the inclusion of regional dispersion modeling in decision support systems for aerially transmitted plant pathogens. The second additional project was entitled “Sustainable resistance against Phytophthora through cisgenic marker-free modification (DuRPh),” and was funded by the Dutch Economic Structure Enhancing Fund. During this project he used simulation modeling to investigate options for the strategic spatial deployment of late blight resistance genes. Currently, he is working as a Postdoctoral researcher for the Theoretical Biology and Evolutionary Genetics groups of Groningen University, the Netherlands. His current project is entitled “Modeling the spread of transgenes.” In this project, which is part of the NWO-ALW research program “Ecology Regarding Genetically Modified Organisms (ERGO),” simulation models will be developed for the spatial dispersal of transgenes (vegetatively or through pollen or seeds) in wild populations.

PE&RC Education Statement Form

With the educational activities listed below the PhD candidate has complied with the educational requirements set by the C.T. de Wit Graduate School for Production Ecology and Resource Conservation (PE&RC) which comprises of a minimum total of 32 ECTS (= 22 weeks of activities)



Review of Literature (5.6 ECTS)

Quantification of the risk of infection from *Phytophthora infestans*, causal agent of potato late blight, in relation to external inputs of viable sporangia (2003)

Writing of Project Proposal (7.0 ECTS)

Quantification of the risk of infection from *Phytophthora infestans*, causal agent of potato late blight, in relation to external inputs of viable sporangia (2004)

Laboratory Training and Working Visits (4.2 ECTS)

- 1 week visit to Dr. Donald Aylor and Dr. Frank Ferrandino at the Connecticut Agricultural Experiment Station, New Haven, USA (2005)
- Working visits to Dacom PLANT Service and Agrovision-Opticrop (4 days) (2007)

Post-Graduate Courses (2.8 ECTS)

- Spatial modeling in ecology; PE&RC (2002)
- Inoculum production; PRI (2004)
- Marie-Curie Fellowship (9 months); Marie-Curie (2002)

Deficiency, Refresh, Brush-up Courses (6.0 ECTS)

- Meteorology and climate; MAQ (2004)

Competence Strengthening / Skills Courses (9.6 ECTS)

- Ninth Workshop of an European Network for development of an Integrated Control Strategy of potato late blight (2005)
- Tenth Workshop of an European Network for development of an Integrated Control Strategy of potato late blight (2006)
- EPPO Conference on Computer Aids for Plant Protection (2006)
- PhD Competence assessment; WGS (2006)
- APS Course on scientific mentoring; APS (2007)

Discussion Groups / Local Seminars and Other Meetings (4.2 ECTS)

Pete made his home at four different research groups (CWE, BFS, MAQ, PRI) as his PhD project was highly interdisciplinary. At each of the four sites, Pete participated in scientific seminars, discussion groups, etc. In total, Pete changed office 6 times between these four departments, in order to take advantage of the skills and knowledge of the staff and researchers there. (2003-2007)

PE&RC Annual Meetings, Seminars and the PE&RC Weekend (0.6 ECTS)

- PE&RC day (2003)
- PE&RC seminar on Influenza Ecology and Pandemics

International Symposia, Workshops and Conferences (9 ECTS)

- Landscape Management for Functional Biodiversity (2006)
- APS Annual conference (2006)
- APS Annual meeting (2007)

Courses in which the PhD Candidate Has Worked as a Teacher

- Systems Analysis, Simulation and Systems Management; BFS, 12 days
- Population Ecology, 2005; CWE, 12 days
- Population Ecology, 2006; CWE, 12 days

Funding

The research described in chapters 2-6 of this thesis was funded by the Dutch Ministry of Agriculture, Nature and Food Quality through the Umbrella Plan Phytophthora (DWK 427) and the Umbrella Plan Phytophthora II (BO06-08), while research described in chapter 7 was financially supported by the DuRPh project: Sustainable resistance against Phytophthora through cisgenic marker-free modification. DuRPh was initiated by the Dutch Ministry of Agriculture, Nature and Food Quality and funded through the “Fonds Economische structuurversterking” (FES). The support is gratefully acknowledged.

